Investigating the role of cellular senescence in skeletal muscle and sarcopenia

Shahjahan Miah Shigdar

Institute of Life Course and Medical Sciences

Thesis submitted in accordance with the requirements of the University of Liverpool for the degree of Doctor in Philosophy

January 2021

Abstract
Senescence was first described by the pioneering work of Hayflick whereby human diploid fibroblasts underwent repeated population doublings, and the cells demonstrated a finite replicative limit in culture. It is now recognised that most replicative cells have the capability to undergo senescence. More recently senescence-like properties have been described in terminally differentiated cells, including skeletal muscle, although the nature of this senescence remains unclear. There is limited data examining the role of senescence in the determination of terminally differentiated tissues such as skeletal muscle.

The overall hypothesis of this thesis was that senescent cells accumulate in old mice, either locally to skeletal muscle or distally, and that they produce an inflammatory Senescence Associated Secretory Phenotype (SASP) which may contribute at least in part to the chronic NF-κB activation and the loss of muscle mass and function seen in the muscles of old compared with adult wild type (WT) mice. This programme of work tested this hypothesis by utilising different models of senescence in vitro and in vivo and using a senolytic and transgenic intervention.

Initial studies examined the potential for mouse skeletal muscle myoblasts (C2C12 myoblasts) to undergo senescence when treated with the DNA damaging agent, etoposide. Treatment of cells with etoposide resulted in cell cycle arrest, increased levels of p21, increased SA-β-Gal activity, and altered morphology, providing proof-of-principle that mononuclear myoblasts can become senescent. Further, the senescent myoblasts produced a proinflammatory SASP detectable in the cell media that was able to increase NF-κB transcription factor activity in mature C2C21 myotubes. Interpretation and comparison of data from senescent cells and control cells proved a challenge since under normal conditions, control myoblasts continue to divide until reaching confluence and contact inhibition occurs. At this point muscle cells initiate differentiation, with expression of some indices common to senescence.

Examination of muscles of old WT mice showed no evidence of the presence of classical senescent cells in muscles of old mice although old mice showed evidence of increased levels of cytokines and chemokines in the plasma. Data suggest that muscle may partially contribute to the increase in some of these plasma cytokines/chemokines by a non-senescent mechanism. In support of this conclusion, studies using either a transgenic or a pharmacological approach to remove whole body senescent cells in old mice had some minor effects on plasma cytokine/chemokine levels but provided no protection against the age-related loss of muscle mass and function.

Evidence for the presence of senescence cells in old mice remains unclear but some studies have suggested that removal of senescent cells provides protection against age-related muscle loss. One potential reason for the difference with the current study is the age of the mice used whereby studies that have demonstrated senescence within skeletal muscle have commonly made use of geriatric (32-months-old) mice suggesting that senescence is only involved in the very late stages of sarcopenia.

Acknowledgments

I would like to thank my supervisors, Professor Anne McArdle, Dr Aphrodite Vasilaki, and Dr Caroline Staunton, for their help and support and all the opportunities they gave me throughout my PhD. I would also like to thank the rest of the research group, especially Professor Jackson, for their guidance and support.

I would like to thank Sue Brooks, Jennifer Judge, Steven Guzman, and the research group at the University of Michigan for their help, support, and data. Thank you for making my first visit to Michigan a wonderful experience.

Thank you to my fellow cohort PhD students, especially Euan Owen for the cytokine data from adult and old mice.

I would also like to thank the Biomedical Service Unit (BSU), especially for their ceaseless support and patience with our experiments.

Finally, I would like to thank my funders – the British Society for Research in Ageing (BSRA), and the Rosetrees Trust, without whom I would not have had this opportunity.

Dedications

To my family and friends,

thank you.

Table of Contents

Figures

Tables

Abbreviations

- ADP — Adenosine Diphosphate
- APS — Ammonium Persulphate
- ATM — Ataxia Telangiectasia-Mutated
- ATP — Adenosine Triphosphate
- ATR — ATM-and-Rad3-related
- BCA — Bicinchoninic acid
- CDK — cyclin-dependent kinase
- CDKI — cyclin-dependent kinase inhibitor
- CuZnSOD/SOD1 — Copper Zinc Superoxide Dismutase
- DAPI — 4’,6-diamidino-2-phenylindole
- DDR — DNA-damage response
- DMEM — Dulbecco’s modified Eagle’s medium
- DNA — Deoxyribonucleic acid
- DSB — Double strand breaks
- EMSA — Electrophoretic Mobility Shift Assay
- g — Grammes
- H_20 — Water
- H2AX — H2A histone family member X
- HBSS — Hepes buffered PBS solution
- IFN-γ — Interferon gamma
- IGF-1 — Insulin growth factor 1
- IGF1 — Insulin-like growth factor 1

• IκB	Inhibitor of nuclear factor kappa B
• IL	Interleukin
• IP10	Interferon Gamma Induced Protein 10
• Kg	Kilogrammes
• KO	Knock-out
• MAPK	Mitogen-activated protein kinase
• MCP1	Monocyte Chemoattractant Protein 1
• M-CSF	Macrophage Colony-Stimulating Factor
• mg	Milligrammes
• MHC	myosin heavy chain
• Mip1α	Macrophage inflammatory protein 1-alpha
• Mip3α	Macrophage inflammatory protein 3-alpha
• MnSOD/SOD2	Manganese Superoxide Dismutase
• mRNA	Messenger RNA
• mtDNA	Mitochondrial Deoxyribonucleic Acid
• mTOR	Mechanistic Target of Rapamycin
• nm	Nano Metre
• NF-κB	Nuclear Factor Kappa-Light-Chain-Enhancer of Activated B cells
• OIS	Oncogene-induced senescence
• PBS	Phosphate buffered PBS
• PCR	Polymerase Chain Reaction
• PI3K	phosphatidyilinositol-3-OH-kinases

- qPCR — Quantitative Polymerase Chain Reaction
- RNA — ribonucleic acid
- RS — Replicative Senescence
- SAHF — Senescence Associated Heterochromatin Foci
- SASP — senescent associated secretory phenotype
- SA-β-Gal — senescence-associated β-galactosidase
- SDS PAGE — Sodium Dodecyl Sulphate-Polyacrylamide Gel Electrophoresis
- SEM — Standard Error of the Mean
- SIPS — stress-induced premature senescence
- TBE — Tris/Borate/EDTA
- TBS — Tris-buffered PBS
- TBST — Tris-buffered PBS, 0.1% Tween 20
- TEMED — Tetramethylethylenediamine
- TNF-α — Tumour Necrosis Factor Alpha
- UV — Ultraviolet
- µM — Micrometre

Chapter 1: General Introduction

1.1 Cellular senescence

The word “senescence” is derived from Latin *senex*, meaning "old" and generally refers to the ageing process. The first introduction to, and demonstration of cellular senescence was led by the pioneering study from Hayflick and Moorhead (1961). Human diploid fibroblasts underwent repeated population doublings, and the cells demonstrated a finite replicative limit in culture. Hayflick and Moorhead named this event senescence, to describe the phenomenon of permanent growth arrest after extensive serial passaging in culture.

This phenomenon is now known as "replicative senescence" (von Zglinicki, 2002). The replicative senescence (RS) described by Hayflick and Moorhead, was attributed to telomere attrition, a process that leads to chromosomal instability and promotes tumorigenesis (Bodnar et al., 1998). A telomere is a region of repeated nucleotide sequences at each end of a chromosome, which protects the end of the chromosome from deterioration, or from fusion with other neighbouring chromosomes (Jiang et al., 2018). The attrition of telomeres ultimately activates the DNA-damage response (DDR), resulting in senescence (von Zglinicki, 2002).

There are other forms of senescence that are not linked to proliferation-dependent telomere attrition, and are similar but not identical to replicative senescence (Section 1.1.1). Many proliferative cell types can undergo stress-induced premature senescence (SIPS) upon exposure to damaging but non-lethal stresses (UV light, ionizing radiation, H_2O_2, hyperoxia, etc.) (Toussaint et al., 2002, Toussaint et al., 2000a, Toussaint et al., 2000b).

First described by Serrano et al. (1997), oncogene-induced senescence (OIS) is a senescent phenotype that depends on the activation and/or overexpression of oncogenes. An oncogene is a gene that has the potential to cause cancer. Serrano et al. (1997) identified that the activation of an oncogenic mutant rat sarcoma viral oncogene homolog (RAS) in cultured cells resulted in senescence. Ultimately, all of these forms of senescence may present some of the hallmarks of senescence (Hernandez-Segura et al., 2017) (Section 1.1.1).

Senescence is an example of antagonistic pleiotropy (Kirkwood and Austad, 2000). Historically, most organisms evolved in environments rich in hazards, which often eliminated older individuals from populations due to selective pressure. Unfortunately, there are not many selective pressures for cellular senescence, allowing senescent cells to accumulate in old age.

1.1.1 Hallmarks of Senescence

There are a number of hallmarks and molecular markers of senescence, some of which are described below senescent cells are diverse and their profiles are dependent on the cell type of origin and methods used to induce the senescence (Wiley et al., 2017). However, the consensus is that senescent cells demonstrate classic morphological changes and express several common markers (Avelar et al., 2020). These include but are not limited to:

- Changes in morphology

Senescent cells undergo important morphological changes, such as becoming flat and enlarged, due to CDK5-dependent activation and increased expression of the cytoskeleton proteins (Yang and Hinds, 2003).

- Cell cycle arrest/absence of proliferative markers

Several molecules play an important role in establishing and maintaining the cell cycle arrest of senescent cells. Of these, p53, p21 and p16 are often used to characterise senescence

- Senescence-associated β-galactosidase (SA-β-GAL) activity

In senescent cells, a lysosomal beta-galactosidase accumulates and can be exploited in a cytochemical assay that leaves a blue precipitate at pH 6.0 (Dimri et al., 1995).

- Chromatin structure (Senescence Associated Heterochromatin Foci [SAHF])

Narita et al. (2003) initially demonstrated that Retinoblastoma (Rb) and other heterochromatin-associated proteins can accumulate on the E2F-responsive promoters in senescent but not quiescent cells. E2F are a group of genes that are involved in the cell cycle regulation (Serrano et al., 1997). These results are associated with more stable repression of E2F responsive genes, permanent cell cycle arrest, and altered heterochromatin formation.

- Senescence associated secretory phenotype (SASP).

A senescent cell is a persisting, metabolically active cell that has undergone widespread changes in protein expression and secretion, ultimately developing the senescence-associated secretory phenotype (SASP) (Evan and d'Adda di Fagagna, 2009, Coppe et al., 2010a, Campisi, 2013). The SASP has also been referred to as the senescence messaging secretome (SMS) or secretome (Kuilman and Peeper, 2009). Coppe et al. (2010a) highlight some of the factors found in the SASP of senescent cells, including cytokines, chemokines, growth factors and regulators, and proteases.

Thus, the SASP is a complex cocktail of compounds capable of influencing the surrounding microenvironment of the senescent cells.

Identification of senescence has been an issue for the field since its inception. None of the markers available are able to detect senescence exclusively (Wiley et al., 2017). Thus, rather than single markers, senescent cells are normally identified by whether they test positive for a range of markers. For example, maturing tissue macrophages (Bursuker et al., 1982) can give false positive results for SA-β-gal activity, and so other indices are required. Furthermore, p53 activation is not required for the SASP (Coppe et al., 2008).

1.1.2 Molecular markers of senescence

1.1.2.1 P53

Tumour protein p53 (tp53), also known as p53, is a crucial protein that plays large role in a number of pathways including: apoptosis, cell cycle arrest, and DNA damage repair (DDR) (Serrano et al., 1997, Ou and Schumacher, 2018). At DNA damage checkpoint, for example when a cell moves from G_1 to S phase, the kinases ATM and ATR become activated, stabilising p53 and preventing its proteasomal degradation (Matsuoka et al., 2000, Ou and Schumacher, 2018). Furthermore, the transcriptional activity of p53 is enhanced, allowing for the transcription cell dependant kinase inhibitors to arrest the cell cycle (Dumaz and Meek, 1999, Ou and Schumacher, 2018).

The importance of p53 is highlighted in transgenic mouse models. Over-expression of p53 has been shown to protect against the development cancer and tumours, at the expense of accelerated ageing phenotypes (Tyner et al., 2002, Maier et al., 2004) (Dumble et al., 2007). Indeed, “super-p53” mice which contained 3 copies of the p53

alleles had normal lifespan, and extended lifespan with the addition of an additional copy of the ARF tumour suppressor (Garcia-Cao et al., 2002, Matheu et al., 2007). Transgenic mice with reduced expression of MDM2 and concomitant increased activation of p53 showed increased resistance to cancer and a normal lifespan (Mendrysa et al., 2006). On the other hand, murine models with reduced functional p53 often result in increased incidences of cancer and poor survival (as reviewed by Lozano (2010)).

1.1.2.2 P21

Cyclin-dependent kinase inhibitor 1, also known as $p21^{Cip1}$ or $p21^{Waf1}$, functions to inhibit cell cycle progression (Xiong et al., 1993) by binding to a range of targets (Gartel and Radhakrishnan, 2005). What distinguishes p21 from other CDKI molecules is that it is a downstream target of p53. The accumulation of p21, a cyclin-dependent kinase inhibitor, suppresses Cyclin E/Cdk2 kinase activity thereby resulting in G1 arrest (Bartek and Lukas, 2001). Transgenic, p21 knockout mice have been shown to be susceptible to osteoarthritis, due in part to increased levels of circulating inflammatory cytokines (Kihara et al., 2018).

1.1.2.3 P16

Phosphorylation of p53 results in increased transcription of $p16^{INK4A}$ (Serrano et al., 1997). First described by (Serrano et al., 1993), cyclin-dependent kinase inhibitor 2A, also known as $p16^{INK4}$, is a tumour suppressor protein under expression of the CDKN2A gene (Nobori et al., 1994). As a cyclin-dependant kinase (CDK) inhibitor, p16 functions to inhibit cell cycle progression (Hara et al., 1996) from G_1 to S phase by binding to CDK 4/6. By doing so, it can no longer bind cyclin D and phosphorylate the

Retinoblastoma protein (pRb). The phosphorylation frees up E2F1 from pRb, allowing E2F1 to enter the nucleus and act a transcription factor for genes related to cell cycle progression.

1.1.2.4 Senescence Associated Heterochromatin Formations (SAHF)

Senescence Associated Heterochromatin Formations (SAHFs) were first described by Narita et al. (2003), who observed that the nuclei of senescent cells contained bright, punctate DNA-stained dense foci which is readily distinguishable from chromatin in normal cells. SAHFs are not associated with cells undergoing quiescence, indicating that SAHF formation is not associated with a reversible exit from the cell cycle (Narita et al., 2003).

SAHF also play a role in the epigenetic regulation of proliferation promoting genes (Narita et al., 2003). An example of which is E2F target genes such as cyclin A (Zhang et al., 2007), which are required for the progression through S-phase of the cell cycle (Pagano et al., 1992). This epigenetic regulation extends further as the SAHF contain no active transcription sites, contributing to the permanent cell cycle arrest we see in senescence. SAHFs can be seen in several models of senescence: Oncogene induces senescence (OIS) (Martin et al., 2010, Michaloglou et al., 2005), and stress induced premature senescence (SIPS) (Narita et al., 2003, Kosar et al., 2011). SAHFs are not to be confused with DNA-SCARS (DNA segments with chromatin alterations reinforcing senescence) (Rodier and Campisi, 2011). SAHF formation and senescence are not always coupled. Several studies have demonstrated this, for instance, activation of AKT and knockdown of PTEN do not cause SAHF formation (Kennedy et al., 2011, Tu et al., 2011). Furthermore, SAHF formation is cell-line dependent (Kosar et al., 2011).

Extensive passaging induced senescence (replicative senescence) of IMR90 and WI38 cells is associated with SAHF, whereas in BJ cells (primary human foreskin fibroblasts) it is not (Narita et al., 2003). This difference in SAHF formation between cell lines is correlated to the p16/pRb pathway and its activation (Kosar et al., 2011).

1.1.2.5 Senescence-associated β-galactosidase activity

The most widely used assay for evidence of senescence is the histochemical detection of β-galactosidase activity at pH 6.0, which is known as senescence-associated β-galactosidase (SA-β-GAL) (Dimri et al., 1995). In senescent cells, a lysosomal beta-galactosidase accumulates and can be exploited in a cytochemical assay that leaves a blue precipitate at pH 6.0 (Lee et al., 2006). SA-β-gal is often used alongside other markers, such as p16 (Hall et al., 2016). Example senescence-associated β-galactosidase in C2C12 cells (Jadhav et al., 2013)

1.1.3 Mechanisms of induction of senescence

1.1.3.1 The Cell Cycle

Understanding the cell cycle is necessary to determine the potential mechanisms of induction of senescence. There exist checkpoints in the cell cycle that regulate the progression of the cell, preventing damaged DNA from progressing through to daughter cells during mitosis. In 2001, Hartwell, Hunt, and Nurse were awarded the Nobel Prize in Physiology and Medicine for the discovery of the two key classes of molecules used in these checkpoints: cyclins and cyclin-dependant kinases (CDKs) (2001). First identified in yeast, cyclins work by forming heterodimers with CDKs, activating the ability of CDKs to phosphorylate key molecules in signalling pathways involved in cell cycle progression (Spellman et al., 1998).

There are four distinct phases of the cell cycle of dividing cells:

G_0 – Also known as the resting phase where cells have left the cell cycle and stopped dividing. This phase encompasses post-mitotic cells, such as muscle or nerves, as well as quiescent and senescent cells. For some cell types, such as terminally differentiated or senescent cells, this arrest is permanent. Whereas for some quiescent cells, like stem cells, they enter and exit the cells cycle when stimulated.

G_1 – The first stage on interphase, the growth phase, where the cells gather resources, grow, and synthesise new proteins and organelles. During G_1 phase, the cell may leave the cell cycle for G_0, or move on to S phase and begin DNA replication. Passage from this phase is controlled by cyclins.

S – S phase, or synthesis phase, is where DNA synthesis occurs. Here, the chromosomes are replicated to provide equal genetic material to each daughter cell in mitosis.

G_2 – This is the second growth phase, where the cells undergo rapid protein synthesis and growth to prepare for mitosis. To pass through to M phase, the cells must pass another checkpoint to identify and DNA damage that may have occurred in S phase. The G2 checkpoint is regulated by p53, which can either repaired the DNA or cause the cell to undergo apoptosis if the damage is irreparable.

M phase – this phase is the physical division of the nucleus (karyokinesis) in to two halves for each of the daughter cells. The M phase is further broken down into more steps: prophase, prometaphase, metaphase, anaphase, and telophase.

Two families of genes that act as inhibitors for cell cycle progression, the cip/kip (CDK interacting protein/Kinase inhibitory protein) gene family and the INK4a/ARF (Inhibitor of Kinase 4/Alternative Reading Frame) gene family. The cip family includes p21, a downstream molecule activated by p53. The INK4a family includes p16, which binds to CDK4 and causes arrest in the G_1 phase (Section 1.1.2).

1.1.3.2 Chemical Inducers of cellular senescence

The number of stimuli that have been identified to induce senescence is continually increasing and the mechanisms involved have been extensively reviewed: (Campisi and d'Adda di Fagagna, 2007, Collado et al., 2007, Collado and Serrano, 2010, Gorgoulis and Halazonetis, 2010, Kuilman et al., 2010, van Deursen, 2014, Salama et al., 2014). A publication by Petrova et al. (2016) has listed and reviewed a number of low molecular weight compounds that can induce senescence (e.g. doxorubicin, H_2O_2), and an example of which is etoposide.

Etoposide, is a chemotherapeutic agent used to treat a wide variety of cancers (Pommier et al., 2010, Montecucco et al., 2015). Etoposide is derived from podophyllotoxin, a toxin found in *Podophyllum peltatum* (AKA American Mayapple). Etoposide was first produced in 1966, and then approved for cancer therapy in 1983 by the U.S. Food and Drug Administration (FDA) (Hande, 1998, Montecucco et al., 2015). Etoposide functions by forming complexes with DNA and the topoisomerase II enzyme, which is used to unwind DNA during mitosis. Complexes of etoposide/topoisomerase II prevents DNA unwinding and the subsequent re-ligation of the DNA strands; and by doing so causes DNA double strand breaks (Pommier et al., 2010, Montecucco et al., 2015). Inhibiting DNA replication drives apoptosis and

has been exploited to eliminate rapidly dividing, cancerous cells (Hande, 1998, Montecucco et al., 2015).

Etoposide has been used in a number of studies to induce senescence to investigate tumour progression in several different cell lines (te Poele et al., 2002), apoptosis in WI38 fibroblasts (Probin et al., 2006), and vimentin cytoskeletal alterations in A549 cells (Litwiniec et al., 2013).

1.1.3.3 The DNA-Damage Response (DDR) and senescence

Damage to nuclear DNA is triggers a rapid response (von Zglinicki, 2002). In cases where the damage is too extensive and not repairable, the cell may undergo apoptosis to prevent propagation of corrupted genomic material (d'Adda di Fagagna, 2008). Cells have several mechanisms termed the DNA-damage response (DDR) to detect DNA damage, signal its presence, and promote DNA damage repair (Jackson and Bartek, 2009).

Two key molecules in DDR signalling are the protein kinases: 1) Ataxia Teleangectasia-Mutated (ATM), and 2) and ATM-and-Rad3-related (ATR), both of which initiate DNA repair or induce cell cycle arrest (Zou, 2007). Two downstream targets of ATM/ATR are the protein kinases CHK1 and CHK2, which work in tandem with ATM/ATR to modulate cyclin-dependent kinase (CDK) activity by activation of the p53 transcription factor.

In healthy cells, p53 levels are low due to p53 binding with MDM2, which targets p53 for nuclear export and then for proteasome-mediated degradation in the cytoplasm (Alarcon-Vargas and Ronai, 2002). Following DNA damage, ATM activates downstream kinase CHK2, which in turn phosphorylates of p53 at S20 (Serine 20) (Matsuoka et al., 2000). Phosphorylation of S20 of p53 blocks the p53/MDM2 interaction, resulting in p53 accumulation in the nucleus. ATM also exerts a second control measure on p53 stability by directly phosphorylating MDM2 on S395 (Maya et al., 2001). This phosphorylation of MDM2 allows the MDM2/p53 interaction but prevents p53 nuclear export to the cytoplasm where degradation would normally occur. ATR also phosphorylates and stabilises p53 at S20 via the ATR-dependent kinase CHK1 (Shieh et al., 2000).

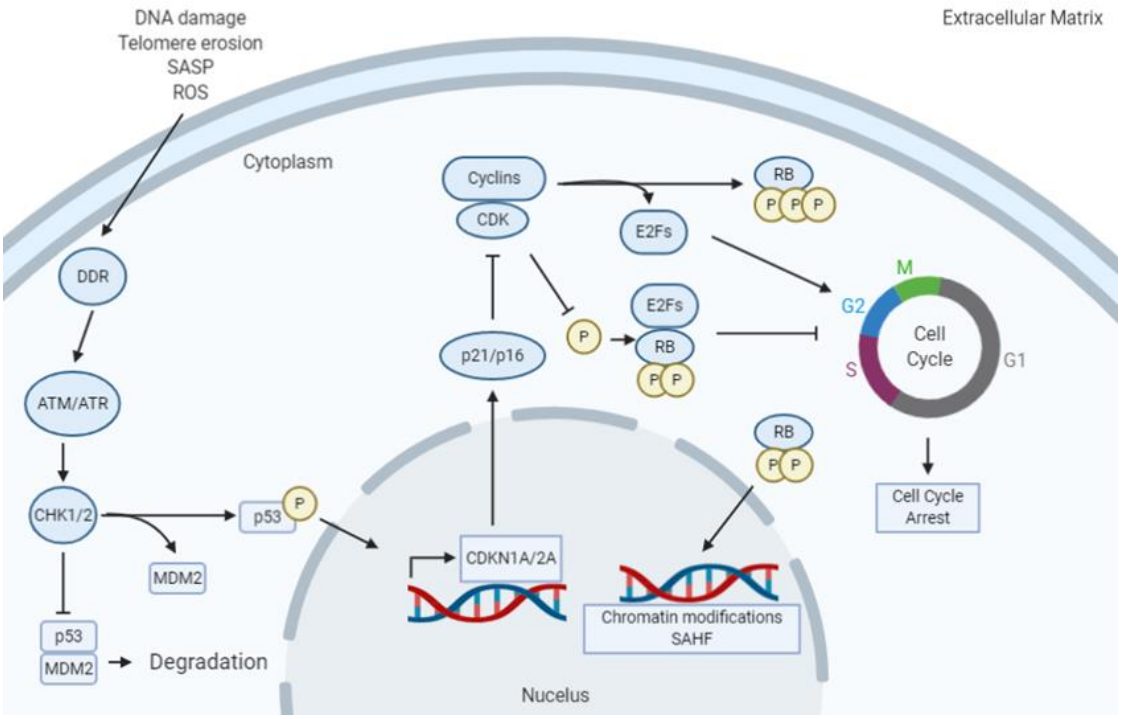

Figure 1.1 Senescence Signalling Pathway.

A simplified description of the cell signalling pathways implicated in establishing and maintaining senescence.

Indeed, p53 can also be phosphorylated at S15 directly by ATM and/or ATR in response to DNA damage, enhancing p53 transcriptional activity (Dumaz and Meek, 1999). Activated p53 then up-regulates transcription of several target genes, many of which are also involved in the DNA damage response (MDM2, GADD45a, and p21/Cip (CDK-interacting protein)). The accumulation of p21, a cyclin-dependent kinase inhibitor, results in the suppression of Cyclin E/Cdk2 kinase activity thereby resulting in G1 arrest (Bartek and Lukas, 2001).

Phosphorylation of p53 also results in increased transcription of $p16^{INK4A}$ (Serrano et al., 1997). Upregulation of $p16^{INK4A}$ leads to the prevention of Retinoblastoma (Rb) phosphorylation. Normally, CDKs phosphorylate Rb to its hyper-phosphorylated form, releasing E2F transcription factors. E2Fs are a group of genes that encode a family of transcription factors in mammalian cells, all of which are involved in regulation of the cell cycle (Serrano et al., 1997). During $p16^{INK4A}$ upregulation, Rb hypo-phosphorylation is inhibitory, resulting in inhibition of E2F-dependent transcription. The cell does not progress from G1 phase into S phase, resulting in cell cycle arrest. Furthermore, to ensure the stable repression of E2F-target genes and permanent cell cycle arrest, Rb promotes heterochromatin formation at E2F-regulated gene promoters. The E2F gene promoters are epigenetically silenced, in a process called Senescence-Associated Heterochromatin Foci (SAHF) formation (Narita et al., 2003).

1.1.4 NF-κB signalling in cellular senescence

Activation of NF-κB occurs in senescent cells and is key to establishing the SASP (Chien et al., 2011). NF-κB (nuclear factor kappa-light-chain-enhancer of activated B cells)

are a family of transcription factors, which regulates a large array of genes involved in different processes of the immune and inflammatory responses (Oeckinghaus and Ghosh, 2009). The NF-κB family is composed of five structurally related monomer proteins: NF-κB1 (p50), NF-κB2 (p52), RelA (p65), RelB, and c-Rel. By binding as various hetero- or homo-dimers, NF-κB mediates transcription of many target genes (Sun et al., 2013). NF-κB family proteins are usually sequestered to the cytoplasm by another family of inhibitory proteins, including the IκB family and related proteins, characterised by the presence of ankyrin repeats (Sun, 2011). Ankyrins are another family of proteins that mediate the attachment of membrane proteins to the membrane cytoskeleton (Bennett and Baines, 2001). The inhibitor of nuclear factor kappa B (IκB) family members of note are: IκBα (inhibitor of κBα), p105, and p100.

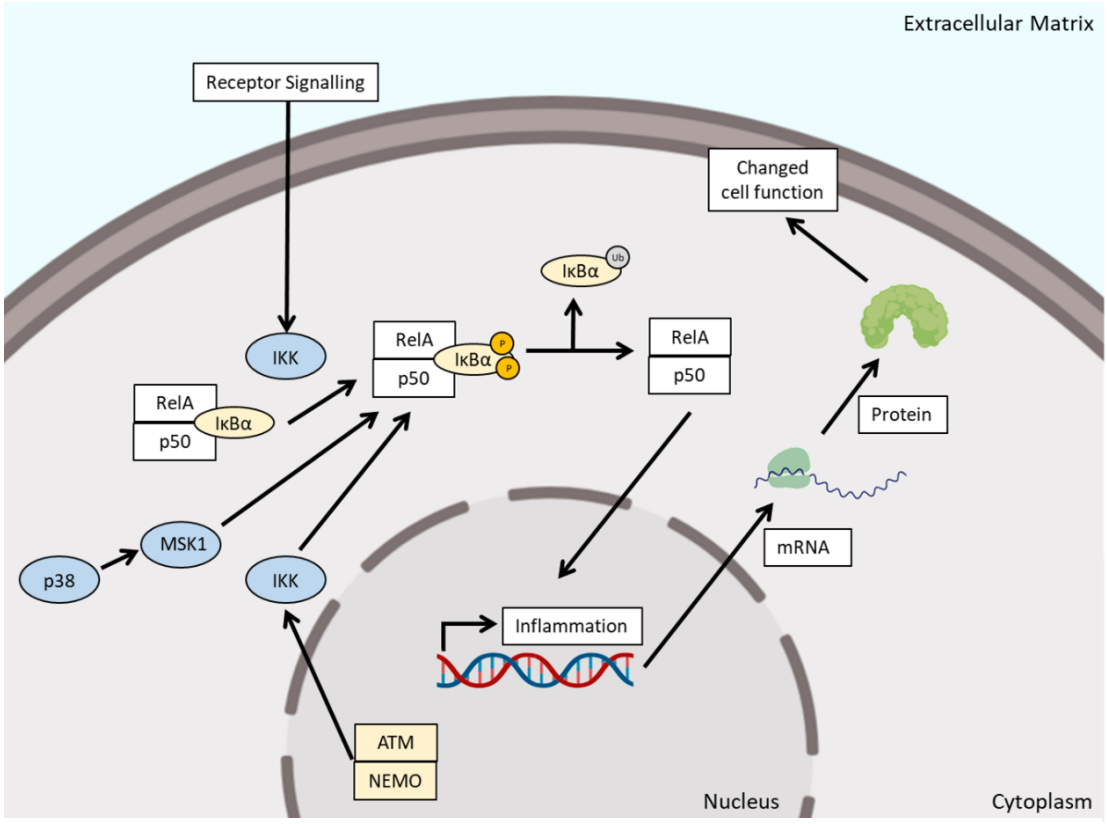

Figure 1.2. NF-κB signalling pathway.

A simplified signalling pathway for canonical NF-κB signalling, in the context of cellular senescence.

Both p105 and p100 are precursor proteins of NF-κB1 and NF-κB2 respectively (Beinke and Ley, 2004). NF-κB activation involves two major signalling pathways, the canonical pathway and the non-canonical (or alternative) pathway. Both pathways are important for regulating immune and inflammatory responses despite their differences in signalling mechanism (Sun, 2011). The focus of this thesis is the canonical pathway.

The primary mechanism for canonical NF-κB activation is the inducible degradation of IκBα, which is triggered through by site-specific phosphorylation by the IκB kinase (IKK) complex (Oeckinghaus and Ghosh, 2009). Upon activation, IKK phosphorylates IκBα at two N-terminal serines, whereby triggering ubiquitin-dependent IκBα degradation by the proteasome (Karin, 1999). Degradation of IκBα results in nuclear translocation of NF-κB members: p50/RelA and p50/c-Rel dimers (Beinke and Ley, 2004).

IKK is composed of two catalytic subunits, IKKα (IKK1) and IKKβ (IKK2), and the regulatory subunit, NF-κB essential modulator (NEMO or IKKγ) (Karin, 1999). NEMO acts as a scaffold for IKK subunits to multimerise, and for activation via trans-auto-phosphorylation, whilst also bringing them in proximity to upstream kinases (E.G. TAK1) (Iwai, 2012, Adhikari et al., 2007). IKK can be activated by different stimuli, including cytokines, growth factors, mitogens, microbial components, and stress agents (Mitchell et al., 2016).

A well-recognized function of NF-κB is regulation of inflammatory responses. Not surprisingly, dysregulated NF-κB activation is a hallmark of chronic inflammatory diseases. Mice lacking NEMO or IKKβ die early during embryogenesis with liver

degeneration, a phenotype like that of p65/RelA-deficient animals (Makris et al., 2000, Pasparakis et al., 2006). Mice lacking IKKα die shortly after birth and show defective epidermal keratinocyte differentiation and skeletal abnormalities (Hu et al., 1999, Pasparakis et al., 2006).

1.1.4.1 Inflammaging and senescence

Inflammaging is the term used to describe the chronic, low-grade systemic inflammation seen in ageing (Franceschi et al., 2000). The source of such inflammatory cytokines is unclear, but this inflammation occurs in the absence of infection and is primarily driven by endogenous signals. A major characteristic of inflammaging is the chronic activation of the innate immune system and macrophages (Franceschi et al., 2000).

Data suggest that besides persistent infections; cell debris, misplaced self-molecules, and misfolded/oxidized proteins are major contributors to inflammaging (Franceschi and Campisi, 2014). One potential contributor to inflammaging are senescent cells and the accompanying senescence associated secretory phenotype (SASP).

1.1.4.2 The role of NF-κB signalling and production of inflammatory cytokines by senescent cells

Several studies have clearly demonstrated that NF-κB plays a significant role in the expression of most SASP factors (e.g. IL-6 and CXCL1) in several models of senescence (Reviewed by Malaquin et al. (2016)).

The molecular mechanisms leading to NF-κB activation in the context of senescence remain poorly defined. However, genotoxic stress activates NF-κB through distinct sumoylation; sumoylation is a post-translational modification which involves addition

of SUMOs (small ubiquitin-like modifiers) (Mabb et al., 2006). In response to DNA damage NEMO is localized to the nucleus as a result of SUMO-1 attachment to NEMO/IKKγ, assisting in the complex formation (Huang et al., 2003). The DDR can also activate NF-κB via ATM (Wu et al., 2006). ATM can interact with NEMO (Miyamoto, 2011), a regulator of the IKK complex. Activation of the DDR results in the export of an ATM/NEMO complex into the cytoplasm. NEMO then binds and activates IKKα/β, degrading IκB proteins. Degradation of IκB then results in the activation of NF-κB (Mitchell et al., 2016).

Alternatively, the p38MAPK pathway may contribute to NF-κB activation. Increased p38MAPK signalling leads to the activation of the mitogen and stress activated protein kinase MSK1 (Kefaloyianni et al., 2006). MSK1 can phosphorylate the p65/NF-κB subunit, resulting in activation (Vanden Berghe et al., 1998). Indeed, small molecule inhibitors of p38 MAP kinase can inhibit secretion of cytokines and the SASP in human fibroblasts (Alimbetov et al., 2016).

1.1.5 Role of Senescence *in vivo*

Senescence can have both positive and negative effects, depending on the context. Originally, senescence was thought of as a tumour suppression mechanism. Several studies to date have reinforced the importance of cellular senescence as a guard against cancer (Serrano et al., 1997, Braig et al., 2005, Collado and Serrano, 2010). This makes sense as the permanent cell cycle arrest described in senescence stands in perfect antithesis to the uncontrolled replication in cancer. Senescent cells can be observed in premalignant stages of tumours, although they disappear in the more malignant stages (Chen et al., 2005). Examples in which senescent cells have been

found include: prostatic intraepithelial neoplasia, lung adenomas, and melanocyte nevi (Michaloglou et al., 2005).

However, other studies have shown that senescent cells develop altered secretory activities (SASP) that may induce changes in the tissue microenvironment, relaxing its control over cell behaviour and instead promoting tumorigenesis (Krtolica et al., 2001).

In liver fibrosis, senescent myofibroblasts accumulate in fibrotic scars following liver damage (Wiemann et al., 2002). These senescent cells attract immune cells, resulting in partial elimination of the fibrotic scars (Krizhanovsky et al., 2008).

Another mechanism in which senescence has a positive role in is wound healing. Jun and Lau (2010) investigated the cell adhesive protein CCN1/CYR61, which is expressed at sites of wound repair (Chen and Lau, 2009). CCN1 was shown to induce senescence in fibroblasts via p53 activation. The resulting senescent fibroblasts have been shown to accumulate in granulation tissues of healing cutaneous wounds in mice and secrete an anti-fibrotic SASP, in wild type mice. Demaria et al. (2014) also investigated the role of senescent cells in wound healing. The P16-3MR animal model (described in Section 1.1.7) was used to demonstrate that senescent cells promote wound healing compared with wound healing in mice where the senescent cells were removed. This protection appears to be due to the senescent endothelial and mesenchymal cells expressing platelet derived growth factor-A (PDGF-A) as part of their SASP, inducing myofibroblast differentiation at the site of injury.

Senescence and the SASP have a central role in tissue remodelling during embryogenesis of mammals, including humans (Munoz-Espin et al., 2013), chickens

(Storer et al., 2013), and quails (Nacher et al., 2006). These findings also suggest that this is a conserved feature of embryonic development across vertebrates.

Senescent cells accumulate in the tissues of aged rodents (Krishnamurthy et al., 2004), primates (Kreiling et al., 2011), and humans (Waaijer et al., 2012, Herbig and Sedivy, 2006). Work by Baker *et al* (Baker et al., 2016, Baker et al., 2004, Baker et al., 2008, Baker et al., 2013, Baker et al., 2011) has shown a causal link between the accumulation of senescent cells and ageing; whereby elimination of senescent cells delays the onset of age related phenotypes (expanded upon in Section 1.1.7.2).

Furthermore, studies show that senescent cells can induce senescence in neighbouring cells through paracrine mechanisms: (Acosta et al., 2013, Nelson et al., 2012, Faggioli et al., 2012). Acosta et al. (2008) suggests that the SASP may act in an autocrine feedback loop to reinforce growth arrest. Senescent cells secrete IL-8, which binds to IL-8 receptor β, inducing senescence in a p53 dependant manner in other cells. This SASP mediated effect on other cells has been called the bystander effect (Nelson et al., 2012).

1.1.6 A comparison of senescence across tissues

A systematic review and meta-analysis of cellular senescence across different tissues with age was performed by Tuttle et al. (2020). The authors identified 38 articles, which together described 83 associations between senescence and chronological age, with pancreas, brain and lung showing the highest correlation. Senescence in adipose, gut, prostate, and thymus tissues was not significantly correlated with age. Senescence associated DNA damage markers had the highest correlation with age, followed by cell cycle regulators, whilst proliferation markers had the lowest

correlation with age. Whilst there was a positive correlation between senescence in skin with age, there was significant heterogeneity within skin sections (dermis, epidermis, facial, and abdominal). This heterogeneity between sub-tissues was also seen in kidneys. The authors then go on to investigate the association of senescence with age where multiple senescent markers have been used in one tissue sample (Tuttle et al., 2020).

The authors go on to investigate the association of senescence markers in multiple tissue sections within a specific tissue. Overall, a positive association between senescence and age was observed, irrespective of the marker used to determine senescence. However, significant heterogeneity was observed within each tissue type, as the expression of senescent markers varied between different subtypes (Tuttle et al., 2020).

There are little data available on senescence within different organ systems from the same individual. Dock et al. (2017) investigated cellular senescence by comparing intra-individual differences in multiple parameters of human T cells in two distinct immune compartments, namely the peripheral blood and gut mucosa. To summarise, changes that occur in CD8+ T cells peripheral blood in ageing are not reflected in T cells from the gut mucosa. Studies that investigated the difference in senescence within tissues of the same organ showed that, despite higher senescence within these tissues, the degree of senescence varied based on the tissue/cell type investigated (Tuttle et al., 2020). Indeed, Chatsirisupachai and colleagues investigated the RNA-Seq-based gene expression of noncancerous tissues from humans and reported

higher and yet varying expression of senescence-associated genes in aged tissue samples (Chatsirisupachai et al., 2019).

Some of these differences may be attributed to post-mitotic tissue within the samples investigated. There has been limited interest in senescence in post-mitotic tissue. However, von Zglinicki et al. (2020) investigated indices of senescence in several different post-mitotic tissues in geriatric mice and showed that post-mitotic tissue, including skeletal muscle fibres can display evidence of senescence. The heterogeneity may also be due to the senescence markers used. Many of the studies used only a single marker to validate cellular senescence, which can cause issues as DNA damage does not always equal cellular senescence (von Zglinicki, 2002), SA-β-Gal is expressed by cells at confluence and quiescent cells, and by some differentiated cells, such as adult melanocytes (Dimri et al., 1995) and maturing tissue macrophages (Bursuker et al., 1982).

1.1.7 Animal models of senescence

1.1.7.1 Senescence Accelerated Mouse-Prone (SAMP) mice

The earliest animal models designed to investigate cellular senescence are the Senescence Accelerated Mouse (SAM) model, described in detail by Takeda et al. (1991). In 1968, several pairs of the AKR/J strain of mice were donated by the Jackson Laboratory (Bar Harbor, USA) to the Department of Pathology, Chest Disease Research Institute, Kyoto University, Japan. Whilst maintaining the strain, researchers identified accelerated onset of age-related pathologies within the population. The strain was refined to produce the first Senescence Accelerated Mouse-Prone (SAMP) mice (Takeda et al., 1981). At present, there are 12 strains of

these mice, all originated from the original strain. SAMP strains include SAMP1-3, 6-ll; and the senescence-resistant inbred strains (SAMR): SAMR1, SAMR4, and SAMR5. These mice showed accelerated onset of age-related pathologies such as loss of fur, coarse skin, lordokyphosis (a measure of sarcopenia), as well as shortened lifespans.

1.1.7.2 INK-ATTAC mice

Baker et al. (2011) designed a transgenic mouse model to examine the effect of the presence and clearance of senescent cells on tissue function. These transgenic mice were based on FAT-ATTAC (fat apoptosis through targeted activation of caspase) mice, a model where adipocytes were induced into apoptosis by administering a synthetic drug AP20187 (Pajvani et al., 2005). The drug induces dimerisation of membrane-bound myristoylated FK506-binding-protein–caspase 8 (FKBP–Casp8) fusion protein, expressed specifically in adipocytes via the Fabp4 promoter. Myristoylation is when a myristoyl group, derived from myristic acid, is covalently attached via an amide bond, to the alpha-amino group of an N-terminal glycine residue.

The FAT-ATTAC model was adapted for the $p16^{INK4A}$ gene, a common marker of senescence where it has been shown to increase in senescent cells (Section 1.1.2). The Fabp4 promoter was replaced with a 2,617-bp fragment of the $p16^{INK4A}$ gene promoter. The mice were named INK-ATTAC, after the INK4A gene.

Baker et al. (2008) investigated the accumulated of senescent cells in ageing using BubR1$^{H/H}$ mice, a mitotic checkpoint protein, a mouse model that suffers from DNA damage due to premature separation of sister chromosomes and is a model of accelerated ageing. These mice have been characterised and display phenotypes such as a shortened lifespan, lordokyphosis (abnormally excessive curvature of the spine), and sarcopenia, amongst other pathologies (Baker et al., 2004). BubR1$^{H/H}$ were bred with p16 knockout mice (p16$^{Ink4a-/-}$) to give BubR1$^{H/H}$: p16Ink4a$^{-/-}$ mice. To determine whether BubR1 may have a role in normal skeletal muscle ageing, protein levels were measured, and transcripts were quantified in the gastrocnemius of 2- and 35-month-old mice. There was an age-related decline in the expression of BubR1 in skeletal muscle, as well as an age-related increase in p16 expression. Gastrocnemius of 2- and 5-month-old BubR1$^{H/H}$ mice also had high p16 expression. Furthermore, BubR1$^{H/H}$ mice showed an increase in SASP components IGFBP2, MMP13, and Pai1. Knocking out p16 in this animal model improved fibre size in gastrocnemius, reduced the instances of lordokyphosis, and reduced the expression of SASP.

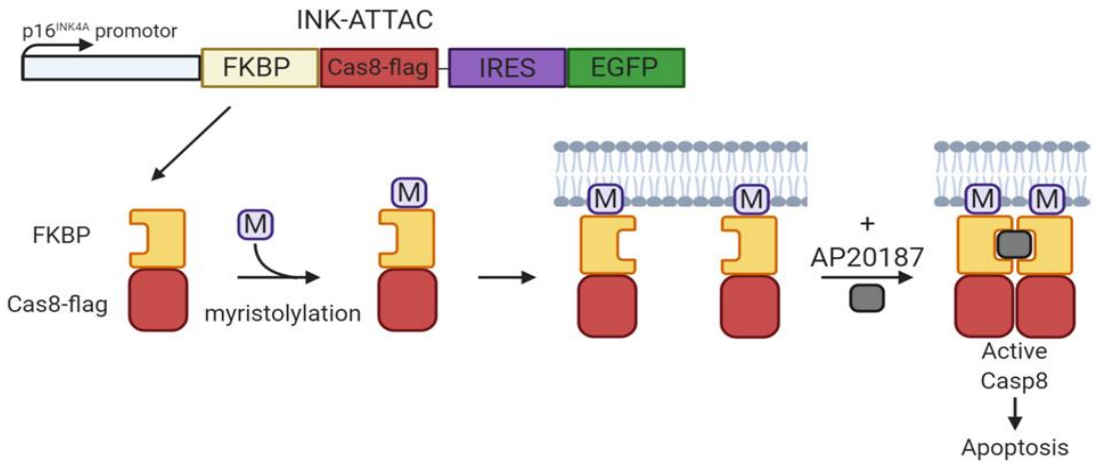

Figure 1.3 Schematic of INK-ATTAC mice transgene

Myristolyated FKBP bound Cas8 dimerise at the cell membrane in the presence of AP20187, inducing apoptosis. Adapted from Baker et al. (2011).

The INK-ATTAC mice were first used by Baker et al. (2011). The authors had crossed the INK-ATTAC model with a BubR1$^{H/H}$ progeroid strain, to investigate the role of cellular senescence in the age-related disorders linked to BubR1$^{H/H}$ progeroid syndromes. Results showed that in the BubR1$^{H/H}$ progeroid mouse background, INK-ATTAC removed p16Ink4a-positive senescent cells upon treatment with AP20187. This study demonstrated that lifelong elimination of p16 positive cells delayed the onset of age-related pathologies in adipose tissue, skeletal muscle, and eye; compared with the BubR1$^{H/H}$ mice alone.

Much of this work was undertaken in mice of or 10 months of age. Baker et al. (2016) revisited the model, using older mice between 12 and 18 months old. Furthermore, two different cohorts of INC-ATTAC mice were established and analysed. The first cohort consisted of mice of a mixed 129Sv (40% ±5%) × C57BL/6J (35% ±5%) × FVB (20% ±5%) genetic background. These mice were treated with 0.2µg/g body weight of AP20817, between 12 and 18 months; and 2.0 µg/g body weight AP20187 thereon. The second cohort was established onto a pure C57BL/6J genetic background, which received 2.0 µg/g body weight AP20187 from 12 months of age until end of life. Both groups received the appropriate vehicle controls.

1.1.7.3 P16-3MR

Another mouse model used to investigate cellular senescence is the p16-3MR model. This animal model was first presented by Demaria et al. (2014). To identify, isolate, and selectively kill senescent cells, the 3MR (trimodality reporter) fusion protein, which contains functional domains of a synthetic Renillaluciferase (LUC), monomeric red fluorescent protein (mRFP) and truncated herpes simplex virus 1 (HSV-1) thymidine kinase (HSV-TK) (Ray et al., 2004) were used. The LUC allows the detection of cells via luminescence. The mRFP further permits sorting of these positive cells from other tissues. Finally, HSV-TK allows selective elimination of p16 expressing cells by ganciclovir (GCV), a nucleoside analogue. GCV has a high affinity for HSV-TK but low affinity for the cellular thymidine kinase. HSV-TK converts GCV into a toxic DNA chain terminator; in non-dividing senescent cells, GCV causes fragmentation of mitochondrial DNA, with subsequent death by apoptosis (Laberge et al., 2013).

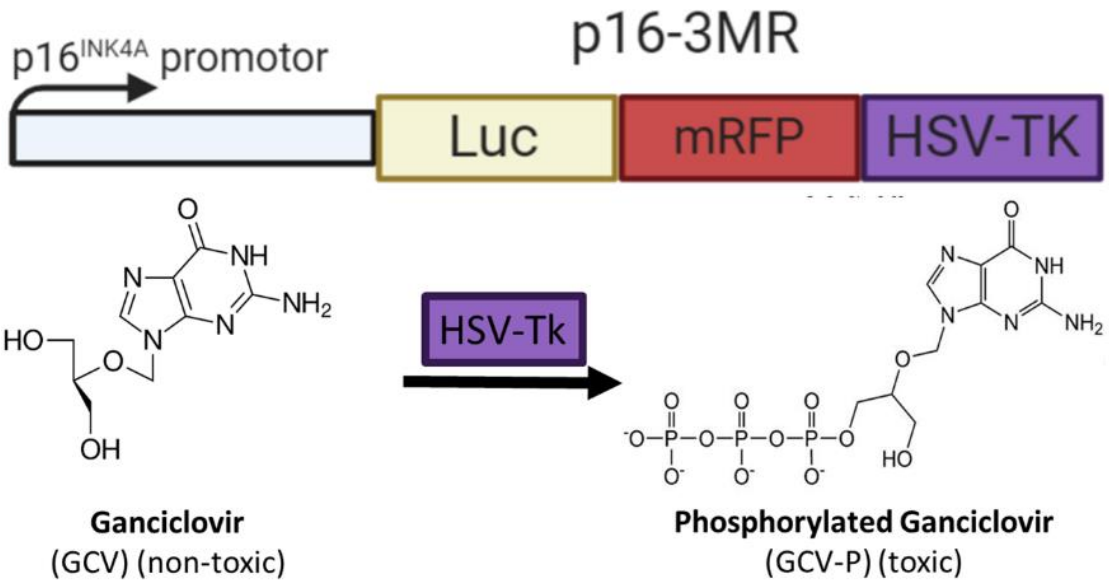

Figure 1.4 Schematic of the p16-3MR transgene.

P16 expressing cells express a fluorescent mRFP, as we all HSV-Tk which phosphorylates GCV to GCV-P inducing apoptosis. Adapted from Demaria *et al.* (2014).

Much of the work conducted using these mice focused on senescent fibroblasts and endothelial cells in response to cutaneous wounds. At the site of injury, senescent cells accelerate wound closure inducing myofibroblast differentiation through the secretion of platelet-derived growth factor AA (PDGF-AA). Elimination of senescent cells resulted in poor wound healing, compared with control mice. The work presented is novel as it is demonstrating a beneficial role of the SASP in tissue repair and adding an evolutionary context to the SASP.

Whilst transgenic animal models provide a powerful tool to investigate the roles of cellular senescence, genetic modifications of humans would not be equally possible. Therefore, a more pharmacological approach would be more appropriate in the development of interventions to remove senescent cells.

1.1.8 Senolytics

Senolytics (from the words "senescence" and "lytic" – destroying) are small molecule compounds that selectively induce the death of, or clearance of senescent cells. The aim of senolytics are to reverse the negative phenotype caused by the presence of senescent cells. Senescent cells accumulate with ageing, and have been linked with the ability to compromise the structure and function of tissue and their microenvironments (Herbig et al., 2006, Krishnamurthy et al., 2004, van Deursen, 2014, Waaijer et al., 2012). In part, this is due to the previously described senescent associated secretory phenotype (SASP), which includes cytokines, chemokines, and matrix remodelling proteins (Section 1.1.5). Several reviews have highlighted the potential role of senescent cells and the SASP in ageing-related conditions (LeBrasseur et al., 2015, Munoz-Espin and Serrano, 2014). Furthermore, studies that

have removed senescent cells via drug-inducible 'suicide' genes (i.e. INK-ATTAC (Section 1.1.7.2), P16-3MR (Section 2.1.2)) showed enhanced health span, and delays in the development in multiple age-related phenotypes in genetically modified progeroid mice (Baker et al., 2011).

Thus, pharmacological interventions that target senescent cells and/or the SASP may potentially ameliorate age-related chronic diseases and disabilities, and even extend health span. Zhu et al. (2016) used a bioinformatics-based approach to identify potent senolytic agents that would induce apoptosis preferentially in senescent cells without damaging proliferating, quiescent, or differentiated cells throughout the body. From this approach, two compounds were selected as candidate senolytics, and were tested *in vivo*: Dasatinib and Quercetin.

Dasatinib, also named Sprycel, is an oral chemotherapy medication used to treat chronic myelogenous leukaemia (CML), and acute lymphoblastic leukaemia (Talpaz et al., 2006). Dasatinib is an inhibitor of multiple tyrosine kinases and platelet-derived growth factor (PDGFR)-β. Dasatinib can have side effects, occasionally including pulmonary oedema, which can occur after months of daily administration (Montani et al., 2012).

Quercetin, a plant flavonol from the flavonoid group of polyphenols can be found in appreciable amounts in organic produce such as fruits, vegetables, leaves, grains, red onions, and kale. Quercetin is used as an ingredient in dietary supplements, beverages, and foods. Quercetin has been reported to be an antioxidant (Williams et al., 2004, Russo et al., 2014).

1.1.8.1 Polyphenols *in vivo*

Dasatinib and quercetin both have short elimination half-lives (Christopher et al., 2008, Graefe et al., 2001), supporting the possibility that their beneficial effects on late-life function and survival are at least partially due to a mechanism that persists long after the drugs are no longer present, such as senescent cell elimination

Xu et al. (2018) transplanted senescent cells into mice and demonstrated that the presence of small number of senescent cells were sufficient to cause persistent physical dysfunction and reduced survival. Furthermore, treatment of these mice and old mice (24- to 27-month-old) with dasatinib (5 mg/kg) and quercetin (50 mg/kg) via oral gavage alleviated physical dysfunction and increased survival in both models.

Ogrodnik et al. (2017) investigated the use of dasatinib and quercetin in INK-ATTAC transgenic mice. AP20187 (10 mg/kg) was administered to 24-month-old mice by intraperitoneal injection every 3 days, for 3 months. For senolytic treatment, dasatinib (5 mg kg 1) and quercetin (10 mg/kg) in combination were administered by oral gavage once per month for 3 months. The elimination of senescent cells by suicide gene-meditated ablation of p16Ink4a-expressing senescent cells in INK-ATTAC mice or by treatment with a combination of the senolytic drugs dasatinib and quercetin reduced overall hepatic steatosis.

Schafer et al. (2017) treated mice with dasatinib plus quercetin to prevent pulmonary disease by potentially clearing senescent cells. The secretome of senescent fibroblasts, which are selectively killed by a senolytic cocktail, dasatinib plus quercetin, is fibrogenic. Thus, these findings establish that fibrotic lung

disease is mediated, in part, by senescent cells, which can be targeted by senolytics to improve health and function.

Roos et al. (2016) treated 24-month-old mice with dasatinib plus quercetin to reduce senescent cell burden and improve vascular function in old mice. C57BL/6J mice were treated with dasatinib and quercetin once per month from 24-27 months of age. This was the first study to demonstrate that chronic clearance of senescent cells improved established vascular phenotypes associated with ageing and chronic hypercholesterolemia and may be a viable therapeutic intervention to reduce morbidity and mortality from cardiovascular diseases related to ageing.

1.1.8.2 Other Senolytics

The earliest, commonly accepted definition of polyphenols, the White–Bate-Smith–Swain–Haslam (WBSSH) definition (Haslam and Cai, 1994) describes polyphenols as water soluble compounds, molecular weight of 500–4000 Da with >12 phenolic hydroxyl groups, and 5–7 aromatic rings per 1000 Da.

Several hundred different polyphenols are found in plant-based foods including vegetables (particularly, broccoli, onion and cabbage), fruits (grapes, pears, apples, cherries. and various berries contain up to 200–300 mg polyphenols per 100 g fresh weight), legumes (soybean), cereals, plant-derived beverages and chocolate (extensively reviewed by Tressera-Rimbau et al. (2017)).

The majority of polyphenols are not absorbed in their native form, but are instead metabolised by intestinal enzymes and/or colonic microflora (Scalbert et al., 2002). These metabolites are further modified to allow entry into the blood and tissues.

Thus the state of the polyphenols that are present in food are often very different to the ones that reach the blood and tissues (Scalbert et al., 2002).

Current research on polyphenols in health and disease has focused on their role as therapeutics, due to their antioxidant and anti-inflammatory properties (Hussain et al., 2016) and this has been extensively reviewed (Serino and Salazar, 2018). The consensus appears to be that improved cardiovascular disease (CVD) outcomes are seen in humans with increased dietary polyphenol consumption.

Fisetin (7, 3', 4'-flavon-3-ol) is a plant-based polyphenol from the flavonoid group. Fisetin can be found in a wide variety of plants, examples of which includes fruits and vegetables such as strawberries, apples, and grapes (Arai et al., 2000).

The role of fisetin as a senolytic is unclear but a study by Yousefzadeh et al. (2018) used fisetin in mice as a senolytic. These authors reported an increase in lifespan, reduction of senescence cell markers as well as reduction of age-related pathologies. The effect appears to be derived from the ability of fisetin to block the PI3K/AKT/mTOR pathway (Syed et al., 2013) (See Section 1.1.8.3), as well as the ability to interfere with cell cycle progression (Gupta et al., 2014). In contrast, fisetin, as well as some other flavonoids, have been described as topoisomerase inhibitors, which may cause DNA damage and carcinogenic effects. Furthermore, whilst fisetin may be safe, metabolites generated from it may have harmful side effects and caution should therefore be used (Kroon et al., 2004).

Fisetin is a sirtuin activating compound, like many other polyphenols. Sirtuins are a heavily conserved class of proteins with deacetylase activity. There are 7 sirtuins in mammals, in 4 different classes: SIRT1-3 are in class I, SIRT4 in class II, SIRT5 in class

III, and SIRT6-7 in class IV (O'Callaghan and Vassilopoulos, 2017). Sirtuins can also be categorized by which subcellular compartment they reside in, SIRT1, 6, and 7 in the nucleus, SIRT3, 4, and 5 in the mitochondria, and SIRT2 is predominately in the cytoplasm (O'Callaghan and Vassilopoulos, 2017). Sirtuins have been shown to extend the life span of simple organisms like yeast, worms and flies (Baur, 2010, O'Callaghan and Vassilopoulos, 2017). However, the efficacy of sirtuins are still being elucidated (Aunan et al., 2016).

1.1.8.3 mTOR signalling

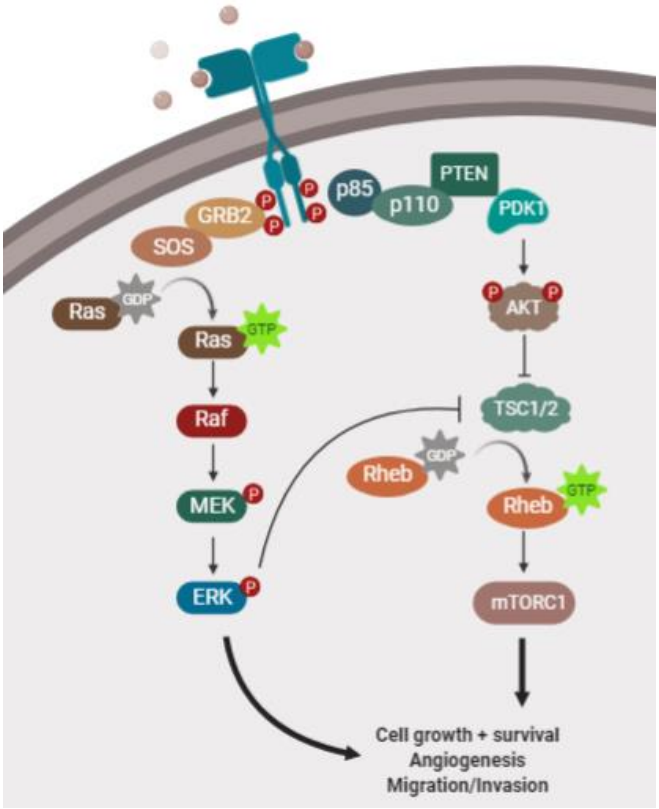

Figure 1.5 The MAPK/ERK and mTOR signalling pathways

The MAPK/ERK pathway (also known as the Ras-Raf-MEK-ERK pathway) communicates mitogen binding to receptors on the cell membrane. These signals are passed along a chain of proteins to elicit cellular effects.

In brief, the binding of mitogen to receptors allows for the GTPase, Ras, to replace GDP with GTP; allowing Ras to activate Raf (MAP kinase kinase kinase, MAP3K, or MEKK). Raf in turn activates Mitogen-activated protein kinase kinase (MAP2K, MEK, MAPKK) which in turn activates mitogen-activated protein kinase (MAPK, MAP kinase). MAPK, originally

called ERK (extracellular regulated kinases), can activate transcription factors, compounding the signalling cascade.

An interesting downstream target of the MAPK/ERK pathway is mTORC1. ERK1 and ERK2 phosphorylate TSC2, inhibiting the GTPase activating protein (GAP) activity of TSC1–TSC2 towards Ras homologue enriched in brain (Rheb) (Ma et al., 2005). Rheb-GTP directly interacts with mTORC1 and strongly stimulates its kinase activity, whereas Rheb-GDP little activity (Long et al., 2005).

The mTOR signalling pathway is a powerful target to modulate ageing and lifespan; as shown by studies in yeast (Kaeberlein et al., 2005), worms (Vellai et al., 2003), flies (Bjedov et al., 2010), and mice (Harrison et al., 2009). In skeletal muscle, mTOR signalling pathways play a key role in cellular growth (Deldicque et al., 2005). Chronic inflammation, as seen with inflammaging and sepsis, has been shown to decrease activation of the mTORC1 signalling pathway, resulting in reduced muscle mass (Frost and Lang, 2011).

Castilho et al. (2009) demonstrated that chronic expression of Wnt1 protein in the epidermis of FVB/N mice results in chronic mTOR signalling and lead to excessive proliferation of epithelial stem cells. This hyper-proliferation led the stem cell to become senescent, expressing SA-β-Gal and p21, and further diminished the stem cell niche. This phenotype could be rescued via inhibition of mTOR signalling pathways.

Chen et al. (2009) constitutively activating of mTORC1, in haematopoietic stem cells (HSC) of mice resulted in the HSCs becoming senescent, expressing p16 and p21. Furthermore, inhibition of mTOR with rapamycin also reversed the age-associated

loss of HSC function, enhancing the immune response of old mice and preserving the pool of HSCs to levels comparable of young mice.

The mTOR signalling pathway promotes the pro-inflammatory phenotype of senescent cells. Laberge et al. (2015) demonstrated that administering rapamycin to senescent fibroblasts suppressed the secretion of inflammatory cytokines as part of the SASP. Rapamycin reduced the mRNA levels of IL-6 and other cytokines and suppressed translation of the membrane-bound cytokine IL-1a. Reduced IL-1a in turn diminished NF-κB transcriptional activity, which controls much of the SASP.

1.1.9 A comparison of senescence in mouse and human cells

Dimri et al. (1995) identified that human fibroblasts have a limited lifespan in culture, and enter terminal growth arrest after 50–80 population doublings. Soon after the limited lifespan of human cells was discovered, a similar phenomenon was described in mouse fibroblasts (Todaro and Green, 1963). One difference between mouse and human cells is that human cells never spontaneously immortalise in culture, whereas murine cells do. Furthermore, the replicative lifespan of murine cells is much lower than that of humans. These differences may be attributed to telomeres (Gorbunova and Seluanov, 2010). A telomere is a region of repeated nucleotide sequences at each end of a chromosome, which protects the end of the chromosome from deterioration, or from fusion with other neighbouring chromosomes (Jiang et al., 2018). Normal human somatic cells (except stem cells), have no detectable telomerase activity, and their telomeres shorten with every division (Harley et al., 1990). In prolonged culture, the telomeres of human fibroblasts reach a critical length and lose protective protein structures. The attrition of telomeres ultimately activates

the DNA-damage response (DDR), resulting in senescence (von Zglinicki, 2002). Human telomeres are on average 8–15 kb long, whilst murine telomeres are much longer, although this varies significantly between rodent species. Indeed, common inbred mouse strains have telomeres of 150 kb, whilst wild mice have shorter 30 kb telomeres (Kipling and Cooke, 1990). Furthermore, telomerase is expressed in multiple tissues of adult mice, and in cultured mouse fibroblasts (Prowse and Greider, 1995). These data suggest that the lower replicative lifespan of murine cells when compared with humans is independent of telomere length and telomerase activity (Gorbunova and Seluanov, 2010).

The reason behind this difference was investigated by Judith Campisi, who demonstrated that mouse fibroblasts do not senesce when cultured in 3% oxygen (Parrinello et al., 2003). Under physiological oxygen concentration, mouse cells proliferate indefinitely, similar to immortalized human cells. Thus, senescence of mouse cells is caused by oxidative stress (Gorbunova and Seluanov, 2010). Indeed, replicative senescent murine fibroblasts under standard culture conditions (20% oxygen), do not express a human-like SASP, and differ from similarly cultured human cells in other respects. However, when cultured in physiological (3%) oxygen and induced to senesce by radiation, mouse cells more closely resemble human cells, including expression of a robust SASP (Coppe et al., 2010b).

Cellular signalling may also be different between murine and human cells. As described in Section 1.1.3.3, senescence is typically activated in a p53 → p21 → pRb dependant manner (Gorbunova and Seluanov, 2010). The majority of mouse fibroblasts that spontaneously escape senescence carry a mutated p53, combined

with data from embryonic fibroblasts lacking p21 undergo senescence normally (Pantoja and Serrano, 1999) suggest that murine cells have different signalling pathways for cellular senescence than humans (Gorbunova and Seluanov, 2010).

1.1.10 Summary

In summary, senescence is proposed to play a major role in the development of age-related pathologies and there is a potential for intervention in this process with senolytics. There is limited data examining the role of senescence in the determination of terminally differentiated tissues such as skeletal muscle.

1.2 Introduction to skeletal muscle

Skeletal muscle is one of three major muscle types within the human body, the others being cardiac muscle and smooth muscle. Skeletal muscle plays a significant role in maintaining posture, motility, and thermoregulation; and can act as a storage for amino acids and carbohydrates (Wolfe, 2006). Skeletal muscle accounts for 40% of total body weight, and 50-75% of total body protein (Frontera and Ochala, 2015).

1.2.1 Skeletal muscle structure and function

The structural design of skeletal muscle is characterised by a logical, hierarchal arrangement of multinucleated, post-mitotic muscle fibres (also referred to as

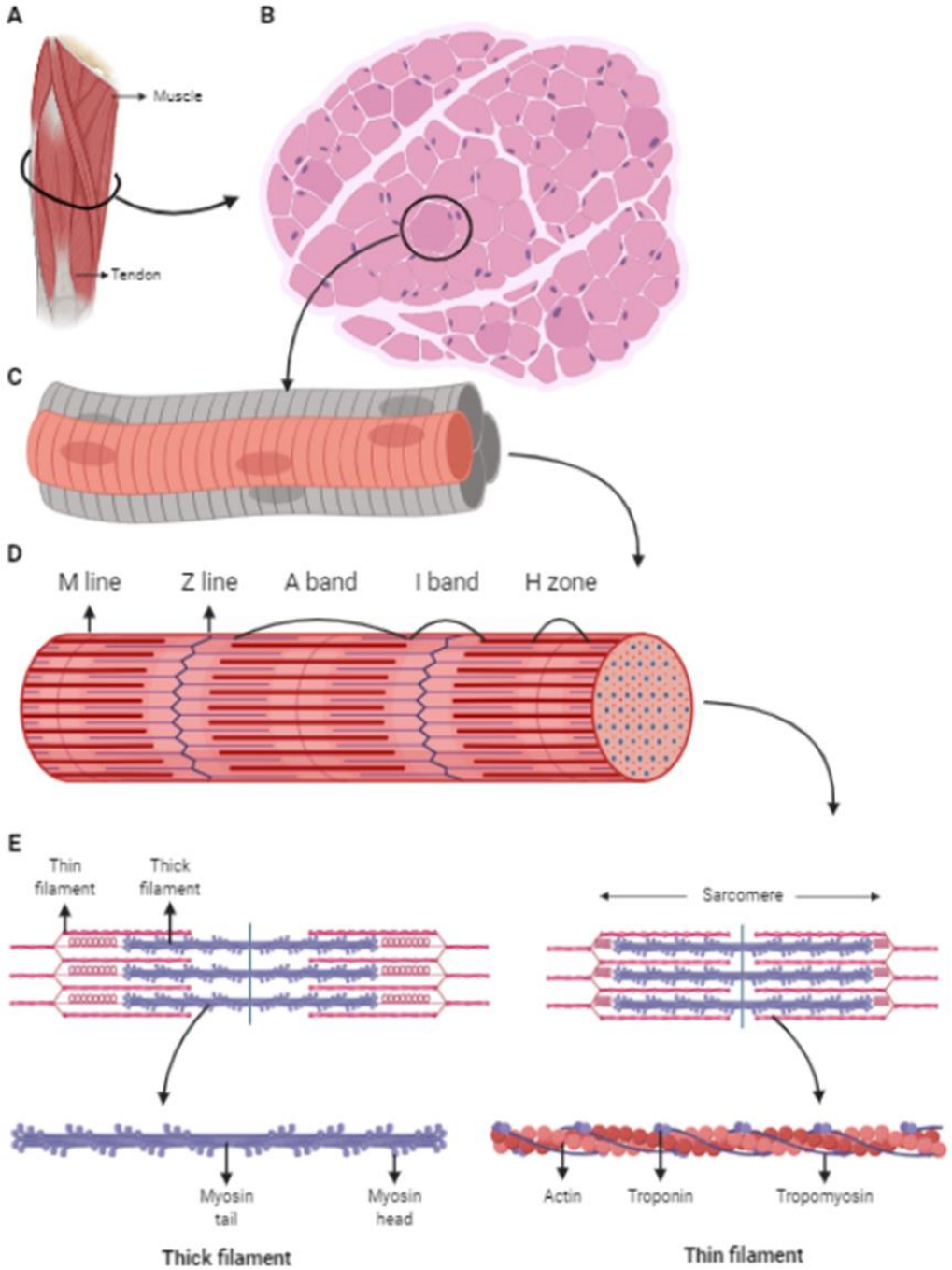

Figure 1.6 Structure of skeletal muscle

The relationship of a whole muscle to a single muscle fibre (A-C). The features of a single myofibril (D). Cytoskeletal components of a myofibril (E). Adapted from (Frontera and Ochala 2015).

myofibres or muscle cells), connective tissue and other cell types (Frontera and Ochala, 2015) (Figure 1.6).

Skeletal muscle is comprised of bundles of muscle fibres surrounded by connective tissue layers called fasciae. Fibres can encompass the entire length of the muscle and are approximately 10-100 µm in diameter. Muscle fibres are formed from the fusion of multiple myoblasts via myogenesis, resulting in a single post-mitotic, multinuclear muscle cell (Figure 1.6C). The force the whole muscle can generate is determined by number of parallel myofibres within these fascicles and the quality of the fascicles. The number of these myofibres in a muscle is determined at birth and little change occurs during life span (Alnaqeeb and Goldspink, 1987, Klein et al., 2003). However, the cross-sectional area of a muscle fibre is very plastic, capable of change throughout life in response to hypertrophy and atrophy (Maughan et al., 1984, Berg et al., 1991). Myofibres are comprised of numerous filaments called myofibrils.

Skeletal muscle has a striated appearance created by overlapping region of thick myosin and thin actin filaments termed the sarcomere (Figure 1.6E). This filament patterning repeats the length of the muscle fibre. As illustrated, a single sarcomere is made up of dark A bands and light I bands. Thin filaments of actin make up the light I bands, whilst the H zones are comprised of myosin. The two sections cross in the A band to create a dark overlap. The A band is separated by a dark line known as the M line, and it is this distance between two Z discs that is known as a sarcomere (Figure 1.6D). Other molecules that play a role in muscle architecture are titin and nebulin. Molecules of titin extend from the Z disc to the M line and act as springs to keep

myosin filaments centred in the sarcomere. Molecules of nebulin extend from the Z disc and are thought to determine the length of associated actin filaments.

1.2.2 Sliding filament theory of muscle contraction

First proposed by Huxley in 1954 (Huxley and Hanson, 1954) and verified in 1957 (Huxley, 1957), the basic mechanism of skeletal muscle contraction is known as the "sliding filament hypothesis" (Figure 1.7) and has been adapted several times.

Skeletal muscle contraction is reliant on nervous input, whereby an action potential arrives at the neuromuscular junction, releasing the neurotransmitter acetylcholine (Ach). Ach causes the depolarisation of the motor end plate, which travels throughout the muscle by the transverse tubules (T-tubules), resulting in the release of calcium (Ca^{2+}) from the sarcoplasmic reticulum (Ashley and Ridgway, 1968). At rest, actin and

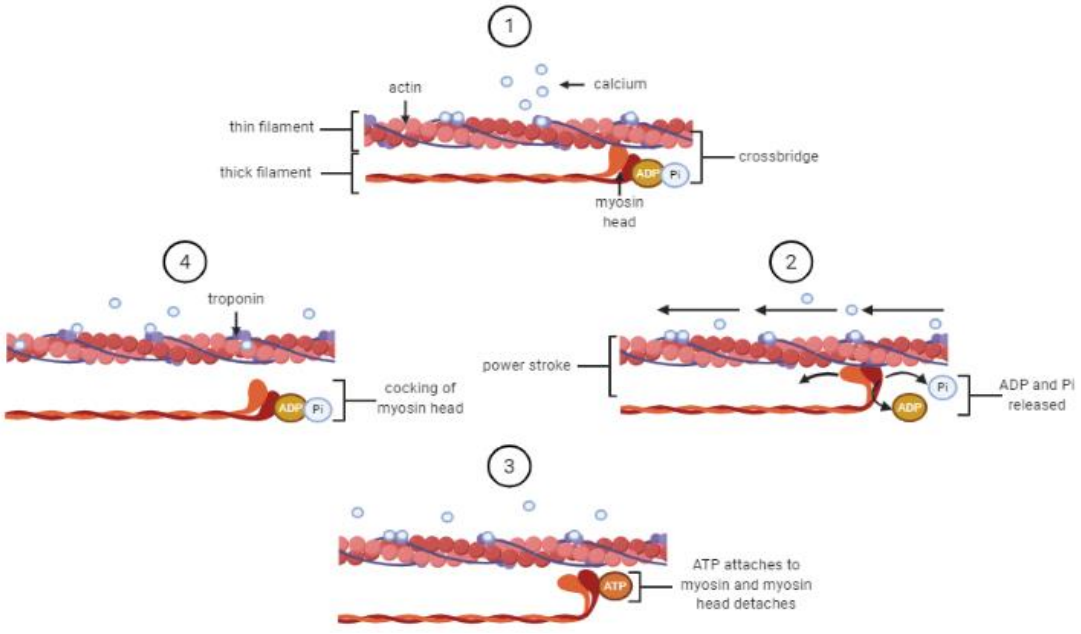

Figure 1.7 Skeletal muscle contraction.

Simplified diagram of the ATP fuelled power stroke of the myosin-actin cross bridge. Ca^{2+} binds to troponin, exposing the acting active site (1). Myosin binds to actin, forming a cross bridge (2). ADP and Pi are released as part of the power stroke (3). ATP binds myosin, uncoupling the cross bridge (4). Adapted from (Frontera and Ochala 2015).

myosin are not cross-linked due to the presence of the troponin-tropomyosin complex. Tropomyosin occupies the niche in the actin filament which contains the myosin binding region (Parry and Squire, 1973). At high concentrations, Ca^{2+} binds to troponin, changing conformational shape; moving tropomyosin from the binding site of actin (Lehman et al., 1994). Myosin filaments can now attach to the actin, forming a cross-bridge. The detailed structure of the myosin head was only described for the first time in 1993 (Rayment et al., 1993) and has further contributed to our understanding of this process (Frontera and Ochala, 2015).

The hydrolysis of ATP into ADP and inorganic phosphate (Pi) releases energy, which enables the myosin to pull the actin filaments inwards and so shortening the muscle. Hydrolysis of ATP strengthens the cross-link between actin and myosin, and this ATPase activity of myosin dictates the speed of the power stroke (Barany, 1967). This occurs along the entire length of every myofibril in the muscle cell. When an ATP molecule binds to the myosin head, the myosin detaches from the actin and the cross-bridge is broken. When the ATP is then hydrolysed, the myosin head can again bind further along the actin filament and repeat the power stroke. This repeated pulling of the actin over the myosin is often known as the ratchet mechanism.

Muscular contraction can last for as long as there is ATP and free Ca^{2+}. Once the impulse stops, the Ca^{2+} is pumped back to the sarcoplasmic reticulum and the actin returns to its resting position causing the muscle to relax. A single power stroke results in only a shortening of approximately 10nm (Spudich, 2001).

1.2.3 Skeletal muscle fibre types

Skeletal muscle can be divided into two types: type I and type II. Fibre types are identified by different isoforms of myosin heavy chain (MHC). MHCs are generally classified into groups: MHC I, MHC IIa, and MHC IIx; due to different isoforms of myosin ATPases: I, IIa and IIx (Brooke and Kaiser, 1970).

Type I fibres are also known as slow twitch fibres. Type I fibres have a red colouring due to large volumes of intracellular myoglobin (Jansson and Sylven, 1983), high density capillary networks (Duey et al., 1997), and high numbers of mitochondria (Ingjer, 1979), compared with type IIB fibres. The energy type I fibres use primarily comes from the oxidative phosphorylation of triglycerides. The amount of ATP these fibres produce give them a high resistance to fatigue, thus making them capable of producing contractions for a long period under aerobic conditions. Type I fibres are typically weaker, producing less force than type 2 fibres (Bottinelli et al., 1996).

Type IIA fibres, also known as fast-twitch oxidative fibres, are usually classified as intermediate fibres. These fibres contain moderate levels of mitochondria, capillaries, and myoglobin when compared with type I and type IIB fibres (Ingjer, 1979, Jansson and Sylven, 1983). Type IIA fibres also make use of glycolysis, oxidative phosphorylation of glycogen, and creatine phosphate as sources of energy. These fibres are used during long-term, anaerobic exercise, and are moderately resistant to fatigue.

Type IIB fibres are known as fast-twitch, glycolytic fibres. Type IIB fibres are generally whiter in colour as they have lower levels of mitochondria, myoglobin, and a less dense capillary network than type I fibres (Ingjer, 1979). Type IIB utilise the glycolysis

of ATP and creatine phosphate for energy. Type IIB fibres are used for short anaerobic exercises that require rapid high forces, and quickly become fatigued; an example of which would be a short distance sprint.

A third type of fast-twitch fibre has also been identified, type IIX. Type IIX fibres have a phenotype and display physical properties in between that of types IIA and B (Schiaffino and Reggiani, 2011).

In humans, the majority of muscles contain type I and type IIA/B/X fibres (Edgerton et al., 1975). These fibre types exist in a spectrum, from purely of one type to a hybrid composition, according to the scheme: I ↔ I/IIA ↔ IIA ↔ IIA/IIX ↔ IIX ↔ IIX/IIB ↔ IIB (Schiaffino and Reggiani, 2011). The proportion of each fibre type can change following exercise (Simoneau et al., 1985). Human single fibres and single myosin molecules force generation have been measured *in vitro* and these studies show that type I myosin (slow) produce less force than type II myosin (fast) (Frontera et al., 2000, Li and Larsson, 2010). However, no differences among sub-types of fast myosin (IIA, IIB, or IIX) were reported (Frontera et al., 2000, Li and Larsson, 2010).

1.2.4 Sarcopenia – loss of muscle mass and function with ageing

The term 'sarcopenia' is derived from the Greek phrase "poverty of flesh" and was first used over 25 years ago (Evans and Campbell, 1993) and has been shown to occur in human (Sousa-Victor et al., 2014) and animal models (Lushaj et al., 2008).

The definition of sarcopenia has since been revised repeatedly. The European Working Group on Sarcopenia in Older People (EWGSOP) (Cruz-Jentoft et al., 2010), the European Society for Clinical Nutrition and Metabolism Special Interest Groups (ESPEN-SIG) (Muscaritoli et al., 2010), the International Working Group on Sarcopenia

(IWGS) (Fielding et al., 2011), the Asian Working Group for Sarcopenia (AWGS) (Chen et al., 2014), and the Foundation for the National Institutes of Health (FNIH) Sarcopenia Project (Studenski et al., 2014) have all published evolving definitions of sarcopenia, based on robust studies in humans. It was only recently that sarcopenia received a clinical definition, consensus diagnostic criteria, International Classification of Diseases 10th Revision (ICD-10) codes or treatment guidelines (Falcon and Harris-Love, 2017). Sarcopenia can be described as an age-related loss of skeletal muscle that may result in diminished muscle strength and functional performance (Falcon and Harris-Love, 2017).

Sarcopenia affects humans from approximately the 4th decade of life (Lexell et al., 1988), with a decrease of 30-50% in skeletal muscle mass and function by approximately 80 years of age (Akima et al., 2001). More recent studies have shown that after the age of 30, about 0.5–1% of skeletal muscle mass is lost per year, with the rate of loss accelerating after the age of 65 (Kyle et al., 2001, Melton et al., 2006). On average, 5–13% of individuals aged over 60 have low skeletal muscle mass, with the prevalence increasing to as high as 50% in those over of 80 (Morley et al., 2014).

Rodents are commonly used as models of human muscle ageing and C57Bl6 mice are the most widely used strain as models of human ageing. The core changes that regulate muscle ageing in humans have been observed in rodents, indicating that mice and rats are model organisms to study human sarcopenia (Demontis et al., 2013). Advantages of using rodent models for investigation of human ageing includes: a mammalian system with a relatively short life span, large cohorts of offspring, and ability for genetic manipulation.

Ageing humans show loss of muscle fibres and rats and mice also show reduced muscle fibres with ageing, particularly in the hind limb muscles (McArdle et al., 2004, Brooks and Faulkner, 1991, Brooks and Faulkner, 1988). The maximum isometric force decreases more than muscle mass during ageing in mice in a similar manner to humans, even when expressed relative to the cross-sectional area of the muscle (Faulkner et al., 1995, Gonzalez and Delbono, 2001). Thus, the age-related loss of muscle strength cannot be solely explained by the loss of muscle mass: both muscle 'quantity' and 'quality' decline in aged animals (Demontis et al., 2013). Studies from our group, colleagues, and the community have shown that the time course and characteristics of contraction-induced muscle injury and recovery are similar for mice (Faulkner et al., 1989, Faulkner et al., 1995), rats (Macpherson et al., 1997, Van Der Meulen et al., 1997), and humans (Faulkner et al., 1993).

1.2.4.1 Mechanisms responsible for the development of sarcopenia

Sarcopenia presents as a reduced muscle mass and function. This may be attributed in part to a decrease in fibre number, with a decreased muscle cross-sectional area, atrophy of the remaining fibres, and poor regeneration following damage (Lexell et al., 1988, Brooks and Faulkner, 1990). There is also evidence for a change in the ratio of type II (fast) fibres to type I (slow) fibres since type II fibres have been shown to be more susceptible than type I fibres to sarcopenia, resulting in a further reduction in maximal force (Larsson et al., 1978, Lexell et al., 1988). However, there are some conflicting studies that provide evidence of no difference in the percentage of type I and type II fibres with age (Lexell et al., 1988). The functional capacity (i.e. strength and power) of skeletal muscle decreases with increasing age to a greater degree than muscle mass itself (Newman et al., 2003).

By the age of 70, the muscle fibre cross-sectional area (CSA) of skeletal muscle is reduced by approximately 30% (Porter et al., 1995). This loss of CSA is accompanied by loss in absolute force generation (Grimby and Saltin, 1983) as well as a decrease in specific force (normalized by CSA) of the remaining muscle (Morse et al., 2005).

One mechanism which may contribute to the development of sarcopenia is the loss of motor units which innervate the muscle (Jackson, 2020). Motor units suffer damage and are subject to turnover, whereby new motor units and terminal axons sprout and regrow to re-innervate the muscle (Delbono, 2003). However, the re-innervation of neuromuscular junctions does not occur as effectively in ageing, resulting in a loss of NMJs in old humans and mice (Larsson and Ansved, 1995). Indeed, A 25–50% reduction in the number of motor neurons occurs in both humans (Tomlinson and Irving, 1977) and mice (Rowan et al., 2012) with ageing. Our group has sought to elucidate the role of denervation in ageing in the development of sarcopenia and frailty (Jackson, 2020).

The mechanisms underlying the development of sarcopenia are not completely understood. It is likely that sarcopenia is a multi-factorial disease with a network of interacting, dysfunctional systems. However, there are several proposed processes:

1.2.4.2 Satellite cells and sarcopenia

Satellite cells are stem cells present in muscle, found between the cell membrane and basal lamina, and are necessary for skeletal muscles to regenerate, especially following injury (Shafiq and Gorycki, 1965). Satellite cells are usually in a quiescent state and are activated during myogenesis and muscle regeneration. The activated satellite cells can then proliferate and either: differentiate to repair damage or self-

renew to maintain the pool of satellite cells. The number of satellite cells has been shown to decline with increasing age (Day et al., 2010). The loss of satellite cells with age may occur in a fibre type specific manner. Verdijk et al. (2014) showed that in humans, type II muscle fibre size was substantially smaller with increasing age in adults and this was accompanied by an age-related reduction in type II muscle fibre satellite cell content. The decrease in number of satellite cells is a potential contributor to the detrimental phenotype of ageing muscle. McKay et al. (2013) showed that satellite cell activation in response to muscle damage was blunted in older adult men and that this was mediated by interleukin-6 (IL-6). Indeed, increased inflammation is chronically evident in the muscles of aged individuals (Vasilaki et al., 2006, Vasilaki et al., 2003).

The decline of the ability of satellite cells to divide following damage may play a role in sarcopenia. However, research by Carlson and Faulkner (1989) showed that the environment of the muscle during regeneration is crucial to successful regeneration. Thus, muscle from a two year old rat was repaired faster and better when grafted into two to three month old rats (Carlson and Faulkner, 1989).

The decline in satellite cell function and so regeneration in an “old” environment may be due to inflammaging and the presence of SASP (Franceschi and Campisi, 2014). Increased TGF-β levels in old individuals have been suggested to have a negative impact on satellite cell function via Wnt signalling pathways, promoting a pro-fibrotic phenotype of satellite cells (Brack et al., 2007). Studies have shown that elevated levels of inflammatory cytokines regulate satellite cell function via the JAK/STAT3 pathway, and inhibition of the JAK/STAT3 pathway improved satellite cell function

(Price et al., 2014, Tierney et al., 2014). The JAK/STAT pathway is also involved in cytokine production, whereby JAK inhibitors decreased cytokine production in senescent preadipocytes (Xu et al., 2015b). Increased p38α/βMAPK signalling has also been shown to be involved in the age-related decline in satellite cell function and proliferative capacity, and the inhibition of the p38α/βMAPK pathway rescued the self-renewal capacity of satellite cells in old age (Bernet et al., 2014, Cosgrove et al., 2014).

A landmark study using the transgenic AMPKγ_3 KO mouse model with inducible depletion of satellite cells showed no effect on muscle fibre size, number, specific force, or myonuclear number between control old mice and old mice with genetically induced satellite cell depletion (Canto et al., 2010). On the other hand, the skeletal muscles of mice depleted of satellite cells showed significantly increased accumulation of collagen and fibrosis associated with ageing, suggesting that the ageing-associated loss of satellite cells contributes to muscle fibrosis in ageing but not to sarcopenia (Section 1.2.4.4) (Canto et al., 2010).

1.2.4.3 Protein turnover and sarcopenia

Protein degradation and synthesis, and the balance between the two play a key role in the homeostasis of skeletal muscle. Studies have investigated protein synthesis and degradation rates in muscles in ageing. Some studies have showed an overall decreased rate of protein synthesis in the muscles of old humans compared with adults (Hasten et al., 2000); with decreased rates of synthesis of individual muscle proteins such as myosin heavy chain proteins (Balagopal et al., 1997). However, studies have shown some conflicting results. Some studies have shown no difference

in protein synthesis rates in muscles of old humans compared with adults (Volpi et al., 2001, Wall et al., 2015).

The ubiquitin-proteasome system (UPS) is a crucial protein degradation system in eukaryotes (Bilodeau et al., 2016). Ubiquitination is a post-translational modification to protein that targets them for proteasomes, which are protein complexes that degrade unneeded or damaged proteins by proteolysis via proteases (Bilodeau et al., 2016). Conflicting evidence exists on the UPS in skeletal muscle, whereby proteasome activity was found decreased (Baehr et al., 2016), unchanged (Bossola et al., 2008), or increased (Altun et al., 2010) in aged rats.

A key enzyme in the UPS system is E3 (ubiquitin ligase), which adds activated ubiquitin to lysine residues on the protein substrate, targeting the proteome for the UPS system. Two inducible E3 ubiquitin ligases have been identified, atrogin-1 (also known as MAFbx), and muscle RING finger protein 1 (MuRF1), both of which have been shown to be responsible for the degradation of the bulk of skeletal muscle protein in various conditions (Gomes et al., 2001, Bodine et al., 2001).

There are increased levels of circulating inflammatory cytokines in old mice, which may stem from the SASP (Campisi and d'Adda di Fagagna, 2007). The SASP induces an unfolded protein response (UPR) in the endoplasmic reticulum in senescent fibroblasts, due to an accumulation of unfolded or damaged proteins (Soto-Gamez et al., 2019). This results in impairment of cell function and autophagy, or the potential to induce senescence within the other stressed cell (Soto-Gamez et al., 2019) and is potential contributor to the loss of protein in ageing (Altun et al., 2010).

1.2.4.4 Fat, fibrosis, and sarcopenia

Fibrosis is the term for the accumulation of extracellular matrix (ECM) (Alnaqeeb et al., 1984, Goldspink et al., 1994). It has been well established that during ageing, fibrosis and infiltration of adipose tissue occurs in skeletal muscle. This decrease in the quality of skeletal muscle is thought to contribute to the age-related impairment in force generation (Faulkner et al., 2011). Satellite cells from old mice have been shown to become fibrogenic, due to canonical Wnt signalling pathway activation; contributing to tissue fibrosis with age (Brack et al., 2007). Collagen, a major component of the ECM, has been shown to accumulate within muscle following incomplete repair post-damage (Serrano and Munoz-Canoves, 2010).

1.2.4.5 ROS, mitochondria, and sarcopenia

Accumulation of mutations in mitochondria and mitochondrial DNA (mtDNA) during ageing have been well characterised (Miquel et al., 1980). ROS derived from the electron transport chain (ETC) are the suspected source of this damage. Mitochondrial DNA is particularly susceptible to damage, especially from ROS, due to fewer repair mechanisms (Clayton et al., 1974).

There is significant evidence to indicate that there are fundamental changes in redox signalling and homeostasis, which occur during ageing (Jackson and McArdle, 2011). Skeletal muscles of old mice demonstrate significant oxidative damage to DNA, lipids, and proteins (Vasilaki et al., 2006). The imbalance in ROS homeostasis may ultimately initiate the upregulation of proinflammatory signals, resulting in chronic inflammation (Meng and Yu, 2010). Oxidative stress, such as muscle derived ROS, is

proposed to activate NF-κB and up-regulate the inflammatory response (Meng and Yu, 2010).

1.2.4.6 Inflammation and sarcopenia

An elevated level of low-grade, chronic systemic inflammation is seen in ageing mammals, called inflammaging (Franceschi and Campisi, 2014). This is characterised by increased serum proinflammatory cytokines such as interleukin-6 (IL-6); and a decrease in anti-inflammatory cytokines like interleukin-10 (IL-10) and interleukin-1 receptor alpha (IL-1ra) (Lio et al., 2002). We have previously demonstration a chronic increase in NF-κB activation in muscles of old compared with adult mice (Vasilaki et al., 2006). Skeletal muscle is a source of cytokines, called myokines (Nielsen and Pedersen, 2008) and such chronic activation of NF-κB in muscles of old mice suggests that the production of cytokines by the muscles may also be increased. Examples of myokines include IL-6, IL-8, and IL-15, which have also been reported to be secreted as part of the senescence associated secretory phenotype (SASP). Such inflammation is proposed to be involved in the development of sarcopenic muscle. Muscle strength (Visser et al., 2002), muscle mass (Schaap et al., 2006), muscle protein synthesis and catabolism (Jo et al., 2012) have all been demonstrated to be affected by inflammatory cytokines.

A positive association between chronically increased serum levels of proinflammatory cytokines such as IL-6 and TNFα and frailty measures such as grip strength have been demonstrated in several epidemiological studies (Leng et al., 2004, Payette et al., 2003, Schaap et al., 2006). Indeed, centenarians have lower levels of IL-6 (Franceschi and Bonafe, 2003). McKay et al. (2013) showed that satellite

cell activation in response to muscle damage was blunted in older adult men and this was mediated by IL-6. IL-6 stimulates the ubiquitin proteasome muscle degradation pathway. Increased concentrations of IL-6 in plasma is associated with increased ubiquitin protein and mRNA expression (DeJong et al., 2005). Furthermore, chronic IL-6 signalling has also been shown to promote insulin resistance in liver, adipose, and skeletal muscle (Kim et al., 2009). Insulin resistance has been shown to supress important pathways involved in muscle synthesis, mainly the Akt-mTOR pathway (Franckhauser et al., 2008).

Jurk et al. (2014) used a NF-κB1$^{-/-}$ mouse model to investigate the effects of chronic inflammation on telomere dysfunction; by increasing ROS-mediated DNA damage and thus accelerated accumulation of senescent cells. 44 weeks old NF-κB1$^{-/-}$ mice showed premature greying and fur loss, as well as kyphosis (loss of muscle mass). Mouse adult (ear) fibroblasts (MAFs) from NF-κB1$^{-/-}$ mice showed increased incidence of senescence, with increased senescence-associated β-galactosidase (SA-β-gal) activity.

In order to examine the influence of systemic circulatory factors on progenitor cells from old mice, Conboy et al. (2005) performed a heterochronic parabiotic pairing between young and old mice. Parabiosis is the sharing of circulatory systems, exposing old mice to factors present in young serum. Parabiosis restored the activation of Notch signalling as well as the proliferation and regenerative capacity of aged satellite cells in a similar manner to the positive effect of the cross-age muscle transplant studies in Carlson and Faulkner (1989).

Immune cells such as neutrophils migrate in response to chemo-attractants, from the blood to a site of infection or tissue damage. Neutrophils release proteases, such as neutrophil elastase, at their leading edge and damaging healthy tissue in the process, resulting in inflammation (Wilson et al., 2017). Furthermore, the efficiency of chemotaxis decreases in ageing, leading to greater tissue damage and secondary systemic inflammation (Wilson et al., 2017).

Cai et al. (2004) has shown that the constitutively active expression of IKKβ causes a significant increase in the expression of the MuRF1 gene in transgenic mice. The IKKβ-expressing mice displayed muscle wasting, which was significantly reduced by crossing them with MuRF1-knockout mice. In contrast, Mourkioti et al. (2006) created a skeletal muscle-specific deletion of IKKβ in transgenic mice, which prevented the expression of MuRF1 gene and atrophy in the skeletal muscles in response to nerve injury. Thus, activation of NF-κB contributed to muscle loss, through the increased expression of MuRF1 E3 ubiquitin ligase in skeletal muscle.

1.3 Evidence of senescence in skeletal muscles in ageing

As skeletal muscle is mainly terminally differentiated, post mitotic tissue, there was initially limited interest in investigating cellular senescence in this tissue. However, there is a body of literature highlighting the presence and influence of senescent cells within skeletal muscle.

Increased expression of senescence markers such as p53 and p21 has been detected in the muscles of mice (Edwards et al., 2007), monkeys (Kayo et al., 2001), and humans (Welle et al., 2004), although the source of these markers is unclear.

Sousa-Victor et al. (2014) demonstrated that satellite cells from geriatric mice (32+ months of old) were unable to maintain their quiescent state, and switch to an irreversible pre-senescence state, caused by de-repression of p16INK4a. Furthermore, satellite cells showed an age-dependent increase in DDR marker γ-H2AX in mice. These cells in turn failed to activate and expand in response to injury, instead converting to a fully senescent state; in a process called 'geroconversion'. Silencing of the p16 gene, CDKN2A, restored the quiescence and regenerative capacity of satellite cells from these geriatric mice.

As discussed in Section 1.1.7.2, Baker et al. (2008) investigated ageing using BubR1 (BubR1 hypomorphic or $BubR1^{H/H}$) progeroid mice, a model of accelerated ageing. These mice have been characterised and display phenotypes such as a shortened lifespan, lordokyphosis, and sarcopenia, amongst others (Baker et al., 2004). These $BubR1^{H/H}$ were crossed with p16 knockout mice ($p16^{Ink4a-/-}$) to give $BubR1^{H/H}$: $p16^{Ink4a-/-}$ mice. To determine the role of BubR1 in normal skeletal muscle ageing, senescence markers in the gastrocnemius of 2- and 35-month-old mice were measured. There was an age-related decline in the expression of BubR1 in skeletal muscle, as well as an age-related increase in p16 expression. Gastrocnemius of 2- and 5-month-old $BubR1^{H/H}$ mice also showed high p16 expression. Furthermore, $BubR1^{H/H}$ mice showed an increase in SASP components IGFBP2, MMP13, and Pai1. Knocking out p16 in this animal model improved fibre size in gastrocnemius, reduced instances of lordokyphosis, and reduced the expression of SASP.

Zhu et al. (2019) have also shown that peri-muscular adipose tissue (PMAT), an ectopic fat deposit surrounding muscle, may drive muscle wasting. Transplanting

PMAT from obese mice into non-obese mice resulted in increased nuclear translocation of FoxO transcription factors. This resulted in the upregulated expression FoxO targets associated with proteolysis (Atrogin1 and MuRF1), and cellular senescence (p19 and p21) in whole muscle lysates. Furthermore, PMAT removal in obese mice attenuated denervation-induced muscle atrophy; suppressing upregulation of genes related to proteolysis and cellular senescence in muscle.

1.3.1 Exercise and cellular senescence

Cellular senescence has been shown to play a role in ageing and inflammation (Hernandez-Segura et al., 2018), however the role of exercise on cellular senescence is an ongoing investigation. Exercise and diet have been shown to be determinant of healthy ageing and sarcopenia (Jackson, 2020). Exercise has been associated with an upregulation of proteins such as telomeric repeat-binding factor 2 (TRF2), telomerase activity and DNA repair pathway Ku proteins which protect DNA, and downregulation of proteins of such as chk2, p16, and p53 in middle-aged athletes (Werner et al., 2009, Rebelo-Marques et al., 2018). Furthermore, although exercise acutely increases oxidative stress, chronic training is associated with antioxidant activity and inferior levels of ROS, favouring the REDOX balance, protecting from DNA damage and subsequently shorter telomere attrition (Gomes et al., 2012, Rebelo-Marques et al., 2018).

Schafer et al. (2016) investigated the effect of "fast-food diet" and exercise on the onset and progression of cellular senescence and the SASP, using adult transgenic p16-EGFP mice. Male mice (8 months old) were fed either a normal diet (ND), "fast-food" diet (FFD), ND + exercise, or FFD + exercise for 16 weeks. The FFD group had

increased body weight, fat mass, circulating insulin levels and β-cell mass compared with the ND control group after treatment. These changes were partially prevented in the FFD + exercise group. The mRNA expression of p16, p21, p53, and SASP cytokines were significantly increased in several tissues (muscle was not measured), SA-β-Gal activity in visceral adipocytes in the FFD group compared with the ND group. Exercise, in both the FFD and the ND group, reduced several indices of senescence and SASP. These findings showed the harmful consequences of excessive nutrient intake and the remarkably protective influence of exercise on this biological process and, in turn, measures of physical, cardiovascular, and metabolic function.

In contrast, Saito et al. (2020) investigated the role of muscle resident senescent fibro-adipogenic progenitor (FAP) cells in the context of muscle regeneration and inflammation. Damage to skeletal muscle/exercise triggers a transient FAP proliferation and protein expression that promotes muscle stem cell differentiation, followed by a return to baseline with apoptosis and subsequent phagocytic clearance of these cells. However, in chronic inflammation, FAP proliferation and protein expression are more robust due to the accumulation of apoptosis-resistant FAPs. The authors investigated the role of FAPs in chronically inflamed environments and hypothesised that the effects of exercise on muscle regeneration or fibrosis depend on the FAP phenotype. The authors showed that FAPs increased after injury in regenerating muscle (barium chloride induced acute muscle injury) (AMI-FAP) and subsequently declined to pre-damage levels. However FAPs continued to accumulate for 14 days after injury by acquiring cell death resistance in degenerating muscle (chronic inflammatory myopathy) (CIM-FAP). In addition, AMI-FAPs acquired increased expression of Cdkn2a, Trp53, p21, and p19Arf, whereas CIM-FAPs showed

decreased expression of senescent factors. Exercise promoted FAP senescence in normal mice, but exercise in CIM mice decreased the expression of senescent factors to levels seen in sedentary CIM mice. AICAR, a cell-permeable APMK activator, was used to induce senescence in FAPs. CIM mice treated with combined exercise and AICAR treatment showed increased stamina, grip strength, and myofibre CSA. In the AMI model, exercise with AICAR treatment resulted in a pro-inflammatory cytokine expression and pro-apoptotic FAP phenotype that promoted muscle regeneration. Taken together, the authors have shown that FAP senescence promotes muscle regeneration by inducing SASP expression and apoptosis, creating a state of regenerative inflammation. FAPs that fail to senescence following AMI or exercise accumulate with an anti-apoptotic and pro-fibrotic phenotype. These findings show that positive role of senescence in tissue repair, similar to that of Demaria et al. (2014). This further highlights the multifaceted nature of senescent cells *in vivo* and that total ablation of senescent cells from an organism may have complex ramifications.

These studies demonstrate that senescent cells may play a role in the age related loss of muscle mass and function with age, and that skeletal muscle may play a role in this, although the nature of the senescence phenotype of skeletal muscle remains unclear.

1.4 Hypothesis and Aims

The overall hypothesis of this thesis was that senescent cells accumulate in old mice, either locally to skeletal muscle or distally and that they produce an inflammatory

SASP that may contribute, at least in part, to the chronic NF-κB signalling and the loss of muscle mass and function seen in the muscles of old compared with adult mice.

This programme of work tested this hypothesis by utilising different models of senescence *in vitro* and *in vivo* and using a senolytic and transgenic intervention.

Chapter 2: Methods

All reagents were purchased from Sigma Aldrich (Poole, U.K) unless stated otherwise. Cell culture supplies were purchased from GibcoBRL (Paisley, U.K).

2.1 Animals

2.1.1 Animal husbandry & Home Office licence permissions

All experiments complied with UK Home Office Animal Licensing Laws for the care and use of laboratory animals. All animals were housed in the specific pathogen free Biomedical Services Unit at the University of Liverpool where they were monitored daily. The animals had standardised lighting system (12-hour light cycles), controlled temperatures (22±2°C) and access to food and water ad libitum.

2.1.2 P16-3MR mice

Twenty-one 20-months-old P16-3MR mice of both genders were given 25mg/kg Ganciclovir by intraperitoneal (I.P) injection in PBS, over 10 days using a regime of 5 days of injections with 2 days of rest. Following I.P injection, mice were treated every 4 weeks with a 5-day course of GCV, until 26 months old where the mice were sacrificed for tissue harvest and force measurement.

2.1.3 Senolytic dietary intervention study

Eighteen 20-months old C57BL/6 male mice were divided into two groups, one of which was fed 500 ppm (500 mg/kg) of fisetin as part of their chow (CRM(P), Special Diet Services, 801722) *ad libitum* (approximately 2.5 mg/day/mouse or 8.7 µM/day/mouse). The second group were fed CRM(P) chow without fisetin. Mice were maintained on the diet for 16 weeks, when force generation of EDL muscle was determined and mice were sacrificed for tissue collection.

2.1.4 Determination of muscle force generation

Muscle force measurements of P16-3MR mice were performed *in situ* at the University of Michigan. Gastrocnemius stimulation, both nerve and by direct muscle activation, were performed *in vivo*. Muscle force measurements of the extensor digitorum longus (EDL) and soleus were also performed *ex vivo*.

The protocol was adapted from McArdle et al. (2004). Mice were anaesthetised with isoflurane and maintained under anaesthesia throughout the procedure. The knee of the right hind limb was fixed. The distal tendon of the extensor digitorum longus (EDL) muscle was exposed and attached to the lever arm of a servomotor (Cambridge Technology). The lever served as a force transducer. The peroneal nerve was exposed, and electrodes were placed across the nerve. The EDL muscle of the contralateral limb served as a non-exercised control.

Stimulation voltage and muscle length were each adjusted to produce maximum twitch force. The optimal length for maximum twitch force is also the optimal length (L_0) for the development of maximum tetanic force (P_0; (Brooks and Faulkner, 1988)). With the muscle at L_0, the P_0 was determined during 300msec of voltage stimulation (10V). The P_0 was identified by increasing the frequency of stimulation at 2-min intervals until the maximum force plateaued. Muscle fibre length (L_f) and cross-sectional area were calculated (Brooks and Faulkner, 1988). For the mice used for the senolytic intervention study, electrodes were also placed directly across the EDL muscle and the procedure above was repeated. This was to determine any deficits due to poor neuronal function.

Following the final measurement, the mouse was removed from the platform. Mice were sacrificed by cervical dislocation and blood was collected from the descending aorta. The mouse was weighed, and the EDL muscles were removed immediately. The muscle length was measured, and mass weighed.

The hind limb muscles and internal organs were weighed and snap frozen in liquid nitrogen. Half of the anterior tibialis (AT) muscle was mounted on to a cork disk, surrounded with mounting medium (O.C.T., Merck, UK), frozen rapidly in liquid nitrogen cooled iso-pentane and sectioned for histological analysis. EDL muscles were pinned and fixed using neutral buffered formalin (NBF), and later stored at 4°C in PBS + 0.1% sodium azide. The specific P0 was calculated as the absolute P_0/ muscle cross-sectional area (Brooks and Faulkner, 2001).

2.2 Cell Culture of C2C12 myoblasts and myotubes

C2C12 cells are an immortalized mouse myoblast cell line. The cell line was initially obtained by Yaffe and Saxel (Yaffe and Saxel, 1977). C2C12 cells are mononuclear myoblasts, capable of rapid proliferation under high serum conditions. C2C12 myoblasts can fuse to form multinucleated myotubes under conditions of low or no serum. This serum deprivation results in functional skeletal muscle cells (McMahon et al., 1994). All media were stored at 4°C and warmed in a heated water bath to 37°C before use. C2C12 Myoblasts were maintained in Dulbecco's modified Eagle's medium (DMEM) supplemented with 10% heat inactivated foetal bovine serum (FBS), 100 U/ml penicillin and 100 µg/ml streptomycin. Cells were grown at 37°C in a humidified 5% CO_2/95% air incubator.

Reagents:

- Dulbecco's Phosphate Buffered PBS (DPBS) (Sigma Aldrich, Dorset, UK)
- 0.25% Trypsin (Sigma Aldrich, Dorset, UK)
- C2C12 growth media
    - Dulbecco's Modified Eagle's Medium
    - 10% (v/v) foetal bovine serum, heat inactivated
    - 100 µmol/ml penicillin, and 0.1 mg/ml streptomycin
    - 4 mM L-glutamine
- C2C12 differentiation media
    - Dulbecco's Modified Eagle's Medium
    - 2% (v/v) horse serum, heat inactivated
    - 100 µmol/ml penicillin, and 0.1 mg/ml streptomycin
    - 4 mM L-glutamine

Method:

Myoblasts were passaged at 65-75% confluence. Cell culture medium was removed and discarded. The cell layer was briefly rinsed with PBS to remove of serum. An appropriate volume of 0.25% (w/v) Trypsin-0.53 mM EDTA/PBS solution was added to the flask and placed into a 37°C in a humidified 5% CO_2/95% air incubator. Myoblasts were observed under an inverted light microscope (Nikon Diaphot, Tokyo, Japan) until the cell layer was non-adherent.

Seven millilitres of growth media was added to neutralise the Trypsin-EDTA solution and the cell suspension was collected before centrifuging the solution at 500g for 5 minutes. The supernatant was discarded, and the cell pellet was aspirated with 10 mL growth media. A 15µL aliquot of resuspended myoblasts were removed at this point for determination of cell number, as described in Section 2.2.5.

A T-75 flask was inoculated with myoblasts at a concentration of between $1.5x10^5$ and $1.0x10^6$ cells/75 cm^2 to maintain a population of cells. Myoblasts were incubated at 37°C in a humidified 5% CO_2/95% air incubator. Alternatively, for experiments such as inducing cellular senescence, myoblasts were seeded into 6 or 12 well plates at $1x10^4$ or $5x10^3$ cells per well respectively and incubated at 37°C in a humidified 5% CO_2/95% air incubator overnight to adhere.

2.2.1 Induction of cellular senescence in C2C12 Myoblasts

Reagents:

- C2C12 growth media
    - Dulbecco's Modified Eagle's Medium
    - 10% (v/v) foetal bovine serum, heat inactivated
    - 100 µmol/ml penicillin, and 0.1 mg/ml streptomycin
    - 4 mM L-glutamine
- etoposide (Sigma, Dorset, UK, E1383)
- Dimethyl Sulfoxide (DMSO) (Sigma Aldrich, Dorset, UK)

Method:

Myoblasts were seeded into 6 or 12 well plates at $1x10^4$ or $5x10^3$ cells per well respectively and incubated at 37°C in a humidified 5% CO_2/95% air incubator overnight to adhere.

Etoposide powder (Sigma, E1383) was reconstituted in Dimethyl Sulfoxide (DMSO) to a concentration of 100 mM, and this was diluted 1 in 10 to a stock concentration of 10mM in growth media. Myoblasts were then treated with different concentrations (30-3.75µM) of etoposide or DMSO carrier control in growth media for 24 hours and incubated appropriately. Etoposide and DMSO containing media was then removed and replaced with standard growth media and further incubated for up to 5 days. Cells were monitored daily to check for progression of senescent morphology, using a light (Nikon Diaphot, Tokyo, Japan) microscope.

2.2.2 Differentiating myoblasts into myotubes

Reagents:

- C2C12 differentiation media
    - Dulbecco's modified eagle's medium
    - 2% (v/v) horse serum, heat inactivated
    - 100 µmol/ml penicillin, and 0.1 mg/ml streptomycin
    - 4 mM L-glutamine

Method:

C2C12 myoblasts were passaged and plated as previously described in Section 2.2and allowed to reach >85% confluence within the well or flask, to promote fusion. Growth media was replaced with differentiation media. Myotubes were differentiated for between 7-10 days, with media changes every 3 days.

2.2.3 Treatment C2C12 myotubes with conditioned media from senescent myoblasts

Reagents:

- Dulbecco's Phosphate Buffered PBS (DPBS) (Sigma Aldrich, Dorset, UK)
- C2C12 growth media
    - Dulbecco's Modified Eagle's Medium
    - 10% (v/v) foetal bovine serum, heat inactivated
    - 100 µmol/ml penicillin, and 0.1 mg/ml streptomycin
    - 4 mM L-glutamine
- C2C12 differentiation media
    - Dulbecco's Modified Eagle's Medium
    - 2% (v/v) horse serum, heat inactivated
    - 100 µmol/ml penicillin, and 0.1 mg/ml streptomycin
    - 4 mM L-glutamine

Method:

Senescent C2C12 myoblasts were prepared as described in Section 2.2.1. DMSO treated cells were used as a vehicle control. Media from these myoblasts was collected at 3, 5, and 7 days post-treatment. C2C12 myotubes were incubated with the media collected from senescent C2C12 myoblasts, for 24 hours in 37°C in a humidified 5% CO_2/95% air incubator. Light microscopic images were recorded before the addition of the media from senescent and controls myoblasts, and 24 hours after treatment. The myotubes were harvested for analysis. Table 2.1 illustrates the workflow in detail.

2.2.4 Measurement of myotube diameter

Four images of C2C12 myotubes were taken at 10x magnification using a light microscope (Nikon Diaphot, Tokyo, Japan). Myotubes in the field of view were analysed using Image J (US National Institutes of Health, Maryland, USA). For each image, myotubes were traced and the minimum Ferets diameter was measured. Measurements for approximately 20 single myotubes from 6 wells were pooled to give an average value per condition.

	Myotubes	7 days Etoposide media	5 days Etoposide media	3 days Etoposide media
Day 1	Seed cells			
Day 2				
Day 3	Differentiation media	Seed cells		
Day 4	Day 1	Treat with Etoposide/DMSO		
Day 5	Day 2	Day 1 – Media change	Seed cells	
Day 6	Day 3 – Media change	Day 2	Treat with Etoposide/DMSO	
Day 7	Day 4	Day 3	Day 1 – Media change	Seed cells
Day 8	Day 5	Day 4	Day 2	Treat with Etoposide/DMSO
Day 9	Day 6 – Media change	Day 5	Day 3	Day 1 – Media change
Day 10	Day 7	Day 6	Day 4	Day 2
Day 11	Day 8	Day 7	Day 5	Day 3
Day 12	Co-culture of media – Image myotubes pre 24 hour treatment and harvest control			
Day 13	Co-culture of media – Image myotubes post 24 hour treatment and harvest			

Table 2.1 Workflow for co-culture experiment.

At day 1, C2C12 myotubes were seeded and differentiated to form myotubes, reaching maturity at day 12. On days 3, 5, and 7, myoblasts were treated with etoposide to generate senescent myoblasts, or the DMSO vehicle controls. On day 12, the conditioned media from the senescent myoblasts were used to treat the mature myotubes, for 24 hours. On day 13, the media was removed and the myotubes harvested.

2.2.5 Determination of cell number

Trypan Blue is commonly used in microscopy for cell counting (Strober, 2015). Trypan blue is an impermeable dye and cannot penetrate the intact cell membranes of live cells, therefore will only stain non-viable cells blue, allowing dead and live cells to be distinguished.

Reagents:

- Dulbecco's Phosphate Buffered PBS (DPBS) (Sigma Aldrich, Dorset, UK)
- 0.025% Trypsin containing EDTA (Sigma Aldrich, Dorset, UK) in DPBS
- C2C12 growth media
    - Dulbecco's Modified Eagle's Medium
    - 10% (v/v) foetal bovine serum, heat inactivated
    - 100 µmol/ml penicillin, and 0.1 mg/ml streptomycin
    - 4 mM L-glutamine
- 0.4% Trypan Blue (Invitrogen, Paisley, UK) in DPBS

Method:

Cells were detached from the surface they were adhered to using trypsin as previously described in Section 2.2, and resuspended in 10 mL fresh growth media. The cell suspension was gently, but thoroughly mixed. Fifteen microliters of cell suspension was mixed 1:1 with trypan blue solution. Ten microliters of the cell suspension was loaded onto a haemocytometer. The numbers of viable cells was determined in triplicate using a light microscope (Nikon Diaphot, Tokyo, Japan) at 10x magnification and an average cell number was calculated.

2.3 Measurement of senescent markers

2.3.1 Cell Viability Assay of C2C12 myoblasts

Cell viability was determined using a LIVE/DEAD© reduced Biohazard Viability/Cytotoxicity Kit (Molecular Probes, UK). The assay determines the viability of samples by exploiting the permeability of the cell to the kit's dyes. SYTO 10 is a cell permeable, fluorescent dye that will stain the entire cell green, including the nucleus. The red fluorescent protein only penetrates the membranes of compromised cells and incorporates into the nucleus; whereby only staining the nuclei of dead cells red. Thus, viable cells are stained green and the nuclei of dead cells are stained red.

Reagents:

- LIVE/DEAD® Viability/Cytotoxicity Kit containing:
    - Component A – SYTO 10 green-fluorescent nucleic acid stain in DMSO
    - Component B – DEAD Red (Ethidium homodimer-1) nucleic acid stain in DMSO/H_2O 1:4 (v/v)
- Hepes Buffer PBS Solution (HBSS) (Sigma Aldrich, Dorset, UK)
- 4% glutaraldehyde (Sigma Aldrich, Dorset, UK) in DPBS
- Sterile H_20

Method:

Briefly, myoblasts were aspirated and washed in HBSS. The myoblasts were then treated with SYTO 10 and DEAD Red diluted 1 in 500 in HBSS; and incubated at room temperature for 15 minutes in the dark. Following this, the staining solution was removed, myoblasts were washed with HBSS and then fixed with 4% glutaraldehyde.

Cells were visualised using a florescent microscope (Nikon Eclipse TE2000, Tokyo, Japan) at 560–520 nm and 700–635 nm wavelengths for the green and red fluorophores, respectively.

2.3.2 Senescence Associated β-Galactosidase Staining

SA-β-gal detection was performed using the Senescence β-Galactosidase Staining Kit (Cell Signalling Technologies, #9860). A lysosomal beta-galactosidase accumulates in senescent cells and can be exploited in a cytochemical assay that produces a blue precipitate at pH 6.0 (Dimri et al., 1995).

Reagents:

- Senescence Associated β-Galactosidase Staining Kit (Cell Signalling Technology, London, UK) containing:
    - 10x Fixative Solution
    - 10x Staining Solution
    - 100x Solution A
    - 100x Solution B
    - X-Gal (5-bromo-4-chloro-3-indolyl-β-D-galactopyranoside)
- N,N-Dimethylmethanamide (DMF), 99% (Sigma Aldrich, Dorset, UK)
- Dulbecco's Phosphate Buffered PBS (DPBS) (Sigma Aldrich, Dorset, UK)

Method:

Twenty milligrams of X-gal were dissolved in 1 ml DMF to prepare a 20 mg/ml stock solution. The solution can be stored at -20°C in foil for up to one month. Myoblasts and tissue sections were prepared as described in Sections 2.2.1 and 2.3.3

respectively. Samples were washed with PBS, and then placed in the Fixative Solution (diluted 1 in 10 in H_20) for 10 minutes at room temperature. Samples were then washed twice with PBS, followed by the addition of the Staining Solution (pH 6.0) (Table 2.2). Samples were then incubated at 37°C overnight, in a low CO_2 environment. The Staining Solution was then removed and replaced with DPBS for imaging under a light microscope (Nikon Diaphot).

	Volume (µL)
1X Staining Solution	930
100X Solution A	10
Solution B	10
20mg/ml X-gal stock solution	50

Table 2.2 Senescence β-Galactosidase Cell Staining Solution.

2.3.3 Immunohistochemical analysis of senescence markers in etoposide treated C2C12 myoblasts

Reagents:

- Dulbecco's Phosphate Buffered PBS (DPBS) (Sigma Aldrich, Dorset, UK)
- Triton X-100 (Sigma Aldrich, Dorset, UK)
- Polyoxyethylene-sorbitan monolaurate (Tween-20) (Sigma Aldrich, Dorset, UK)
- 4% Paraformaldehyde (PFA) in DPBS
- Blocking solution
    - 10% donkey serum (Sigma Aldrich, Dorset, UK) in DPBS

- Diluting solution
    - 0.25% sodium azide (Sigma Aldrich, Dorset, UK), 0.25% of donkey serum, and 0.2% Triton in DPBS
- Primary antibody
    - anti-p21 antibody [EPR3993] (ab109199)
- Secondary antibody
    - Goat anti-rabbit 488
- DAPI (4',6-diamidino-2-phenylindole)) (Sigma Aldrich, Dorset, UK)
- Vector Shield aqueous mounting solution

Method:

C2C12 myoblasts were seeded on to coverslips in a 6 well plate and treated with etoposide to induced senescence as described in Section 2.2.1. The cells were then washed with PBS, and ice-cold 4% PFA was added to each sample for 5 minutes at room temperature. Cells were then aspirated to remove the PFA, followed by three washes with PBS. Myoblasts were then incubated for 1 hour at room temperature in blocking solution.

Primary antibody, anti-p21 antibody [EPR3993] (ab109199) (1 in 400), was diluted in the diluting solution. Blocking solution was removed and the myoblasts were incubated in primary antibody overnight at 4°C.

Myoblasts were then washed three times with DPBS before the secondary antibody was added. Anti-rabbit 488 secondary antibody was used, diluted 1 in 1000 in diluting solution. Cells were incubated for 1 hour at room temperature in the dark. Myoblasts

were then washed twice time with DPBS and then DAPI (1 in 10,000 in dH_20) was added and cells were incubated for a further 10 minutes at room temperature in the dark. Myoblasts were washed three times with PBS to remove any excess antibody and DAPI. Cells were then sealed under a cover slip using Vector Shield aqueous mounting solution. Finally, the cells were washed with distilled water.

Cells were then imaged using a fluorescent microscope (Nikon Eclipse TE2000) using IP Lab 3.0 Software.

2.3.4 Cryosectioning of frozen mouse tissue

Reagents:

- Optimal Cutting Temperature (OCT) compound (Sigma Aldrich, Dorset, UK)
- Isopentane (Sigma Aldrich, Dorset, UK)
- Histological cork (Sigma Aldrich, Dorset, UK)
- SuperFrost Plus™ Adhesion Microscopy slides (Sigma Aldrich, Dorset, UK)

Methods:

Muscle harvested from sacrificed mice were mounted transversely on to a histological cork. The cork and tissue were covered in OCT resin and snap frozen in liquid nitrogen cooled iso-pentane. Frozen muscle blocks were stored at -80°C long term. Frozen muscle sections were acclimatised to -24°C before sectioned at 12µM thickness using a cryostat (Leica CM1800, Wetzlar, Germany) set to -24°C. Sectioned tissues were then adhered to microscopy slides and stored at -20°C.

2.3.5 Sudan Black B staining or autofluorescence measurement of muscle tissue sections for evidence of lipofuscin

Reagents:

- Sudan Black B (SBB)
- Ethanol
- Formaldehyde

Methods:

Methods were adapted from Evangelou and Gorgoulis (2017).

Preparation of SBB solution:

0.7g of SBB (BDH, Athens, Greece) was dissolved in 70% ethanol, covered with parafilm, and thoroughly stirred overnight at room temperature. This was then filtered through filter paper and then filtered again using a frittered glass filter of medium porosity with suction. Throughout the process it was important to avoid ethanol evaporation, which results in precipitation of the stain and so the solution was stored in an airtight container.

Staining Procedure:

Frozen muscle sections were mounted onto SuperFrost slides prepared as described in Section 2.3.3, were fixed in 1% (wt/vol) formaldehyde/PBS for 1 min at room temperature and then washed three times at room temperature with PBS. Tissue was then incubated for 5 min in 50% ethanol and then for another 5 min into 70% ethanol. Coverslips with fixed tissue were incubated for 2 min in 70% ethanol. In order to avoid precipitation of SBB on tissue the following two steps were crucial:

1) A drop from freshly prepared SBB was placed on a clean slide. The slide with the tissue was placed face down on the SBB. Staining was observed under the microscope.

2) Either the coverslip or the slide was carefully lifted and any SBB present on the edges of the tissue-slide was removed manually with tissue paper.

The tissue sections were then washed with 50% ethanol and counterstained with 0.1% Nuclear Fast Red (NFR) (Sigma, Athens, Greece) for 10 min., and mounted into 40% Glycerol/TBS mounting medium. SBB staining was considered positive when perinuclear and cytoplasmic aggregates of blue-black granules were evident inside the tissue.

For autofluorescence imaging, unstained muscle sections were imaged under a Zeiss LSM 800 confocal microscope at 20x magnification between 530 nm to 660 nm.

2.3.6 Immunohistochemical analysis of muscle sections for senescence markers

Reagents:

- PBS (0.01% tween 20) for washes
- PBS
- Tween 20 (Sigma Aldrich, Dorset, UK)
- Bovine Serum Albumin (Sigma Aldrich, Dorset, UK)
- 4% PFA (Sigma Aldrich, Dorset, UK)
- PBS (0.1% Triton)
- Goat Serum (Sigma Aldrich, Dorset, UK)
- Primary antibodies
    - Anti p21 [EPR3993] (ab109199) (Abcam, Cambridge, UK)

- Anti p16 [2D9A12] (ab54210) (Abcam, Cambridge, UK)

- Secondary antibody
  - Alexa Fluor® 488 Goat anti-rabbit (Sigma Aldrich, Dorset, UK)
- Rhodamine wheat germ agglutinin (WGA) (Sigma Aldrich, Dorset, UK)
- Vector Shield mounting media with DAPI (Sigma Aldrich, Dorset, UK)
- Cover slips (Sigma Aldrich, Dorset, UK)

Methods:

Muscle sections were prepared on microscopes slides, as described in 2.3.3. Muscle sections were washed once with ice cold PBS for 5 mins. Sections were then fixed with ice cold 4% PFA for 10 mins at RT. Sections were washed three times for 5 mins with PBS (0.01% Tween 20). Sections were permeabilised with 0.1% Triton (0.1%) in PBS for 10 mins at RT, followed by another 3x5 mins wash. Sections were then incubated with 10% goat serum, 1% BSA, and 0.1% tween 20 in PBS, at RT for an hour. Sections were then incubated overnight at 4°C in 1% BSA, 0.1% tween 20 in PBS, containing either anti-p21 or anti-p16 antibodies, at a 1 in 100 dilution.

Following the overnight incubation, sections were washed 3x5 mins and incubated with a 1:1000 dilution of Alexa Fluor® 488 Goat anti-rabbit secondary antibody in 1% BSA, 0.1% tween 20 in PBS for 1 hr at RT. Sections were washed 3x5 mins and stained with Rhodamine WGA diluted 1 in 1000 for 10 mins at RT. Sections were was washed 3x5 mins as previously described, then finally with sterile water. Sections were mounted with VectaShield Hardset medium containing DAPI (Sigma Aldrich, Dorset, UK).

2.4 Protein Quantification

2.4.1 Generation of tissue homogenates

Frozen mouse tissue was ground into a fine powder using a pestle and mortar under liquid nitrogen. C2C12 cell pellets or ground tissue powder was then lysed in 100µL RIPA lysis buffer, on ice for 30 mins. The cell debris was then centrifuged out at 10,000g for 10 mins, at 4°C. The protein content was then determined using a protein assay.

2.4.2 Bicinchoninic acid assay of tissue or cell homogenates

The Bicinchonic acid (BCA) assay is used in the detection of the concentration of proteins in a sample via a standard curve of protein of a known concentration. The BCA assay is based on the method originally described by Smith et al. (1985). The assay works by exploiting Cu^{2+} protein complex formation. First, the peptide bonds in protein reduce Cu2+ ions from the copper (II) sulphate to Cu^{+} (a temperature dependent reaction). The amount of Cu^{2+} reduced is proportional to the amount of protein present in the solution. Next, two molecules of BCA chelate with each Cu^{+} ion, forming a purple-coloured complex that strongly absorbs light at a wavelength of 562 nm. The reduction of Cu^{2+} to Cu^{+} is proportional to the protein content of the sample in question. This results in the formation of purple coloured salt complex with Cu^{+}, which can be quantified using a spectrophotometer (Olson and Markwell, 2007).

- Pierce™ BCA Protein Assay Kit (Sigma Aldrich, Dorset, UK) containing:
    - BCA Reagent A - containing sodium carbonate, sodium bicarbonate, bicinchoninic acid and sodium tartrate in 0.1M sodium hydroxide
    - Reagent B - 4% cupric sulphate

- Albumin Standard Ampules, 1mg/mL, bovine serum albumin (BSA) in 0.9% PBS and 0.05% sodium azide

Vial	Volume of Diluent (µL)	Volume and Source of BSA (µL)	Final BSA Concentration (µg/mL)
A	0	200 of Stock	1000
B	100	100 of vial A	500
C	100	100 of vial B	250
D	100	100 of vial C	125
E	100	100 of vial D	62.5
F	100	100 of vial E	31.25
G	100	100 of vial F	15.625
H	100	0	0 = Blank

Table 2.3 Preparation of Diluted Albumin (BSA) Standards

Method:

The BCA assay was performed by generating a standard curve of protein to use as a standard from a stock solution of BSA (1mg/mL) (Table 2.3).

Twenty microliters of protein standard or tissue homogenates were loaded in triplicate into a 96 well plate. One hundred and eighty microliters of Reagent B, diluted 1 in 50 in Reagent A, was added to each well, and was incubated at 37°C for 30 minutes. Absorbance was measured using a spectrophotometer (SPECTRO-star Nano, BMG Labtech, Offenburg, Germany) at 570nm. The protein standard curve was used to quantify the protein content of the samples.

2.4.3 Bradford Assay of tissue or cell homogenates

The Bradford protein assay is a colorimetric protein assay based on the use of the dye Coomassie Brilliant Blue G-250 (Coomassie G-250 or Coomassie Blue). The dye exists in three forms:

- Cationic (doubly protonated, red)
- Neutral (green)
- Anionic (stable, unprotonated, blue)

Under normal conditions, the dye is predominantly in the doubly protonated red cationic form (A_{max} = 470 nm). However, when the dye binds to protein, it is converted to a stable unprotonated blue form (A_{max} = 595 nm) (Figure 2.1 Coomassie Brilliant Blue G-250 reaction).

The blue protein bound dye form is detected at 595 nm using a spectrophotometer. The neutral, green form of the does not interfere with measurement in the Bradford assay since it has an A_{max} of 650 nm.

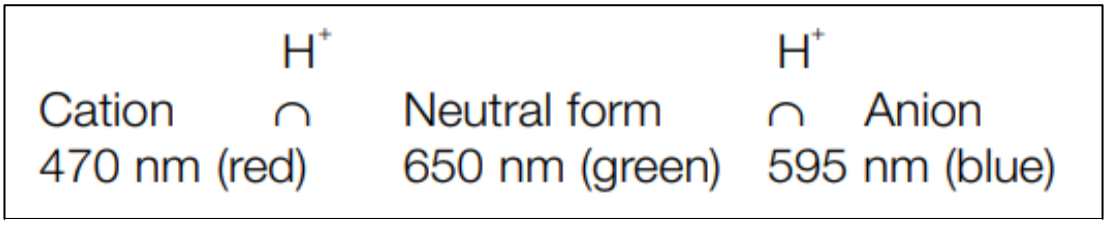

Figure 2.1 Coomassie Brilliant Blue G-250 reaction.

Reagents:

- Bovine Serum Albumin (BSA) (Sigma Aldrich, Dorset, UK) in H_2O
- Bradford Reagent (B6916) (Sigma Aldrich, Dorset, UK)

Method:

The Bradford assay was performed first by generating a standard curve of protein as a standard from a stock solution of BSA (1mg/mL) (Table 2.3).

Twenty microliters of protein standard or tissue homogenates were loaded in triplicate into a 96 well plate. One hundred and eighty microliters of room temperature, Bradford reagent was added to each well. Absorbance was measured using a spectrophotometer (SPECTRO-star Nano, BMG Labtech, Offenburg, Germany) at 595 nm. The protein standard curve was used to quantify the protein content of the samples.

2.5 Western blotting of tissue homogenates for detection of senescence markers

The western blot (sometimes called the protein immunoblot) is a widely used technique to detect specific proteins in a sample homogenate, extract, or lysate (Section 2.4.1).

In brief, the sample undergoes protein denaturation, followed by gel electrophoresis. A synthetic or animal-derived primary antibody was generated that recognises and binds to a specific target protein. The electrophoresis membrane is washed in a solution containing the primary antibody before excess antibody is washed off. A secondary antibody is added which recognises and binds to the primary antibody. The secondary antibody is tagged with a fluorescent protein and is visualised using immunofluorescence in this case, allowing detection of the specific target protein.

2.5.1 Sodium Dodecyl Sulphate-Polyacrylamide Gel Electrophoresis (SDS PAGE)

Reagents:

- Resolving Acrylamide Gel
    - 4x ProtoGel Resolving Buffer (Tris/SDS) (Geneflow, Litchfield, UK)
        - 1.5 M Tris-HCl, 0.4% SDS; pH 8.8
    - ProtoGel Acrylamide (30% Solution at 37.5:1 acrylamide/methylene bisacrylamide solution ratio 10% ammonium persulphate (APS) (Sigma Aldrich, Dorset, UK) in H_2O
    - N,N,N′,N′-tetramethylethylene-diamine (TEMED) (BioRad, Hertfordshire, UK)
- Stacking Acrylamide Gel
    - ProtoGel Stacking Buffer (Tris/SDS) (Geneflow, Litchfield, UK)
    - ProtoGel Acrylamide (30% Solution at 37.5:1 acrylamide/methylene bisacrylamide solution ratio)
    - 10% ammonium persulphate (APS) (Sigma Aldrich, Dorset, UK) in H_2O
    - N,N,N′,N′-tetramethylethylene-diamine (TEMED) (BioRad, Hertfordshire, UK)
- Running Buffer
    - Tris-Glycine 10x Stock
        - 250 mM TRIZMA® base (Sigma Aldrich, Dorset, UK)
        - 2 M Glycine (Sigma Aldrich, Dorset, UK)
        - 1% (w/v) SDS (Sigma Aldrich, Dorset, UK)
    - 4x sample loading buffer

- 20 mM Tris pH 6.8
- 10% (v/v) glycerol
- 2% (w/v) SDS
- 10% (v/v) β-mercaptoethanol

- PageRuler™ Plus Prestained Protein Ladder, 10 to 250 kDa (ThermoFisher, Massachusetts, US)

Method

Protein content of samples was been determined as described in Section 2.4. The 4x sample loading buffer was added to the samples at a 1 in 4 dilution. Samples were then denatured at 95°C for 5 minutes using heating block. Following this, samples thoroughly vortexed and were briefly centrifuged at 12,000 g for 2 minutes to collect to the bottom of the tube.

	10% Resolving Gel	**4% Stacking Gel**
H_2O	4.1 mL	6.1 mL
Acrylamide	3.4 mL	1.3 mL
Resolving Buffer/Stacking Buffer	2.5 mL	2.5 mL
10% APS	100 µL	100 µL
TEMED	10 µL	10 µL

Table 2.4 SDS PAGE formula

Resolving and stacking gels were prepared using the formula described in Table 2.4. Gels were cast using Mini-PROTEAN Tetra Cell Casting Stand & Clamps (BioRad, Hertfordshire, UK). Ten millilitres resolving gel was added to 1.5 mm glass plates to set and 100% ethanol was added on top of the resolving gel to prevent air bubble

formation. Ethanol was removed and 5 mL 4% stacking gel was added and a well comb was inserted.

Gels were placed into a Mini-PROTEAN® Tetra Electrode Assembly (BioRad, Hertfordshire, UK). The tank was filled to the appropriate level with 1x running buffer.

Fifty micrograms of samples were loaded into each well of the gel, 3 µL protein ladders was added to a separate well. Electrophoresis was carried out at 60V for approximately 20 minutes or until samples had reached resolving gel. The voltage was then increased to 120V and electrophoresis continued for an hour or until the loading dye had reached the bottom of the gel. Gels were then transferred onto a nitrocellulose membrane for western blotting, as described in Section 2.5.2.

2.5.2 Western Blotting

Reagents:

- Anode 1 Buffer (pH 10.4)
    - 0.3M Tris (Sigma Aldrich, Dorset, UK)
    - 20% (v/v) Methanol (Sigma Aldrich, Dorset, UK)
    - dH_2O
- Anode 2 Buffer (pH 10.4)
    - 25mM Tris (Sigma Aldrich, Dorset, UK)
    - 20% (v/v) Methanol (Sigma Aldrich, Dorset, UK)
    - dH_2O
- Cathode Buffer (pH 7.6)
    - 40mM 6-amino n hexanoic acid (Sigma Aldrich, Dorset, UK)
    - 20% (v/v) Methanol

- 10x Tris-Buffered PBS (TBS) (pH 7.6) Stock
    - 200 mM TRIZMA® base (Sigma Aldrich, Dorset, UK)
    - 1.4 M NaCl (Sigma Aldrich, Dorset, UK) in dH_2O
    - dH_2O
- Wash Buffer (pH 7.6)
    - 1 in 10 dilution of 10x TBS Stock
    - 0.1% (v/v) polyoxyethylene-sorbitan monolaurate (Tween-20) (Sigma Aldrich, Dorset, UK)
    - dH_2O

Method:

The Geneflow blotting system (Gene flow, Litchfield, UK) comprises of two graphite panels containing electrodes. Whatman No1 filter paper was used as a buffer reservoir. Following electrophoresis, the SDS PAGE gels were removed from the Mini-PROTEAN® Tetra Electrode Assembly (BioRad, Hertfordshire, UK), removed from glass plates; and the stacking gel was discarded. The resolving gel, the filter paper, and the nitrocellulose membrane were assembled as described in Figure 2.2, placed

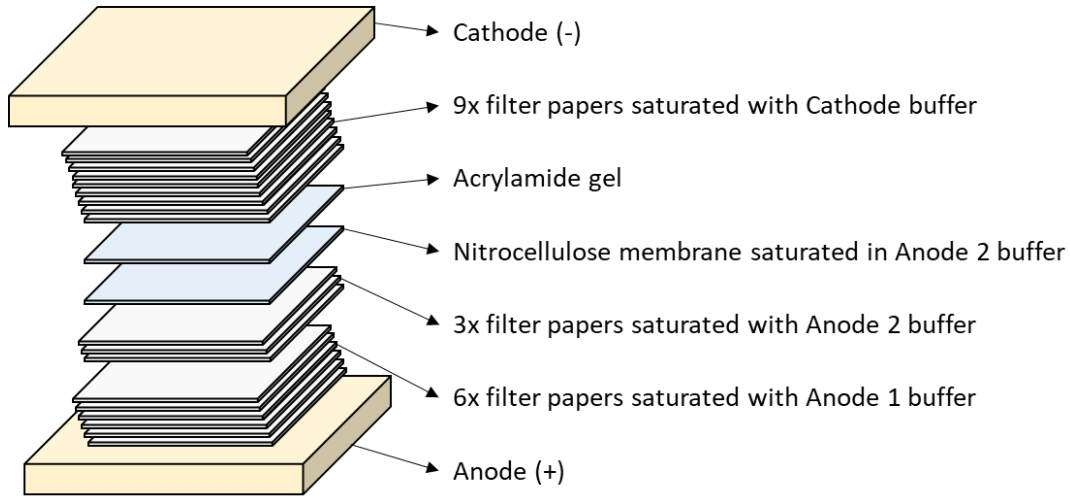

Figure 2.2 Schematic of western blot semi dry transfer assembly.

between the electrode plates and exposed to a current of 0.8mA/cm^2 gel, for 75 minutes. Following transfer, the gel was discarded, and the nitrocellulose membrane was stained with Ponceau S solution (Sigma, Dorset, UK) to ensure equal loading and transfer of proteins. Images of the membrane were recorded using the ChemiDoc imaging system (BioRad, Hertfordshire, UK). The Ponceau S solution was thoroughly removed from the membrane with liberal washes of wash buffer. Membrane could then be used for analysis for specific proteins.

2.5.3 Analysis of membranes for specific proteins

Reagents:

- 10x Tris-Buffered PBS (TBS) (pH 7.6) Stock
    - 200 mM TRIZMA® base (Sigma Aldrich, Dorset, UK)
    - 1.4 M NaCl (Sigma Aldrich, Dorset, UK) in dH_2O
    - dH_2O
- Wash Buffer (pH 7.6)
    - 1 in 10 dilution of 10x TBS Stock
    - 0.1% (v/v) polyoxyethylene-sorbitan monolaurate (Tween-20) (Sigma Aldrich, Dorset, UK)
    - dH_2O
- Blocking buffer
    - 5% milk powder in Wash Buffer
- Primary antibody
    - anti-p21 antibody [EPR3993] (ab109199) (Abcam, Cambridge, UK)
- Secondary antibody

- IRDye® 800CW Goat anti-Rabbit (LI-COR, Cambridge, UK)

Method:

Following a transfer and removal of the Ponceau S staining described in Section 2.5.1, the membrane was then blocked for 1 hour at room temperature using 10 mL blocking buffer containing milk powder. Following this, the membrane was incubated overnight at 4°C with the primary antibodies listed in Section 2.5.5. After this incubation, the membranes were washed 3x5 minutes with wash buffer. The species-specific secondary antibody was added as listed in Section 2.5.5 to the membranes in blocking buffer, for 1 hour at room temperature. After another 3x5 minutes washes with wash buffer, images of the membranes were captured on the LI-COR Odyssey® CLx Imaging System (LI-COR, Cambridge, UK) at the 800nm wavelength.

2.5.4 Western blotting analysis

Following imaging of the membrane, the intensity of each protein band on the membrane was measured using ImageJ software (US National Institutes of Health, Maryland, USA).

2.5.5 List of Primary antibodies

2.5.5.1 H2AX

Rabbit polyclonal antibody to gamma H2A.X (phospho S139) (Abcam, Cambridge, UK) in 0.021% PBS, 1.764% Sodium citrate, 1.815% Tris; 0.1% Sodium azide. Detects a band of approximately 15 kDa. Used at 1 in 1000 dilution.

2.5.5.2 IKBα

Rabbit monoclonal [E130] antibody to IKBα (Abcam, Cambridge, UK) in 40% Glycerol, 0.05% BSA, 0.01% Sodium azide; pH 7.2. Detects a band of approximately 35 kDa. Used at 1 in 1000 dilution.

2.5.5.3 p65

Rabbit monoclonal (D14E12) antibody to NF-κB p65 (Cell Signalling Technology, London, UK) in 10 mM sodium HEPES (pH 7.5), 150 mM NaCl, 100 µg/ml BSA, 50% glycerol; <0.02% sodium azide. Detects a band of approximately 65 kDa. Used at 1 in 1000 dilution.

2.5.5.4 Phosphorylated p65

Rabbit monoclonal (93H1) antibody to Phosphorylated NF-κB p65 (Ser536) (Cell Signalling Technology, London, UK) in 10 mM sodium HEPES (pH 7.5), 150 mM NaCl, 100 µg/ml BSA, 50% glycerol; <0.02% sodium azide. Detects a band of approximately 65 kDa. Used at 1 in 1000 dilution.

2.5.5.5 $p21^{CIP1}$

Rabbit monoclonal [EPR3993] antibody to p21 (Abcam, Cambridge, UK) in 40% Glycerol, 0.05% BSA, 0.01% Sodium azide; pH 7.2. Detects a band of approximately 21 kDa. Used at 1 in 1000 dilution.

2.5.5.6 p53

Mouse monoclonal (D14E12) antibody to p53 (Cell Signalling Technology, London, UK) in 10 mM sodium HEPES (pH 7.5), 150 mM NaCl, 100 µg/ml BSA, 50% glycerol; <0.02% sodium azide. Detects a band of approximately 53 kDa. Used at 1 in 1000 dilution.

2.6 Quantitative PCR for senescence markers

2.6.1 RNA Extraction

Reagents:

- TRIzol™ Reagent (Life technologies, Warrington, UK)
- Chloroform (Sigma Aldrich, Dorset, UK)
- Isopropanol (Sigma Aldrich, Dorset, UK)
- Ethanol (Sigma Aldrich, Dorset, UK)
- RNase-free water (Sigma Aldrich, Dorset, UK)

Method:

To extract RNA, frozen muscle samples were ground into a fine powder under liquid nitrogen using a pestle and mortar. One millilitre of TRIzol™ was added per 50–100 mg of ground tissue to the sample and lysed by passing through a needle and syringe. Samples were then incubated for 5 minutes to permit complete dissociation of the nucleoproteins complex. Chloroform (0.2 mL) was added per 1 mL of TRIzol™ Reagent used for lysis. The tubes were securely capped and incubated for 3 minutes.

Samples were centrifuged for 15 minutes at 12,000g at 4°C. The mixture separates into a lower red phenol-chloroform, and interphase, and a colourless upper aqueous phase. The aqueous phase containing the RNA was transferred to a new tube.

In order to isolate the RNA, 0.5 mL of isopropanol was added to the aqueous phase, per 1 mL of TRIzol™ Reagent used for lysis. Samples were then incubate for 10 minutes followed by centrifugation for 10 minutes at 12,000g and 4°C. Total RNA precipitate forms a white gel-like pellet at the bottom of the tube. Supernatant was

discarded. To wash the RNA, the pellet was resuspended in 1 mL of 75% ethanol per 1 mL of TRIzol™ Reagent used for lysis. The sample was briefly vortexed then centrifuged for 5 minutes at 7500g at 4°C. The supernatant was discarded, and the RNA pellet was left to air dry for 5–10 minutes. Finally, the pellet was resuspended in 20–50µL of RNase-free water heated to 40°C in a heating block. Sample RNA concentration and purity was determine using a Nanodrop (Thermoscientific, Cheshire, UK).

2.6.2 cDNA Synthesis

Reagents:

- iScript cDNA Synthesis Kit (BioRad, Cambridge UK) containing:
    - 5x iScript Reaction Mix
    - iScript Reverse Transcriptase
    - Nuclease free water

Methods:

Component	**Volume per reaction (µL)**
5x iScript Reaction Mix	4
iScript Reverse Transcriptase	1
Nuclease free water	<15
Sample RNA (1µg)	Variable
Total Volume	20

Table 2.5 cDNA synthesis reaction

RNA was isolated and quantified as described in Section 2.6. Samples and reagents were thawed on ice when necessary. CDNA synthesis reactions were generated as described in Table 2.5.

Complete reaction mixes containing RNA template were incubated in a thermal cycler using Table 2.6:

Step	**Duration /Temperature (minutes/°C)**
Priming	5 min/25°C
Reverse transcription	20 min/46°C
RT inactivation	1 min/95°C
Hold	Hold/4°C

Table 2.6 cDNA thermal cycler settings

2.6.3 Quantitative PCR

Reagents:

- cDNA
- Sybrgreen master mix (Thermoscientific, Cheshire, UK)
- Primers (Invitrogen, Cheshire, UK)

Methods

cDNA was diluted 1 in 40 with RNAse free water and 3µl of diluted cDNA was added into 96 well plates. A master mix consisting of 5 µL of Sybrgreen, 1µL of forward primer and 1 µL of reverse primer was prepared for each sample and 7 µL were added to cDNA). Plates were then sealed, pulse centrifuged for 5 seconds and placed in the

thermal cycler (Starlab, Hertfordshire, UK) for thermo cycling (Table). Forty cycles were performed.

2.7 Multiplex Cytokine Analysis

For multiplex cytokine analysis, the Luminex Bio-Plex Multiplex immunoassay kit (BioRad, Hertfordshire, UK) was used. The Luminex is a colour coded, magnetic bead based multiplex assay that measures multiple cytokines, chemokines, and growth factors in a single sample.

The basic principle behind the technique is the same as those use in normal sandwich ELISAs or western blotting. The beads used in the assay are fused to a specific primary antibody. The biomarker or target of interest is bound by the specific primary antibody, which in turn is bound by a biotinylated secondary detection antibody. This complex is then detected by a streptavidin-phycoerythrin (PE) conjugate (Figure 2.3).

The magnetic, fluorescent 5.6 µm beads on which all these complexes form are detected by the Bio-Plex 200 system (BioRad, Hertfordshire, UK). The flow cytometry-based system uses dual lasers: one at 635 nm to classify the beads unique fluorescent coating and determine which analyte is being detected. The second laser set at 525 nm defines the magnitude of the PE-derived signal, which is directly proportional to the amount of analyte bound (Figure 2.3).

The beads are coloured using a proprietary mix of an infrared and a red coloured dye. The distinct colouring can readily generate bead sets with a unique combination of the dyes used. Fluorescent excitation of the beads with one wavelength of light generates two observable emissions wavelengths, which differ between the different

bead's sets used. By combining each unique bead set with a specific antibody, the assay allows for high throughput multiplexing.

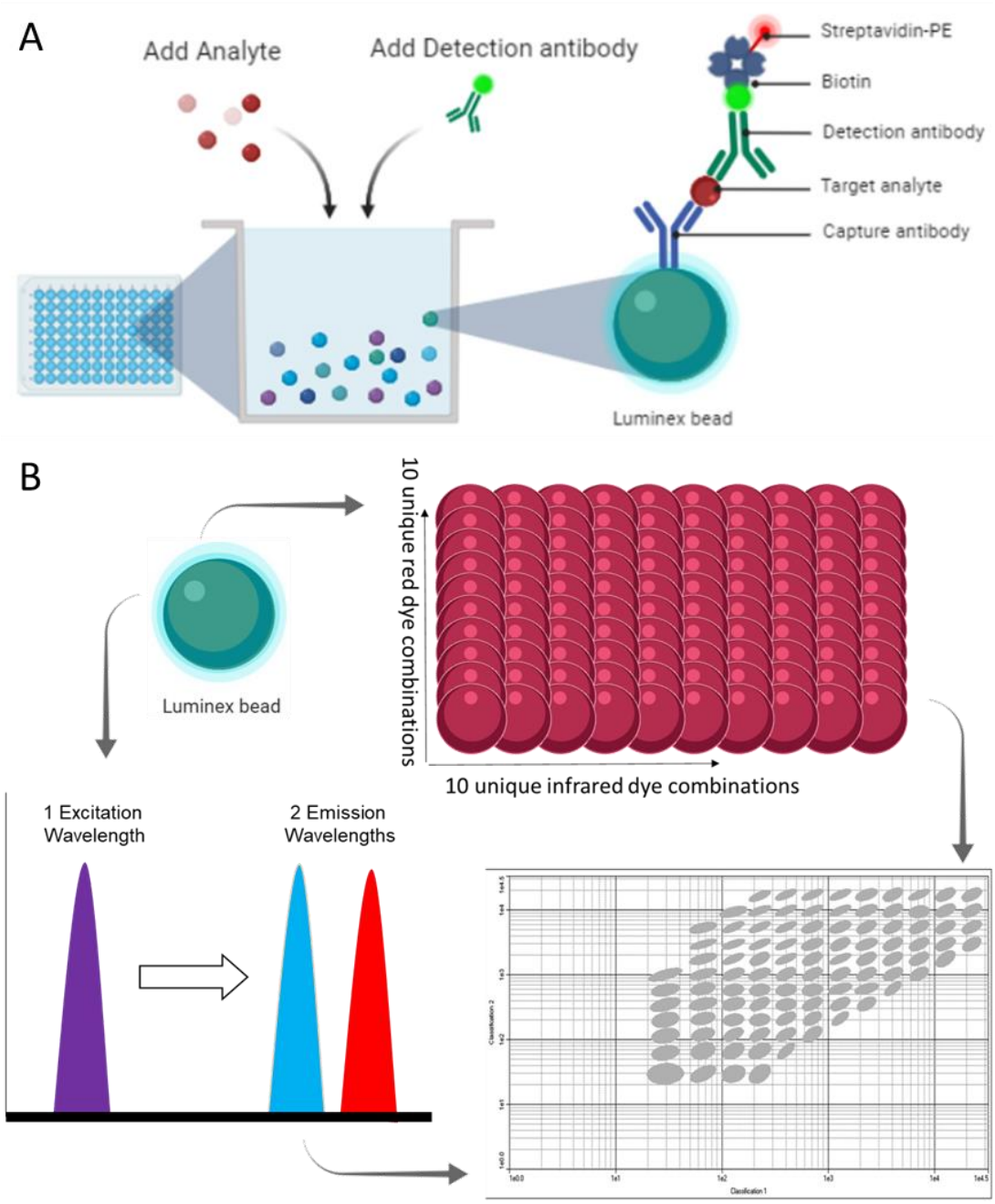

Figure 2.3 Overview of Luminex Assay.

(A) A visual representation of how the beads capture specific analytes and complexes with them to yield a fluorescent signal. (B) The dual lasers of the flow cytometer analyse the bead profile and fluorescence intensity, yielding a specific target and concentration. Reproduced from BioRad product information page.

Reagents:

- Bio-Plex® Pro™ Mouse Cytokine 23-plex Assay (#M60009RDPD) containing:
    - Coupled magnetic beads (10x)
    - Detection antibodies (10x)
    - Lyophilised cytokine standards
    - Detection antibody diluent HP
    - Standard diluent
    - Assay buffer
    - Wash buffer (10x)
    - Streptavidin-PE (100x)
    - 96 well, flat bottom, black assay plate

Method:

Senescent C2C12 myoblast was prepared as described in Section 2.2.1. The media was collected from the myoblasts and stored at -80°C. Lyophilised standards provided were reconstituted in 250 µL cell culture medium. Standard was vortexed for 5 seconds then incubated on ice for 30 minutes. A seven-point standard curve was prepared as described in Table 3.4. Culture medium was used as a diluent to match the samples. The 10x magnetic beads were vortexed thoroughly for 30 seconds. For a 96 well plate, 570 µL of the 10x magnetic coupled beads was diluted 1 in 10 in assay buffer. The 1x magnetic bead solution was stored on ice in foil. The 1x bead solution was vortexed for 30 seconds and 50 µL was added to each well. The plate was placed onto the magnetic plate holder and washed twice by adding 100 µL of 1x wash buffer to each well. Fifty microliters of the standards, blank, and samples were loaded on to

the plate, vortexing thoroughly throughout. The plate was sealed and placed on a plate shaker at 850 ± 50 RPM for 30 minutes at room temperature. The Detection antibodies (10x) were prepared by vortexing the 10x detection antibody stock bottle for 20 seconds followed by a 30 second centrifugation to collect the entire reagent. For a 96 well plate, 300 µL of the 10x detection antibody stock was diluted 1 in 10 in detection antibody diluent. The plate was washed three times and 25 µL of the 1x detection antibody solution was added to each well. The plate was placed on the shaker at 850 ± 50 RPM for a further 30 minutes at room temperature. The 1x Streptavidin-PE (SA-PE) solution was prepared by vortexing the 100x SA-PE stock solution for 5 seconds followed by a 30 second centrifugation to collect the entire solution. Sixty microlitres of the 100x SA-PE stock was diluted in 1 in 100 in assay buffer; and kept away from light. The plate was washed three times and 50 µL of the 1x SA-PE solution was added to each well. The plate was placed on to the shaker at 850 ± 50 RPM for a further 10 minutes at room temperature. Finally, the SA-PE was discarded, and the plate was washed three times and 125 µL of Assay buffer was added to each well. The plate was placed back on a plate shaker at 850 ± 50 RPM for 30-seconds before absorbance was determined on the Bio-Plex 2000 system (BioRad, Hertfordshire, UK).

Standard	Volume of Diluent (µL)	Volume and Source (µL)
S1	0	250 of reconstituted standard
S2	150	50 from S1
S3	150	50 from S2
S4	150	50 from S3
S5	150	50 from S4
S6	150	50 from S5
S7	150	50 from S6
Blank	150	0

Table 2.7 Preparing a fourfold dilution series for the Luminex

2.8 Electromobility Shift Assay (EMSA) for NF-κB transcription factor activity

An electrophoretic mobility shift assay (EMSA) (AKA: mobility shift electrophoresis, gel shift assay, gel mobility shift assay, band shift assay, or gel retardation assay) is an electrophoresis technique used to study protein/DNA or protein/RNA interactions. EMSAs can be used to identify sequence-specific, DNA-binding proteins (such as transcription factors) in crude lysates and, in conjunction with mutagenesis, to identify the important binding sequences within the upstream regulatory region of a given gene.

The current, modern form of the assays differs little from the original protocols described by Fried and Crothers (1981), and Garner and Revzin (1981). There are also precursors to this technique in earlier literature (Eisinger, 1971, Chelm and Geiduschek, 1979, Varshavsky et al., 1976).

Reagents:

- Extraction buffer (pH 7.9):
    - 25% (v/v) glycerol
    - 0.42M NaCl
    - 1.5mM $MgCl_2$
    - 0.2mM EDTA
    - 0.5mM dithiothreitol (DTT)
    - 0.5mM Phenylmethylsulphonyl fluoride (PMSF)
    - 20mM HEPES (N-2-hydroxyethylpiperazine -N'-2-ethanesulfonic acid)
- EMSA Gel Solution
    - 5 mL 40% Acrylamide: bis-Acrylamide (29:1) solution (BioRad, Hertfordshire, UK)
    - 2 mL, 1 M Tris, pH 7.5
    - 7.6 mL 1 M Glycine
    - 160 µL 0.5 M EDTA, pH 8.0
    - 26 mL dH_20
    - 200 µL 10% APS
    - 30 µL TEMED
- Binding Reactions
    - 10x binding buffer
        - 100 mM Tris, 500 mM KCl, 10 mM DTT; pH 7.5
    - 25 mM DTT, 2.5% Tween-20
    - Poly (dI-dC) 1 µg/µL in 10 mM Tris, 1mM EDTA; pH 7.5
    - 100 mM $MgCl_2$
    - 200 mM EDTA, pH 8.0

    - 50% Glycerol
    - 50 nM NF-κB Oligo (IRDye® 700) (LI-COR, Cambridge, UK)
    - dH_2O
- 10x Orange loading dye (LI-COR, Cambridge, UK)
- 10x TBE Stock
    - 1 M Tris base
    - 0.9 M Borate
    - 10 mM EDTA (pH 8.0)
    - dH_20

Method:

Protein extracts of cells were prepared according to the method described Mosser et al. (1988). C2C12 cell pellets or ground muscle powder (Section 2.4.1) were lysed in the extraction buffer, sonicated, and centrifuged at 10,000g for 10 minutes at 4°C (Eppendorf Centrifuge 5402, London, U.K.). The supernatants were then removed, rapidly frozen in liquid nitrogen and stored at -80°C for future analysis. The protein content of supernatants was determined via Bradford assay as DTT interferes with the BCA assay (Brown et al., 1989).

The EMSA was performed using the Hoefer® SE400 Air-Cooled Vertical Protein Electrophoresis Unit (ThermoFisher, Manchester, UK). EMSA gel solution was prepared and was poured between two glass plates (18x16 cm) in clamp assemblies, a 1.5 mm thick comb was placed between the plates and the gels set.

Sample lysates were mixed with an equal volume of EMSA binding reaction, described in Table 2.8. Samples were incubated with the binding reaction at room temperature in the dark for 30 minutes. Following the incubation, 2 µL Orange loading dye was added to each sample and loaded into the EMSA gel. The electrophoresis chamber was covered in foil to prevent bleaching of the fluorophores. Electrophoresis was performed at 160V for 90 minutes, at 4°C. The bands were imaged on the LI-COR Odyssey® CLx Imaging System (LI-COR, Cambridge, UK).

	Volume (µL)
10x binding buffer	2
25 mM DTT, 2.5% Tween-20	2
Poly (dI-dC) 1 µg/µL in 10 mM Tris, 1mM EDTA; pH 7.5	1
100 mM $MgCl_2$	1
200 mM EDTA, pH 8.0	1
50 nM NF-κB Oligo (IRDye 680)	1
dH_2O	2
Protein extract + dH_2O	10

Table 2.8 EMSA binding reaction

2.8.1 Competition and Supershift experiments

To verify that the results from gel shift mobility assay do not arise from non-specific binding of probes to protein/DNA complexes, competition experiments and supershift assays were performed.

Figure 2.4 illustrates the potential bands detected during an EMSA and supershift assays. In supershift experiments, the addition of antibodies to the reaction is used to determine the identity, as well as the specificity of the binding protein. If the antibody recognizes the DNA-protein complex, the antibody can bind and produce a 'heavier' labelled band (supershift band). Since the extra mass of the antibody will result in slower migration in the gel than the original DNA-protein complex, thus "shifting" the band up the gel. Competition analyses take two forms: specific and non-specific. In the specific reactions, the unlabelled competitor DNA is an identical sequence as the original labelled probe. For non-specific reactions, DNA fragments or oligonucleotides with different sequences from the original probe are used. Thus, if the band is specific, the addition of the unlabelled, specific competitor should decrease the intensity of the band. The addition of the unlabelled, non-specific competitor should leave the specific band unchanged.

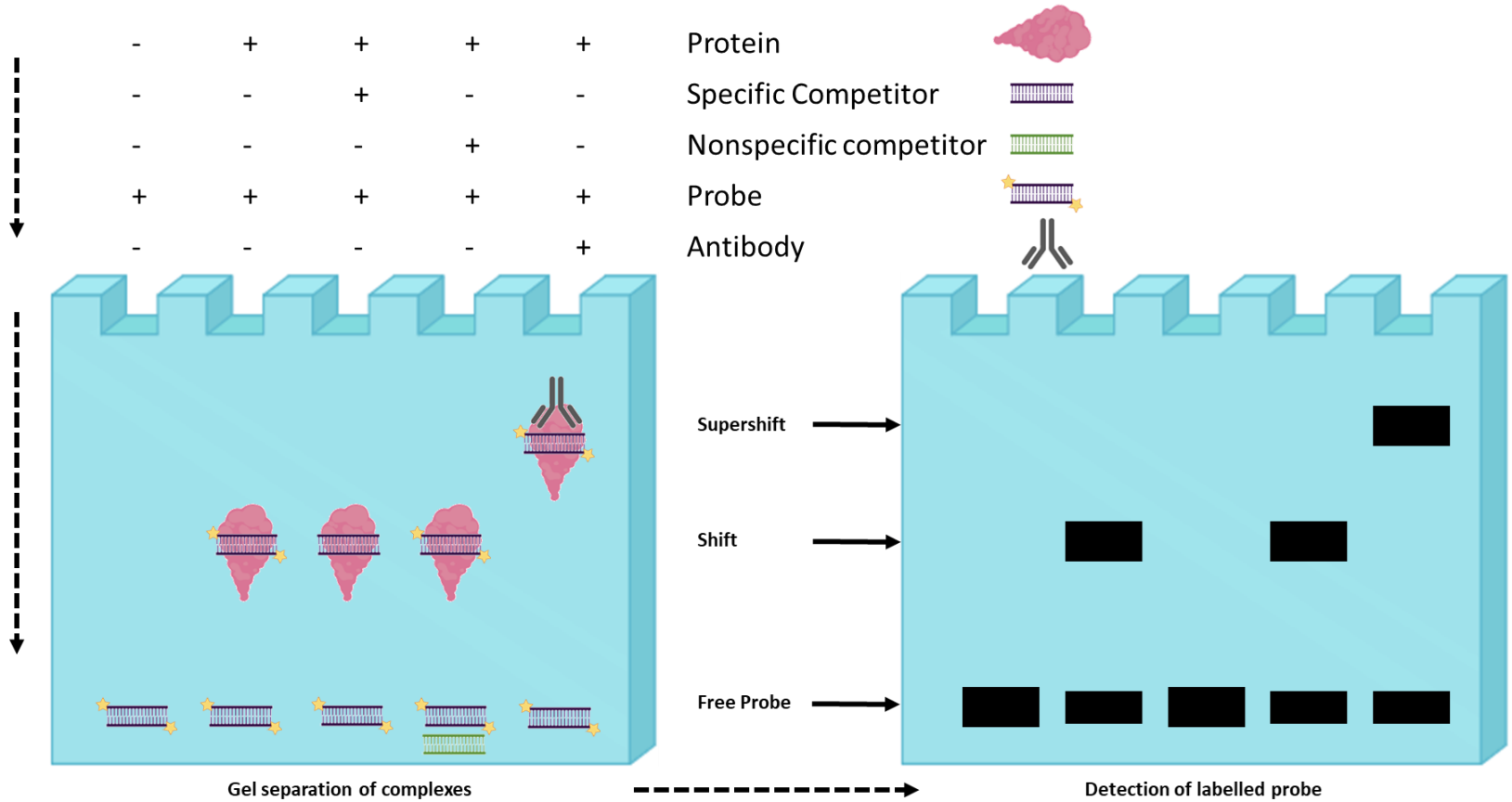

Figure 2.4 Overview of the gel shift assay method.

Protein/DNA complexes are detected using fluorescent DNA probes for specific transcription factors. Addition of antibody specific to protein complex of interest increases the mass of the sample, reducing its ability to migrate through the gel.

2.9 Gene Ontology Term Analysis

WebGestalt (2019 release) was used to perform the Overrepresentation Enrichment Analysis for each of the gene ontology categories (Biological Process, Cellular Component and Molecular Function). The list of mouse genes was analysed against the reference option of genome. The significance level was FDR<0.05 and the multiple test adjustment was done using the Benjamini–Hochberg method.

To help better visualize the GO terms obtained from the analysis above described, the tool REViGO was used. The p-values here considered were the FDR values obtained previously, with the *mus musculus* database option used for the GO terms.

2.10 Statistics

Graphs were plotted and statistics were calculated with GraphPad Prism® Version 6.5. Data are expressed as mean ± standard error of the mean (SEM). *P < 0.05. Grubbs test was used when appropriate to identify outliers within the sample population. Column statistics were then used on the data set to identify normality.

Chapter 3: An *In vitro* Model of Cellular Senescence in C2C12 Muscle Myoblasts

3.1 Introduction

3.1.1 Cellular Senescence

The first introduction to, and demonstration of cellular senescence was led by Hayflick and Moorhead (1961), describing Replicative Senescence (RS), one of the methods of inducing cellular senescence in cells. There are several ways of inducing cellular senescence, not linked to proliferation dependent telomere shortening demonstrated by Hayflick and Moorhead (1961). Many proliferative cell types can undergo stress-induced premature senescence (SIPS) upon exposure to damaging but non-lethal stresses (UV light, ionizing radiation, H_2O_2, hyperoxia, etc.) (Toussaint et al., 2000b), and oncogene-induced senescence (OIS) which is a senescent phenotype that depends on the activation and/or overexpression of oncogenes (Serrano et al., 1997).

This study focuses on the use of etoposide (Section 1.1.3.2) to induce a stress-induced premature senescence (SIPS) (Section 1.1.3.3) via DNA damage, triggering a DNA-damage response (DDR) (Section 1.1.3.3) (von Zglinicki, 2002).

3.1.2 Etoposide and the DNA Damage Response

Etoposide induces of senescence (Section 1.1.3.2). Etoposide forms complexes with DNA and the topoisomerase II enzyme, used to unwind DNA during mitosis. Complexes of etoposide/topoisomerase II prevents unwinding and the subsequent re-ligation of the DNA strands; causing DNA strands to break (Pommier et al., 2010). The resulting DNA damage response results in a permanent cell cycle arrest and cellular senescence (Section 1.1.3.3).

DNA damage can be in the form of single or double strand breaks (DSBs) which activates the DDR and triggers DNA repair or cell cycle arrest (Zou, 2007). DNA DSBs have been shown to both indirectly and directly promote the phosphorylation and activation of p53, a key protein in cell cycle arrest (Saito et al., 2002).

3.1.3 The Role of Cell dependant Kinase Inhibitors in Cell Cycle Arrest

One of the hallmarks of a senescent cell is that they enter a metabolically active state of permanent growth arrest, triggered by the p53/p21 and/or $p16^{INK4A}$/Rb tumour suppressive pathways; downstream of the DDR pathway (Section 1.1.3.3).

Tumour protein 53 (TP53, or p53), is a gene that codes for a protein that regulates the cell cycle and functions as a tumour suppressor. The p53 protein has been shown to increase during cellular senescence (Serrano et al., 1997). When phosphorylated, p53 stimulates the expression of numerous genes that regulate cell cycle arrest and/or promote cellular senescence. An example of which is p21, which p53 transcriptionally upregulates by direct promoter binding of the CDKN1A gene (Tahara et al., 1995).

$p21^{Cip1}$, also known as $p21^{Waf1}$, cyclin-dependent kinase inhibitor 1, or CDK-interacting protein 1; is a cyclin-dependent kinase (CDK) inhibitor (CDKI) triggers G1-phase cell cycle arrest by inhibiting the cell cycle regulatory kinases CDK4 and CDK2 (He et al., 2005).

Phosphorylation of p53 also results in increased transcription of $p16^{INK4A}$ (Serrano et al., 1997). Upregulation of $p16^{INK4A}$ leads to the prevention of Retinoblastoma (Rb) phosphorylation, resulting in inhibition of E2F-dependent transcription. E2F are a group of genes that encode a family of transcription factors in mammalian cells, all

of which are involved in the cell cycle regulation (Serrano et al., 1997). The cell does not progress from G1 phase into S phase, resulting in cell cycle arrest.

Furthermore, to ensure the stable repression of E2F-target genes and cell cycle arrest, Rb promotes heterochromatin formation at E2F-regulated gene promoters. The E2F gene promoters are epigenetically silenced, in a process called Senescence-Associated Heterochromatin Foci (SAHF) formation (Narita et al., 2003); a marker of senescence.

3.1.4 Markers of cellular senescence

Senescent cells are diverse; dependant on the cell type of methods used to induce senescence, and the cell type (Wiley et al., 2017). None of the current markers are completely specific for senescence and are used in combination to characterise cellular senescence. Several markers of senescence were described in Section 1.1.1, which include:

- Changes in morphology
- Cell cycle arrest/absence of proliferative markers
- Expression of Senescence-associated β-galactosidase (SA-β-gal) activity
- Changes in Chromatin structure (Senescence Associated Heterochromatin Foci [SAHF])
- Production of Senescence associated secretory phenotype (SASP).

3.1.5 The Senescence Associated Secretory Phenotype (SASP) produced by senescent cells *in vivo*: role in the development of sarcopenia

Senescent cells can have both a positive and negative role *in vivo*; primarily implemented via the senescence associated secretory phenotype (SASP), which has also been called the senescence messaging secretome (SMS) (Section 1.1.5).

The SASP can have a detrimental effect on normal physiology and results in pathology, an example of which may be sarcopenia. Studies show that senescent cells can induce senescence in neighbouring cells through paracrine mechanisms: (Acosta et al., 2013, Nelson et al., 2012, Faggioli et al., 2012). This SASP mediated effect has been called the bystander effect (Nelson et al., 2012, von Zglinicki et al., 2020). Muscles from both old mice and humans have been shown to accumulate $p16^{INK4a}$ and SA-β-gal positive cells (Sousa-Victor et al., 2014, von Zglinicki et al., 2020), with a reduced regenerative capacity (Bernet et al., 2014). Inactivation of $p16^{INK4a}$ in transgenic mice rejuvenates aged satellite cells and promoted muscle regeneration upon injury (Cosgrove et al., 2014) (Section 1.1.7). Clearance of $p16^{INK4a}$ expressing satellite cells also ameliorated sarcopenia in a mouse model (Baker et al., 2011) (Section 1.1.7). This highlights that senescent satellite cells may be detrimental in the context of sarcopenia.

3.1.6 The role of NF-κB in the Senescence Associated Secretory Phenotype of senescent cells

Several studies have clearly demonstrated that NF-κB plays a significant role in the mRNA expression of most SASP factors (e.g. IL-6 and CXCL1) in several models of senescence (Reviewed by Malaquin et al. (2016)). In normal, stress-free conditions,

NF-κB is inhibited by its interaction with cytoplasmic IκB, preventing nuclear translocation. In stressed conditions, IκB kinase (IKK) initiates the degradation of IκB, allowing for nuclear accumulation and post translational modifications (e.g. phosphorylation, acetylation) of NF-κB. Ultimately resulting in NF-κB activation (Karin, 1999). The molecular mechanisms leading to NF-κB activation in the context of senescence remain poorly defined. Work by Acosta et al. (2008) suggests that the SASP may act in an autocrine feedback loop to reinforce growth arrest.

3.1.7 Hypothesis

The hypothesis was that senescent cells accumulate in muscle during ageing. The proinflammatory SASP activates NF-κB in old muscles which then contribute to the pro-inflammatory phenotype of the mouse. The nature of senescent cells in unclear but it was hypothesised that mononuclear myoblasts present in muscles can express senescence markers and that these cells have a detrimental effect on mature muscle cells.

This hypothesis was tested by inducing and characterising senescence in C2C12 myoblasts as a proof of principle. Furthermore, C2C12 myotubes will be treated with the conditioned media containing the SASP from the senescent cells to investigate the effect on activation NF-κB activity in multinuclear myotubes.

3.2 Methods

3.2.1 Inducing cellular senescence in C2C12 myoblasts

C2C12 myoblasts were seeded into 12 well plates and treated as described in Section 2.2.1. Briefly, myoblasts were seeded into 12 well plates at $5x10^3$ cells per well and incubated at 37°C in a humidified 5% CO_2/95% air incubator overnight to adhere. Etoposide powder (Sigma, E1383) was reconstituted in Dimethyl Sulfoxide (DMSO) to a concentration of 100 mM, and this was diluted 1 in 10 to a stock concentration of 10mM in growth media. Myoblasts were then treated with different concentrations (30-3.75µM) of etoposide or DMSO carrier control in growth media for 24 hours and incubated appropriately. Etoposide or DMSO control containing media was then removed and replaced with standard growth media and further incubated for up to 5 days. Cells were monitored daily to check for progression of senescent morphology, using a light (Nikon Diaphot, Tokyo, Japan) microscope.

3.2.2 Viability of etoposide treated C2C12 myoblasts

C2C12 myoblasts were seeded into 12 well plate and treated as described in Section 2.2.1. Cell viability was determined using a LIVE/DEAD© reduced Biohazard Viability/Cytotoxicity Kit (Molecular Probes, UK) as described in Section 2.3. Cells were counted in 3 fields of view, in 3 unique wells, at a 10x magnification for each treatment, and quantified.

3.2.3 Proliferation of etoposide treated C2C12 myoblasts

C2C12 myoblasts were seeded into 6 well plate and treated as described in Section 2.2.1. Treated C2C12 myoblasts in a 6 well plate well were aspirated from the well using trypsin as described in Section 2.2.5, 1-5 days post treatment. The initial

number of seeded cells was used to signify day 0 ($1x10^4$). Cells were counted using Trypan blue and the cell number plotted over time.

3.2.4 Senescence Associated β-Galactosidase staining of cells

C2C12 myoblast were seeded and treated as described in Section 2.2.1. SA-β-gal detection was performed using the Senescence β-Galactosidase Staining Kit (Cell Signalling Technologies, #9860) (Section 2.3.2). C2C12 myoblasts were immersed and incubated at 37°C overnight, in a low CO_2 environment. The staining solution was then removed, cells were rinsed with DPBS and imaged under a light microscope (Nikon Diaphot, Tokyo, Japan). Cells were counted in 3 fields of view, in 3 unique wells, at a 10x magnification for each treatment, and quantified.

3.2.5 Western blotting for markers of senescence in C2C12 myoblasts

C2C12 myoblasts were seeded into 6 well plates and treated as described in Section 2.2.1. The cells were aspirated form the wells using trypsin and lysed as described in Section 2.4.1 and protein concentrations quantified as described in Section 2.4.2. Samples were then denatured and loaded onto acrylamide gels and proteins resolved, as described in Section 2.5.1. Following transfer of proteins to a nitrocellulose membrane using the Geneflow blotting system (Section 2.5.2), membranes were blocked in 5% milk and incubated with primary antibodies (Table 3.1) at 4°C overnight. Membranes were washed 3x5 minutes and incubated with the secondary antibody (Table 3.1) for 1 hour at room temperature. Membranes were then washed for 3x5 minutes and images of the membranes were captured on the LI-COR Odyssey® CLx Imaging System (LI-COR, Cambridge, UK) at a wavelength of

800nm.

3.2.6 Immunofluorescent analysis of senescence markers in etoposide treated C2C12 myoblasts

C2C12 myoblasts were seeded into 12 well plate and treated as described in Section 2.2.1. Fluorescent staining of the C2C12 cells was performed as described in Section 2.3.3.

Primary Antibody Target	Dilution in 5% milk	Secondary antibody	Secondary antibody dilution
P65	1 in 1000	IRDye® 800CW Goat anti-Rabbit (LI-COR, Cambridge, UK)	1 in 15,000
p53	1 in 1000	IRDye® 800CW Goat anti-Mouse (LI-COR, Cambridge, UK)	1 in 15,000
p21	1 in 1000	IRDye® 800CW Goat anti-Rabbit (LI-COR, Cambridge, UK)	1 in 15,000
p16	1 in 1000	IRDye® 800CW Goat anti-Rabbit (LI-COR, Cambridge, UK)	1 in 15,000
IKBα	1 in 1000	IRDye® 800CW Goat anti-Rabbit (LI-COR, Cambridge, UK)	1 in 15,000

Table 3.1 Antibody dilutions for western blotting of senescence markers in C2C12 cells

3.2.7 Multiplex cytokine analysis of the media from etoposide treated C2C12 myoblasts

C2C12 myoblasts were seeded into 6 well plates and treated as described in Section 2.2.1. The media from these cells were collected and analysed for cytokine content by Luminex, as described in Section 2.7. Cytokine values were normalised to the protein content of the wells, which was analysed by protein quantification (Section 2.4).

3.2.8 Analysis of myotubes treated with SASP from senescent myoblasts: effect on Electromobility Shift Assay (EMSA) for NF-κB transcription factor activity and myotube diameter

C2C12 myoblasts and myotubes were seeded into several plates as described in Section 2.2.3. Myotubes were treated with media collected from senescent and control myoblasts. The treated myotubes were analysed by EMSA, as described in Section 2.8. The bands were quantified as described in Section 2.5.4. for determination or myotube diameter, images of myotubes were taken at 10x magnification using a light microscope (Nikon Diaphot, Tokyo, Japan). Myotubes in the field of view were analysed using Image J (US National Institutes of Health, Maryland, USA). For each image, myotubes were traced and the minimum Ferets diameter was measured. Measurements for approximately 20 single myotubes from 6 wells were pooled to give an average value per condition.

3.3 Results

3.3.1 Viability of etoposide treated C2C12 myoblasts

Figure 3.1 shows fluorescent images of C2C12 myoblasts treated with 3.75 µM (B), 7.5 µM (C), 15 µM (D), and 30 µM (E) etoposide; as well as those treated with DMSO vehicle control (A) for 24 hours. C2C12 myoblasts treated with etoposide showed a dose dependant loss of viability following treatment with increasing concentrations of etoposide for 24 hours. Quantification of viable cells (F) showed a significant loss of viability when cells were treated with 15 µM and 30 µM etoposide, when compared with DMSO treated control cells ($P<0.05$). No significant effect on viability was seen when cells were treated with the lower concentrations of etoposide (3.75 µM and 7.5 µM) when compared to the DMSO treated control cells.

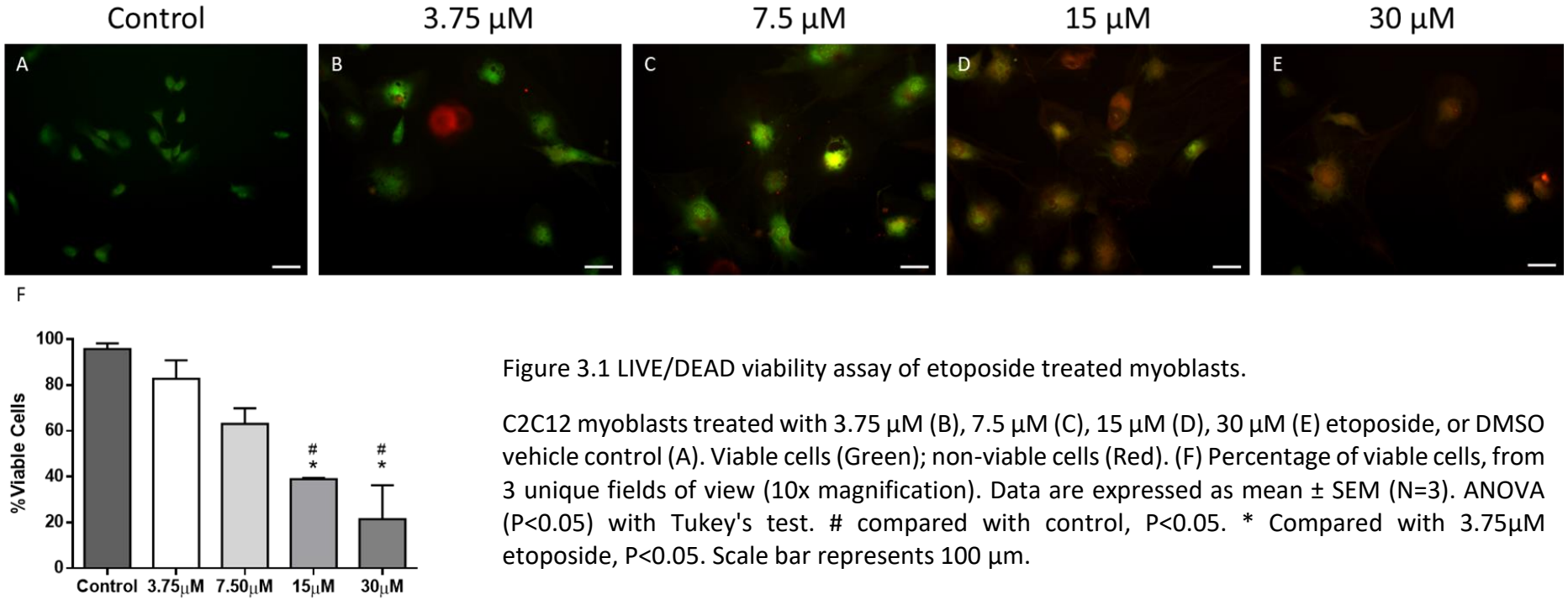

Figure 3.1 LIVE/DEAD viability assay of etoposide treated myoblasts.

C2C12 myoblasts treated with 3.75 µM (B), 7.5 µM (C), 15 µM (D), 30 µM (E) etoposide, or DMSO vehicle control (A). Viable cells (Green); non-viable cells (Red). (F) Percentage of viable cells, from 3 unique fields of view (10x magnification). Data are expressed as mean ± SEM (N=3). ANOVA ($P<0.05$) with Tukey's test. # compared with control, $P<0.05$. * Compared with 3.75µM etoposide, $P<0.05$. Scale bar represents 100 µm.

3.3.2 Proliferation of etoposide- and DMSO-treated C2C12 myoblasts

Figure 3.2 shows the cell number of C2C12 myoblasts treated with 3.75 µM etoposide or DMSO vehicle control for 24 hours, analysed for a further 5 days of culture. Myoblasts treated with DMSO increased in cell number, peaking at 3 days of culture. The myoblasts treated with etoposide did not increase in cell number following treatment. Treatment of myoblasts with etoposide for 24 hours appeared to halt cellular division permanently when compared with DMSO treated controls since cell division did not return following removal of etoposide. Thuds, a significant difference in total cell number were seen at 3 days following-etoposide treatment when compared with the equivalent time point in the DMSO control cells ($P<0.05$).

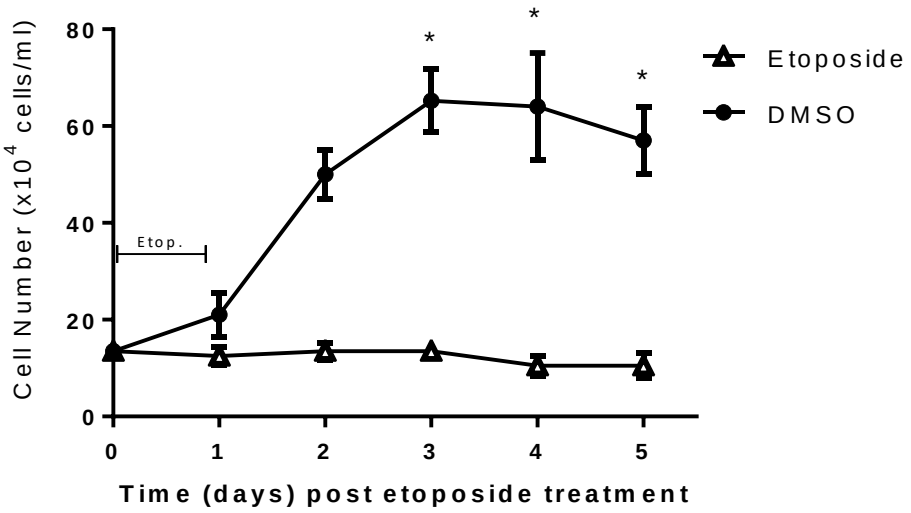

Figure 3.2 Cell number of C2C12 myoblasts treated with etoposide.

C2C12 myoblasts treated with 3.75 µM etoposide or DMSO for 24, and cell number was measured across 5 days of culture. Data are expressed as mean ± SEM. ANOVA ($P<0.05$) with Tukey's test. * $P<0.05$.

3.3.3 SA-β-gal activity of etoposide- and DMSO- treated C2C12 myoblasts

Figure 3.3 shows representative bright field images of DMSO treated control C2C12 myoblasts and myoblasts stained for SA-β-gal activity after 5 days after treatment with 3.75 μM (B), 7.5 μM (C), 15 μM (D), and 30 μM (E) etoposide. Blue pigments show positive staining. Quantified number of SA-β-gal positive cells are shown in (F).

Treatment with etoposide resulted in a substantial increase in SA-β-gal staining, whereby approximately 35% of the etoposide treated cells showed SA-β-gal staining, whereas the DMSO control cells showed no detectable activity. Little difference in the number of positive cells was seen between the different concentrations of etoposide treatment used. Furthermore, changes in the morphology of etoposide treatment myoblasts, compared with DMSO treated, or untreated control cells were evident in Figure 3.1 and Figure 3.3. The etoposide treated cells had a flatter appearance and covered a larger surface area.

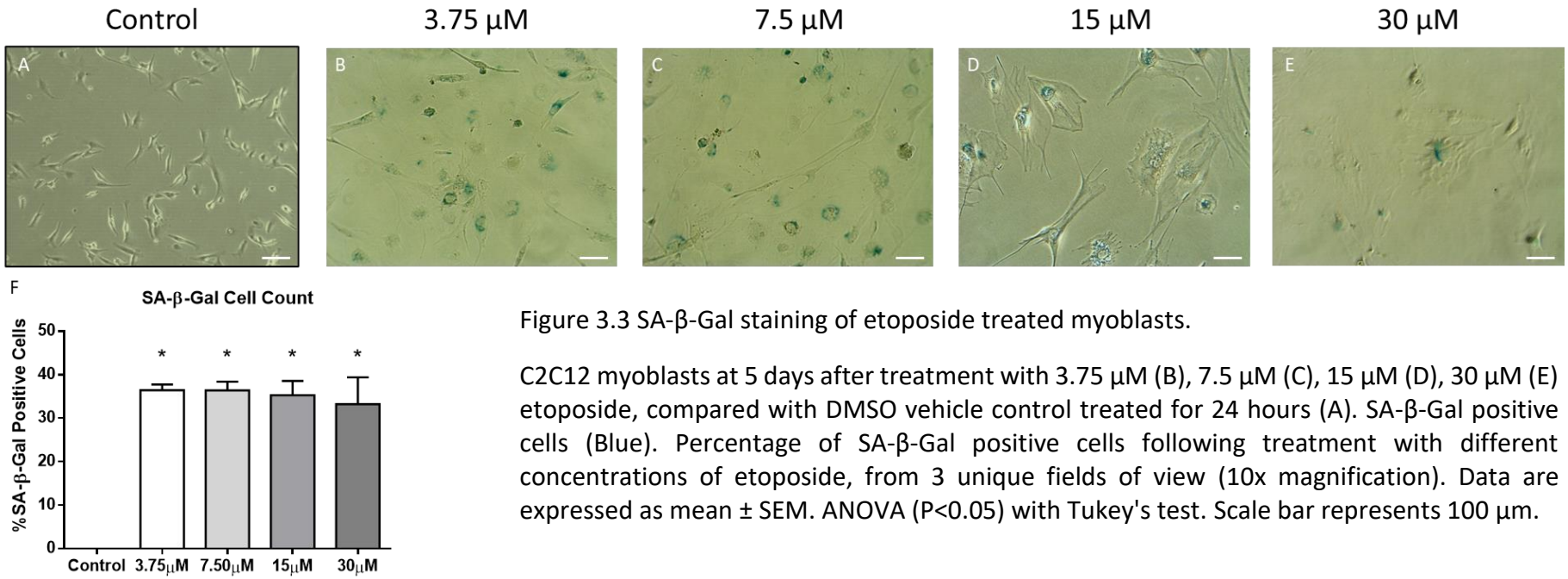

Figure 3.3 SA-β-Gal staining of etoposide treated myoblasts.

C2C12 myoblasts at 5 days after treatment with 3.75 µM (B), 7.5 µM (C), 15 µM (D), 30 µM (E) etoposide, compared with DMSO vehicle control treated for 24 hours (A). SA-β-Gal positive cells (Blue). Percentage of SA-β-Gal positive cells following treatment with different concentrations of etoposide, from 3 unique fields of view (10x magnification). Data are expressed as mean ± SEM. ANOVA ($P<0.05$) with Tukey's test. Scale bar represents 100 µm.

3.3.4 Detection of senescence markers in etoposide treated C2C12 myoblasts

Figure 3.4 shows the protein levels of the senescence markers: p53, p21, and p16; in untreated C2C12 myoblasts and in cells at 1, 3, or 5 days after 24-hours of treatment with 3.75 μM etoposide, or DMSO treated controls. Inflammation markers p65 and IKBα were also investigated. Etoposide treated myoblasts showed elevated levels of p21 following treatment, at 3 days following treatment. The IKBα protein levels decreased following etoposide treatment, suggesting this as a mechanism of NF-κB activation. The proteins p65, p53, and p16 were not consistently detected in any sample (positive control was excluded, data not shown).

Figure 3.5 shows the localisation of p21 in the nuclei of etoposide treated C2C12 myoblasts, which was absent in the untreated control cells. Some localization of p21 was also seen in the DMSO treated control cells. Etoposide treated cells showed an altered morphology, a larger flattened shape compared with the untreated or DMSO control myoblasts. The etoposide treated cells also showed a larger nuclear space, with punctate DAPI staining, which was absent in untreated or DMSO treated cells. In agreement with the western blot analysis, control untreated cells contain low levels of p21 and evidence of positively stained cells was rare by immunostaining. In contrast, DMSO treatment resulted in some non-significant increase in p21 levels (Figure 3.4) and some increased p21 staining; particularly in the cells that seem to have begun to fuse into myotubes at the 5 day time point (Figure 3.5), although this was not as evident as the increase seen in etoposide treated myoblasts.

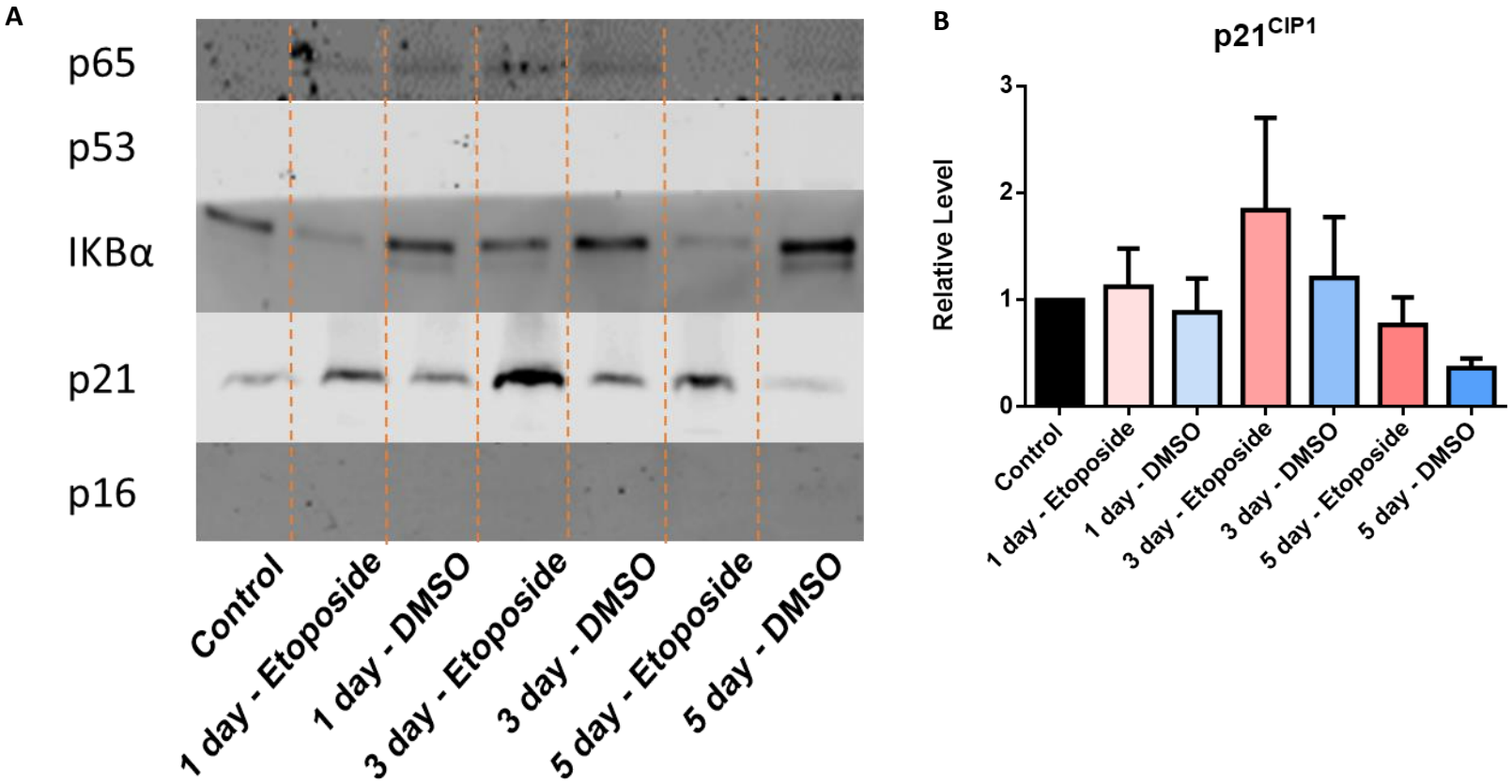

Figure 3.4

(A) Protein levels of p65, IKBα, p53, p21, and p16, of C2C12 myoblasts 1, 3, or 5 days after 24-hour treatment with 3.75 µM etoposide, DMSO treated and untreated actively proliferating myoblasts. (B) Quantification of the relative intensity of p21 levels within etoposide treated, DMSO treated, or untreated, proliferating C2C12 myoblasts (n=3). ANOVA ($P<0.05$) with Tukey's test

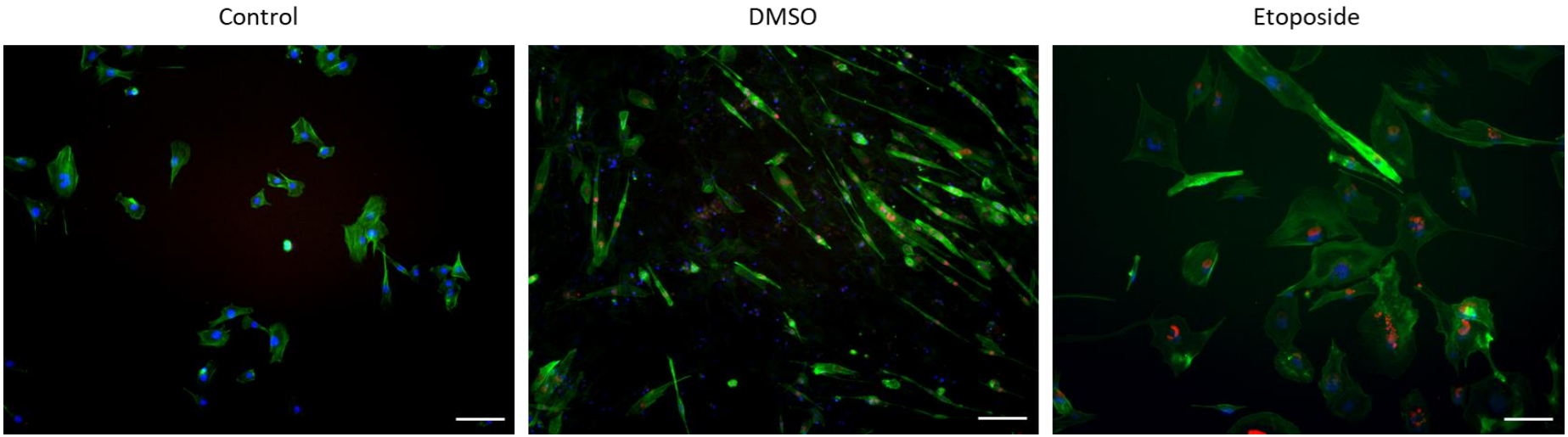

Figure 3.5

C2C12 myoblasts 5 days after 24-hour treatment with 3.75 µM etoposide, DMSO treated, and untreated, proliferating C2C12 myoblasts. Cells were stained for p21 (Red), phalloidin (Green), and DAPI (Blue). Scale bar represents 100 µm.

3.3.5 Analysis of the SASP from etoposide- and DMSO-treated C2C12 myoblasts.

Figure 3.6 shows the cumulative cytokine content of the SASP secreted into the media of etoposide treated myoblasts after either 1, 3, or 5 consecutive days incubation, compared with DMSO treated, and untreated myoblasts. The media contained the cytokines produced across the entire incubation period and so has the limitation that the value represents the whole time and so may both mask larger acute release but also does not account for degradation of released proteins. Media from etoposide treated cells showed significantly increased IL-2, IL-6, IL-12(p40), IL-17, Eotaxin, KC, MCP-1 and RANTES, when compared with untreated controls when collected over the full time period Of interest is that this increased production of SASP by etoposide treated myotubes was accompanied by decreased levels of Iκ-B in myotubes, inferring increased activation NF-κB (Figure 3.4). IL-2, IL-6 IL-12(p40) were significantly higher in media collected at each time point than the corresponding DMSO treated control. Media from DMSO treated cells showed also significantly higher levels of Eotaxin, KC, and MCP-1 when compared to untreated actively dividing myoblasts, particularly at later time points when myoblasts had reached contact inhibition.

To investigate the potential issue of cytokine degradation in the media over time, one-hour samples were also analysed at each time point. Figure 3.7 shows the acute cytokine content of the SASP secreted into the media of etoposide treated myoblasts for 1 hour at 1-, 3-, or 5-days incubation, compared with media from DMSO treated and untreated, actively dividing myoblasts. The increase in a number of the values

over the full time period was reflected in those measured acutely for one hour at each time point, particularly for IL-2, Eotaxin and RANTES.

3.3.6 Effects of treating C2C12 myotubes with SASP enriched media from senescent C2C12 myoblasts on NF-κB DNA binding activity.

Figure 3.8 shows representative images of C2C12 myotubes after 24-hour treatment with SASP conditioned media from senescent C2C12 myotubes, or DMSO vehicle treated myoblasts. DMEM differentiation media was used as a control. An untreated control was added as the quantification of the cytokines produced by DMSO treated myoblasts showed increased levels of the cytokines Eotaxin, KC, and MCP-1 when compared to untreated controls. No significant differences were seen in myotube fibre diameters between etoposide- and DMSO-treatment.

Figure 3.9 shows a representative EMSA of NF-κB/p65 transcription factor activity in C2C12 myotubes after treatment with the SASP enriched media from senescent C2C12 myoblasts. Quantification of the EMSA bands showed that the myotubes treated with media from the senescent myoblasts had increased NF-κB/p65 activity when compared with the myotubes treated with media from DMSO treated myoblasts, as well as untreated myotubes and myotubes with a media change alone.

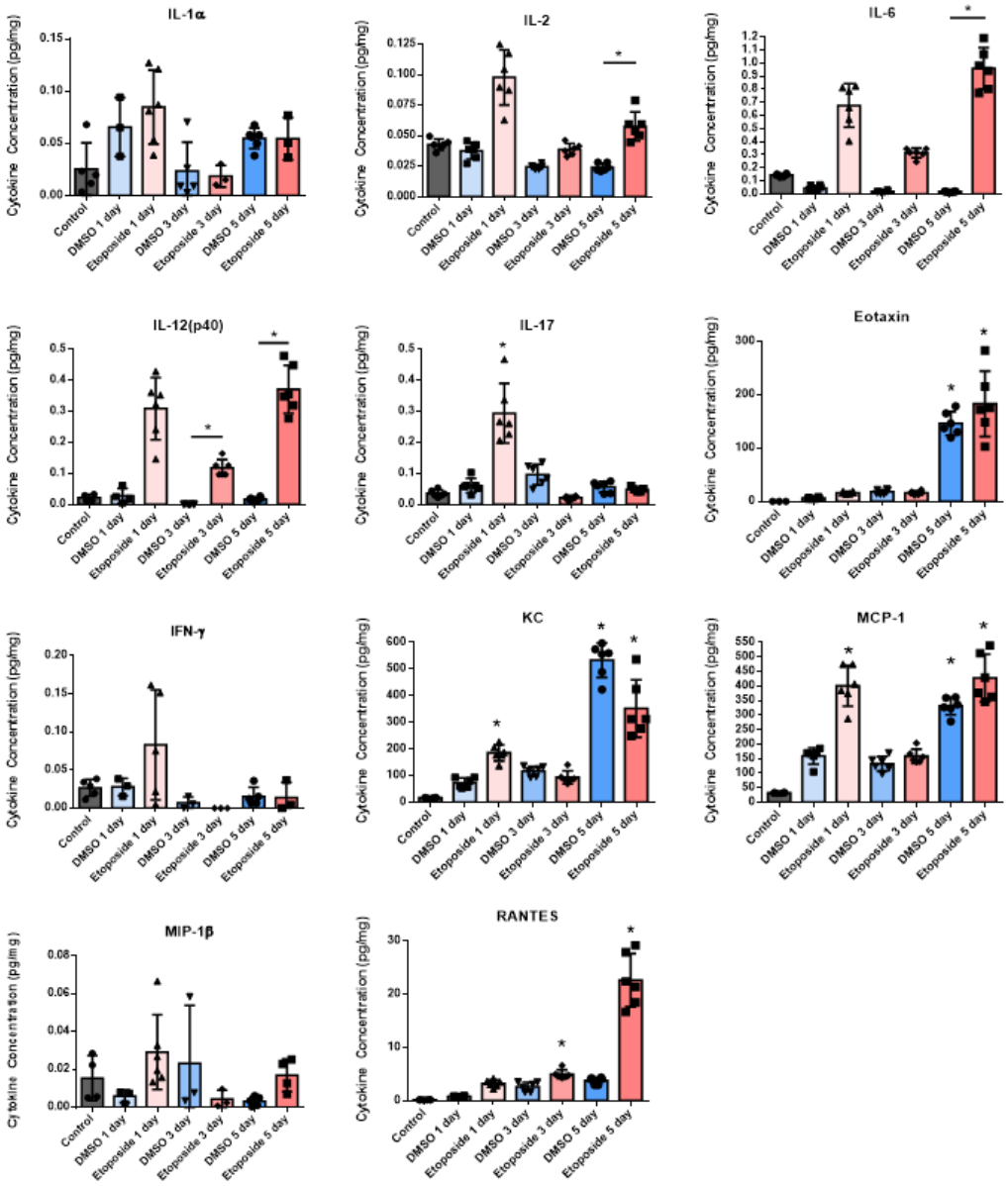

Figure 3.6 Cytokine analysis of the total SASP from senescent compared with proliferating C2C12 myoblasts.

The cumulative cytokine content of the media from C2C12 myoblasts treated with 3.75 µM etoposide collected after 1, 3, or 5 days following treatment, compared with DMSO treated and untreated, proliferating C2C12 myoblasts. Data are expressed as mean ± SD (N=3-6). ANOVA ($P<0.05$) with Tukey's test. * compared with control, $P<0.05$.

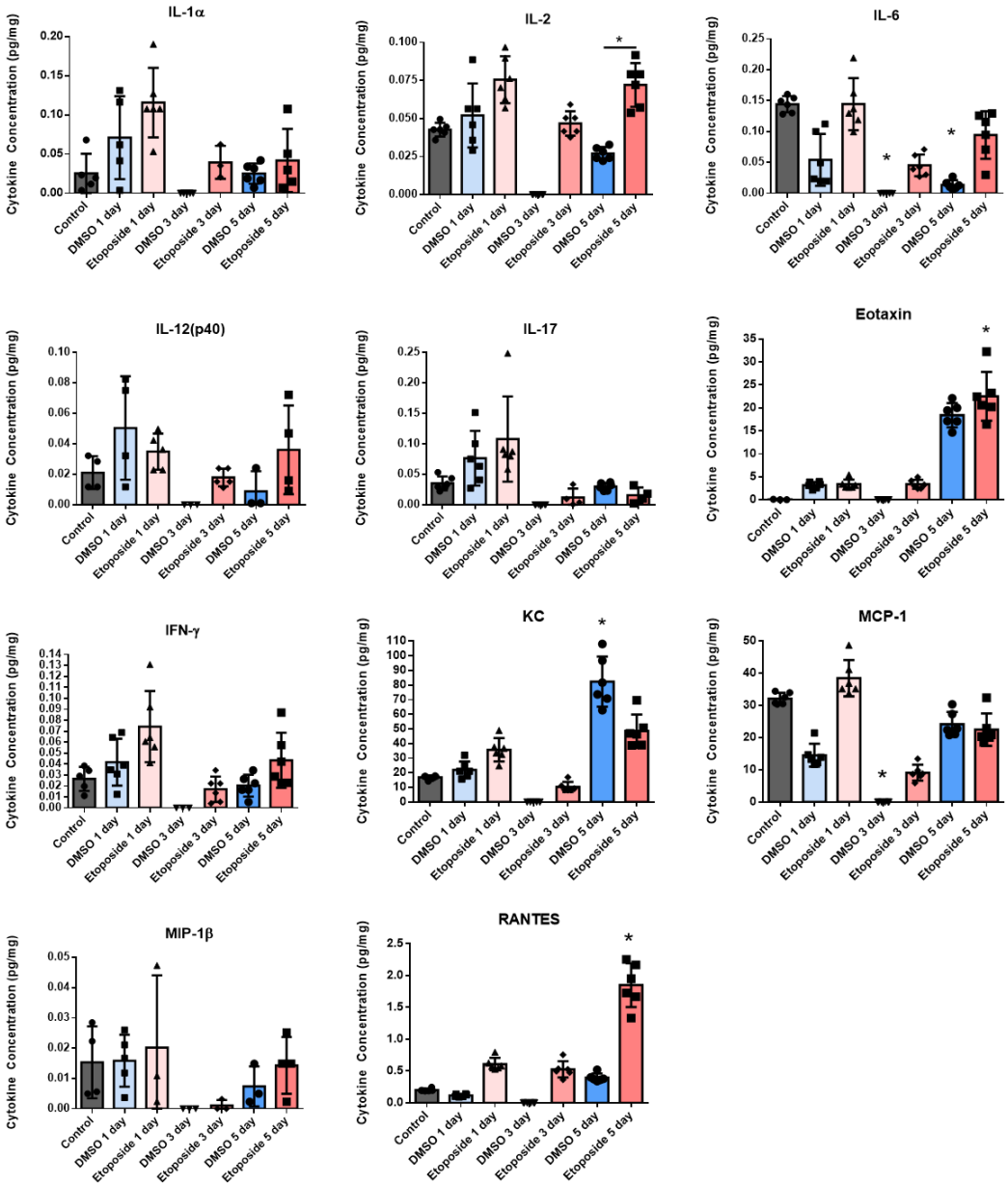

Figure 3.7 Cytokine analysis of the acute SASP from senescent compared with proliferating C2C12 myoblasts.

The acute cytokine content of the media from C2C12 myoblasts treated with 3.75 µM etoposide collected for 1 hour at 1, 3, or 5 days after treatment, compared with DMSO treated and untreated, proliferating C2C12 myoblasts. Data are expressed as mean ± SD (N=3-6). ANOVA ($P<0.05$) with Tukey's test. * compared with control, $P<0.05$.

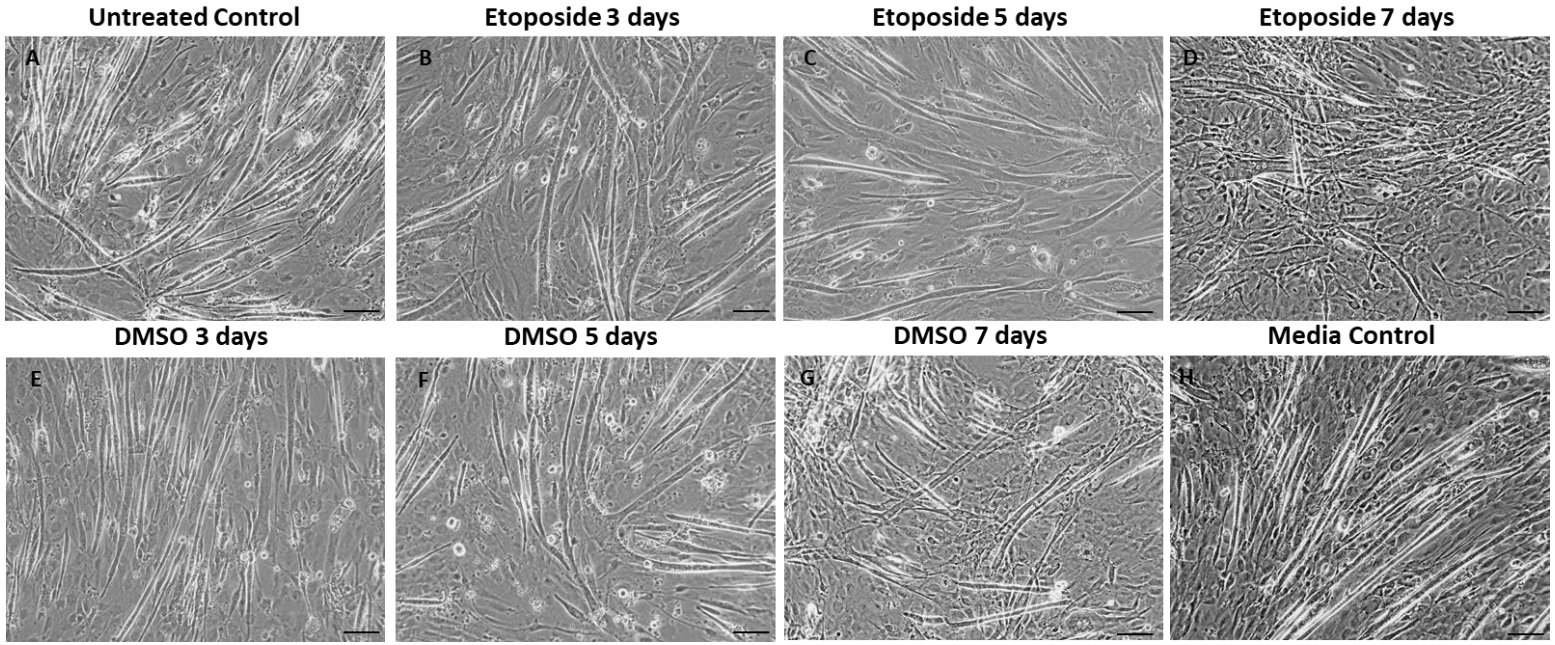

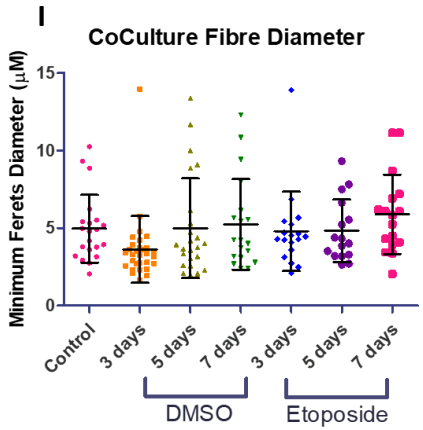

Figure 3.8

Representative images of C2C12 myotubes treated with conditioned media for 24 hours, from etoposide treated C2C12 myoblasts 3, 5, or 7 days past etoposide treatment (B-D), compared with untreated myotubes (A). Conditioned media from DMSO treated myoblasts (E-G) and differentiation media (H) were used as controls. (I) Minimum Ferets diameter of myotubes fibres after 24-hour treatment with conditioned media from etoposide treated or DMSO treated myoblasts. Data are expressed as mean ± SEM. ANOVA ($P<0.05$) with Tukey's test. Scale bar represents 100 µm.

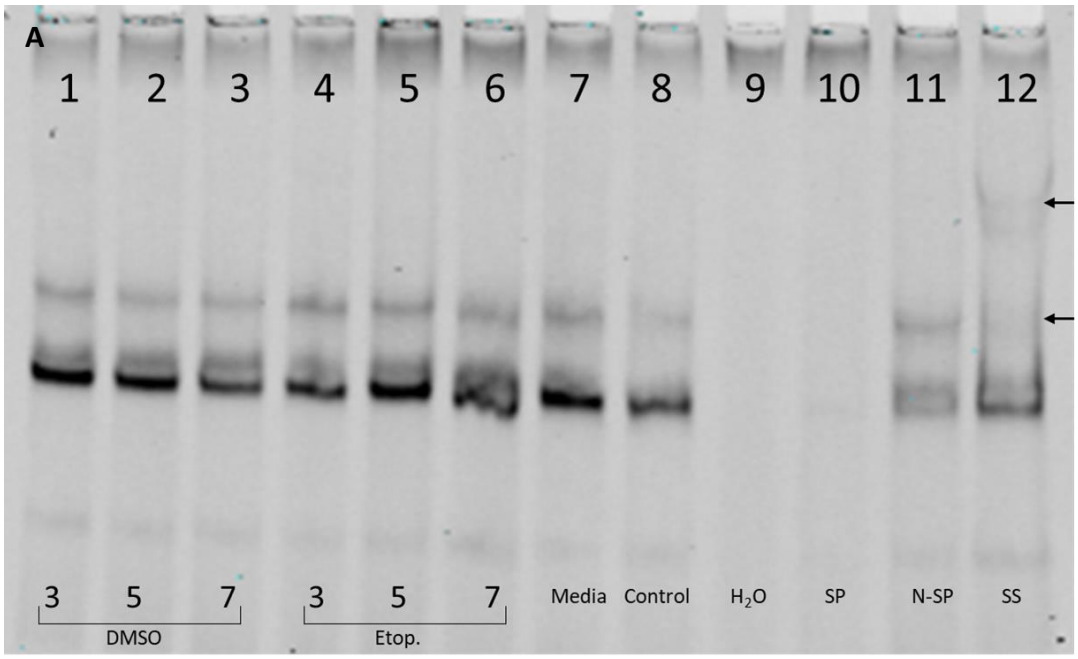

Cells were treated with SASP from:			
Lanes	**Sample**	**Lanes**	**Sample**
1.	DMSO 3 days	7.	Media control
2.	DMSO 5 days	8.	Untreated control
3.	DMSO 7 days	9.	No protein
4.	Etoposide 3 days	10.	Specific competitor
5.	Etoposide 5 days	11.	Non-specific competitor
6.	Etoposide 7 days	12.	Super shifted using anti-p65 antibody

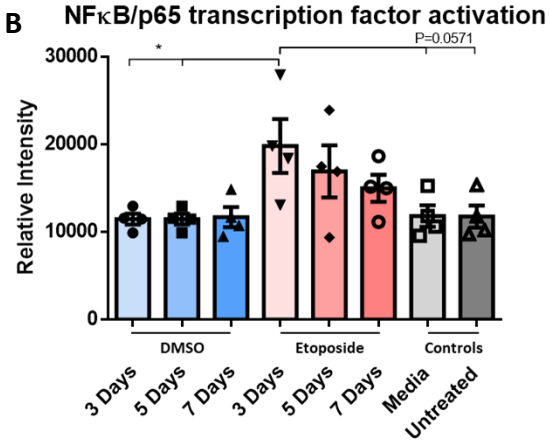

Figure 3.9 EMSA for NF-κB/p65 transcription factor DNA binding activity in C2C12 myotubes cultured in SASP enriched media.

(A) Representative EMSA of C2C12 myotubes treated with SASP enriched media collected, from senescent (etoposide treated) or DMSO vehicle treated C2C12 myoblasts. Myotubes were treated for 24 hours and the fibres collected for EMSA, looking for NF-κB/p65. Arrows represent migration of supershifted bands. (B) Quantification of data. Data are expressed as mean ± SEM. ANOVA ($P<0.05$) with Tukey's test.

3.4 Discussion

The aims of this study were to establish a model of senescence in C2C12 myoblasts and examine the effect of SASP produced by the cells on the activity of NF-κB in myotubes, as a potentially bystander effect of senescent cells on myotubes. Data presented here demonstrated that treatment of C2C12 myoblasts with etoposide resulted in increased evidence of several hallmarks of senescence; including altered morphology, permanent arrested cell growth, increase in senescence markers particularly p21, and the production of an inflammatory SASP detectable in the cell media. Treatment of C2C12 myotubes with media from senescent myoblasts resulted in an increased NF-κB DNA binding activity, suggesting that the presence of such cells is likely to have a detrimental effect on multinuclear myotubes.

3.4.1 Treatment C2C12 myoblasts with etoposide induced senescence

There are a significant number of small molecules which are widely used to induce senescence in experimental models, extensively reviewed by Petrova et al. (2016). As discussed in Section 3.1.2, etoposide is a topoisomerase II inhibitor widely used as a chemotherapeutic agent. Like other topoisomerases, etoposide treatment has been used in several other tissue culture models to induce senescence. Five days of etoposide treatment has been shown to be sufficient to generate a senescent phenotype in other cell types (Nagano et al., 2016). Probin et al. (2006) treated WI38 cells with 20 μM etoposide for 24 hours and identified a senescent phenotype, with an increase in p53 and p21 signalling; as well as γH2AX phosphorylation. Litwiniec et al. (2013) treated A549 cells with 0.75–3 μM etoposide for 72 hours and saw a senescent like morphology, positive SA-β-gal activity as well as increased p21 expression.

The decrease in myoblast viability following the treatment with relatively high concentrations of etoposide can be attributed to cytotoxic effects; the DNA damage caused by etoposide

results in DNA double strand breaks (Pommier et al., 2010), and data suggests that higher doses of etoposide caused a significant loss in viability, and subsequent death.

In this study, trypan blue was used to determine cell number at different time points following treatment to identify whether the etoposide treated C2C12 myoblasts were in growth arrest. The cell numbers of etoposide treated myoblasts remained the same over 5 days of culture despite the removal of the etoposide after 24 hours, unlike the DMSO vehicle treated cells. This demonstrated growth arrest, for up to 5 days after etoposide treatment, suggesting potential permanent growth arrest.

Several studies have induced senescence in C2C12 myoblasts through various means: (Chen et al., 2020) (Hwang et al., 2018), (Sosa et al., 2018), (Jadhav et al., 2013), (D'Orazi et al., 2000). However, this is the first demonstration of the use of etoposide to induce senescence in C2C12 myoblasts.

3.4.2 C2C12 myoblasts demonstrated characteristic features of senescence

There is not a single universal biomarker that identifies senescence in cells. Therefore, researchers have identified several common indices of senescence, as described in Section 3.1.4, that are used in tandem to identify cellular senescence.

SA-β-gal staining is a common marker for senescence in tissue. C2C12 myoblasts treated with etoposide displayed positive β-gal staining when compared with untreated or DMSO vehicle control cells (Section 3.1.4). Similar staining was seen in a study by Jadhav et al. (2013), where C2C12 myoblasts were treated with 50 µM C2-ceramide for 8 hours; resulting in higher β-gal staining when compared with controls. The limitation of this assay is that whilst increased SA-β-gal activity is associated with cellular senescence, the assay is not completely specific for senescence. For example, cells at confluence can show increased β-gal activity, as can some

differentiated cells, such as adult melanocytes (Dimri et al., 1995) and maturing tissue macrophages (Bursuker et al., 1982).

As previously discussed, one biomarker alone is not sufficient to confirm that cells were senescent. Previous studies have shown increased p21 staining in the nuclei of C2C12 cells (Wang and Walsh, 1996). In this study, we also examined the levels of p21 in control and treated cells. Etoposide treated myoblasts had higher protein levels of p21 than the cells treated with DMSO vehicle control, at 3 days following etoposide treatment (Figure 3.4). The levels of p21 protein appeared to be increasing from day 1-3 and decreasing by day 5. Previous studies have shown that 3–5 days of p21 overexpression can induce senescence in tumour cells (Chang et al., 1999). Transcriptional silencing of E2F genes responsible for cell cycle progression could result in the upregulation of p21, reinforcing cell cycle arrest (Narita et al., 2003).

The quantification of p21 protein content by western blotting or immunohistochemistry in etoposide treated cells compared with DMSO treated cells is complicated. Senescent cells demonstrate growth arrest and an increase in cell volume. In contrast, DMSO treated cells continue to replicate, finally resulting in temporary growth arrest when confluent, where they begin to terminally differentiate into myotubes. Thus, the numbers of etoposide treated cells plateaued following the 24-hour treatment, whilst the DMSO treated cells carried on dividing and reached a plateau once they had reached confluence within the plate at 5 days of culture. Indeed, p21 may have played a role in establishing permanent cell cycle arrest following etoposide treatment, but may not be crucial in the maintenance of growth arrest since only minor effect of confluence was seen in p21 immunohistochemical identification when DMSO treated cells reached confluence at the 5 day time point (Narita et al., 2003). During

myogenesis, precursor cells irreversibly withdraw from the cell cycle as they differentiate into mature myotubes and this complicates the measurement of indices of senescence, particularly p21. Upregulation of p21 is a critical regulatory event that establishes the post-mitotic state with additional development of resistance to apoptosis; such coordinated regulation of cell proliferation and cell death provides a mechanism to deposit muscle mass during embryonic development (Walsh, 1997).

The changes in morphology of the C2C12 myoblasts demonstrated characteristic senescent morphology. Senescent myoblasts *in vitro* present with a larger, flatter morphology than their original, non-senescent shape (Jadhav et al., 2013). Thus, etoposide treated myoblasts were significantly larger than the untreated and DMSO treated control cells. This, accompanied by altered DAPI staining, resembling senescence associated heterochromatin formations (SAHFs) within the etoposide treated cells was not evident in the untreated or DMSO treated control cells (Narita et al., 2003). This further complicated the quantification of the content of proteins such as p21 since levels are normalised to total protein content. However, in this instance, each cell may contain significantly more total protein. Thus, higher levels of p21 per unit protein in the nucleus then reflects more p21 per nuclei in a larger cell and so considerably more per cell. The effects of this are unclear.

From the findings described, we can conclude the etoposide treatment of C2C12 myoblasts resulted in a senescent phenotype, and that DMSO treated cells did not induce senescence, although some minor evidence of increased p21 staining was evident, likely due to contact inhibition at confluence. It is intriguing that little evidence of p16 or p53 were evident in these cells despite changes in other indices suggesting that the cells were senescent.

3.4.3 Characterising the SASP produced by senescence C2C12 cells

To characterise the secretory profile of the senescence C2C12 myoblasts, media was collected at 1, 3, and 5 days after etoposide treatment and examined by multiplex ELISA system. Data showed that etoposide treated, senescent C2C12 myoblasts produce a proinflammatory secretory profile that contained cytokines that have been reported as part of the SASP in other cells (Coppe et al., 2010a).

The levels of IL-2, IL-6, IL-12(p40), IL-17, Eotaxin, KC, MCP-1, and RANTES were significantly increased in the media of etoposide treated, senescent myoblasts collected at specific time points following treatment. Since it was possible that cytokines may have degraded during incubation in the media over a 5-day period, we also examined the acute release of cytokines in the media for 1 hour at each of the time points and these data confirmed increases in a number of these cytokines. Eotaxin, KC, and MCP-1 were also increased in the media of DSMO treated myoblasts compared with untreated actively proliferating myoblasts. One explanation for this is similar to the discussion of p21 above, that the DMSO treated cells were capable of dividing to confluence, where cells may start to differentiate to form myotubes. Ge et al. (2013) have shown that cytokines play a role in the differentiation process of C2C12 cells from myoblast to myotubes and the increase in cytokine levels seen in the media of DMSO treated myoblasts could be due to normal differentiation programming of C2C12 myoblasts, potentially ruling out a direct role of these cytokines in senescence *per se*.

3.4.4 Treatment of C2C12 myotubes with media containing the SASP from senescent C2C12 myoblasts promoted inflammation.

To examine the effect of the presence of senescent cells on mature muscle myotubes *in vivo*, C2C12 myotubes were treated with the media containing the SASP from senescent C2C12

myoblasts at 3, 5, and 7 days after etoposide treatment. The 1-day time point was excluded and replaced with the 7-day time point to capture any longer-term effects on myotubes (as the 1-day time point contained etoposide and so would complicate interpretation). Increased activation of canonical p65/NF-κB transcription factor was seen in the myotubes treated with SASP containing media compared with media from the DMSO-treated, fresh DMEM, or from untreated control cells. However, this was not accompanied by any significant changes in fibre diameter, although a significantly longer period may be needed to detect atrophy.

These findings are supported by other studies. A systematic review and meta-analysis by Bano et al. (2017), highlights the role inflammation on the development of muscle atrophy and sarcopenia. Muscle from old mice and humans have been shown to accumulate $p16^{INK4a}$ and SA-β-gal positive senescent satellite cells (Sousa-Victor et al., 2014), and this is proposed to reduce regenerative capacity of the muscle (Bernet et al., 2014). Inactivation of $p16^{INK4a}$ rejuvenated satellite cells of old mice and promoted muscle regeneration following injury (Cosgrove et al., 2014). Clearance of $p16^{INK4a}$ expressing satellite cells has also been shown to ameliorate sarcopenia in a mouse model (Baker et al., 2011). Highlighting that the presence of senescent satellite cells in muscle may play a role in the development of sarcopenia, beyond inhibiting regeneration. Studies in our laboratory and others (McArdle et al., 2019) have shown that the muscles of old mice and humans demonstrate a chronic increase in NF-κB activation (Vasilaki et al., 2003). The activation of NF-κB in myotubes by SASP from senescent cells provides compelling proof-of-principle that the local effects of SASP may be a mechanism by which NF-κB is chronically activated in old mice and humans (Vasilaki et al., 2003).

3.5 Conclusions

The aims of this chapter were to develop and validate a model of senescence in C2C12 myoblasts and further, to investigate if senescent cells produced a proinflammatory SASP that contributed to the increased NF-κB activity evident in muscle of old mice. Data suggest that treatment of C2C12 myoblasts with etoposide resulted in evidence of several the hallmarks of senescence and could provide insight into how senescent myoblasts may affect mature myotubes *in vivo*. This in turn provides an explanation as to why a chronic inflammatory profile and increased NF-κB activity is seen in skeletal muscle of old mice and humans. Thus, it is evident that at least C2C12 myoblasts can become senescent and that SASP produced by the senescent cells can activate NF-κB in C2C12 myotubes. Whether such effects are evident *in vivo* is unclear.

Chapter 4: Characterising senescence in skeletal muscle of adult and old mice *in vivo*

4.1 Introduction

The presence of senescent cells in skeletal muscle of old rodents and humans is currently unresolved. Several studies have suggested that skeletal muscle contains senescent cells or indeed that terminally differentiated muscle fibres can demonstrate evidence of increased indices of senescence (da Silva et al., 2019), potentially induced by the presence of non-muscle senescent cells (the bystander effect) (Nelson et al., 2012, da Silva et al., 2019, von Zglinicki et al., 2020). Others have suggested that although muscle fibres themselves do not 'senesce', the detrimental effects of an increase in the local presence of non-muscle senescent cells play a major role in the development of sarcopenia.

4.1.1 The role of senescence in inflammation-mediated sarcopenia

The mechanisms by which sarcopenia occurs are unclear, but there is evidence that a chronic inflammation has a detrimental effect on muscle mass and function (Reviewed by Bano et al. (2017)). Muscle strength (Visser et al., 2002), muscle mass (Schaap et al., 2006), muscle protein synthesis and catabolism (Jo et al., 2012) have all been shown to be affected by inflammation. However, there is no consensus as to the source of this systemic inflammation.

The elevated level of low-grade, chronic systemic inflammation, called inflammaging, seen in old mammals is characterised by increased serum levels of proinflammatory cytokines including the components of the SASP, IL-6 and TNFα (Franceschi and Campisi, 2014). The source of these cytokines is unclear but it is hypothesised that the presence of increasing numbers of senescent cells in old age contributes to this chronic systemic inflammation (Campisi and d'Adda di Fagagna, 2007) and so to sarcopenia. Studies where senescent cells were transplanted into muscle showed that the presence of senescent cells had a detrimental

effect on muscle (da Silva et al., 2019), supporting a role for the increased presence of senescent cells in the development of sarcopenia.

Chronically activated NF-κB is evident in the skeletal muscle of old mice (Vasilaki et al., 2006). The mechanism by which this occurs are not clear. Evidence suggests that increased extracellular levels of pro-inflammatory cytokines can activate NF-κB in muscle (Lightfoot et al., 2014), possibly via increased mitochondrial production of ROS (Lightfoot et al., 2014). The chronic activation of NF-κB can lead to activation of degenerative pathways (Thoma and Lightfoot, 2018) and so play a direct role in the development of sarcopenia. Skeletal muscle has also demonstrated an ability to be a potential source of cytokines, called myokines (Nielsen and Pedersen, 2008). Examples of myokines include IL-6, IL-8, and IL-15, which have also been reported to be secreted as part of the senescence associated secretory phenotype (SASP) in other cell types (Coppe et al., 2010a),potentially further contributing to the circulating levels of pro-inflammatory cytokines.

There are two primary possibilities for senescence in skeletal muscle *in vivo*, 1) that the chronic systemic inflammation from a local or distant site resulted in the activation of NF-κB in muscle cells and the muscle production of cytokines contributes further to the systemic inflammatory cytokines or 2) that muscle cells themselves demonstrate some indices of senescence in old age.

4.1.2 Evidence of senescence in skeletal muscle fibres

Several markers of senescence have been identified and are routinely used to identify the presence of senescent cells in tissues. However, not all indices are evident in all senescent cells and some are notoriously difficult to identify (Hernandez-Segura et al., 2018).

Whilst skeletal muscle contains a range of different cell types such as fibroblasts and adipocytes, muscle fibres are terminally differentiated, multinucleated post-mitotic tissue. Due to the terminally differentiated nature of the muscle fibres, there has been little interest in investigating cellular senescence. However, there is emerging albeit confusing evidence of the presence of senescent-like cells within skeletal muscle tissue. Such evidence for the presence of senescent cells in skeletal muscle is however unclear. Few studies have examined the expression of senescence markers in other terminally differentiated cells, but the implication of such changes is also confusing. Studies have demonstrated increases in some indices of senescence in skeletal muscle, but others demonstrate no change (see von Zglinicki et al. (2020) for current review).

Increased expression of senescence marker such as p53 and p21 have been detected in whole lysates of skeletal muscles of old mice (Edwards et al., 2007), monkeys (Kayo et al., 2001), and humans (Welle et al., 2004). However, detection of senescence in skeletal muscle is complicated due to the composition of the tissue and a muscle lysate will undoubtedly contain several other cell types. Mature multinuclear skeletal muscle fibres comprise much of the tissue, but resident 'stem' or satellite cells are also present in the tissue where they are responsible for successful regeneration of muscle fibres following muscle damage (Sousa-Victor et al., 2014). The number of satellite cells present in muscle declines during ageing (Day et al., 2010).Indeed, the cell composition of muscle can change with age, complicating any whole tissue homogenate analysis.

Sousa-Victor et al. (2014) investigated satellite cell regeneration in wild-type mice of 2–3 (young), 5–6 (adult), 20–24 (old) and 28–32 (geriatric) months of age, and hypothesised that the environment of the satellite cells may induce irreversible changes that inhibit muscle

maintenance in ageing. The authors demonstrated that the number of satellite cells decreased in old mice versus adult, but did not decrease further in geriatric mice. Satellite cells from mice of different ages or the SAMP8 accelerated ageing model (Section 1.1.7.1) were transplanted in to young mice, which resulted in decreased muscle fibre number and size with increasing age of the donor/SAMP8 mice. These results indicate that geriatric age induces intrinsic alterations in muscle stem-cell regenerative functions, which cannot be rejuvenated by a young host environment. In order to identify these intrinsic alterations, global gene expression changes were investigated. Whilst there was divergent gene expression between young, adult and old mice, the satellite cells from geriatric mice had a cluster that was enriched for genes associated with cellular senescence, including CDKN2A (p16). To investigate the role of p16 in satellite cells, Bmi1-/- premature ageing mice were also investigated via gene expression analysis and showed increased senescence gene expression. Silencing of p16 via shRNA in geriatric satellite cells downregulated p16 expression and significantly restored activation early after injury, whilst reducing the expression of senescence-associated genes. Silencing p16 in transplanted geriatric cells also restored the cells ability to self-renew. The shift in these geriatric satellite cells from quiescent to senescent is called 'geroconversion', and is explained by an imbalance in the p16INK4a/Rb/E2F axis, as described in Section 1.1.3.3. Forced p16 expression promoted geroconversion of young satellite cells during regeneration and in vitro myogenesis whilst depletion of p16 prevents geroconversion from occurring.

Muscle tissue also contains a number of other cell types due to the presence of blood vessels containing immune and other cells as well as fibroblasts, endothelial cells, adipose tissue neuronal tissue etc. (Berry et al., 2013), and these cell types have been shown to senescence

(von Zglinicki et al., 1995, Akbar et al., 2016, Jurk et al., 2012, Imamura et al., 1983). Studies show that senescent cells can induce senescence and tumorigenesis in neighbouring cells through paracrine mechanisms: (Acosta et al., 2013, Nelson et al., 2012, Faggioli et al., 2012, Coppe et al., 2010a). This SASP mediated effect has been called the bystander effect (Nelson et al., 2012) and is evident in transplantation of senescent cells into mice (Xu et al., 2017, da Silva et al., 2019). These senescence cells, as well as potentially 'senescent' muscle fibres may contribute to the pro-inflammatory phenotype and chronic NF-κB activation seen in muscles of old mice (Vasilaki et al., 2006).

4.1.3 Hypothesis and aims

The hypothesis was that there is an increase in senescence cells near or within skeletal muscle of old mice, when compared with adult mice. Further, that these senescent cells are producing a proinflammatory SASP driving increased NF-κB activity within the muscle fibres of old mice.

The aim of this chapter was to determine the presence of senescent cells within muscle of adult and old mice including the potential of muscle of adult and old mice to produce pro-inflammatory cytokines as SASP.

4.2 Methods

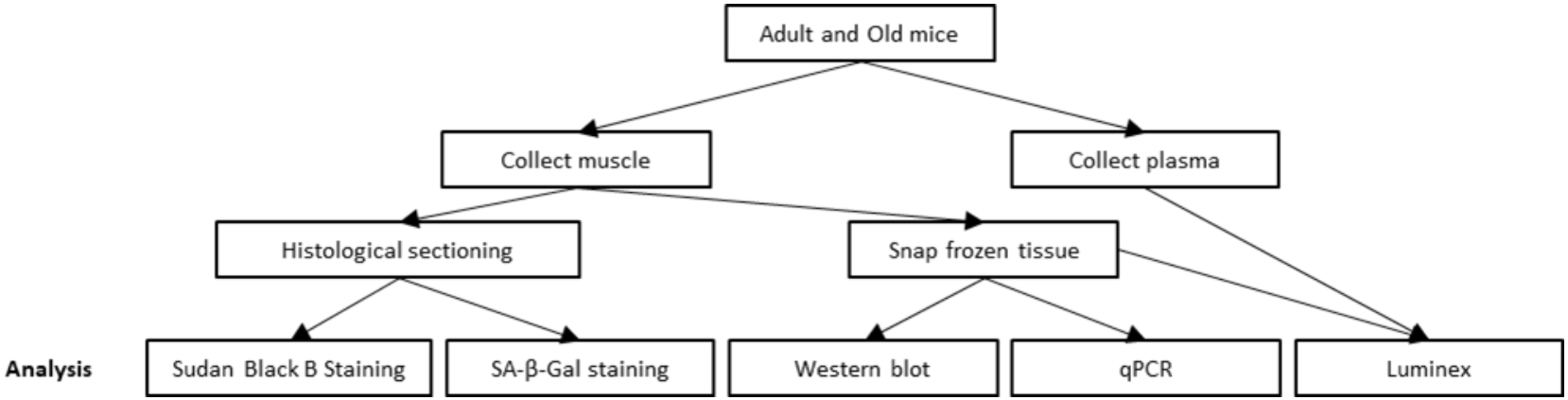

Figure 4.1 A brief overview of the methodology used for this chapter.

Adult (8-12 months-old) and old (24 months-old) mice were culled, and their blood and hind limbs muscles collected. The plasma of these mice was used for multiplex cytokine analysis. The skeletal muscle was prepared for either immuno-histological sectioning and staining, or the whole muscle was lysed for protein and mRNA content and assayed for senescence markers.

4.2.1 Western blotting for senescence markers

Gastrocnemius muscle from adult and old mice were ground under liquid nitrogen, lysed, and homogenised as described in Section 2.4.1 and protein concentrations quantified as described in Section 2.4.2. Samples were then denatured and loaded into acrylamide gels and proteins resolved, as described in Section 2.5.1. Following transfer of proteins to a nitrocellulose membrane using the Geneflow blotting system (Section 2.5.2), membranes were blocked in 5% milk and incubated with primary antibodies (Table 4.1) at 4°C overnight. Membranes were washed 3x5 minutes and incubated with the secondary antibody (Table 4.1) for 1 hour at room temperature. Membranes were then washed for 3x5 minutes and, images of the membranes were captured on the LI-COR Odyssey® CLx Imaging System (LI-COR, Cambridge, UK) at a wavelength of 800nm.

Primary Antibody Target	**Dilution in 5% milk**	**Secondary antibody**	**Secondary antibody dilution**
p53	1 in 1000	IRDye® 800CW Goat anti-Mouse (LI-COR, Cambridge, UK)	1 in 15,000
p21	1 in 1000	IRDye® 800CW Goat anti-Rabbit (LI-COR, Cambridge, UK)	1 in 15,000
p16	1 in 1000	IRDye® 800CW Goat anti-Rabbit (LI-COR, Cambridge, UK)	1 in 15,000

Table 4.1 Antibody dilutions for western blotting of senescence markers in skeletal muscles of adult and old mice

4.2.2 Quantitative PCR for senescence markers

Gastrocnemius muscle from adult and old mice were ground into a fine powder under liquid nitrogen (Section 2.4.1), lysed in TRIzol™ Reagent (Life technologies, Warrington, UK) and the mRNA was extracted (Section 2.6.1). The mRNA was then reverse transcribed and quantified as described in Section 2.6.2. Qualitative PCR was performed as described in Section 2.6.3, using primer sequences specific for p53, p21, and p16 (Table 4.2). Ct values were normalised to the housekeeper gene PPIA (Gong et al., 2016).

Target	Forward Sequence	Reverse Sequence
p53	AGGGTCCATATCCTCCA	AATGCAGACAGGCTTTGC
p21	ATTCCATAGGCGTGGGACCT	TCCTGGGCATTTCGGTCAC
p16	AATCTCCGCGAGGAAAGC	GTCTGCAGCGGACTCCAT
PPIA	GGCAAATGCTGGACCAAAC	CATTCCTGGACCCAAAACG

Table 4.2 Primer sequences for senescence markers

4.2.3 Senescence Associated β-Galactosidase staining of muscle sections

Gastrocnemius muscle from adult and old mice were cryosectioned as described in Section 2.3.4. SA-β-gal detection was performed using the Senescence β-Galactosidase Staining Kit (Cell Signalling Technologies, #9860) (Section 2.3.2). Muscle sections were immersed and incubated at 37°C overnight, in a low CO_2 environment. The staining solution was then removed, muscle sections were rinsed with DPBS and imaged under a light microscope (Nikon Diaphot, Tokyo, Japan).

4.2.4 Sudan Black B staining of muscle sections for lipofuscin

Gastrocnemius muscle from adult and old mice were cryosectioned as described in Section 2.3.4. Sudan Black B staining was performed on muscle sections as described in Section 2.3.5. Muscle sections were imaged under a light microscope (Nikon Eclipse Ci, Tokyo, Japan).

4.2.5 Immunohistochemistry for senescence markers in etoposide- and DMSO-treated C2C12 myoblasts

Gastrocnemius muscle from adult and old mice were cryosectioned as described in Section 2.3.4. Muscle sections incubated with primary antibodies (Table 4.3) at 4°C overnight. Muscle sections were washed 3x5 minutes and incubated with the secondary antibody (Table 4.3) for 1 hour at room temperature.

Primary Antibody Target	Dilution	Secondary antibody	Dilution
p53	1 in 100	Alexa Fluor® 488 Goat anti mouse (Sigma Aldrich, Dorset, UK)	1 in 10, 000
p21	1 in 100	Alexa Fluor® 488 Goat anti rabbit (Sigma Aldrich, Dorset, UK)	1 in 10,000
p16	1 in 100	Alexa Fluor® 488 Goat anti rabbit (Sigma Aldrich, Dorset, UK)	1 in 10,000

Table 4.3 Immunohistochemistry antibody dilutions of senescence markers

4.2.6 Multiplex Cytokine Analysis

Adult and old mice were sacrificed by cervical dislocation and blood was collected from the descending aorta. Blood was centrifuged at 10,000g for 10 mins at 4°C, and the plasma

collected. Gastrocnemius muscle from the same mice were collected and the plasma were analysed using a Bio-Plex® Pro™ Mouse Cytokine 33-plex Assay (#12002231) (Section 2.7).

4.2.7 Gene Ontology Term Analysis

WebGestalt (2019 release) was used to perform the Overrepresentation Enrichment Analysis for each of the gene ontology categories (Biological Process, Cellular Component, and Molecular Function). The list of mouse genes was compared against the reference option of genome. The significance level was FDR<0.05 and the multiple test adjustment was performed using the Benjamini–Hochberg method.

To help better visualize the GO terms obtained from the analysis above described, the tool REViGO was used. The p-values here considered were the FDR values obtained previously, with the *mus musculus* database option used for the GO terms.

4.3 Results

4.3.1 Molecular markers of senescence in muscle of adult and old mice.

No statistically significant differences were seen in the abundance of p53, p21, and p16 proteins between muscles of adult and old mice (Figure 4.2). A significant decrease in p53 mRNA expression was seen in muscles of old when compared with adult mice. Although no significant difference was seen in p21 and p16 mRNA levels in muscles of old compared with adult mice, mean levels of these indices also appeared to be <50% of levels in muscles of adult mice (Figure 4.2).

4.3.2 Detection of senescence markers in histological sections of muscle from adult and old mice.

Figure 4.3 shows SA-β-Gal staining of 12µm thick sections of gastrocnemius muscle from adult and old mice. No detectable evidence of positive staining for β-Gal was seen in any of the serial sections from a number of biological replicates (n=4) of samples from muscles of mice of both ages. Both sudan black staining and auto-fluorescence was used to examine muscle for the presence of lipofuscin. Figure 4.4 shows Sudan Black B staining of gastrocnemius muscle sections from adult and old mice for evidence of the accumulation of lipofuscin. No detectable staining of lipofuscin was seen in the serial muscle sections from biological replicates (n=4) using this method. Figure 4.5 shows sections of gastrocnemius muscle of adult and old mice that were analysed for fluorescent lipofuscin granules by auto-fluorescence. In this instance, the muscle from old mice showed significantly more auto-fluorescence than the muscle from adult mice. No significant differences in the presence of p21

(Figure 4.6) and p16 (Figure 4.7) content of old mice muscle sections was seen when compared with muscle sections from adult mice.

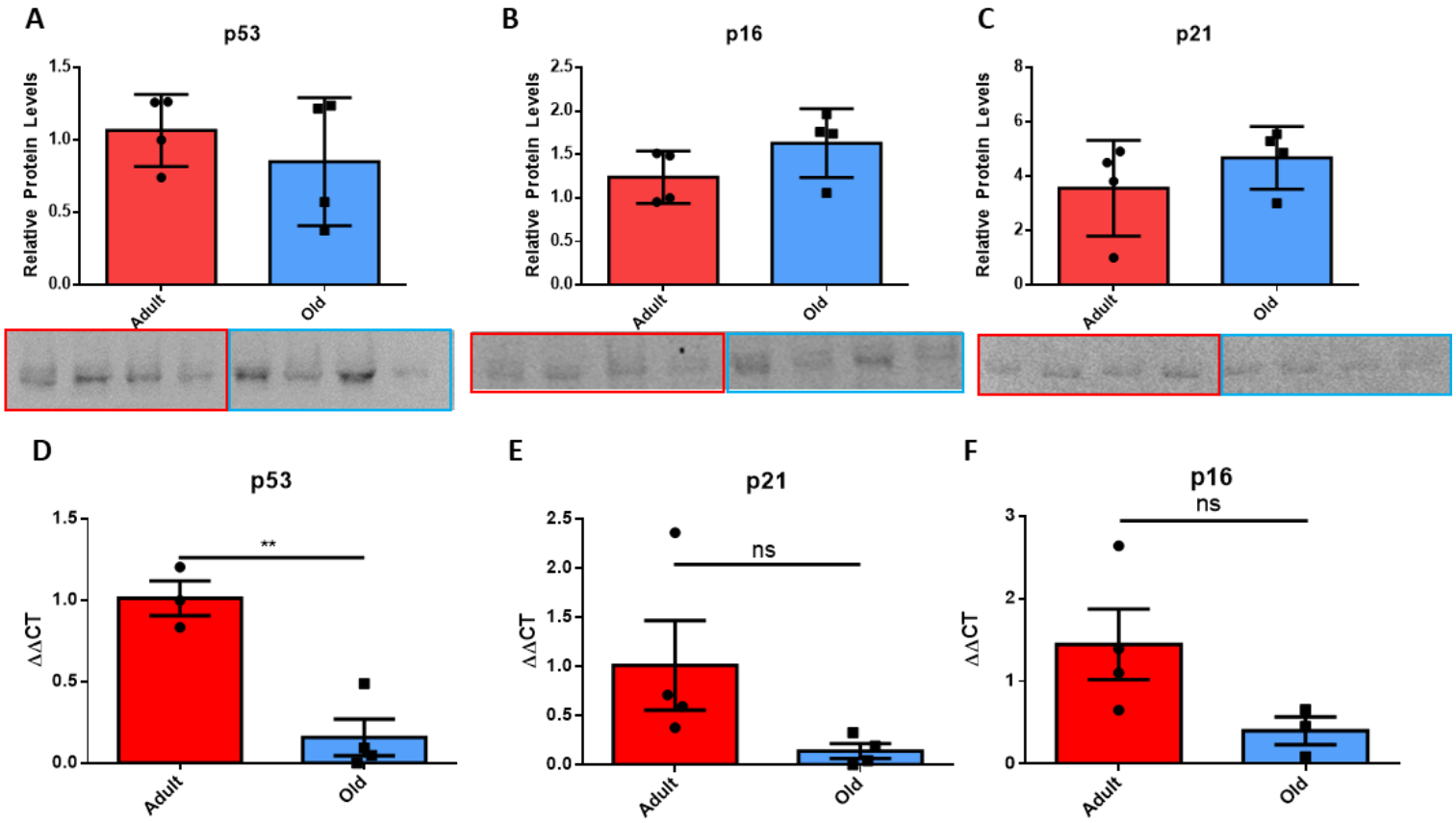

Figure 4.2
Relative protein levels of p53 (A), p16 (B), and p21 (C), in gastrocnemius muscles of adult (10 months) or old (24 months) WT mice. Relative expression of p53 (D), p16 (E), and p21 (F), in gastrocnemius muscles of adult (10 months) or old (24 months) C57BL6 mice. Data are presented as mean ± SEM (N=4), *P > 0.05, Student's T-Test.

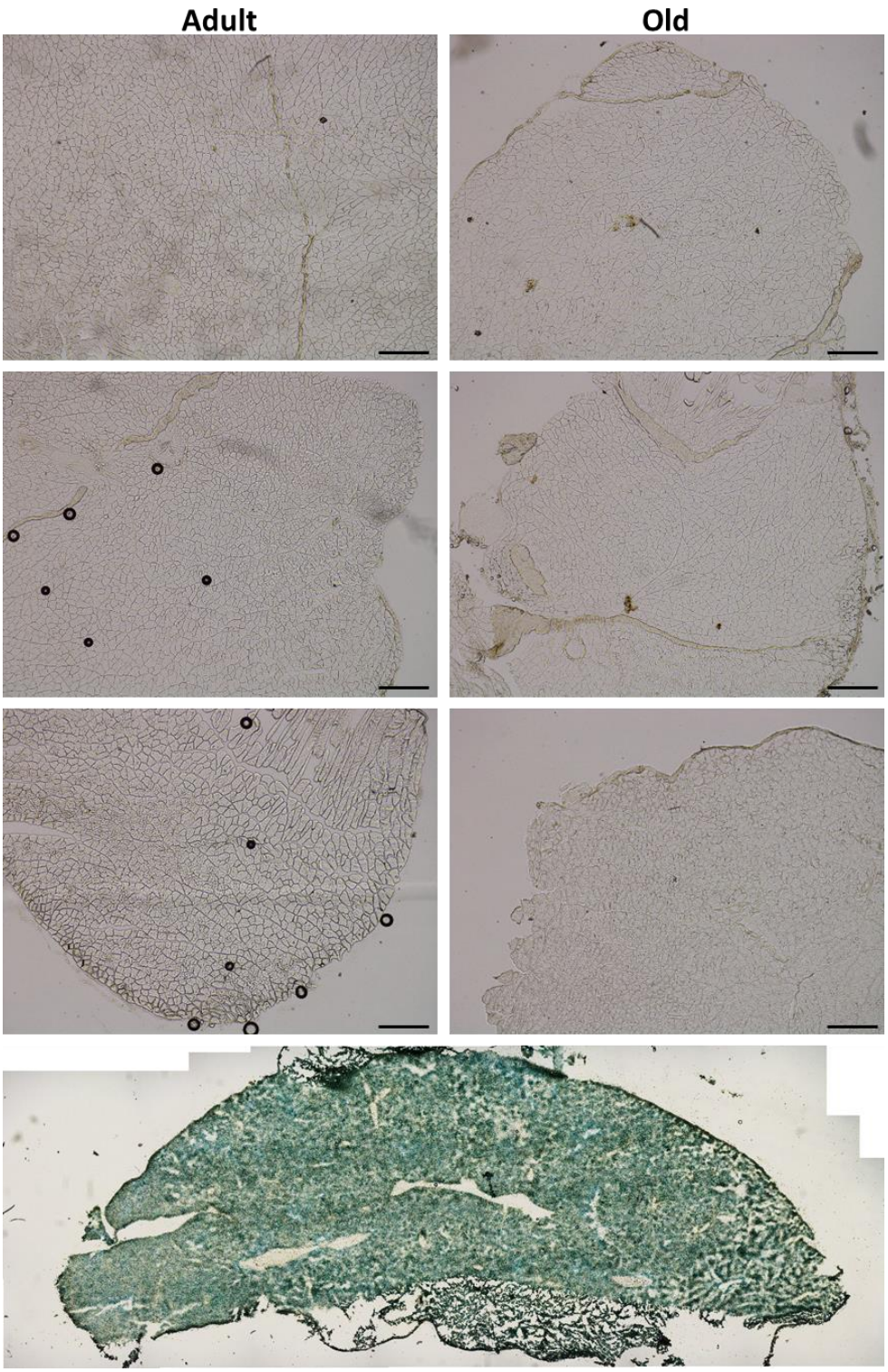

Figure 4.3

Representative transverse muscle sections (12µm) of gastrocnemius muscle stained for SA-β-Gal activity, adult (left) and old (right) WT mice. Liver was used as a positive control (bottom). Positive staining is blue, negative is brown. Scale bar represents 100 µm.

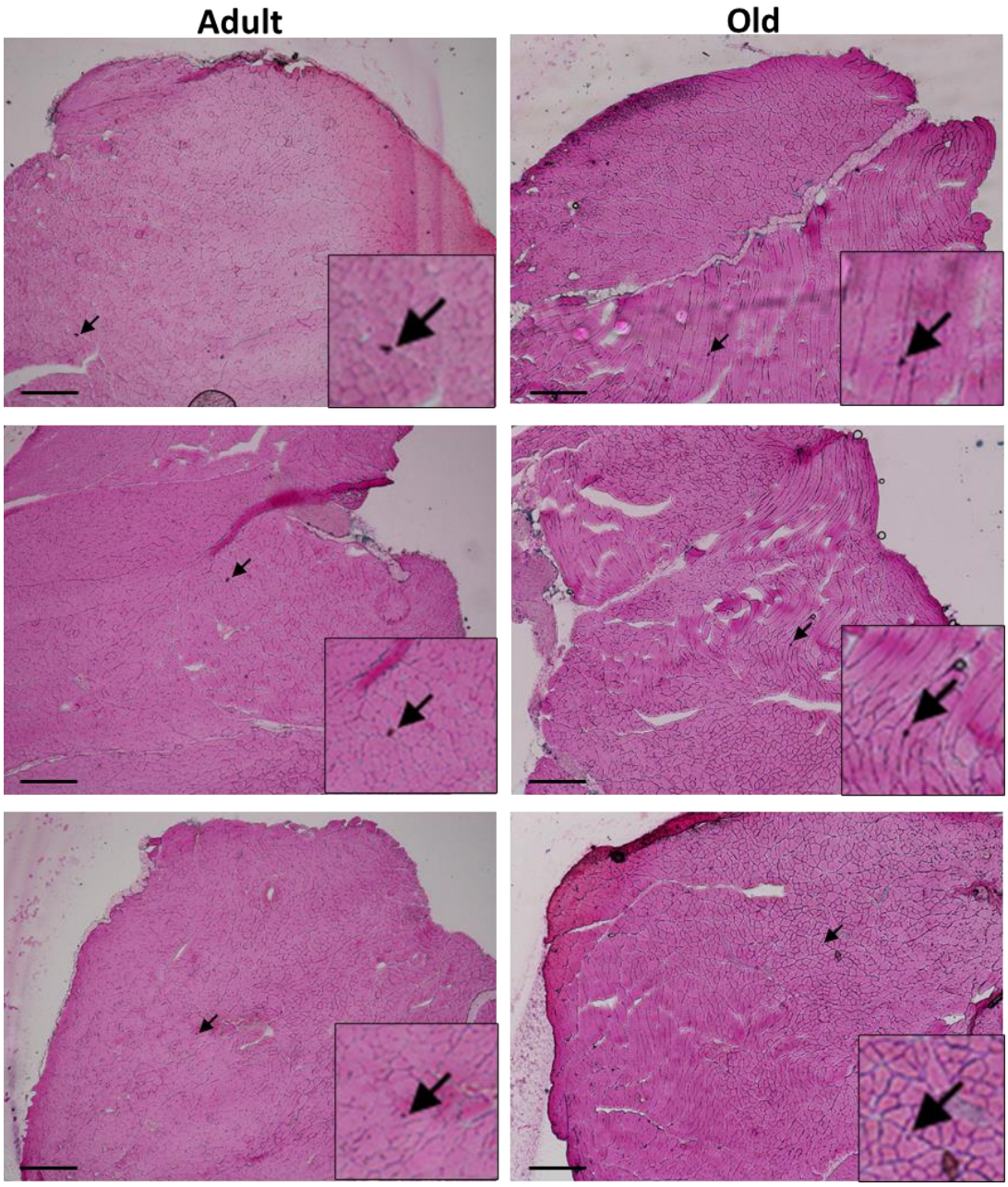

Figure 4.4 Sudan Black B staining of gastrocnemius muscle from adult and old mice.

Representative transverse (12µm) sections of gastrocnemius muscle stained with Sudan Black B for lipofuscin from adult (left) and old (right) WT mice. Counterstained with Nuclear Fast Red (pink). Positive staining is black/blue, negative is pink/purple. Scale bar represents 100 µm.

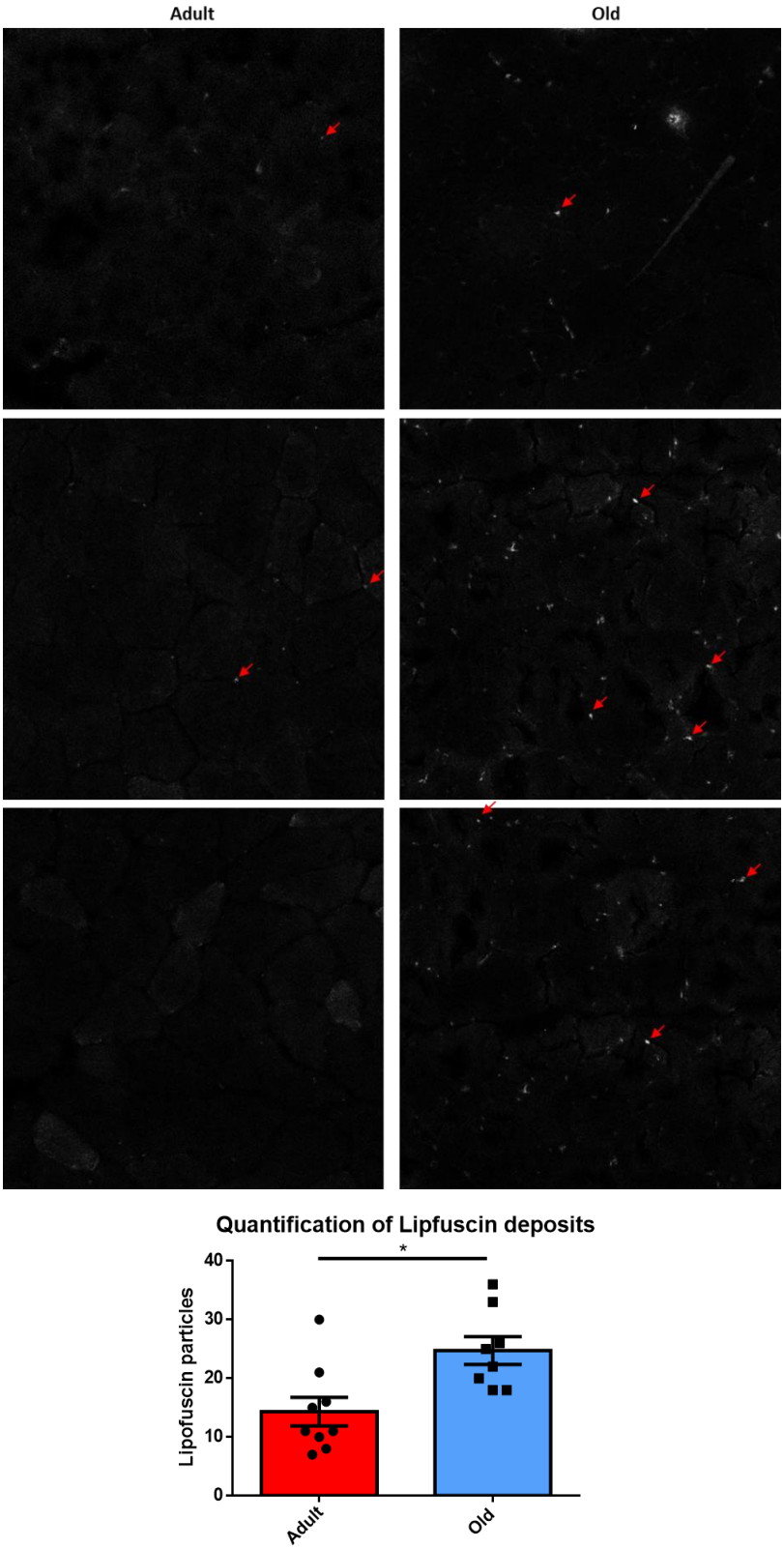

Figure 4.5 Detection and quantification of lipofuscin particles by autofluorescence within the gastrocnemius muscle from adult and old mice.

Transverse (12µm) sections of gastrocnemius muscles imaged for lipofuscin auto-fluorescence from adult (left) and old (right) WT mice.

4.3.3 Immunohistochemical staining for the senescence marker p21

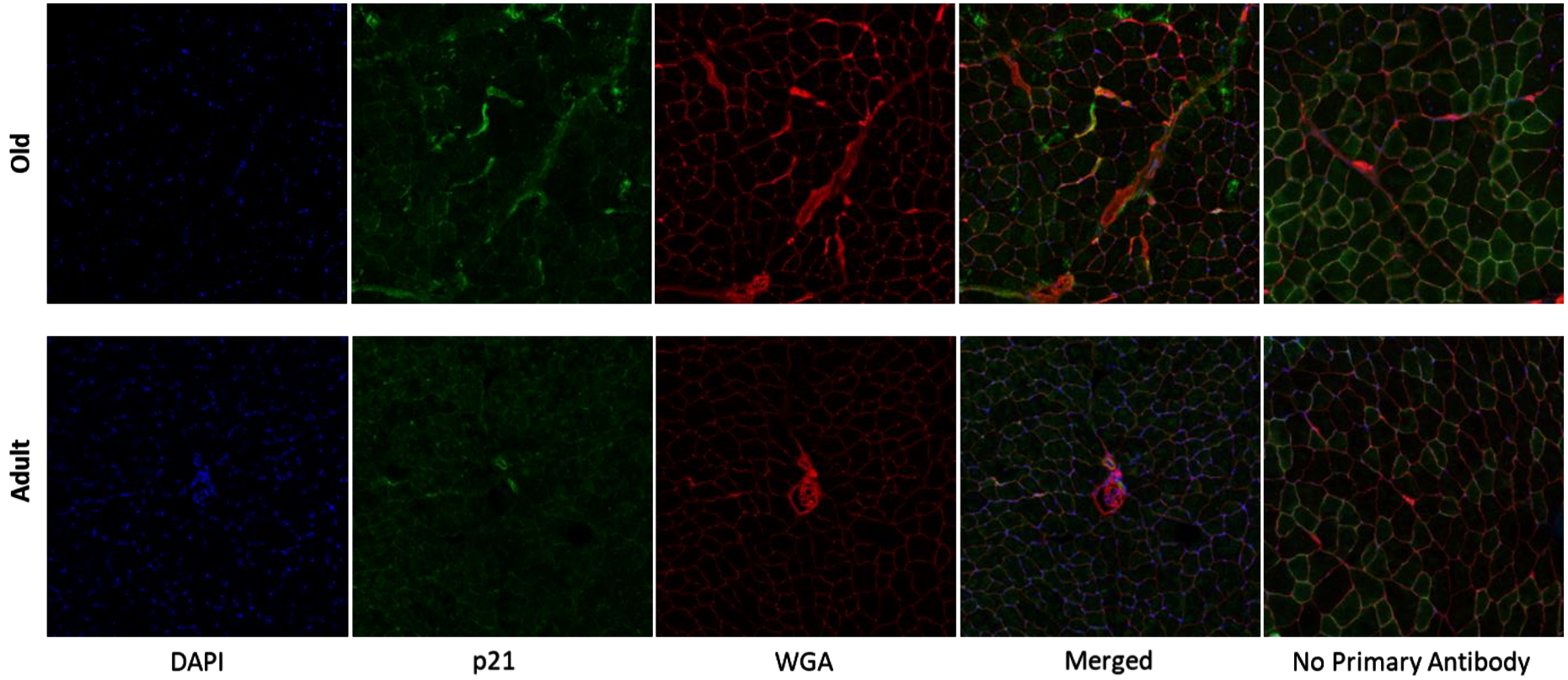

Figure 4.6

Transverse sections of anterior tibialis muscle sections (12µm) stained for p21 (green), WGA (red), and DAPI (blue) from adult (bottom) and old (top) WT mice.

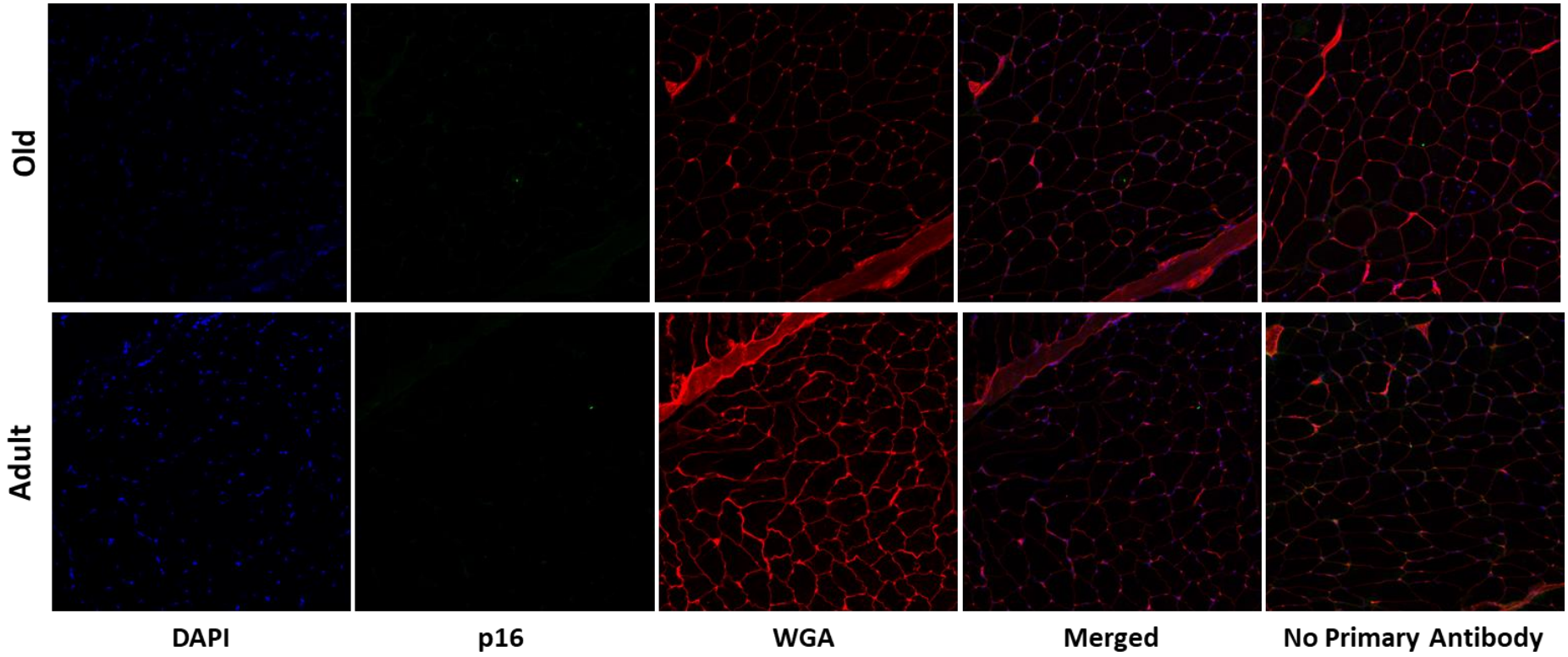

Figure 4.7

Transverse sections of anterior tibialis muscle sections (12µm) stained for p16 (green), WGA (red), and DAPI (blue) from adult (bottom) and old (top) WT mice.

4.3.4 Multiplex cytokine analysis of plasma and muscle from adult and old mice

Data from the multiple cytokine analysis of plasma and muscle lysate from adult and old WT mice are shown in Figure 4.8 and Figure 4.9.

Of the 33 cytokines measured, 12 were significantly increased in plasma of old mice compared with adult mice (Figure 4.8). In contrast, cytokine analysis of lysates from gastrocnemius muscle of adult and old mice (Figure 4.9) showed that GM-CSF and MIP-2 were the only two cytokines with significantly higher levels in muscles of old compared with adult mice.

Gene ontology (GO) term analysis on biological process was performed for the cytokines significantly higher in old mouse plasma compared to adult plasma (Figure 4.10).

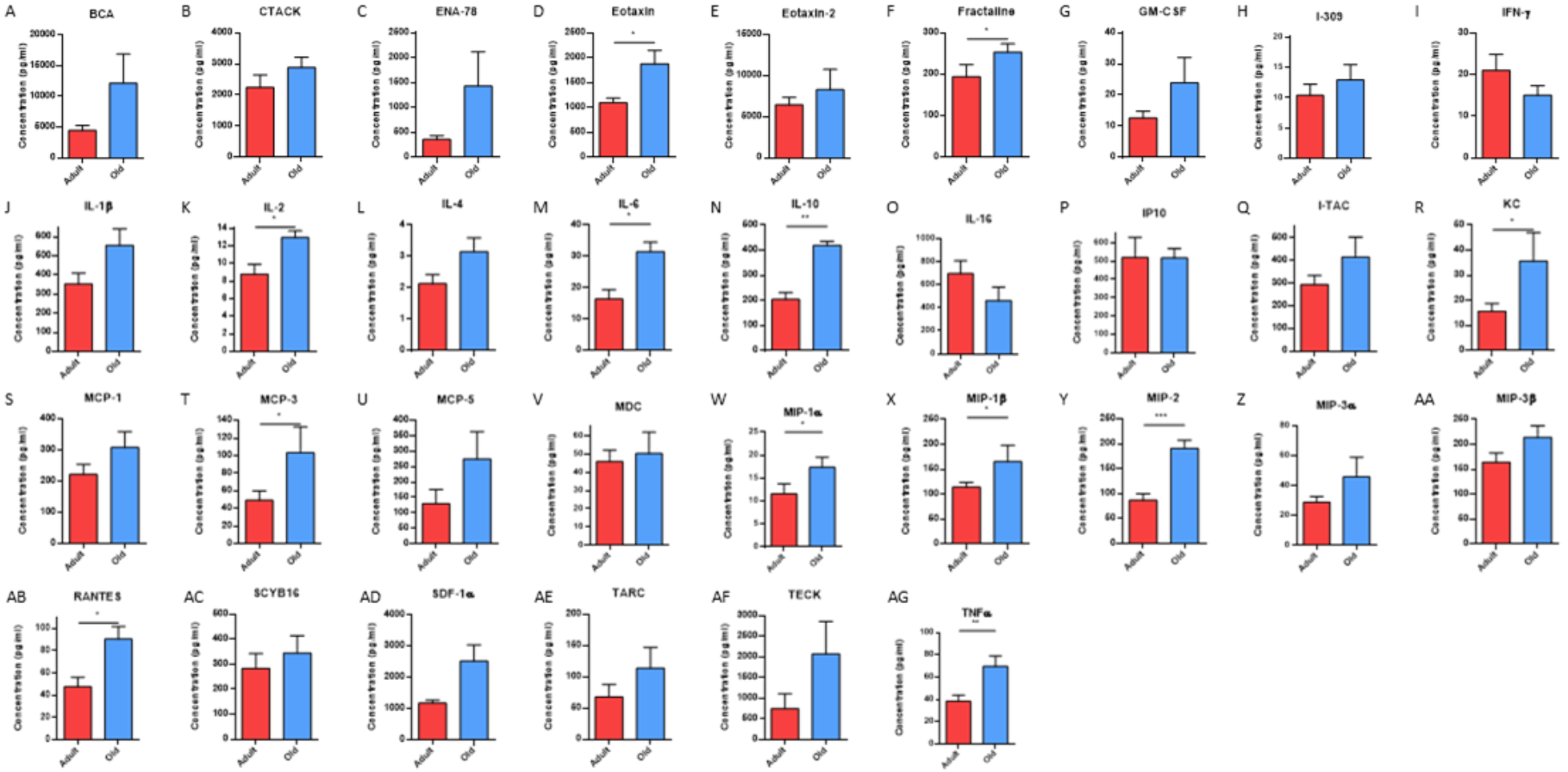

Figure 4.8

Plasma cytokine/chemokine concentrations (pg/ml) from adult (red) and old (blue) WT mice (A-AG). Data are presented as mean ± SEM. *P>0.05

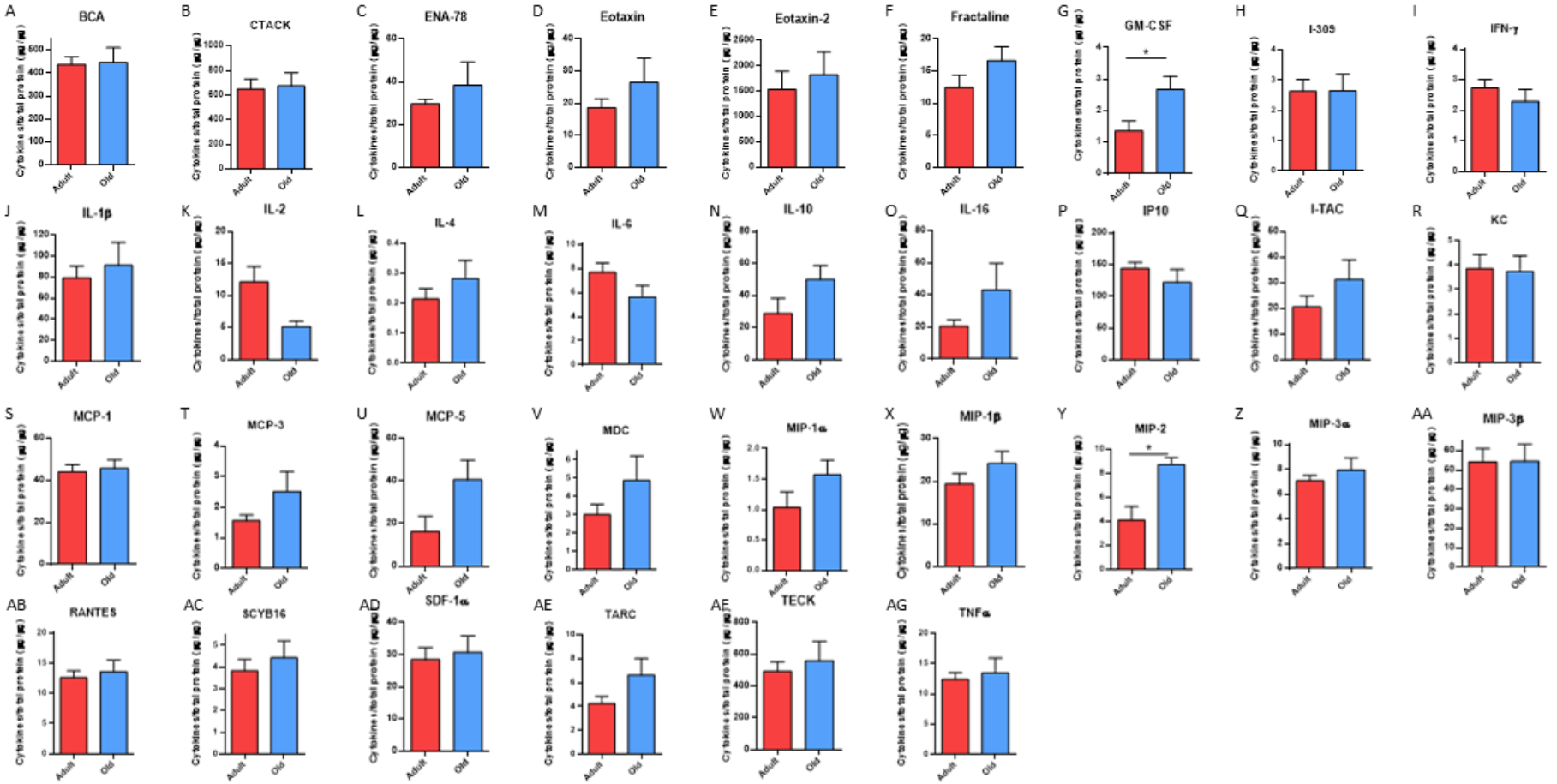

Figure 4.9

Tissue cytokine/chemokine concentrations normalised to gastrocnemius protein (µg/µg) from muscles of adult (red) and old (blue) WT mice. Data are presented as mean ± SEM. *P>0.05

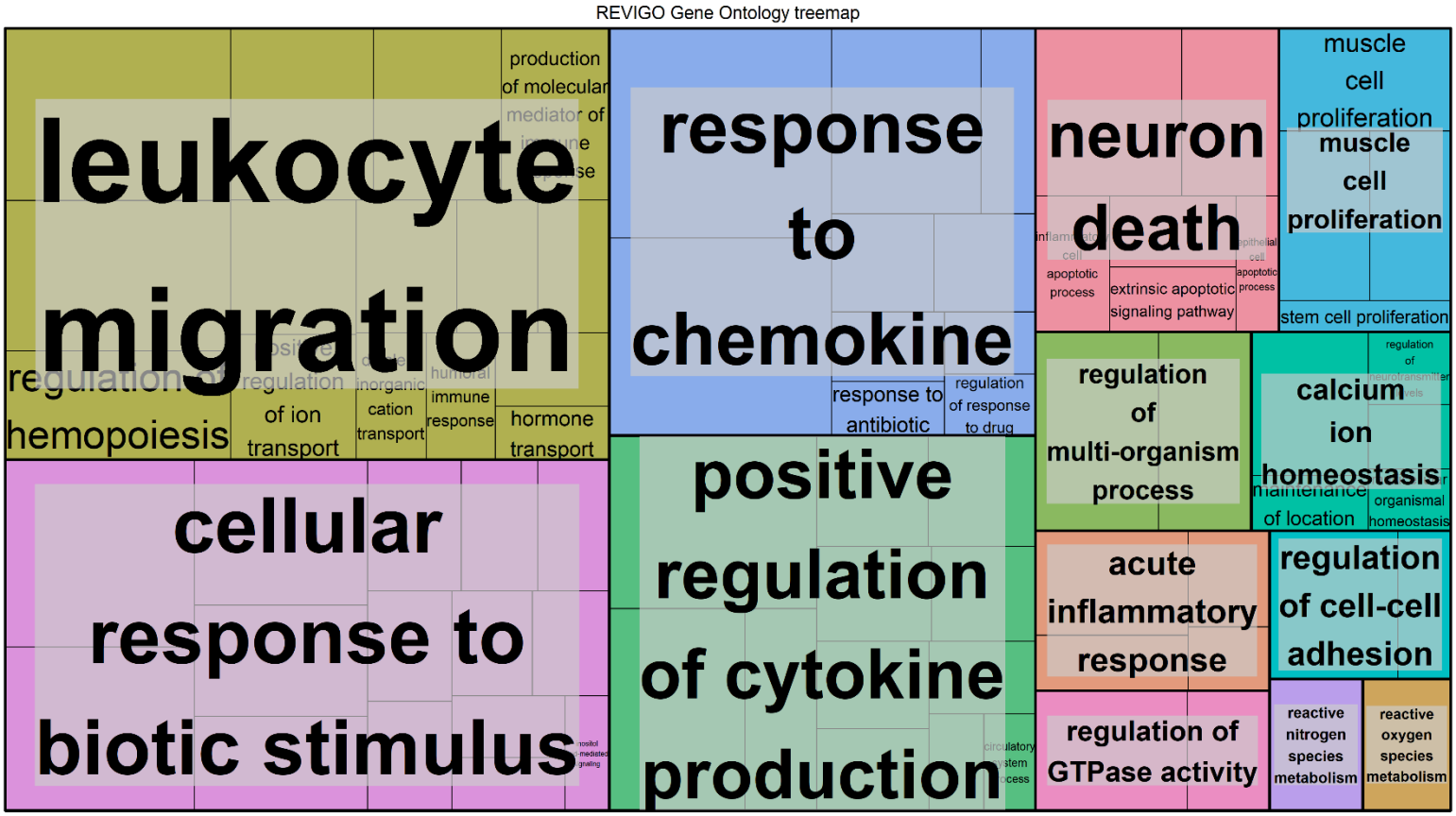

Figure 4.10

GO term analysis of the cytokines significantly increased in the plasma of old WT mice compared with adult WT mice. Box size was based on FDR values (<0.05) from gene ontology analysis using Web Gestalt. Figure produced using Revigo.

4.4 Discussion

The aims of this chapter were to examine skeletal muscles of adult and old mice for evidence of senescence. This was achieved by examination of muscles for common markers of senescence including: SA-β-Gal activity, senescence markers (e.g. p21), as well as the evidence for the increased production of SASP.

4.4.1 Characterisation of senescence markers in the skeletal muscle of adult and old mice

4.4.1.1 Protein and mRNA levels of p16 and p21 in the muscles of adult and old mice.

Both p16 and p21 play a key role in the development of cellular senescence (Coppe et al., 2010a). No significant differences were seen in p16 and p21 protein abundance in the skeletal muscle from adult and old mice. The mRNA from skeletal muscle of adult and old mice was also examined. The level of p53 mRNA was significantly decreased in muscles of old mice compared with adult mice. Jeyapalan et al. (2007) reported no differences in p53 levels in skeletal muscle nuclei comparing young and very old baboons (Jeyapalan et al., 2007). There was also a significant decrease in the mRNA levels of both p21 and p16 in muscles of old compared with adult mice. Feng et al. (2007) demonstrated decreased p53 and p21 transcriptional activity in various tissues in aging C57BL/6 female mice, from 6 to 20 months old in several tissues including skeletal muscle. Sousa-Victor et al. (2014) performed qPCR on muscle satellite cells (SCs) from adult and old mice to investigate the effects of ageing on SCs. These authors reported no significant changes in p16 mRNA levels in the SCs from 20-24 months old C57BL/6 mice compared with 5-6 months old adult mice, and only saw a significant increase in p16 mRNA levels in 28-32 months old geriatric mice. Edwards et al. (2007) reported increased p53, p21, p16 expression within the gastrocnemius muscle of 25 months old mice compared with 5 months old adult mice. In contrast to Jeyapalan et al.

(2007), (da Silva et al., 2019) did indeed find increased p53 levels within skeletal muscles of 32-months old mice. Thus, there is little consensus on the evidence of changes in these proteins in muscle of mice with increasing age. There are several potential reasons for these discrepancies. The differences may be due to methodological approaches. Both Sousa-Victor et al. (2014) and Edwards et al. (2007) performed qPCR to analyse p53 and p21 expression in old mice. For both studies, old mice were approximately 24/25 months old. Edwards et al. (2007) prepared samples from whole muscle lysates whilst Sousa-Victor et al. (2014) used isolated SCs. As previously mentioned, muscle tissue contains a range of other cell types that contribute to the muscle bulk and its cellular composition may change during ageing. Indeed, p16 is not specific to senescent cells and positive p16 staining has been reported in normal healthy T-cells (Akbar and Henson, 2011). Other tissues (e.g., adipocytes or immune cells) may in fact be senescent and contributing to the p53 and p21 mRNA levels and thus the senescent profile of the whole muscle analysed although that was not evident in our studies. In addition, other studies in our laboratory have demonstrated that, during ageing, the mRNA levels do not always reflect the protein levels of specific proteins (Owen et al, unpublished).

4.4.1.2 Immunohistochemistry for SA-β-Gal and Lipofuscin

Another canonical marker of cellular senescence is the lysosomal enzyme, beta-galactosidase, which is proposed to be specific to senescent cells and not evident in quiescent cells or terminally differentiated cells (Debacq-Chainiaux et al., 2009). However, Debacq-Chainiaux et al. (2009) have proposed that SA-β-Gal staining may occur in quiescent cells induced by confluency or serum starvation, in immortalized cells (Cristofalo, 2005).

No evidence of SA-β-Gal activity was seen in any of the muscle sections from either adult or old mice (Figure 4.3). There have been limited studies to date examining the SA-β-Gal activity

in skeletal tissue. Since skeletal muscle is mainly post-mitotic, it is a poor target for examining cellular senescence. Sousa-Victor et al. (2014) performed SA-β-Gal analysis of isolated satellite cells from adult, old and geriatric (28-32 months old) C57BL6 mice. Their data showed no positive SA-β-Gal staining in the satellite cells of adult and old mice, but positive staining as evident in the geriatric mice. However, these analyses were performed on isolated satellite cells, and do not describe whether multinucleated muscle fibres themselves were positive for SA-β-Gal.

Lipofuscin can be detected by using the natural auto-fluorescent properties, or it can also be detected using Sudan Black B staining (Glees and Hasan, 1976). Sudan Black B is a highly lipophilic agent that exhibits high affinity to the lipid compartment of lipofuscin (Gatenby and Moussa, 1949). Lipofuscin is an aggregate of oxidised proteins, lipids, and metals, and is considered a hallmark of ageing (Brunk and Terman, 2002). Lipofuscin accumulates in various tissues and species with age, particularly post mitotic tissues such as the brain and cardiac and skeletal muscle (Brunk and Terman, 2002) although this isn't consistently seen (Ikeda et al., 1985). An explanation for the latter may be that the pathways which drive senescence and the accumulation of lipofuscin, functions independently of the ability of a cell to divide, as demonstrated in neurons (Jurk et al., 2012) and adipocytes (Minamino et al., 2009). Lipofuscin has also been shown to accumulate during replicative senescence of cells such as human fibroblasts (von Zglinicki et al., 1995) and in resident satellite cells in muscles of older humans (Roth et al., 2000). Increased granular deposits of lipofuscin were evident by auto-fluorescence in muscle sections from old mice compared with muscles of adult mice although no difference was evident when Sudan Black B staining was used. The difference in findings using the two different methods is unclear. An increase in deposits of lipofuscin in muscles of old mice is in agreement with current literature, where lipofuscin granules accumulate with

ageing (Kakimoto et al., 2019) and particularly in skeletal muscle (Tohma et al., 2011). However, the potential increase in lipofuscin granules due to the increased presence of senescent cells is in contrast to the other findings in this Chapter, showing little evidence of changes in other indices of senescence... Change in fibre type, as seen in muscles of old mice can also result in changes in lipofuscin content of muscles (Roth et al., 2000). The positioning of the granules in the transverse sections of muscles also suggests that it may be outside of the muscle cells in some instances, possibly evident in satellite cells, although this was not examined in detail. In conclusion, in the absence of any more specific indices of senescence, it is likely that that the increase seen in this instance is due to a non-specific increase in oxidation with advancing age, evident in muscles of old mice. There is significant evidence to indicate that there are fundamental changes in redox signalling and homeostasis, which occur during ageing (Jackson and McArdle, 2011). Skeletal muscles of old mice demonstrate significant oxidative damage to DNA, lipids, and proteins (Vasilaki et al., 2006). The imbalance in ROS homeostasis may ultimately initiate the upregulation of proinflammatory signals, resulting in chronic inflammation (Meng and Yu, 2010). Oxidative stress, such as muscle derived ROS, is proposed to activate NF-κB and up-regulate the inflammatory response (Meng and Yu, 2010).

4.4.2 Characterisation of the inflammatory cytokine profiles of adult and old mice

Figure 4.10 shows gene ontology (GO) term analysis of the cytokines shown to be significantly elevated in the plasma of old mice compared with adult mice, showing common motifs in the functions of the cytokines. GO terms are descriptors that assigns terms to genes, allowing for hierarchically classification. The logical structuring of these hierarchies allows queries to be performed, looking for similar terms between groups of genes. Through GO term analysis, several common motifs were identified:

4.4.2.1 Chemotaxis and the immune system

The largest field, with the highest FDR (false discovery rate) values and most overlapping functions was “leukocyte migration”, “response to chemokines”, and “positive regulation of cytokine production”. Chemotaxis, as the name suggests is when an organism moves in response to a chemical stimulus of some kind. An example of which are bacteria, that make use of chemotaxis to move towards nutrients and away from hazards. In the context of multicellular organisms, cytokines, and chemokines; chemotaxis refers to the movement and migration of immune cells.

Immune cells such as neutrophils migrate in response to chemoattractant. Neutrophils release proteases, such as neutrophil elastase, damaging healthy tissue in the process, resulting in inflammation (Wilson et al., 2017). The efficiency of chemotaxis decreases with age, resulting in greater inflammation and damage when compared with adults (Wilson et al., 2017).

4.4.2.2 Skeletal muscles as a source of cytokines

Skeletal muscle comprises approximately 40% of total body mass, and has been shown to be a source of cytokines, called myokines (Nielsen and Pedersen, 2008, Janssen et al., 2000). Indeed, IL-6 expression increases significantly in skeletal muscle following exercise where it is proposed to have beneficial effects (Steensberg et al., 2000). However, a chronic increase in IL-6, for example in plasma results in increased ubiquitin protein and mRNA expression in muscle, resulting in muscle degradation (DeJong et al., 2005). IL-6 binds to the glycoprotein 130 (gp130) or CD130 receptor, and shares several functions with other cytokines such as IL-11, leukaemia inhibitory factor (LIF), oncostatin M (OSM), granulocyte colony-stimulating factor (G-CSF), and IL-12 (Ohtani et al., 2000).

Data in this study show an increase in a number of cytokines/chemokines in the plasma of old compared with adult mice, but a limited number elevated in the muscle of old mice, where significant increases were seen only in GM-CSF and MIP-2, with MIP-2 only common to increases seen in these in plasma of old compared with adult mice. Cytokines are produced by tissues and rapidly released. It may therefore be possible that this results in little difference in absolute protein levels of cytokines in muscles of old verses adult mice and so

Cytokines	Plasma	Muscle
BCA-1/CXCL13		
CTACK/CCL27		
ENA-78/CXCL5		
Eotaxin/CCL11		
Eotaxin-2/CCL24		
Fractalkine/CX3CL1		
GM-CSF		
I-309/CCL1		
IFN-γ		
IL-1β		
IL-2		
IL-4		
IL-6		
IL-10		
IL-16		
IP-10/CXCL10		
I-TAC/CXCL11		
KC/CXCL1		
MCP-1/CCL2		
MCP-3/CCL7		
MCP-5/CCL12		
MDC/CCL22		
MIP-1α/CCL3		
MIP-1β/CCL4		
MIP-2/CXCL2		
MIP-3α/CCL20		
MIP-3β/CCL19		
RANTES/CCL5		
SCYB16/CXCL16		
SDF-1α/CXCL-12		
TARC/CCL17		
TECK/CCL25		
TNFα		

Table 4.4

Summary table of the cytokines significantly increased in the plasma and/or muscle of old mice compared with adult mice. Green, increased; Grey, no difference.

determination of protein levels of cytokines alone in muscle tissue is a limitation of this study. Indeed, mRNA analysis of muscle from old versus adult mice from our laboratory supports this possibility for IL-6 (Owen et al, unpublished) where muscle levels of mRNA for IL-6 were also increased in old compared with adult mice, although a full range of cytokine/chemokines was not assessed. Cytokines/chemokines may be produced by cells within the muscle and result in altered local concentrations, for example at the location of the peripheral nerve, but may not alter plasma levels of these molecules. Thus, further data from our laboratory has also demonstrated an increase in the release of several cytokines from isolated muscle fibres from old compared with adult mice, including Eotaxin and MCP-1 (Owen at al, unpublished)

Data from Chapter 3 suggests that myoblasts have the capability of senescence and release increased levels of cytokines/chemokines including IL-2, IL-6, Eotaxin, KC and MCP-1. However, although these cytokines/chemokines are released by senescent cells (Chapter 3), such release in not exclusive to senescent cells and data presented in this Chapter suggest that resident senescent cells in muscle tissue are not a major source of these cytokines since no evidence of the presence of local senescent cells was seen. However, data suggest that the source of some cytokines may still be the muscle fibres themselves in a so-called bystander effect although the release is limited and non-muscle cells in the muscle bulk cannot be ruled out as an alternative source.

The chemokines, MIP-1α, MIP-1β, and MIP-2, belong to the MIP (Macrophage Inflammatory Proteins). MIP-1α and -1β, have been shown to be secreted as part of the SASP (Coppé et al., 2010). MIP-2 is transcriptionally controlled by NF-κB (Burke et al., 2014). MIP-2 levels were significantly higher in the muscle lysates of old mice when compared with adult mice suggesting that muscle may in part be a source of this cytokine. MIP-2, as well RANTES and

MCP-1, have been shown to increase in the plasma of aged rats on a high-fat diets, when compared with control diet rats, due to greater deposits of long-chain fatty acid esters creating inflammatory cross-talk with the sarcopenic muscles (Laurentius et al., 2019). Zhu et al. (2019) have also proposed that peri-muscular adipose tissue (PMAT), an ectopic fat deposit surrounding muscle, may drive muscle wasting.

Granulocyte–macrophage colony stimulating factor (GM-CSF) functions to activate and recruit granulocytes to sites of tissue damage (Hammond et al., 1995, Francisco-Cruz et al., 2014) and is proposed to play a major role in tissue remodelling (Sacramento et al., 2009). A study examining the effect of transient expression of GM-CSF shows an increase in the number of 'healing' M1-like macrophages immediately after traumatic muscle injury promoting muscle recovery (Martins et al., 2020). Skeletal muscle of old mice accumulates focal areas of damage and so increased production of GM-CSF by skeletal muscle may be a response by the muscle to promote efficient muscle repair.

Data showed significant changes in a number of other cytokines in plasma of old compared with adult mice although the source of these cytokines is unclear. The effect of these on muscle mass and function is also unclear, but the individual cytokines may have specific effects. TNFα has been shown to directly upregulate the NF-κB pathway via IκB kinase (IKK). Activation of the transcription factor NF-κB in muscle results in myofibre atrophy and activation of the ubiquitin-proteasome pathway (Li and Reid, 2000, Ladner et al., 2003, Cai et al., 2004). Furthermore, treatment of mice with TNFα caused suppression of the Akt-mTOR pathway, resulting in decreased protein synthesis (Pijet et al., 2013).

Fractalkine structure differs from typical cytokines. The soluble version is a potent chemo-attractant of T-cells and monocytes, whilst the cell-bound form promotes the strong adhesion of leukocytes (Bazan et al., 1997). In an effort to identify new biomarkers of ageing, Deng et al. (2019) investigated the cytokine profile of the serum from young and old mice. From their panel Fractalkine, amongst others, was significantly higher expressed in the plasma of old mice when compared to young, which agrees with the data presented in this Chapter.

IL-10 was also significantly higher in the plasma of old compared with adult mice. IL-10 was first discovered in 1991 by de Waal and colleagues (de Waal Malefyt et al., 1991a, de Waal Malefyt et al., 1991b), IL-10 was initially reported to suppress cytokine secretion, antigen presentation, and CD4+ T cell activation. As an anti-inflammatory cytokine, it inhibits the synthesis of IFN-γ, IL-2, IL-3, TNF-α, and GM-CSF by cells such as macrophages and Th1 cells (Moore et al., 1993). However, it has also been shown to stimulate thymocytes, mast cells and B cells (Moore et al., 1993). IL-10 has also been shown to be a myokine, and is increased in plasma following exercise (Ostrowski et al., 2000). The role in plasma of old mice is unclear but it may be an attempt by muscle to counteract the pro-inflammatory environment.

The transcription factor NF-κB plays a significant role in the expression of inflammatory cytokines and the SASP (Malaquin et al., 2016, Lopes-Paciencia et al., 2019). Elevated levels of NF-κB have been shown in the skeletal muscle of old mice and humans, when compared with adults (Vasilaki et al., 2006, Cuthbertson et al., 2005). Senescent cells accumulate in other tissues throughout the body with age throughout the body and may be a source of the SASP (Baker et al., 2016). Indeed, There is evidence to suggest that the SASP secreted by senescent cells within adipose tissue reduces the expression of contractile proteins and induces insulin resistance in human muscle cells (Sachs et al., 2019).

The pro-inflammatory cytokines produced as SASP can contribute to the plasma cytokine pool of old individuals and can promote further NF-κB activation in several tissues, producing more inflammatory cytokines , creating a vicious feedback loop. This SASP mediated feedback loop has been described as the bystander effect (Nelson et al., 2012). Whereby senescent cells can induce senescence like behaviour in neighbouring cells through paracrine mechanisms (Acosta et al., 2013, Nelson et al., 2012, Faggioli et al., 2012). As skeletal muscle is a source of cytokines (myokines), such a bystander effect may also have a substantial effect on circulating cytokine levels since muscle comprises a substantial proportion of the body (Lutz and Quinn, 2012, Nielsen and Pedersen, 2008), creating a vicious circle.

4.5 Conclusion

In summary, analysis of muscles of adult and old mice has provided little evidence of classical senescence in any cell types present in muscle tissue. Data examining protein levels of cytokines in muscle of old compared with adult mice suggest that muscle may partially contribute to the increase in plasma cytokines evident in plasma of old mice, but suggest that the source of the majority of cytokines seen in plasma is not primarily muscle tissue. It may be that muscle rapidly produces and secretes cytokines and so changes in intracellular protein levels will not be evident, but such cytokines produced by muscle may still have a local effect on peripheral nerves for example.

To elucidate the role of the presence of senescent cells distant to the muscle on plasma cytokine profiles and changes in muscle function during ageing, models are required to eliminate senescent cells form the whole body.

Chapter 5: Removal of senescent cells in p16-3MR mice: effect on age-related loss of skeletal muscle

5.1 Introduction

The ability to eliminate senescent cells in transgenic mouse models has allowed the examination of the effect of the presence or accumulation of senescent cells distant to tissues during ageing on tissues such as skeletal muscle. Most senescent cells express the tumour suppressor p16INK4a, which prevents cell cycle progression from the G1 to S phases by inhibiting two cycle-dependent kinases, CDK4 and CDK6 (Section 1.1.3.1). The expression of this protein has been exploited to develop transgenic mouse models aimed at eliminating p16-positive senescent cells (Demaria et al., 2014, Baker et al., 2016).

5.1.1 The p16-3MR mouse model

The p16-3MR mouse model (Section 1.1.7.3) allows the investigation of the role of the presence of senescence cells in ageing in several tissues, allowing the selective elimination of senescent cells *in vivo*. The model was first described by Demaria et al. (2014) in order to investigate the role of cellular senescence in wound healing. A Bacterial Artificial Chromosome (BAC) was used to inactivate the original $p16^{INK4a}$ gene and drive 3MR expression instead. The P16-3MR mice have genes, which contain functional domains of

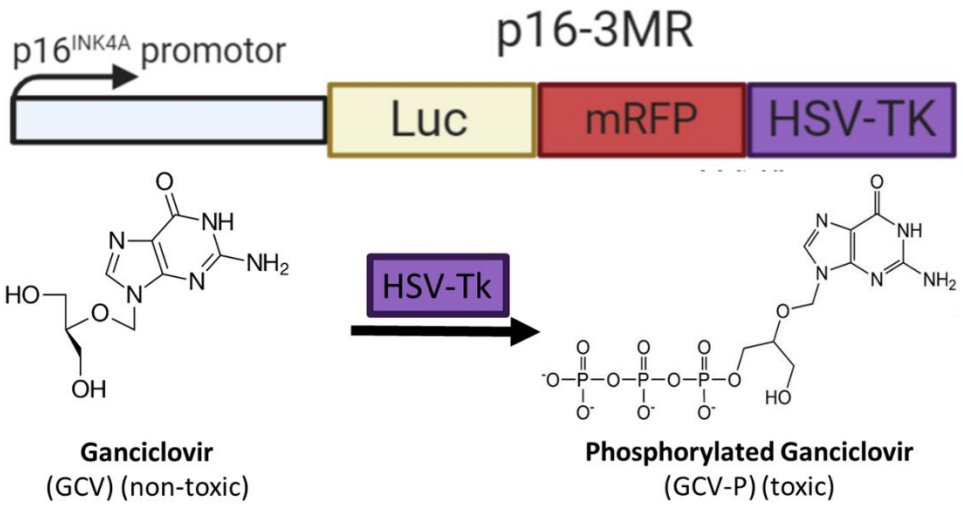

Figure 5.1 Schematic of the p16-3MR transgene.

Adapted from Demaria *et al*. (2014).

Renilla luciferase (LUC), monomeric red fluorescent protein (mRFP), and a truncated herpes simplex virus (HSV)-1 thymidine kinase (TK) under control of the full $p16^{ink4a}$ promoter (Figure 5.1). The LUC and mRFP are both fluorescent reporter proteins, which allow for detection of 3MR expressing. HSV-TK allows for selective elimination of $p16^{ink4a}$ expressing cells by ganciclovir (GCV), a nucleoside analogue. GCV has a high affinity for HSV-TK but low affinity for the cellular TK (Laberge et al., 2013). HSV-TK converts GCV into a toxic DNA chain terminator in 3MR expressing cells which competes with deoxyguanosine triphosphate for incorporation into nascent DNA chains, leading to DNA synthesis termination (Laberge et al., 2013). Production of toxic GCV-P by HSV-TK results in damage to nuclear and mitochondrial DNA, causing caspase-dependent apoptosis of p16 expressing cells, and so loss of these cells (Laberge et al., 2013). The P16-3MR mice provided novel insight in to the role of senescent cells in wound healing (Demaria et al., 2014). Data from this study showed that the presence of senescent cells increased with age in many tissues (visceral fat, kidneys, and lungs), evidenced by an increased level of luminescence, starting ~18 months of age. GCV treatment of old (20–24 months) mice efficiently eliminated senescent cells as determined by reduced total body luminescence, SA-β-gal staining, and p16 mRNA levels in biopsies of visceral fat (Demaria et al., 2014). These data demonstrate that the model was effective in removal of senescent cells. However, the effects of elimination of p16 expressing senescent cells on the musculoskeletal system was not examined in this study.

A loss of skeletal muscle mass is seen in old mice, with a 20-30% loss of muscle mass and function by 24-26 months of age (Brooks and Faulkner, 1991, McArdle et al., 2004). Similar rates of loss of motor units are observed in electromyography studies in ageing (Campbell et al., 1973). The mechanisms by which sarcopenia occurs are unclear, but the role of senescence in this muscle loss has received some attention recently.

Senescent cells produce a proinflammatory cytokines via the SASP (Coppe et al., 2010a).

Muscle strength (Visser et al., 2002), muscle mass (Schaap et al., 2006), muscle protein synthesis and catabolism (Jo et al., 2012) have all been shown to be affected by inflammation, suggesting a potential mechanism by which sarcopenia develops. Age-related loss of muscle mass and function is associated with an increased chronic activation of NF-κB in muscles of old mice (Vasilaki et al., 2006). The mechanisms by which this occurs are unclear, but activation would undoubtedly contribute to further local increases in the production and concentrations of pro-inflammatory cytokines and proteolytic processes leading to loss of muscle mass and function (Lightfoot et al., 2014).

The role of the presence of senescence cells distant to muscle on muscle function have been examined using a similar transgenic mouse model, known as INK-ATTAC mouse model (Section 1.1.7.2). Briefly, when exposed to the synthetic molecule AP20187, p16 expressing cells in these transgenic mice undergo caspase-induced apoptosis (Baker et al., 2011). AP20187 is a ligand, which induces the homodimerisation of fusion proteins, which contain a specific mutant of the FKBP domain (Mabe et al., 2014). In order to examine the role of senescence in ageing, the INK-ATTAC mice were crossed with another mouse line with accelerated ageing, BubR1$^{H/H}$ mice (Baker et al., 2008). BubR1$^{H/H}$ mice have been characterised and display accelerated onset of age-related phenotypes such as a shortened lifespan, lordokyphosis (abnormally excessive curvature of the spine), and sarcopenia, amongst others; within 3-5 months (Baker et al., 2004). BubR1$^{H/H}$;INK-ATTAC mice treated with AP20187 from weaning age until 10-months old showed significantly larger mean gastrocnemius fibre diameter and exercise ability, when compared with vehicle treated mice (Baker et al., 2011). To investigate the effect of senescent cell clearance later in life when age-

related phenotypes are apparent in BubR1$^{H/H}$ mice, Baker et al. (2011) started AP20187 treatment of BubR1$^{H/H}$;INK-ATTAC mice at 5 months instead of weaning age and analysed the mice at 10 months old. Ten-month-old AP20187 treated mice had larger mean gastrocnemius fibre diameter and exercise ability, when compared with vehicle treated mice (Baker et al., 2011). The same authors later performed similar experiments with older cohorts of mice, but the INK-ATTAC model was bred into a C57BL/6 WT background rather than the model of accelerated ageing. In this study, gastrocnemius fibre diameter was preserved in 18-month-old female mice following AP20187 treatment compared with untreated WT mice (Baker et al., 2016).

These data suggest that senescent cells may play a role in age-related decline of skeletal muscle mass and function, and that removal of senescent cells from the mice may preserve muscle mass and function.

5.1.2 Hypothesis and aims

The hypothesis was that the presence of senescent cells distant to the muscle during ageing contributes to the development of sarcopenia by the increased production of pro-inflammatory cytokines (SASP). Removal of p16 positive senescent cells in old P16-3MR mice during ageing will result in a reduction in the number of senescent cells in the whole body, reduced plasma cytokine concentrations and preserve muscle mass and function.

This hypothesis was investigated by determining the effects of removal of P16 positive senescent cells in P16-3MR mice on plasma cytokine concentrations and indices of skeletal muscle function and inflammation in mice.

5.2 Methods

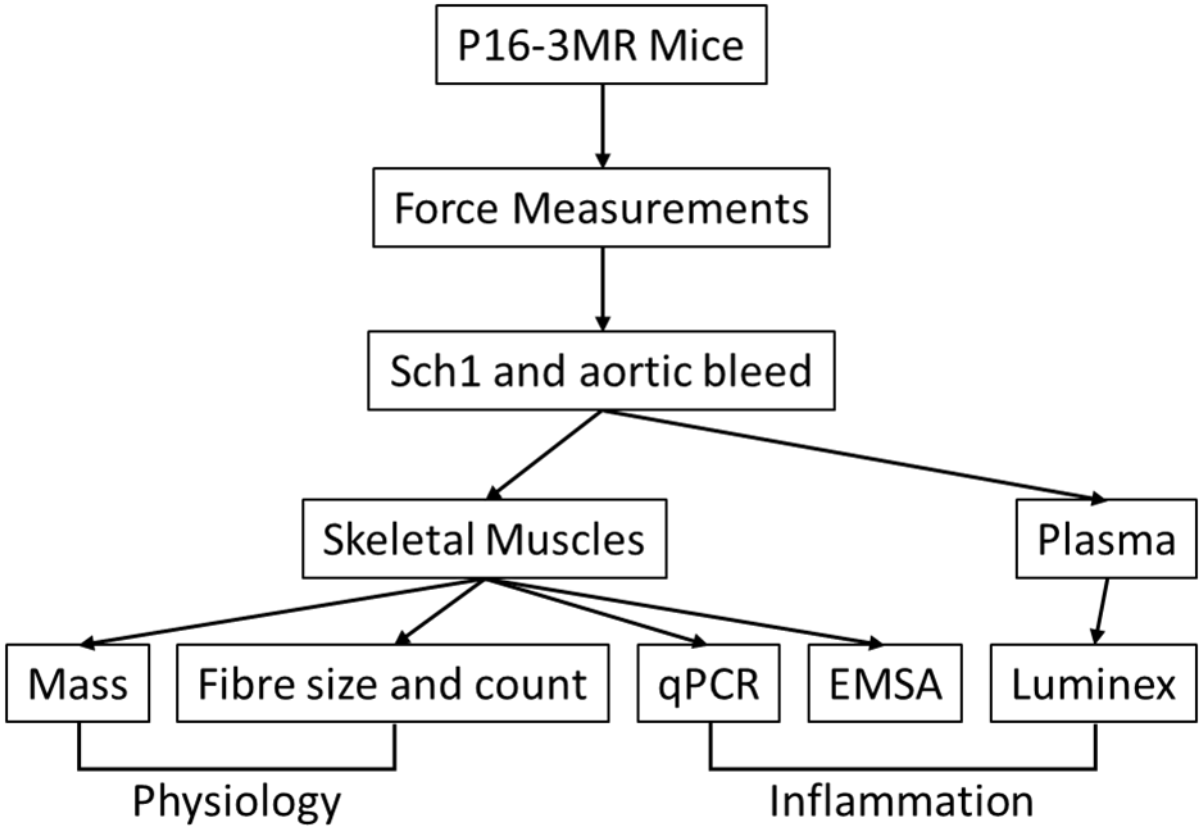

Figure 5.2 Overview of methodology used for Chapter 5

Following GCV treatment, muscle force measurements were recorded. The mice were then culled for plasma and tissue collection. The plasma and the skeletal muscles were analysed for cytokine levels.

5.2.1 GCV treatment of P16-3MR mice

This was a collaborative study with Dr Brooks at the University of Michigan and Drs Richardson and Van Remmen at Oklahoma. The mice were treated with GCV at Oklahoma and analysis of muscle function was carried out at the University of Michigan. This allowed additional muscle analyses although sample collection was limited and a mixed sex cohort was used.

Twenty-one 20-month-old P16-3MR mice of both genders were treated with 25mg/kg

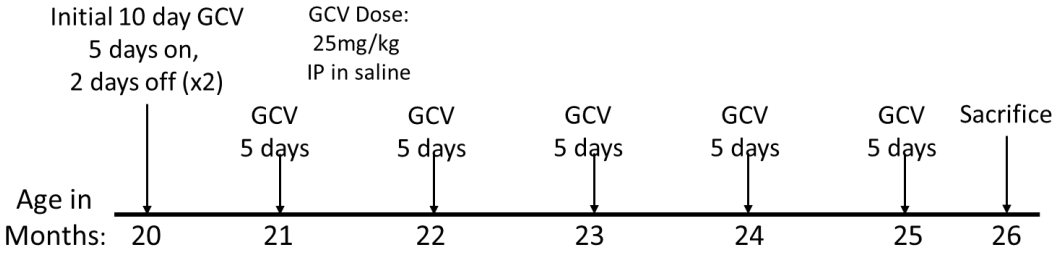

Figure 5.3 Experimental design for treatment of P16-3MR mice with GCV.

P16-3MR mice received repeated doses of GCV or PBS to ablate senescent cells.

Ganciclovir by intraperitoneal (I.P) injection in PBS, or with PBS only as control, using a regime of 5 days of injections with 2 days of rest (Laberge et al., 2013). Following I.P injection, mice were treated every 4 weeks with a 5-day course of GCV, until 26 months old where the mice were sacrificed for tissue harvest and muscle force measurements.

5.2.2 Measurements of force generation of muscles *in situ and ex vivo*

Muscle force measurements were performed *in situ* at the University of Michigan. Gastrocnemius stimulation, both nerve and by direct muscle activation, were performed *in vivo*. Muscle force measurements of the extensor digitorum longus (EDL) and soleus were also performed *ex vivo*. Muscles were carefully dissected and placed at resting length into a Mammalian Ringer's solution at 37oC and gassed with O_2/CO_2. Muscles were attached to a force transducer and maximum tetanic tension determined (Brooks et al., 1995). The *in situ*

analysis of gastrocnemius function allows determination of maximum muscle contractile forces when activated by nerve stimulation compared with activation by electrodes placed across the muscle surface, bypassing neural stimuli. Any difference between the two measures provides information regarding a reduced nerve function, potentially demonstrating a proportion of denervation of the muscle. Analysis of both EDL and soleus muscle function ex vivo provides muscle stimulation only but will demonstrate differential effects on muscles that are primarily comprised of type I or type II fibres.

5.2.3 qPCR of inflammatory markers

Quantitative PCR for cytokines was performed at the University of Michigan and so the nature of cytokines analysed was limited to those that had been shown to be reduced in previous studies (Baker et al., 2016). Data were normalised to 18S.

5.2.4 EMSA for NF-κB transcription factor activity

EMSA was performed on the gastrocnemius muscles of GCV and PBS treated P16-3MR mice. The samples and protocol were performed as described in Section 2.8, and 100µg of muscle lysate was used.

5.2.5 Multiplex cytokine analysis

Blood samples from P16-3MR mice were collected into EDTA coated microcentrifuge tubes from the descending aorta. Samples were centrifuged at 10,000g for 10 mins at 4° and the plasma collected. Multiplex cytokine analysis for pro-inflammatory cytokines was performed as described in Section 2.7.

5.3 Results

5.3.1 Effects of GCV treatment of p16-3MR mice on muscle mass and morphology.

Data are presented either as separate sexes or pooled (Figure 5.4). No significant difference was seen in the body weight of GCV treated compared with PBS treated P16-3MR mice, when either presented as separate sexes or pooled. Treatment of P16-3MR mice with GCV resulted in preservation of muscle mass in male, but not female mice (Figure 5.4) whereby the masses of the TA, soleus, and GTN of GCV treated male mice were significantly higher than those of PBS treated P16-3MR mice, and the masses of the EDL and quadriceps just failed to reach statistical significance. Although some evidence of increased muscle mass in male mice was seen, this was due to the cohort of mice being larger, since no significant differences in muscle masses were seen when normalised to body weight (Figure 5.4G-L).

No significant differences in fibre size distribution were seen between the GCV and PBS treated groups of either sex (Figure 5.5A and B). No significant differences were seen in fibre type composition of GTN muscles between GCV and PBS treated P16-3MR mice (Figure 5.5C).

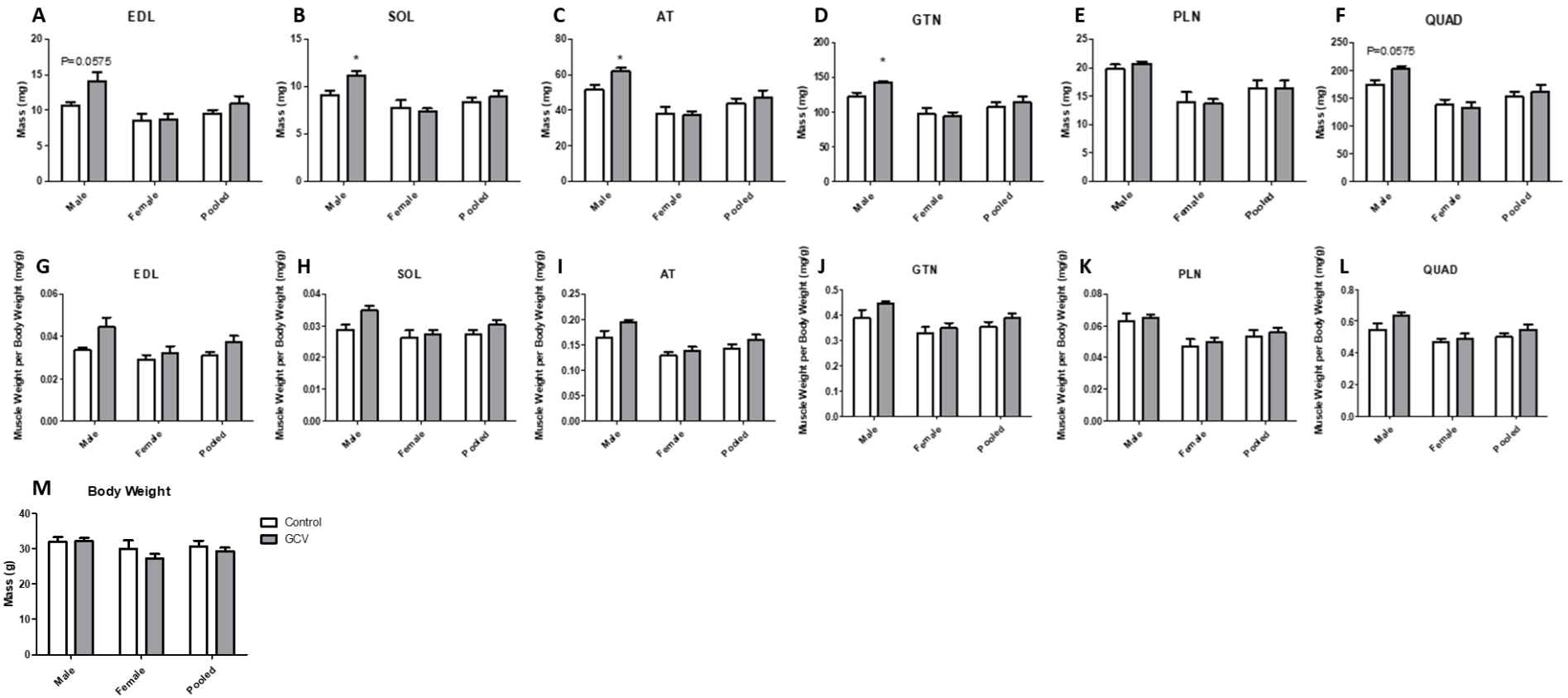

Figure 5.4 Hind limb muscle mass of GCV or PBS treated p16-3MR mice

Mass (mg) of the hind limb muscles: EDL (A), SOL (B), AT (C), GTN (D), PLN (E), and QUAD (F) of male, female, and pooled GCV and PBS treated (control) P16-3MR mice. Muscle weights of EDL (G), SOL (H), AT (I), PLN (K), GTN (J), and QUAD (L); normalised to body weight (mg/mg) of male, female, and pooled GCV and PBS treated (control) P16-3MR mice. Body weight (g) of male, female, and pooled GCV and PBS treated P16-3MR mice (M). Data are presented as mean ± SEM. Significance determined using Student's T-Test.

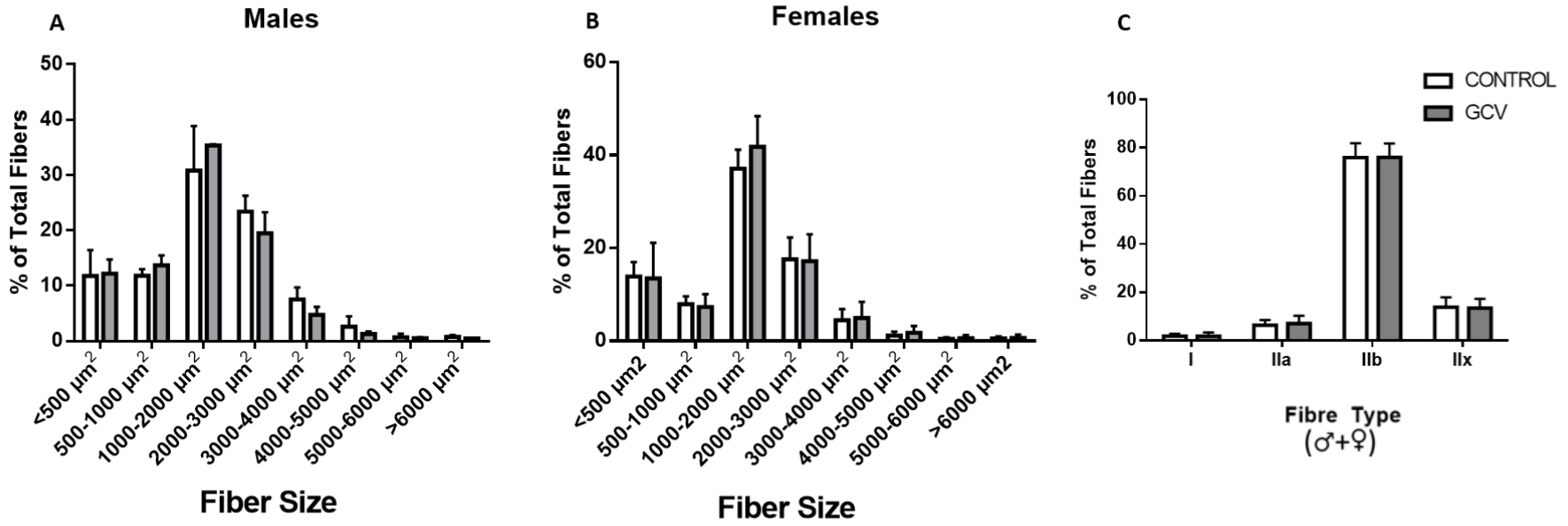

Figure 5.5 Fibre size and type analysis of PBS treated (control) or GCV treated p16-3MR mice.

Fibre size distribution in GTN muscles of GCV and PBS treated male (A), female (B) or mixed sex (C) P16-3MR mice. Data are presented as mean ± SEM, N=3-6.

5.3.2 Effects of GCV or PBS treatment of P16-3MR mice on muscle force generation.

Treatment of P16-3MR mice with GCV had no effect on force generation by several muscles of male or female mice compared with PBS treated P16-3MR mice. Thus, no significant differences in absolute tetanic force (P_0 (mN)) (Figure 5.7) or specific force (kN/m^2) (Figure 5.6) were seen in either male or female GCV treated mice when compared with PBS treated mice.

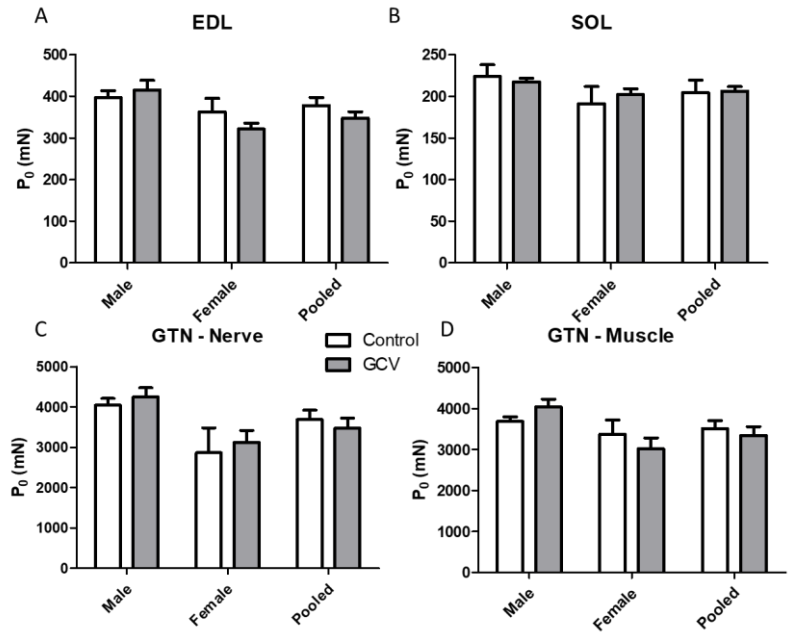

Figure 5.7 Absolute tetanic force generation by hind limb muscles of GCV and PBS treated P16-3MR mice.

Absolute force (mN) of EDL (A), Soleus (B), and nerve (C) or muscle (D) stimulated GTN of male and female GCV or PBS treated P16-3MR mice. Data are presented as mean ± SEM, N=3-6. Student's T-test.

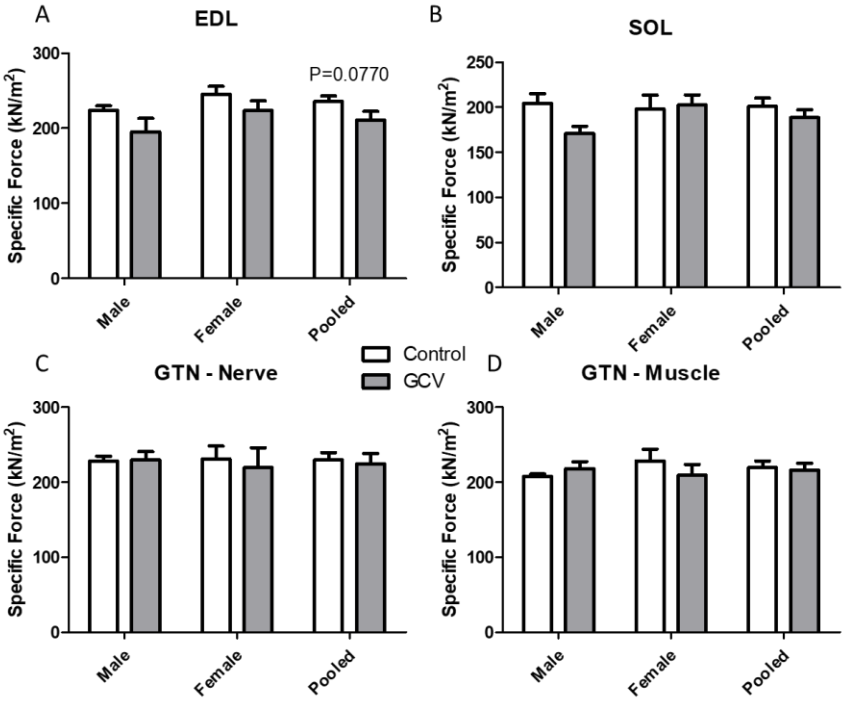

Figure 5.6 Specific force generation by hind limb muscles of GCV and PBS treated P16-3MR mice.

Specific force (kN/m^2) of EDL (A), Soleus (B), and nerve (C) or muscle (D) stimulated GTN of male and female GCV and PBS treated P16-3MR mice. Data are presented as mean ± SEM, N=3-6. Student's T-test.

5.3.3 Effects of GCV or PBS (control) treatment of P16-3MR mice on the inflammatory cytokine profile of plasma and muscle.

Figure 5.10 and Figure 5.11 show the cytokine profile of the plasma of GCV or PBS treated P16-3MR mice. Since no effect of sex on muscle function was seen, samples were combined. There was a tendency for several cytokines to be decreased in the plasma from GCV treated compared with PBS treated mice although only the values for G-CSF reached significance when compared with PBS treated control mice.

Surprisingly, DNA binding of the NF-κB/p65 transcription factor was significantly increased in GTN muscle of GCV treated P16-3MR mice when compared with muscle from PBS treated control mice (Figure 5.8).

No significant differences were seen in the mRNA levels of IL-6 or TNF-α in the AT and GTN muscles of PBS treated and GCV treated P16-3MR mice (Figure 5.9).

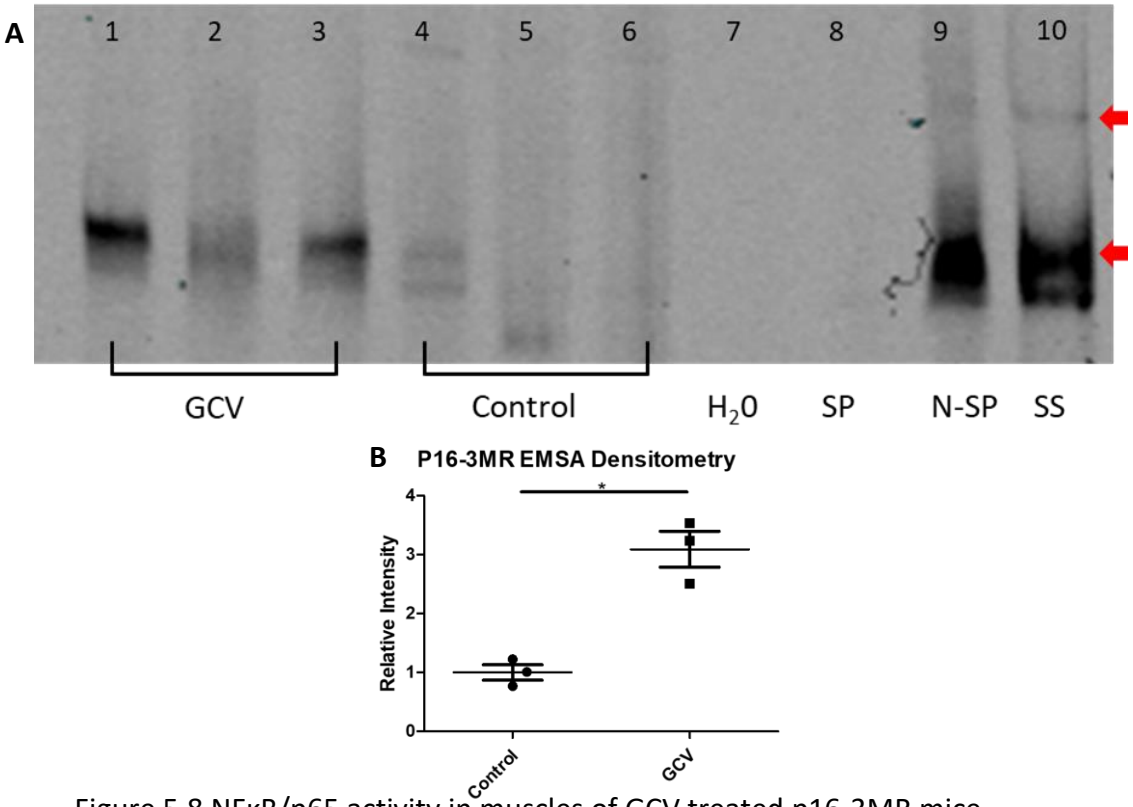

Figure 5.8 NFκB/p65 activity in muscles of GCV treated p16-3MR mice.

(A) EMSA for NFκB/p65 transcription factor binding in the gastrocnemius of GCV and PBS treated P16-3MR mice. (B) Densitometry. SP, Specific competitor. N-SP, Non-specific competitor. SS, Supershift. Data are mean ± SEM. *P<0.05, Student's T Test. Top red arrow displays supershifted band from bottom red arrow.

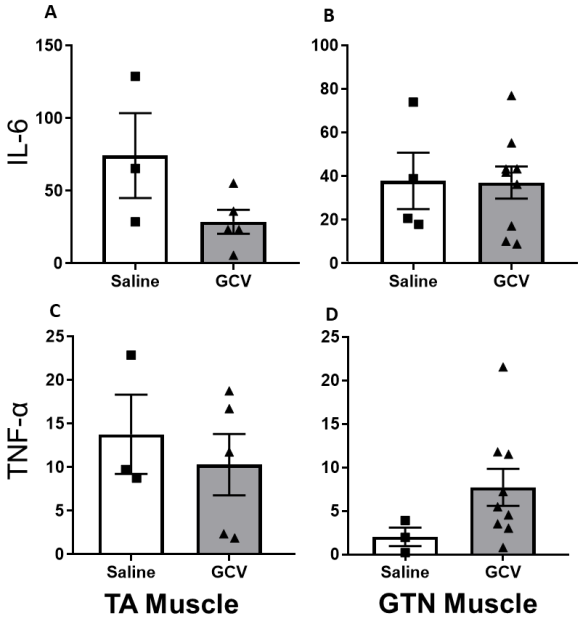

Figure 5.9 Cytokine mRNA levels in muscle of PBS or GCV treated p16-3MR mice.

Fold changes in expression of IL-6 and TNF-α, in TA and GTN from GCV or PBS (control) treated p16-3MR mice, normalised to 18S. Data are mean ± SEM, N=3-6. Significance tested with ANOVA.

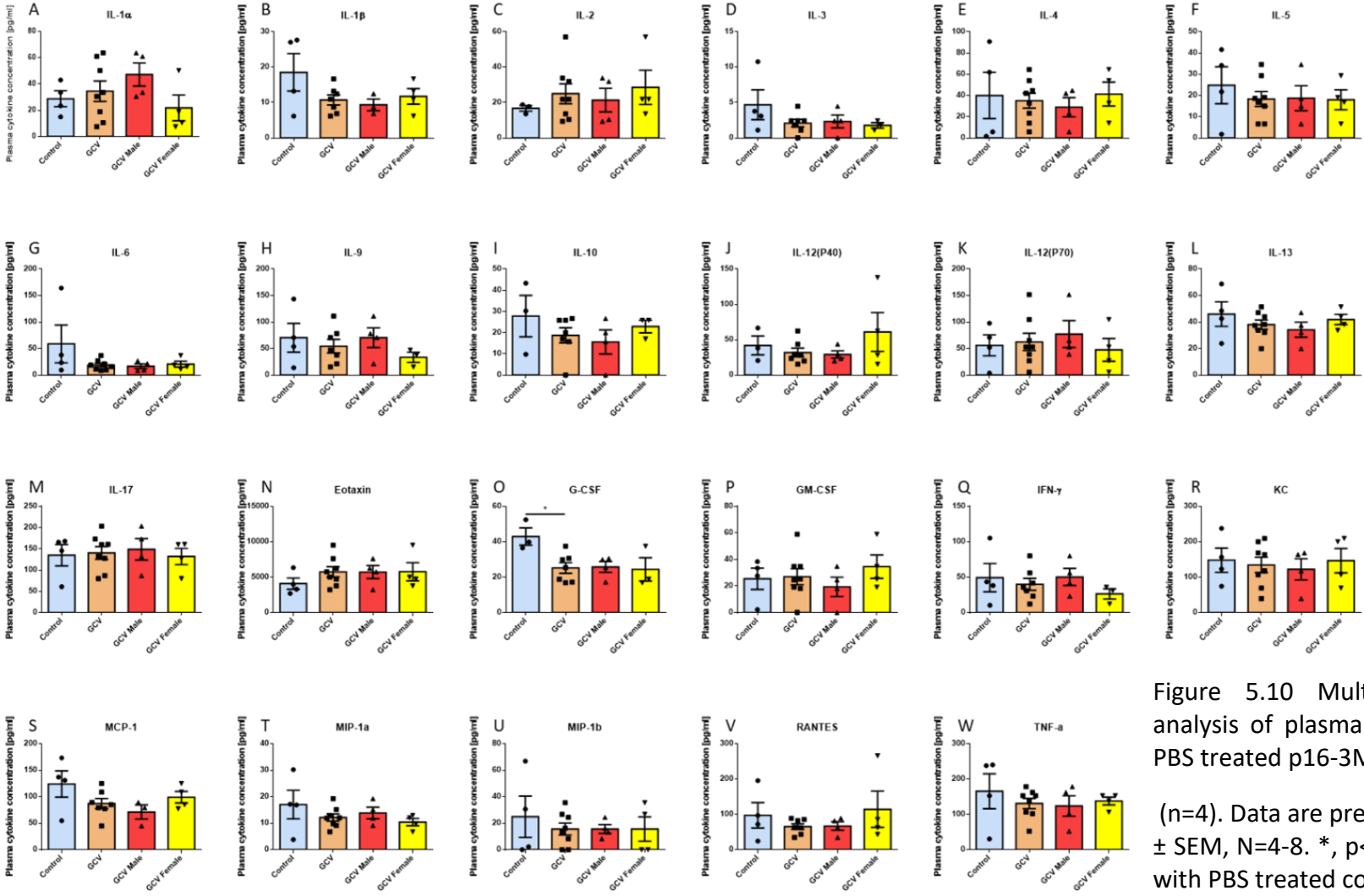

Figure 5.10 Multiplex cytokine analysis of plasma from GCV and PBS treated p16-3MR mice.

(n=4). Data are presented as mean ± SEM, N=4-8. *, p<0.05 compared with PBS treated control data.

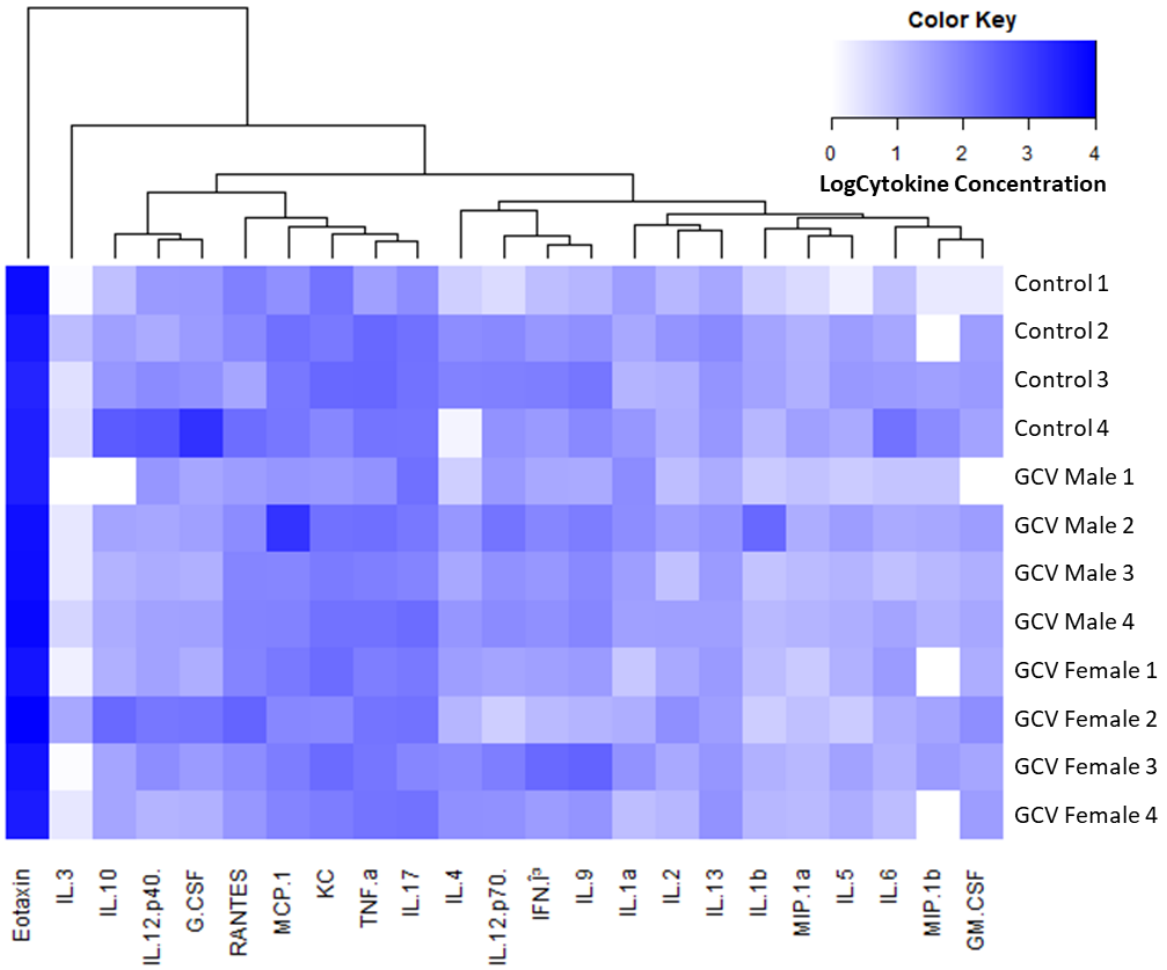

Figure 5.11 Heatmap and Dendritic Clustering of cytokines from the plasma of GCV and PBS treated p16-3MR mice.

Cytokine concentrations plotted on a log10 scale. (n=4 per group).

5.4 Discussion

The aims of this study were to determine the effects of the whole body removal of senescent cells on plasma cytokine concentrations and indices of skeletal muscle inflammation and to examine whether removal of senescent cells from old P16-3MR mice following treatment with ganciclovir resulted in preservation of skeletal muscle including mass and function compared with that of PBS (control) treated P16-3MR mice.

5.4.1 Effects of elimination of p16 expressing cells from p16-3MR mice on skeletal muscle mass and function.

Male p16-3MR mice treated with GCV showed a small but significant preservation of mass of most muscles measured; with others, just missing significance compared with muscles of PBS treated p16-3MR mice (Figure 5.4). This preservation was not seen in female p16-3MR mice treated with GCV compared with PBS treated p16-3MR mice. However, when data were normalised to body weight, there were no significant differences in muscle mass, in either gender of p16-3MR mice suggesting that the mice in the GCV-treated group were generally larger than the PBS-treated control mice. Since body weight was not recorded prior to treatment, it was not possible to determine whether the treatment was responsible for this. Treatment of female p16-3MR mice with GCV resulted in no significant differences when compared with the PBS treated p16-3MR mice. These data show that GCV treatment and so removal of p16 cells provides little protection from the age-related loss of muscle mass in either sex. A characteristic of sarcopenia is an age-related loss of muscle fibres (Lexell et al., 1988) and an atrophy of the remaining fibres, with type II (fast-twitch) fibres demonstrating a greater reduction in cross-sectional area, when compared with the size of type I fibres (slow-twitch) fibres (Lexell et al., 1988). Data showed that there was no significant difference in

fibre size between the GCV treated and the PBS treated mice. Therefore, elimination of p16 expressing cells did not preserve fibre number or size in old mice. No effect of GCV treatment was seen on force generation (Figures 5.6 and 5.7) and little effect was seen on fibre size distribution, suggesting that the increase in body mass seen was not relevant and that depletion of P16 positive cells in old mice had little effect on muscle function.

5.4.2 Effects of elimination of p16 expressing cells from p16-3MR mice on plasma cytokine levels.

The findings from this study are in contrast to other studies. Demaria et al. (2014) treated of p16-3MR mice with GCV via daily intraperitoneal (IP) injections for 5 consecutive days at 25 mg/kg in PBS. In the study presented in this Chapter, p16-3MR mice were treated with the same dosing regimen used by Demaria *et al*, but across the longer period of 4 months. Supplemental Figure 2E from Demaria *et al* (Figure 5.12) shows the time course of total body luminescence for p16 in p16-3MR mice at 12, 18, 20, and 24 months of age, indicative of the

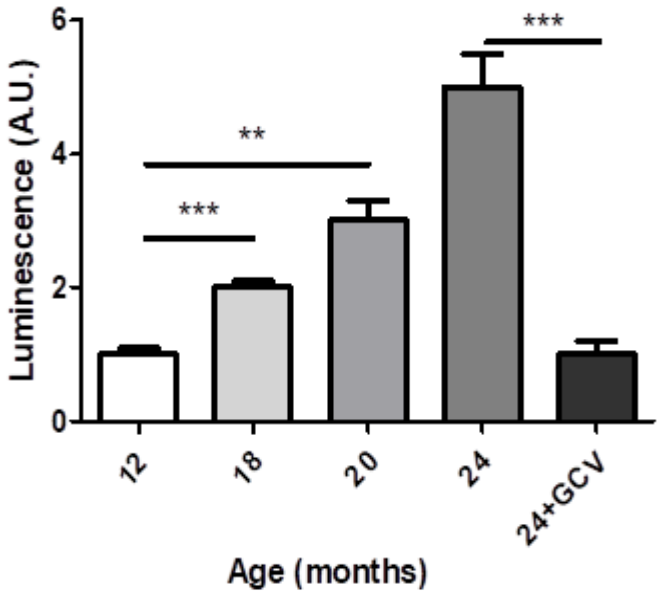

Figure 5.12 Total body luminescence of p16 expressing cells of p16-3MR mice with increasing age.

Adapted from supplemental figure 2E of Demaria *et al*. (2014).

accumulation of p16 positive senescence cells. Significant increases in luminescence, reflecting a concomitant increase in senescent cells were seen. Luminescence was significantly increased in 24-month old p16-3MR mice when compared with 12-month old p16-3MR mice. GCV treatment of 24-month-old p16-3MR mice decreased total luminescence to that of 12-month-old untreated p16-3MR mice.

The current study in this Chapter did not examine luminescence in these mice. GCV treatment results in the acute removal of senescent cells although the time course of removal and repletion is unclear. It is unlikely although possible that the treatment did not result in complete and persistent removal of senescent cells in our model. It may also be possible that prolonged treatment of mice with GCV has a detrimental effect on mice and unfortunately, no untreated control mice or GCV treated old WT mice were included in this study.

Whilst the effect of removal of senescent cells on skeletal muscle mass and function was not investigated in the Demaria et al. (2014) study, decreased concentrations of SASP factors interleukin-6 (IL-6), interleukin-15 (IL-15), and MMP-3 were reported in the fat of GCV-treated p16-3MR mice. It is well documented that senescent cells produce a SASP (Baker et al., 2016). The SASP is proposed to contribute to the altered cytokine profile of the plasma in old age and the levels of a substantial number of cytokines are elevated in plasma of old mice (Section 4.4.2). The levels of some of these cytokines are also changed in muscles of old mice, (Section 4.4.2) and it is proposed that this occurs via activation of NF-κB in muscle, (Vasilaki et al., 2006), potentially by the bystander effect. GCV-mediated elimination of senescent cells should therefore reduce the levels of SASP-related cytokines in the plasma and muscle with normalisation of the level of activation of NF-κB. However, in the current study, GCV treatment of p16-3MR mice had little effect on the plasma cytokine levels compared with PBS

treated mice, except for G-CSF, which was significantly decreased when compared with PBS treated old p16-3MR mice. Although mRNA analyses were limited in this study, GCV treatment had no significant effect on IL-6 and TNF-α mRNA levels in the AT or GTN muscles when compared with PBS treated p16-3MR mice. These data contradict other studies where senescent cells have been eliminated from whole mice. The inflammatory SASP makers, including IL-6, IL-1α, and TNFα were examined in the gastrocnemius of INK-ATTAC mice (Baker et al. (2016). IL-6 increased significantly from 12- to 18-months of age, and AP20187 treatment resulted in reduced expression to levels similar to that of 12-month-old mice (Baker et al. (2016). IL-1α and TNFα did not change in expression with age, however, administration of AP20187 also resulted in significantly lower expression of IL-1α and TNFα in muscles of these mice. Such changes in IL-6 were not reproduced in the study presented here (Baker et al. (2016).

In contrast to the hypothesised normalisation of NF-κB activation, treatment of p16-3MR mice with GCV resulted a large and significant *increase* in DNA binding activity of NF-κB although this was not accompanied by a major change in muscle cytokine production. A comparison of plasma cytokine levels in mice with P16 positive senescent cells removed, with cytokines shown to be modified in old WT mice in Chapter 4 (Table 5.1) shows no effect of removal of senescent cells on any of the cytokines elevated in plasma of old compared with adult mice. Together, these data suggest that elimination of senescent cells in old mice had little effect on plasma cytokine levels with the exception of G-CSF, muscle production of cytokines or muscle mass and function suggesting no major role for P16 positive senescent cells in age-related loss of muscle mass and function.

	Old mouse models	
Cytokines	WT	P16-3MR
BCA-1/CXCL13		-
CTACK/CCL27		-
ENA-78/CXCL5		-
Eotaxin/CCL11		
Eotaxin-2/CCL24		-
Fractalkine/CX3CL1		-
G-CSF	-	
GM-CSF		
I-309/CCL1		-
IFN-γ		
IL-1α	-	
IL-1β		
IL-2		
IL-3	-	
IL-4		
IL-5	-	
IL-6		
IL-9	-	
IL-10		
IL-12(p40)	-	
IL-12(p70)	-	
IL-13	-	
IL-16		-
IL-17	-	
IP-10/CXCL10		-
I-TAC/CXCL11		-
KC/CXCL1		
MCP-1/CCL2		
MCP-2/CCL8	-	-
MCP-3/CCL7		-
MCP-5/CCL12		-
MDC/CCL22		-
MIP-1α/CCL3		
MIP-1β/CCL4		
MIP-2/CXCL2		-
MIP-3α/CCL20		-
MIP-3β/CCL19		-
RANTES/CCL5		
SCYB16/CXCL16		-
SDF-1α/CXCL-12		-
TARC/CCL17		-
TECK/CCL25		-
TNFα		

Table 5.1

Summary of the cytokines measured in the plasma of old compared with adult mice, and the plasma of GCV treated P16-3MR compared with PBS treated mice. Green, significantly increased; Red, significantly decreased; Grey, no difference; White, not measured.

5.4.3 The effects of G-CSF on skeletal muscle

Despite no evidence of an effect of elimination of P16 positive cells from old mice on cytokines known to be elevated in plasma of old compared with adult WT mice. The effect of elimination of p16 positive cells on granulocyte-colony stimulating factor (G-CSF) is intriguing. G-CSF is also known as colony-stimulating factor 3 (CSF3). G-CSF is a 25kD secreted glycoprotein encoded by the CSF3 gene. G-CSF has a significant role in the regulation of neutrophils, as G-CSF receptor-deficient mice are characterised by neutropenia; a reduced capacity to respond to infection with neutrophils (Liu et al., 1996). G-CSF has not been identified as a member of SASP for any other cell. G-CSF is secreted by almost all tissues in response to a number of inflammatory stimuli such as IL-1, LPS, and TNF-α (Roberts, 2005). G-CSF is used therapeutically to stimulate the bone marrow, resulting in the production and release of hematopoietic stem cells (HSCs) in to the blood (Deotare et al., 2015). Studies have shown that human myotubes that undergo cyclic mechanical strain secrete IL-6, IL-8, MCP-1, and G-CSF (Peterson and Pizza, 2009). Furthermore, G-CSF has been shown to be asymmetrically expressed in satellite cells. G-CSF positively affects the satellite cell population during multiple stages of differentiation in fibres cultured *ex vivo* (Hayashiji et al., 2015). It may decrease bone mineral density in mice (Hayashiji et al., 2015). Thus, it is tempting to speculate that a decrease in G-CSF as seen in the current study denotes a potentially reduced production of HSCs, reducing the immune cell population and represents a potential detrimental effect of the treatment. Disruption of satellite cell growth may also deplete the cell pool, inhibiting muscle growth and repair, potentially contributing to sarcopenia in the longer term (Hayashiji et al., 2015) although no worsening of sarcopenia was seen in the current study.

5.4.4 Comparison with the INK-ATTAC mouse model

Studies examining the effect of elimination of p16 positive cells on age-related loss of muscle mass and function are limited. A similar model that also made use of genetically modified mice to remove senescent cells was reported by Baker et al. (2016). These authors made use of the INK-ATTAC strain, as well as the P16-3MR mice (Section 1.1.7.2). The INK-ATTAC transgenic mouse model was also used to selectively eliminate p16 positive, senescent cells. The model has been used to investigate several senescence related pathologies. Examples include age-related bone loss (Farr et al., 2019, Farr et al., 2017, Kim et al., 2019), age-dependent hepatic steatosis (Ogrodnik et al., 2017), neurogenesis (Ogrodnik et al., 2019), kidney disease (Valentijn et al., 2018), heart regeneration (Lewis-McDougall et al., 2019), adipogenesis (Xu et al., 2015a), diabetes, (Aguayo-Mazzucato et al., 2019), and atherosclerosis (Roos et al., 2016).

Baker et al. (2016) showed that INK-ATTAC mice bred onto two different backgrounds, C57BL/6 and C57BL/6-129Sv-FVB (a model of different white fat depots) show a loss of spontaneous movement and exploratory behaviour from 12 to 18 months of age (Baker et al., 2016). Abnormal movement and behaviour were rescued to levels equal to 12-month-old mice by the administration of AP20187 (Section 1.1.7.2) with the concomitant removal of senescent cells. In contrast, exercise time, distance, and work were not improved in 18-month-old INK-ATTAC treated with AP20187 , when compared with 18 month old control mice (Baker et al., 2016). Physiological measures of the fitness and gastrocnemius weight of 18-month-old INK-ATTAC mice was not significantly increased with AP20187 treatment, in both genders (Baker et al., 2016). Gastrocnemius fibre diameter was significantly greater in 18-month-old female AP20187 treated INK-ATTAC mice when compared with untreated

controls, however, male AP20187 treated INK-ATTAC mice were not significantly affected (Baker et al., 2016).

There are some differences between Baker et al. (2016), and the study performed in this chapter in addition to the use of different transgenic animal models (INK-ATTAC versus p16-3MR).The published work of Baker only examined 18-month-old mice whilst 26-month-old mice were used in this current study. With that in mind, the data presented in Baker et al. (2016) contrast with our own. Data presented in the current study show no effect on tetanic force generation by GTN muscles using either nerve or direct muscle stimulation (Figure 5.7), when compared with PBS treated (control) p16-3MR mice. Furthermore, SASP and inflammatory markers IL-6 and TNFα were measured in the gastrocnemius of both studies via qPCR. Baker et al. (2016) reported an approximately 50% decrease in IL-6 and TNFα expression within the muscle of 18-month-old female INK-ATTAC mice. In the current study, no significant differences were reported in IL-6 or TNFα mRNA levels within the muscle of 26-month-old p16-3MR mice compared with muscles of PBS treated control mice. The reasons for these differences are unclear. It may be due to the difference in protocols or the nature of the samples used for the qPCR in this study. In the current study, surprisingly, the EMSA for NF-κB transcription factor activity showed increased activity in muscles of GCV treated compared with PBS treated control mice. This increase may be due to a direct effect of chronic treatment of mice with GCV or an effect of removal of senescent cells although the mechanism by which this is acting is unclear. Such increases in NF-κB transcription factor activity may therefore be potentially masking any changes seen from removal of p16 positive senescent cells. One drawback of the study was the lack of a control old WT group receiving ganciclovir alone.

5.4.5 The use of P16-3MR mice in other studies

P16-3MR mice have been used for several other studies investigating senescence and age-related pathologies. Examples of these include senescent chondrocytes and osteocyte in the development of osteoarthritis (OA) (Jeon et al., 2017, Kim et al., 2019), Acute myeloid leukaemia (AML) (Abdul-Aziz et al., 2019), intervertebral disc degeneration (IDD) (Patil et al., 2019), immune-senescence in irradiated mice (Palacio et al., 2019), and the role of senescent astrocytes in cognitive decline (Yabluchanskiy et al., 2020). None of these studies investigated the effects of removing senescent cells on muscle mass and function. However, some have reported a decrease in the expression of pro-inflammatory cytokines such as: IL-6, IL-1β (Jeon et al., 2017) (anterior cruciate ligament), IL-1α, IL-6, TNFα (Kim et al., 2019) (bone marrow-derived macrophages), IL-6, IL-8, MIP-3a (Abdul-Aziz et al., 2019) (bone marrow stem cells), and plasma levels of IL-1α, IL-6, IL-10, KC, MCP-1, VEGF (Palacio et al., 2019). The decrease in the expression of the pro-inflammatory cytokine IL-6 is the most common result following GCV treatment in these varying studies. These effects were not seen in the current study, both at the mRNA level and at the protein level in circulating plasma. These differences may have occurred due to the different GCV treatment regimens utilised by this study. Furthermore, not only were the ages of the mice studies different, but they were also subject to unique experimental procedures to investigate each of the authors' hypotheses.

5.4.6 Limitations of this and other studies

The lack of study of females is a major limitation in a large number of studies. Women and non-human female mammals are underrepresented in studies, whereby researchers assume results from males apply to females (Beery and Zucker, 2011). Researchers avoid the inclusion of females because of concerns that hormonal cycles decrease the homogeneity of study populations and confound effects of experimental manipulations (Beery and Zucker, 2011).

Many drug studies using males often generate different results from those for women (Soldin and Mattison, 2009). The study presented in this Chapter contained mixed sex groups and it was not possible to separate sexes in most analyses due to the small sample number. Experimental designs should include batches of sex and aged matched males/females as females differ from males at a cellular, molecular, and whole organism level. A recent analysis of gene expression in mice demonstrated substantially sexual dimorphic expression in the brain, liver and adipose tissue and whilst both sexes make the same steroid hormones they are inevitably found in different quantities (Yang et al., 2006).

Another limitation to the study is that all p16 expressing cells of the P16-3MR mice would be eliminated with GCV treatment. T-cells express high levels of p16 (Liu et al., 2009), and highly differentiated T-cells show some similarities with senescent cells (Pangrazzi and Weinberger, 2020). It is proposed that removal of p16 positive cells in an effort to remove senescent cells may also influence T-cell populations and removal of p16 expressing T-cells would have an impact on the plasma cytokine profile of the GCV treated mice. Baker et al. (2016) Examined CD4+, CD8+, CD44hi/CD4+, and CD44hi/CD8+ T-cell populations in peripheral blood mononuclear cells in INK-ATTAC mice. However, this study showed that removal of p16 expressing cells had little effect on T cell populations. CD4+ T-cell populations decreased with age, but clearance of senescent cells at 18 months of age had no effect on T-cell population size when compared with the untreated controls. Examination of T-cell populations was out of the scope of the current study.

Despite the obvious benefits of removing proinflammatory senescent cells, there may negative consequences to the organism. Grosse et al. (2020) investigated cellular senescence in organismal ageing with two different strains of transgenic mice. The first line (p16-Cre/R26-

DTA) acted as a reporter and identified that age-induced p16 senescence is a slow process that manifests around 10–12 months of age in mixed C57BL/6J and 129/SvJ background mice. Furthermore, the majority of these p16 reporter cells were vascular endothelial cells mostly in liver sinusoids (LSECs), and to lesser extent macrophages and adipocytes. The second strain examined by these authors was the INK-ATTAC strain discussed previously, whereby continuous or acute elimination of p16 expressing senescent cells disrupted the blood-tissue barriers. Senescent liver sinusoids (LSECs) removal via INK-ATTAC were not replaced with healthy LSECs but instead resulted in fibrosis. This ultimately resulted in liver and perivascular tissue fibrosis and health deterioration of the mice. Of interest is that when *ex vivo* isolated LSECs were treated with the senolytics Dasatinib and Quercetin, there was no significant effects reported. Furthermore, when 10-month-old p16-Cre/R26-mTmG mice were treated with these senolytics for 5 weeks, a significant difference in p16 expressing macrophages was reported when compared with vehicle control mice, but LSECS and adipocytes were not affected. These differences may have arisen from the fact that senescent cells are heterogeneous, and that each method of senescent cell removal may have specificity for a subset of senescent cells.

5.5 Conclusion

In summary, removal of p16 expressing, senescent cells from P16-3MR mice by GCV treatment had no effect on preserving muscle mass or on muscle function. Furthermore, the GCV treatment to remove p16 positive senescent cells had very specific effects on the plasma pro-inflammatory cytokine G-CSF and no effect on tissue expression of inflammatory cytokines. There were some limitations to the current study. , The differences reported between this study and other reported findings may be attributed to the nature of the GCV

treatment, the age and sex of the mice, and the experimental protocol. Data are complicated by the need to include a number of control groups in such transgenic studies and, whereas genetic intervention to remove and investigate cellular senescence remains a powerful tool, this does not translate to an immediate treatment for humans. Pharmacological intervention with molecules designed to eliminate senescent cells provides a simpler model and could prove to be an effective tool in removing senescent cells and identifying their contributions to age-related pathologies such as sarcopenia and inflammaging.

Chapter 6: The effects of intervention with the senolytic fisetin on muscle mass and function in old mice

6.1 Introduction

6.1.1 Senolytics

Senolytics (from the words “senescence” and “lytic” – destroying) are small molecule compounds that selectively induce the death/clearance of senescent cells (Xu et al., 2018). The aim of senolytics are to reverse the negative effects of senescence cells on ageing (Xu et al., 2018). The mechanisms by which the presence of senescent cells are deleterious are thought to be at least in part to the previously described senescent associated secretory phenotype (SASP), which includes pro-inflammatory cytokines, chemokines, and matrix remodelling proteins (Section 1.1.5) (Coppe et al., 2008). Several reviews have identified the potential role of senescent cells and the SASP in aging-related conditions (Munoz-Espin and Serrano, 2014, LeBrasseur et al., 2015, da Silva et al., 2019). Studies that have removed senescent cells *in vivo* via inducible removal of p16 expressing senescent cells have shown enhanced health span and delays in the development of multiple age-related phenotypes in genetically modified progeroid mice, including age-related loss of muscle mass and strength (Baker et al., 2016, Baker et al., 2008, Baker et al., 2011).

Thus, pharmacological interventions that target senescent cells and/or the SASP provide a potential therapeutic approach to ameliorate age-related chronic diseases, disabilities and possibly extend health span. Zhu et al. (2016) used a bioinformatics-based approach to identify potent senolytic agents that would activate cell death pathways and trigger apoptosis preferentially in senescent cells without damaging non-senescent, proliferating, quiescent, or differentiated cells throughout the body. From this bioinformatic screen, two compounds were selected as candidate senolytics, and were tested *in vivo*: The tyrosine kinase inhibitor Dasatinib and the polyphenol Quercetin (see Section 1.1.8).

In a related study, Xu et al. (2018), where senescent cells were transplanted into mice, both of these drugs were shown to have a positive effect on muscle loss. Even a small number of senescent preadipocytes (0.2-1x10^6 cells) were sufficient to cause significant decreases in grip strength, hanging endurance, maximal speed, and more when compared with control mice. Furthermore, mice with senescent cells transplanted into them showed significant decreases in lifespan when compared with untreated mice and experimental-control mice. Dasatinib and quercetin were administrated via oral gavage 1 month prior to analysis. The administration of senolytics to both senescent cell-transplanted younger and naturally aged mice alleviated physical dysfunction, with measures in grip strength, hanging endurance, maximal speed equalling or greater than control mice. Dasatinib and quercetin treatment also increased post-treatment survival and reversed the negative effects of the transplanted cells on lifespan compared to that of control mice.

The senolytics dasatinib and quercetin have been used in human trials, and have resulted in significant improvement thus far (Hickson et al., 2019). The open label Phase 1 pilot study administered 3 days of oral dasatinib (100mg) and quercetin (1000mg) to subjects with diabetic kidney disease. Significant decreases in p16, p21, SA-β-gal activity, and circulating SASP factors (including IL-1α, IL-6, MMP-9, and MMP-12) were reported in adipocytes, epidermal cells within 11 days of treatment.

6.1.2 Polyphenols as senolytics

Polyphenols are small, water soluble compounds (Haslam and Cai, 1994). Several hundred different polyphenols are found in plant-based foods (Extensively reviewed by Tressera-Rimbau et al. (2017)). Current research on the role of polyphenols in health and disease has focused on their antioxidant and anti-inflammatory properties (Hussain et al., 2016). Many

polyphenols are not absorbed in their native form but are instead metabolised by intestinal enzymes and/or colonic microflora. These metabolites are further modified to allow entry into the blood and tissues (Scalbert et al., 2002). Indirect evidence of the absorption of polyphenols through the gut barrier is the increase of the antioxidant capacity of the plasma following the consumption of polyphenol-rich foods (Scalbert et al., 2002). The effects of polyphenols in human health have been extensively reviewed by Serino and Salazar (2018), and reported improved cardiovascular disease (CVD) outcomes in humans with increased dietary polyphenol consumption; amongst other changes. This is part due to two reasons. The first is that polyphenols are reducing agents and thus scavenge free radicals, and participate in the regeneration of other antioxidants such as vitamin E (Scalbert et al., 2002). The second is that some polyphenols have shorter, more specific effects. For example, isoflavone phytoestrogens are associated with a lower risk of hormone-dependent diseases and have well-documented pseudo-estrogenic properties (Scalbert et al., 2002).

6.1.3 Fisetin as a senolytic

Fisetin (7, 3', 4'-flavon-3-ol) is a plant based polyphenol from the flavonoid group, and can be found in a wide variety of plants (Arai et al., 2000). The concentration of fisetin in these sources ranged from 2-160 µg/g. Individuals typically consume approximately 0.4 mg of Fisetin per day (Arai et al., 2000). Like other polyphenols, fisetin is a sirtuin activating compound (Section 1.1.8) and has been shown to extend the life span of simple organisms like yeast, worms and flies (Baur, 2010). The effect appears to be derived from the ability of fisetin to block the PI3K/AKT/mTOR pathway (Syed et al., 2013), as well as interfere with cell cycle progression (Gupta et al., 2014). A number of studies have demonstrated that fisetin has the potential to prevent and/or inhibit various chronic inflammation-related conditions (Pal et al., 2016b).

Yousefzadeh et al. (2018) examined the effects of a range of polyphenols on senescent murine and human fibroblasts. In this study, the effects of fisetin on senescent cells was tested in INK-ATAC mice (Section 1.1.7.2), progeroid p16 reporter mice (C57BL/6 $p16^{Luc/+}$; $Ercc1^{+/-}$ and FVB/n $p16^{+/Luc}$; $Ercc1^{+/\Delta}$), and old C57BL/6 WT mice. The publication is a little confusing since the mouse models, age, and methods of fisetin delivery vary throughout the study.

The mice treated were either given a diet containing fisetin (500mg/kg) or an oral gavage (100mg/kg). Progeroid luciferase p16 reporter mice treated with fisetin as part of their diet over 10 weeks showed significantly less total body luminescence when compared with vehicle fed control mice. This treatment resulted in a decreased presence of senescent cells in internal organs (fat, spleen, liver, and kidneys) in fisetin fed mice when compared with control mice (Yousefzadeh et al., 2018). Furthermore, old C57BL/6 WT mice (22-24 months old) given fisetin by oral gavage showed reduced senescent cell content (SA-ß-gal) and pro-inflammatory immune cells (T-cells, and natural killer (NK) cells) within the adipose tissue compared with vehicle treated mice and young mice (Yousefzadeh et al., 2018).

To investigate the effects of fisetin on lifespan, 20-month old WT mice were fed a diet containing fisetin, which resulted in a substantial extension of median and maximal lifespan to approximately 32-months, when compared with vehicle treated mice. Several tissues (brain, kidneys, liver, and lungs) had reduced age-related pathology and reduced the expression of senescence and SASP markers in the fisetin treated group compared to the control mice (Yousefzadeh et al., 2018).

Thus, fisetin has the potential to be a therapeutic agent to combat age-related pathologies, in mice at least. Indeed, a phase II trial has been initiated to determine whether fisetin may alleviate frailty, inflammation, and related measures in older adults (NCT03675724).

However, little is currently known about the effects of fisetin on skeletal muscle mass and function in old WT mice and humans.

6.1.4 Fisetin treatment and cell signalling

Fisetin has been proposed to modulate many signalling pathways. At lower doses (3.4-50 µM), fisetin targets Aurora B kinase by inhibiting kinetochore and centromere localization. This results in immature segregation of chromosomes, premature cessation of mitosis without cytokinesis, and ultimately aneuploidy (Gollapudi et al., 2014). At higher doses of fisetin (30-100 µM), DNA replication enzymes, topoisomerase I and II, are inhibited which results in chromosomal breakage (Lopez-Lazaro et al., 2010, Olaharski et al., 2005).

Much work has been undertaken to investigate the role that fisetin plays is cancer in studies both *in vivo* and *in vitro*. Treatment of cancer cells with fisetin resulted in:

Inhibition of cell cycle progression by targeting cyclins and cyclin-dependant kinases (CDKs). Fisetin forms a complex with human CDK6 and inhibits its activity with an IC_{50} of 0.85 µM (Sung et al., 2007, Salmela et al., 2009).

Inhibition of NF-κB DNA binding activity and signalling within several cancer cell lines (Pal et al., 2015, Pal et al., 2016a, Pal et al., 2014). Indeed, EMSA data has shown that 50 µM fisetin treated H1299 cells suppressed TNF-induced NF-κB activation within 6 hours (Sung et al., 2007).

PC3 cells were treated with 40, 80 and 120 µM of fisetin for 48 hours inhibited the activity of mTOR by 6, 11 and 25%, respectively (Suh et al., 2010). It also increased apoptosis via inhibition of the expression of PI3K, phosphorylation of AKT, expression and phosphorylation of mTOR, and mTOR complex formation (Suh et al., 2010, Chien et al., 2010).

Indeed, Fisetin was reported to reverse the acquired cisplatin-resistance in A549-CR lung cancer cells (Zhuo et al., 2015). Fisetin (40 µM) in combination with cisplatin (10 µM) showed intense suppression of cell viability and induction of apoptosis as compared to cells treated with fisetin and cisplatin alone, possibly via inactivating MAPK pathways as well as suppressing Survivin expression (Zhuo et al., 2015).

6.1.5 Hypothesis

Skeletal muscle mass and function is decreased in old mice and is accompanied by an increase in plasma cytokine levels and increased NF-κB activity in skeletal muscle. The hypothesis was that the polyphenol fisetin would reduce the burden of senescent cells in old mice, reducing pro-inflammatory cytokine levels in the plasma, and reduce the chronic NF-κB activation seen in skeletal muscle; ultimately preserving muscle mass and function.

This was investigated by treating old WT mice with fisetin as part of their diet from 20 to 24 months old, to investigate the pro-inflammatory cytokine levels in the plasma, and the NF-κB activity within the skeletal muscles and the effect on muscle mass and function.

6.2 Methods

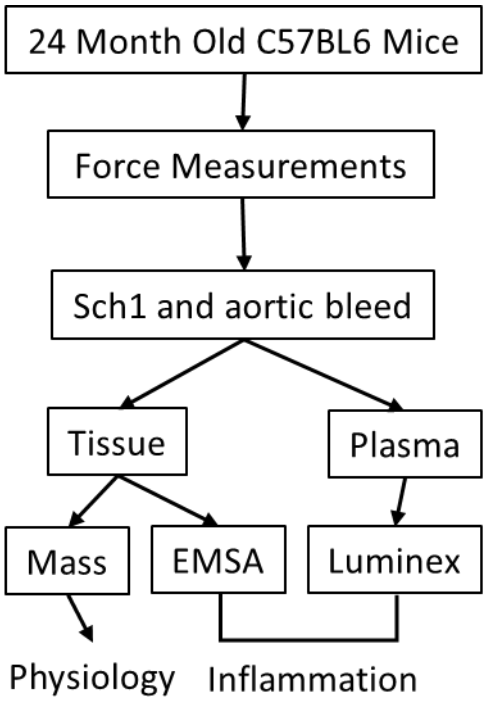

Figure 6.1 A brief overview of the methodology used for this chapter

Eighteen 20-month-old C57BL/6 mice were treated with fisetin (500mg/kg) as part of their normal diet for 4 months. Following this, muscle force generation was determined. The mice were culled, and tissue and plasma removed and stored. The plasma was used for cytokine analysis whilst the muscle was weighed and then analysed for NF-κB activity.

6.2.1 Senolytic intervention study

This study was undertaken in the animal research facility at the University of Liverpool. Eighteen male C57BL/6 WT mice (20 months) were randomly divided in to two groups, one of was fed fisetin (500 mg/kg) as part of their normal chow (CRM(P), Special Diet Services, 801722) *ad libitum* (approximately 2.5 mg/day/mouse or 8.7 µM/day/mouse). The second group were fed CRM(P) chow without fisetin. Mice were maintained on the diet for 16 weeks and monitored weekly to determine any changes in body weight. After 16 weeks, force generation of EDL muscle was determined and mice where then sacrificed for tissue and plasma collection.

6.2.2 Force measurements

The protocol was adapted from McArdle et al. (2004). Mice were anaesthetised with isoflurane and maintained under anaesthesia throughout the procedure. The knee of the right hind limb was fixed. The distal tendon of the extensor digitorum longus (EDL) muscle was exposed and attached to the lever arm of a servomotor (Cambridge Technology, Cambridge, UK). The lever served as a force transducer. The peroneal nerve was exposed, and electrodes were placed across the nerve. The EDL muscle of the contralateral limb served as a non-exercised control. Stimulation voltage and muscle length were each adjusted to produce maximum twitch force. The optimal length for maximum twitch force is also the optimal length (L_0) for the development of maximum tetanic force (P_0; (Brooks and Faulkner, 1988)). With the muscle at L_0, the P_0 was determined during 300msec of voltage stimulation at 8-10V. The P_0 was identified by increasing the frequency of stimulation at 2-min intervals until the maximum force plateaued. The electrodes were then moved to provide direct activation of the muscle, the voltage increased to 30V and the maximum tetanic force was re-measured. Muscle fibre length (Lf) and cross-sectional area were calculated (Brooks and Faulkner, 1988).

Following the final measurement, the mouse was removed from the platform, blood was collected from the descending aorta and mice were sacrificed by cervical dislocation. Mice were weighed, and all hind limb muscles and internal organs were removed post-mortem, weighed, and snap frozen in liquid nitrogen. Half of the anterior tibialis (AT) muscle was mounted on to a cork disk, surrounded with mounting medium (O.C.T., Merck, UK), frozen rapidly in liquid nitrogen cooled iso-pentane. EDL muscles were pinned and fixed using neutral buffered formalin (NBF), and later stored at 4°C in PBS + 0.1% sodium azide. The specific P_0 was calculated as the absolute P_0/muscle cross-sectional area (Brooks and Faulkner, 2001).

6.2.3 EMSA for NF-κB activity in muscle

EMSA was performed on the gastrocnemius (GTN) muscles of mice in both groups. The samples and protocol were performed as described in Section 2.8, and 100μg of muscle lysate was used.

6.2.4 Luminex analysis of plasma cytokine content

Blood from old mice was collected post-mortem from the descending aorta. The blood was centrifuged for 10 mins at 10,000g at 4°C, and the plasma collected. Luminex was performed as described in Section 2.7.

6.3 Results

6.3.1 Effect of Fisetin treatment on the survival and body weight of old mice

Figure 6.2 shows percent weight change of mice treated with fisetin or on the normal control diet. No significant differences were seen in the body weight of the fisetin treated group (32.4 ± 1.0g), when compared with the control group (31.2 ± 1.2g) (Figure 6.2A). No significant differences were seen in the percent weight lost in the fisetin treated group (5.36±3.55%), when compared with the control group (5.45±4.24%) (Figure 6.2B). The survival plot of the two populations were not significantly different; between 20 and 24 months of age, one mouse died due to natural causes in each group over the time frame of the study (Figure 6.2C).

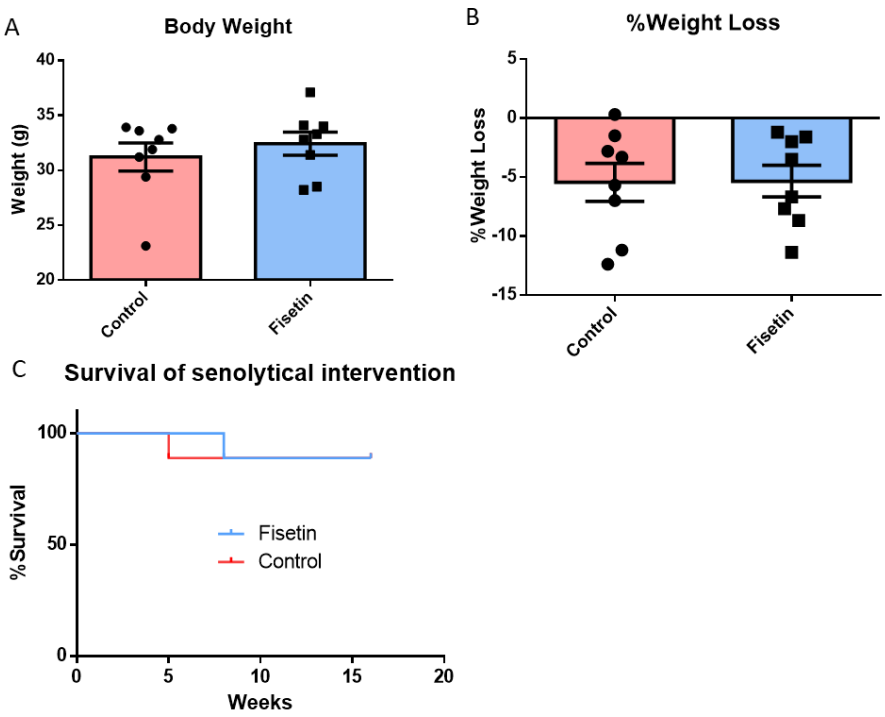

Figure 6.2 Effects of fisetin treatment on body weight and survival of mice

(A) Body weight of mice after 4 months of treatment with fisetin or control diet. (B) The percent loss of body mass of mice after 4 months of treatment with fisetin or fed the control diet, when compared with initial body weight at 20 months. (C) Survival curve of mice in each group over 16 weeks of study. Data are presented as mean ± SEM. N= 8.

6.3.2 Effect of Fisetin treatment on the organ weights of old mice

No significant differences were seen in the weight of the heart (2133 ± 158mg) (Figure 6.3A), lungs (2300 ± 89.55mg) (Figure 6.3B), kidneys (4965 ± 167.2mg) (Figure 6.3C), and spleen (783.3 ± 49.45mg) (Figure 6.3D), of fisetin treated mice, when compared with the heart (2080 ± 294mg) (Figure 6.3A), lungs (2241 ± 85.58mg) (Figure 6.3B), kidneys (4672 ± 126.0mg) (Figure 6.3C), and spleen (945.5 ± 95.72mg) (Figure 6.3D), of mice fed the control diet.

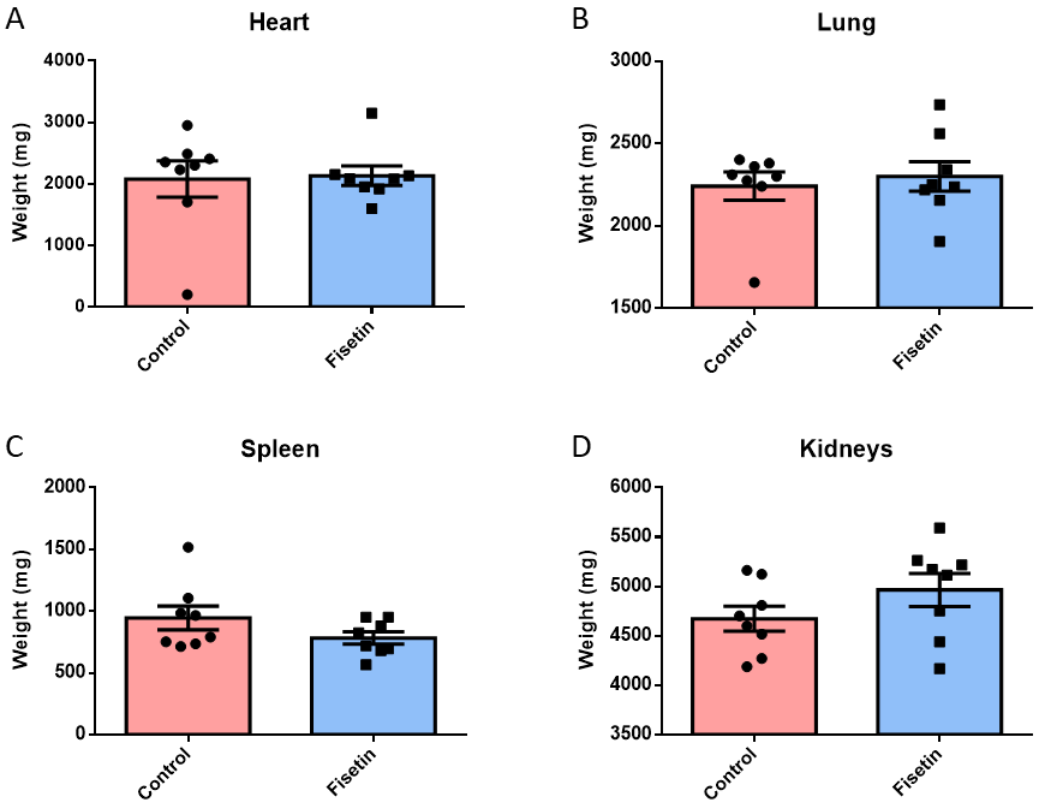

Figure 6.3 Organ weights following fisetin treatment

Weights of the heart (A), lung (B), spleen (C), and kidneys (D) of mice treated with fisetin or fed the control diet. Data are presented as mean ± SEM. N=8

6.3.3 Effect of fisetin treatment on the muscle mass of old mice

Figure 6.4 shows the mean muscle mass (Figure 6.4A-E) or the muscle mass normalised to body weight (Figure 6.4F-J) of fisetin treated and control mice. No significant differences were seen in the absolute muscle or normalised weight of fisetin treated mice when compared with mice fed the control diet.

6.3.4 Effect of Fisetin treatment on force generation of the EDL muscles of old mice

No significant differences were seen in maximum tetanic force generation (Figure 6.5A) or specific force generation (Figure 6.5) of EDLs of fisetin treated mice when compared with control mice. This lack of difference was evident whether the EDL was activated by nerve stimulation or by direct muscle activation.

6.3.5 Multiple cytokine analysis of the plasma from fisetin treated and control mice

Figure 6.6 shows multiple cytokine data of the plasma collected from fisetin treated and control mice. MCP-1 was significantly decreased in plasma of fisetin treated mice compared with that of control mice. The plasma level of G-CSF approached significance (P=-0.0525) in fisetin treated mice compared with that of control mice, whereby the level was higher in plasma of fisetin treated mice.

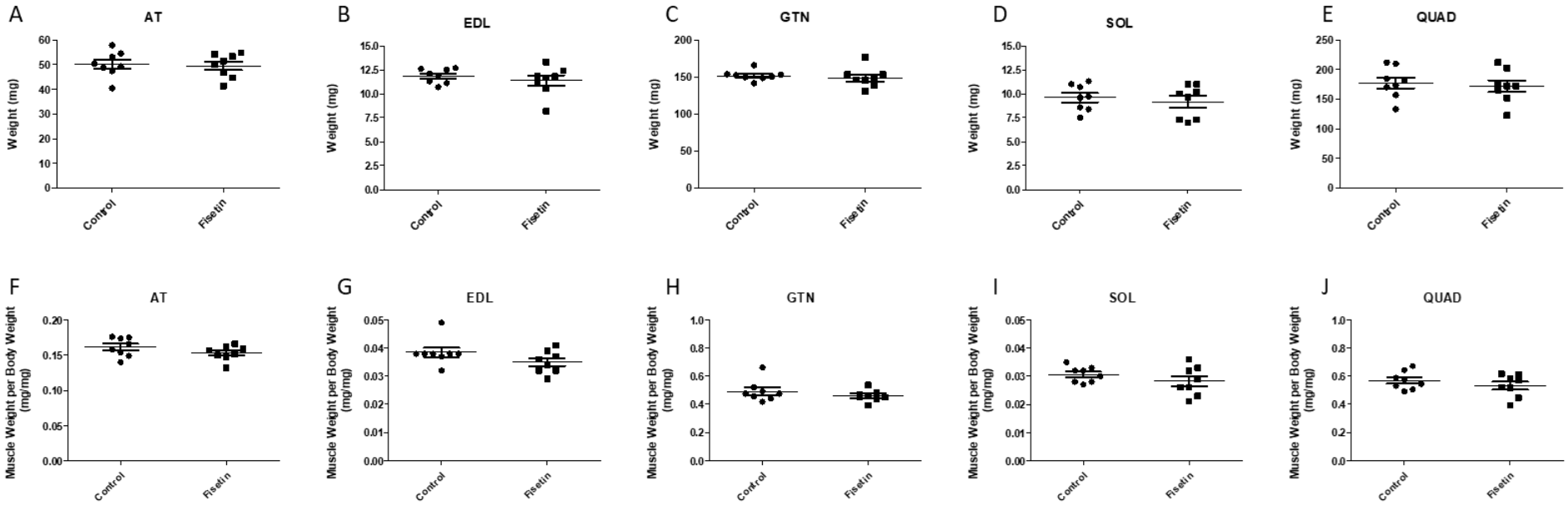

Figure 6.4 Hind limb muscle weights of fisetin treated mice after 4 months of senolytic treatment compared with mice fed the control diet.

The absolute weight (mg) and the muscle weight normalised to body weight (mg/mg) of: AT (A+F), EDL (B+G), GTN (C+H), SOL (D+I), and Quadriceps (E+J) of control or fisetin treated mice. Data are mean ± SEM.

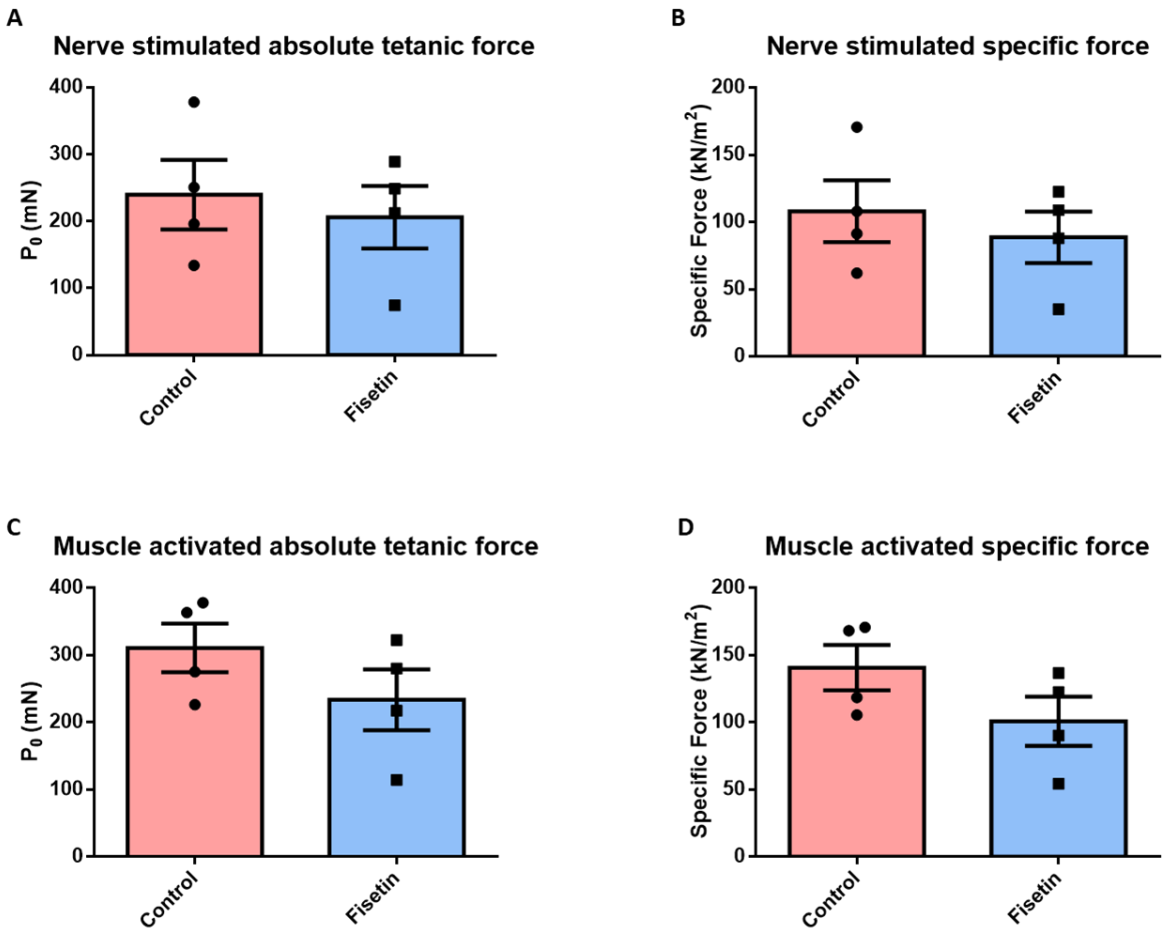

Figure 6.5 Force generation by EDL muscles of fisetin treated and control mice.

The tetanic (A+C) and specific (B+D) force of the EDL muscle from fisetin treated and control mice. The specific Po was calculated as the absolute Po/muscle CSA. Data are presented as mean ± SEM.

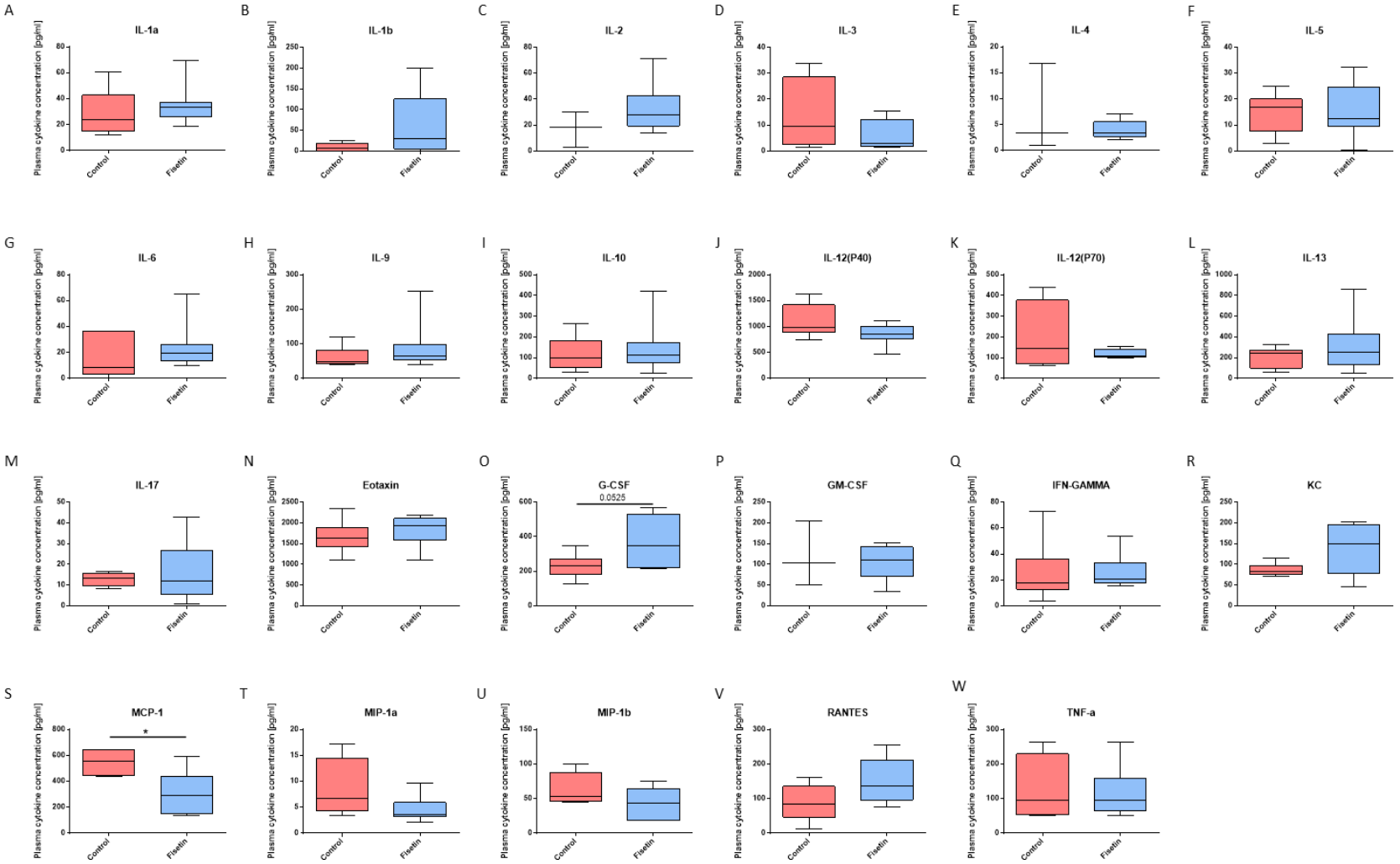

Figure 6.6 Multiple cytokine analysis of plasma from mice after 4 months of treatment with fisetin compared with control mice.

Plasma cytokine concentrations (pg/ml) of fisetin treated or control mice. Data are presented as mean ± SEM. Significance tested via Student's T-test.

6.3.6 NF-κB activity in skeletal muscle of fisetin treated and control mice

DNA binding of the NF-κB/p65 transcription factor was very variable in both groups but not different in GTN muscle of fisetin treated mice when compared with muscle from control old mice (Figure 6.7).

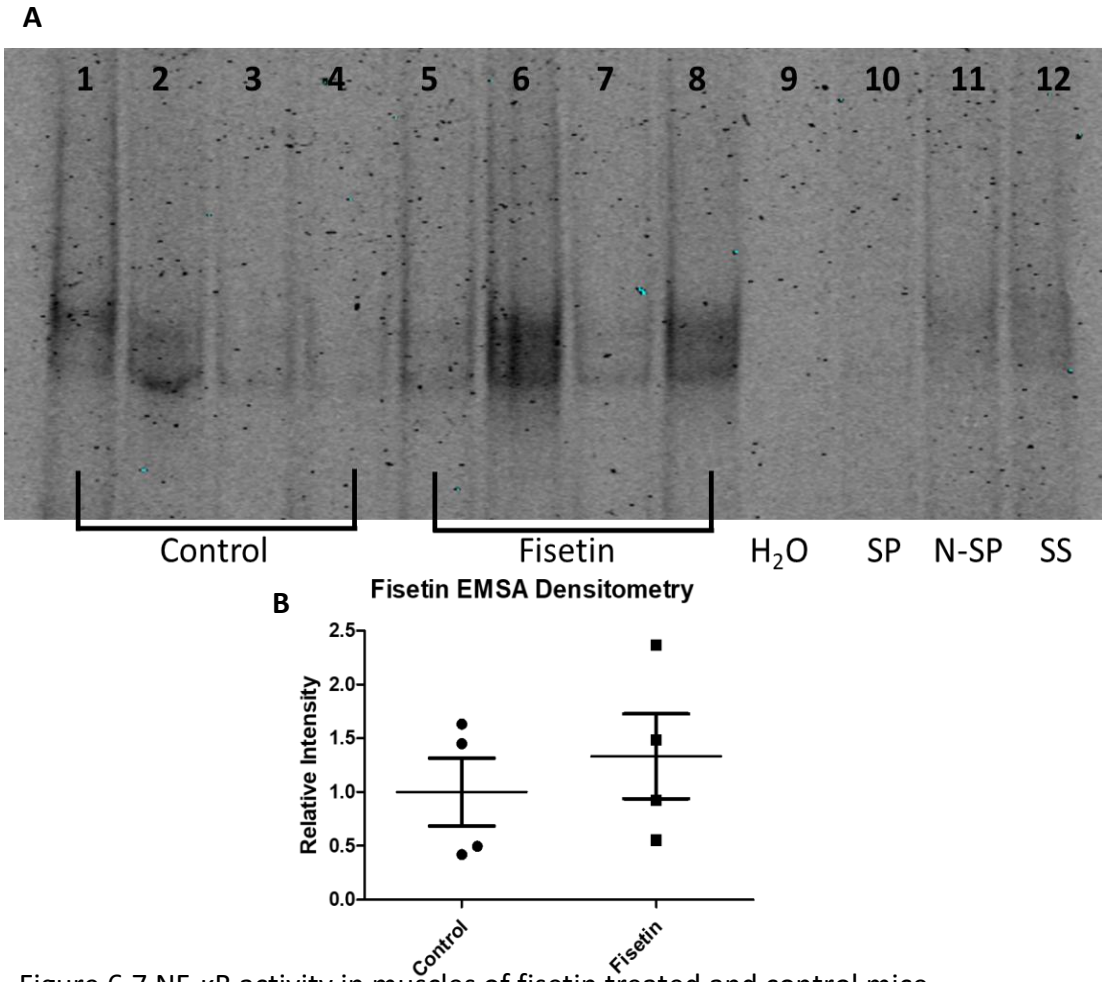

Figure 6.7 NF-κB activity in muscles of fisetin treated and control mice.

(A) Representative EMSA for NF-κB/p65 transcription factor DNA binding in the GTN of fisetin treated and control mice. (B) Quantification of the densitometry. SP, Specific competitor. N-SP, Non-specific competitor. SS, Supershift. Data are presented as mean ± SEM. Significance tested via Student's T-Test.

6.4 Discussion

We hypothesised that the polyphenol fisetin would reduce the burden of senescent cells in old mice, reducing pro-inflammatory cytokine levels in the plasma, and reducing the chronic NF-κB activation seen in skeletal muscle; ultimately preserving muscle mass and function. This was investigated by treating old WT mice with fisetin as part of their diet from 20 to 24 months old, to investigate the pro-inflammatory cytokine levels in the plasma, and the NF-κB activity within the skeletal muscles and the effect on muscle mass and function.

Age (months)		**6**	**12**	**24**
Body Weight (g)	Average	30.1	32.9 **a**	30.0
	SEM	0.8	0.8	0.7
Heart (mg)	Average	197.2	240.2	205.7
	SEM	13.4	30.8	8.8
Lungs (mg)	Average	208.3	240.9 **a**	228.5
	SEM	12.1	11.4	12.8
Liver (mg)	Average	1580.3	1758.4	1212.1 **a,b**
	SEM	76.2	130.9	127.7
Kidneys (mg)	Average	402.9	496.8 **a**	450.1
	SEM	12.5	23.9	35.5
Spleen (mg)	Average	70.8	100.3 **a**	66.9 **b**
	SEM	5.4	7.4	10.6
Brain (mg)	Average	388.4	386.7	383.1
	SEM	31.4	25.4	22.7
Heart OW/BW	Average	6.5	7.2	5.0 **a,b**
	SEM	0.3	0.8	0.6
Lungs OW/BW	Average	6.9	7.3	6.7
	SEM	0.3	0.3	1.4
Liver OW/BW	Average	52.3	53.3	39.1 **a,b**
	SEM	1.5	3.4	9.8
Spleen OW/BW	Average	2.3	3.0 **a**	5.6
	SEM	0.1	0.2	3.0

Table 6.1 Body weight of C57BL/6 mice on a standard diet over time

(Nye et al, unpublished)

6.4.1 The effect of fisetin treatment on body weight of old mice

A decline in the body weight of mice is evident after 20 months of age (Vanhooren and Libert, 2013). Unpublished data from our laboratory have shown that C57Bl/6 mice fed a standard diet lose body weight by 24 months old (Table 6.1, Nye *et al*, unpublished). The body weights of the control treated (31.2 ± 1.2g) and fisetin treated (32.4 ± 1.0g) old mice were not significantly different at the end of treatment. This suggests that inclusion of fisetin in the diet of the mice did not affect the palatability of the chow. Yousefzadeh et al. (2018) did not report body mass following dietary fisetin treatment of mice. However, no significant differences in body weight were reported in a 9 month long dietary fisetin treatment of mice from 3-12 months of age (Currais et al., 2014).

6.4.2 Fisetin treatment, survival, and potential toxicity

The survival plot of the two groups were also not significantly different suggesting no adverse effects of the diet on the lifespan at this age (20-24 months old). These findings suggest that fisetin appeared to have no immediate or long-term effects on the health of the mice that would result in increased mortality. Yousefzadeh et al. (2018) reported a significant improvement in median lifespan in a cohort of fisetin treated mice when compared with control mice. However, the median lifespan of the control group in their study was greater than 24 months of age, which was the endpoint for this current study. Fisetin (25 mg/kg) has not been shown to result in any signs of measurable toxicity, and is readily absorbed and distributed to blood vessels (Krasieva et al., 2015). Moreover, fisetin can be detected within the brain and

other distal organs at 40 minutes after oral administration (25 mg/kg) and remains detectable for up to 2 hours (Krasieva et al., 2015).

Other studies have investigated the toxicity of fisetin over shorter periods of time. Mice were orally administered 2000 mg/kg body weight of fisetin, examined for 48 hours and sacrificed; again, no indications of toxicity were observed (Maher, 2015). Effects of long-term feeding of fisetin on health were also evaluated and no significant differences in body weights were seen between control and fisetin-fed animals given fisetin (25 mg/kg body weight) in their diets for 9 months (Currais et al., 2014). Following sacrifice, Currais et al. (2014) examined lungs, spleen, liver, kidneys, heart, stomach, intestine, testes and ovary and no evidence of toxicity was seen following fisetin treatment.

6.4.3 Fisetin treatment and organ weights

Data from our laboratory have shown a significant reduction in the weights of a number of organs including heart, lung and kidneys and a significant increase in spleen mass with advancing age (Table 6.1). The weights of the organs of the fisetin treated mice were not significantly different when compared with the control mice, suggesting that treatment of mice with fisetin had no effect on age-related changes in weights seen in these tissues. The study by Yousefzadeh et al. (2018) did not report on internal organ weights but did report a decrease in senescence markers in the fat, spleen, liver, and kidneys of fisetin fed progeroid p16-reporter mice when compared with control progeroid p16-reporter mice. Jung et al. (2013) investigated the effects of fisetin treatment on a high fat, diet-induced obesity. Treatment of mice with fisetin, alongside the high fat diet, reduced weight gain and accumulation of white

adipose tissue, via suppression of mTORC1 signalling and reduced differentiation of pre-adipocytes (Jung et al., 2013).

Fisetin has been shown to have no significant toxic effects on the lungs, liver, spleen, kidneys, heart, stomach, intestine, or reproductive organs; at doses as high as 2g/kg (Currais et al., 2014) and our current study. In models of diabetic rats, a month of fisetin treatment significantly decreased blood glucose levels, increased insulin levels, and reduced glycosylation of red blood cells (Prasath and Subramanian, 2011). In the liver and kidneys of these treated rats, fisetin restored the activity of glycolytic pathway enzymes and inhibited the activity of gluconeogenic pathways (Prasath and Subramanian, 2011).

6.4.4 Fisetin treatment of old mice: effect on muscle mass and force generation of the EDL muscle

The maximum tetanic force generated by muscles of 24 month old WT mice is generally decreased by 30-40%, specific force by 10-15% (McArdle et al., 2004) and muscle mass is decreased by 20-30% . The muscle masses or maximum tetanic and specific force generation of muscles of fisetin treated mice was not significantly different when compared with that of control mice whether the muscle was activated by nerve stimulation or direct muscle activation. These data suggest that fisetin did not provide any protection against age-related loss of muscle mass and function. Indeed, there was a trend to decrease in the absolute force generation in the EDL from the fisetin treated mice, when compared with the control mice.

These findings are contrary to the hypothesis that removal of senescent cells would improve muscle function by eliminating the SASP. Fisetin treatment and inflammation

Data in Chapter 4 show that the plasma levels of a number of cytokines were elevated in old compared with adult mice. When comparing similar data from the fisetin treated group with the control group, the only significant effect on plasma cytokine levels was a decrease in Monocyte chemotactic protein-1 (MCP-1). Yousefzadeh et al. (2018) also saw a specific and significant decrease in plasma circulating MCP-1 in mice treated with fisetin compared with control mice. A comparison of changes in plasma cytokine levels in plasma in old compared to adult WT mice, and the fisetin treated mice together with their controls (Table *6.2*).

The source of plasma MCP-1 is unclear and since plasma MCP-1 levels were not affected by ageing, these effects are unlikely to be due to the removal of senescent cells. MCP-1 is a chemokine and member of the small inducible cytokine family, playing a crucial role in the recruitment of monocytes and T lymphocytes into tissues (Baggiolini, 1998); and is expressed by adipocytes (Gerhardt et al., 2001). MCP-1 was found to impair glucose uptake (Sartipy and Loskutoff, 2003) and was shown to impair insulin signalling in skeletal muscle at physiological levels (200 pg/ml); via ERK1/2 activation but does not involve activation of the NF-κB pathway (Sell et al., 2006).

Table 6.2

Summary table of the cytokines measured in the plasma of old mice compared with adult mice, and fisetin treated mice compared with control mice. Green, significantly increased; Red, significantly decreased; Grey, no difference; White, not measured.

	Old mouse models	
Cytokines	**WT**	**Fisetin**
BCA-1/CXCL13		-
CTACK/CCL27		-
ENA-78/CXCL5		-
Eotaxin/CCL11		
Eotaxin-2/CCL24		-
Fractalkine/CX3CL1		-
G-CSF	-	p=0.0525
GM-CSF		
I-309/CCL1		-
IFN-γ		
IL-1α	-	
IL-1β		
IL-2		
IL-3	-	
IL-4		
IL-5	-	
IL-6		
IL-9	-	
IL-10		
IL-12(p40)	-	
IL-12(p70)	-	
IL-13	-	
IL-16		-
IL-17	-	
IP-10/CXCL10		-
I-TAC/CXCL11		-
KC/CXCL1		
MCP-1/CCL2		
MCP-2/CCL8	-	-
MCP-3/CCL7		-
MCP-5/CCL12		-
MDC/CCL22		-
MIP-1α/CCL3		
MIP-1β/CCL4		
MIP-2/CXCL2		-
MIP-3α/CCL20		-
MIP-3β/CCL19		-
RANTES/CCL5		
SCYB16/CXCL16		-
SDF-1α/CXCL-12		-
TARC/CCL17		-
TECK/CCL25		-
TNFα		

6.4.5 Comparison of the current study with published studies.

Yousefzadeh et al. (2018) noted that the effect of fisetin treatment was greater on p16-expressing cells than on p21 expressing cells, at least in subcutaneous fat. Although the current study saw no increase in p21 or p16 in muscle tissue, the nature of senescent cells in non-muscle tissue of old mice was not examined. If p21 expressing cells are dominant at 24-26 months old, this might explain the lack of effects in the current studies.

In other studies, specific ablation of p16 expressing senescent cells had a profound effect on muscle. Whilst weight or force generation was not reported, an improvement in fibre diameter was reported and greater mobility was seen in the p16 ablated mice compared to the control mice (Baker et al., 2016, Baker et al., 2011).

Data from Sousa-Victor et al. (2014) showed that there were no significant increases in p16 expression in satellite cells from old (24 months) mice, when compared with adult (12 months). von Zglinicki et al. (2020) reported significantly increased expression of p16 and p21 in the muscles of very old (32 months) mice when compared with adult (8 months) mice, and also saw significantly increased nuclear p21 in the old mice. These data, and more discussed in Section 4.4.1.1 suggest that: A) skeletal muscle show significantly increased markers of cellular senescence, but only once mice are classed as “geriatric” (32-months old); and B) cellular senescence in muscle may be based more on changes in p21 activity, rather than p16.

6.5 Conclusion

Fisetin treatment had no significant effects in preserving the loss of hind limb muscle mass and EDL function with age, when compared with control treated old mice.

Fisetin treatment resulted in a significant decrease in the plasma concentration of MCP-1 when compared with control treatment mice although this cytokine was not elevated in plasma of old WT mice. Fisetin treatment had no significant effect on NF-κB transcription factor binding activity in muscle, when compared with that of control old mice. Overall, fisetin treatment had a no effect regarding preserving muscle mass and function in mice of this age, as well as little effect in reducing the pro-inflammatory plasma cytokines. Recent studies suggest that skeletal muscle does not contain a significant population of senescent cells until the mice are significantly older (da Silva et al., 2019, von Zglinicki et al., 2020) despite showing sarcopenia by 24 months old. The mice used in this study were 24 months old, and therefore would have a limited pool of senescent cells. Therefore, it may be that the effects of a senolytics would have marginal effects on skeletal muscle at this age.

Chapter 7: General Discussion and Future Directions

7.1 Hypothesis.

The overall hypothesis of this thesis was that senescent cells accumulate in old mice, either locally to skeletal muscle or distally, and that they produce an inflammatory SASP which may contribute at least in part to the chronic NF-κB signalling and the loss of muscle mass and function seen in the muscles of old compared with adult mice. This programme of work tested this hypothesis by utilising different models of senescence *in vitro* and *in vivo* and using a senolytic and transgenic intervention.

7.2 Aims of the thesis

The aims of the work reported in this thesis were to:

1. Establish an *in vitro* model of cellular senescence in muscle cells by inducing and characterising senescence in C2C12 myoblasts. Furthermore, C2C12 myotubes were treated with the conditioned media containing the SASP from the senescent cells to investigate the effect of the SASP on activation of NF-κB activity in mature multinucleated myotubes.
2. To determine the presence of senescent cells within muscle of adult and old WT mice including the potential of muscle of adult and old mice to produce SASP.
3. To determine the effects of senescent cell removal on plasma cytokine concentrations and indices of skeletal muscle inflammation, as well as muscle mass and function in old P16-3MR mice treated with gancyclovir to remove P16 positive cells compared with PBS treated old P16-3MR mice.

4. To determine the effects of pharmacological removal of senescent cells by treating old WT mice with the senolytic fisetin as part of their diet over several months and investigate muscle mass and function, the pro-inflammatory cytokine levels in the plasma, and the NF-κB activity within the skeletal muscles.

7.3 Summary of the findings of the thesis

The major findings of this work were:

1. Treatment of C2C12 myoblasts with etoposide, a well-studied small molecule capable of causing DNA damage and inducing senescence, resulted in a dose dependant loss of cell viability. Low concentrations of etoposide induced senescence in C2C12 myoblasts, and these cells showed many hallmarks of senescence, including increased protein levels of p21, increased SA-β-Gal activity, SAHF, and altered morphology. Furthermore, the senescent myoblasts produced a proinflammatory SASP detectable in the cell media that was able to increase NF-κB transcription factor activity in mature C2C21 myotubes. These findings suggest that C2C12 myoblasts can become senescent and that the SASP produced can activate NF-κB in mature muscle myotubes.
2. Muscles of old (24-months-old) WT mice did not show any significant change in indices of senescence (p16, p21, p53, SA-β-Gal) when compared with muscles of adult (8-12-month-old) mice. These findings provide little evidence of the presence of classical senescent cells in muscles of old mice. Old mice showed evidence of increased levels of potential SASP components in the plasma although the role of senescent cells in the production of these

cytokines/chemokines is unclear. Data examining levels of cytokines in muscle of old compared with adult mice suggest that muscle may partially contribute to the increase in some plasma cytokines evident in plasma of old mice but suggests that the source of many cytokines seen in plasma is not primarily muscle tissue. However, it may be that muscle rapidly produces and secretes cytokines and so changes in intracellular protein levels will not be evident, but such cytokines produced by muscle may still have a local effect on peripheral nerves for example.

3. GCV treatment of old (20 to 24-months-old) P16-3MR mice to remove p16 expressing senescent cells both local and distant to muscle showed no significant effect on muscle mass or function, compared with vehicle treated P16-3MR control mice. GCV treatment of P16-3MR mice resulted in a minor effect on the plasma cytokine/chemokine profile of old mice and had no effect of reducing the NF-κB transcription factor activity in muscle of these old mice.
4. In a similar manner to the study using P16-3MR mice, treatment of old (20 to 24-months-old) WT mice with fisetin as part of their diet had no significant effect on muscle mass or function, when compared with vehicle treated control mice. Only MCP-1 was significantly lower in the plasma of fisetin treated old mice compared with age-matched control mice, although this cytokine had not been identified as elevated in plasma of old compared with adult WT mice. No significant differences were seen in NF-κB transcription factor activity in the muscles of fisetin treated compared with control mice.

7.4 General discussion

7.4.1 Senescence in a cell culture model.

One of the major challenges of the current study was the establishment of a suitable cell culture model allowing accurate determination of cytokine release by senescent cells. The study described in Chapter 3 used a DNA damaging agent, etoposide to successfully induce senescence in myoblasts, providing proof-of-principle that myoblasts were capable of senescence. However, quantification of cytokine/chemokine release by cells proved challenging.

The senescent cells demonstrated growth arrest and an increase in cell volume following treatment with etoposide. In contrast, DMSO treated cells continue to actively divide, finally resulting in temporary growth arrest when confluent at ~ 5 days following seeding in the current experiments, where they begin to terminally differentiate into myotubes. The indices of senescence may also be involved in this contact inhibition and differentiation process in muscle cells and so comparison of the levels of such indices in these 'control' cells with that of senescent cells may be misleading. In addition, there is considerable discussion on the method of normalisation of cytokine/chemokine release into the media from the different groups of cells. Wells of senescent cells will have less cells than those of DMSO-treated control wells of cells, but the senescent cells are much larger. It is anticipated that a comparison of the expression of cytokine/chemokine release data will be different if expressed per unit of protein in each well or per cell. Both will be particularly informative but care in interpretation is recommended.

7.4.2 Senescence in skeletal muscle tissue

The first introduction to, and demonstration of cellular senescence was led by the pioneering study from Hayflick and Moorhead (1961). Since then, cellular senescence has become far more widely studied, with a number of hallmarks of senescence being identified (Hernandez-Segura et al., 2018). However, senescent cells are diverse and their profiles are dependent on the cell type of origin and how senesce was induced (Wiley et al., 2017). Of these hallmarks, of interest is the senescence associated secretory phenotype (SASP), a cocktail of cytokines, chemokines, and proteases secreted by senescent cells (Coppe et al., 2010a). Indeed, the SASP has been hypothesised to be a contributor to the age-related increase in inflammation, termed inflammaging (Franceschi and Campisi, 2014). This increase in inflammation has a negative effect on tissue structure and function, increasing the development of several age-related pathologies, including sarcopenia.

The mechanisms underlying the development of sarcopenia are not completely understood. It is likely that sarcopenia is a multi-factorial disease with a network of interacting, dysfunctional systems (Larsson et al., 2019). However, data has shown that increased inflammation that occurs with ageing is likely to play a major role (Bano et al., 2017).

As part of this thesis, it was hypothesised that senescent cells accumulate with age in old mice, either locally or distant to skeletal muscle. These senescent cells produce an inflammatory SASP which contributes to the chronic NF-κB activation and inflammation seen in muscle ageing, contributing to the activation of degradation

pathways and loss of muscle mass and function seen in old mice (Lightfoot et al., 2014).

Similar studies have proposed a role for senescence in inflammation and the development of age-related pathologies, including the development of sarcopenia (Demaria et al., 2014, Baker et al., 2016). Despite these studies, the literature supporting the presence of senescent cells in skeletal muscle is heterogeneous (Jeyapalan et al., 2007, Edwards et al., 2007, Sousa-Victor et al., 2014, da Silva et al., 2019). The differences between these data may be due to methodological approaches. Indeed, data presented as part of this thesis show that whilst muscle cells have the capability to senescence *in vitro*, there is little evidence of this occurring within muscle *in vivo*, at least up to the age of 24 months, when considerable loss of muscle mass is evident.

Skeletal muscle is mainly comprised of post-mitotic multinucleated muscle fibres, and there has been limited interest in investigating senescence in post-mitotic tissue. However, von Zglinicki et al. (2020) investigated indices of senescence in several different post-mitotic tissues in geriatric mice and showed that post-mitotic tissue, including skeletal muscle fibres can display evidence of senescence. Studies using transgenic mice for whole body removal of senescent cells (Baker et al., 2016) or senolytic treatment (Yousefzadeh et al., 2018), have also demonstrated improvements in several measures of physical mobility in old mice. However, when muscle mass and function were investigated as part of this current thesis, using both transgenic mouse models (Chapter 5) and senolytic treatment (Chapter 6), no significant preservation of muscle mass and function were seen.

One potential reason for the difference between the current study and those discussed above may be due to the age of the mice used.

7.4.3 Senescence may only be evident in very old (geriatric) mice.

Studies that have demonstrated senescence within skeletal muscle, have commonly made use of geriatric (32-months-old) mice (Sousa-Victor et al., 2014, von Zglinicki et al., 2020, da Silva et al., 2019, Baker et al., 2016). Geriatric mice represent a human approximately in their 80th decade of life (Ackert-Bicknell et al., 2015). Skeletal muscle accounts for 40% of total body weight, and 50-75% of total body protein (Frontera and Ochala, 2015). A decrease of 30-50% in skeletal muscle mass and function had been reported in adult by approximately 80 years of age (Akima et al., 2001). More recent studies have shown that after the age of 30, about 0.5–1% of skeletal muscle mass is lost per year, with the rate of loss accelerating after the age of 65 (Kyle et al., 2001, Melton et al., 2006). On average, 5–13% of individuals aged over 60 have low skeletal muscle mass, with the prevalence increasing to as high as 50% in those over of 80 (Morley et al., 2014). Geriatric mice will also show substantially increased indices of cancer and so caution needs to be taken when interpreting data from such studies.

The data, together with the data presented in this thesis suggest that the accumulation of senescent cells may only occur in very old (>32 month) mice. Loss of muscle mass and function occurs at ~18 months onward in mice and so the presence of senescent cells is only evident at a time point when substantial sarcopenia is evident, suggesting that senescence plays little role in the development of sarcopenia in mice. In contrast, data show substantial inflammaging at the time of the development of sarcopenia, suggesting an association between an elevation in

plasma cytokine/chemokine levels and the development of sarcopenia and this was not affected by removal of senescent cells. Muscle may contribute in part to these cytokines/chemokines but data suggest there are additional, likely non-senescent sources of cytokines/chemokines seen in plasma of old mice (Larsson et al., 2019, Bano et al., 2017).

7.4.4 Use of transgenic mouse models to eliminate senescent cells

Several landmark studies by Baker *et al* (2016, 2013, 2011, 2008, 2004) have investigate the role of senescence in the development of age-related pathologies using progeroid mouse models crossed with a transgenic mouse model that can both report and selectively eliminate senescence cells (Section 1.1.7.2). To summarise their findings in the context of sarcopenia and frailty, elimination of senescent cells from the whole organism result in delayed onset of age-related pathologies in adipose tissue, skeletal muscle, and eye. Increases in health span and several measures of fitness, as well increases in gastrocnemius mass were reported following senescent cell elimination. Furthermore, a decrease in the level of inflammatory cytokines was reported in the plasma and muscles of these mice following senescent cell elimination. The difficulty with interpreting these data are that mice of several different ages and genetic backgrounds are used throughout all of the studies. Whilst these findings are novel, they were again reported in geriatric mice, and as previously discussed, whilst the muscles of geriatric mice may show indices of senescence, old (24-months-old) do not appear to, particularly in skeletal muscle. Therefore, the effects of eliminating senescent cells from an old mouse with age-related pathology remain uncertain. The elimination of senescent cells that accumulate in other tissues that are not skeletal muscle would influence the SASP and inflammation. Indeed,

whilst the effect of removal of senescent cells on skeletal muscle mass and function was not investigated in the Demaria et al. (2014) P16-3MR study, decreased concentrations of inflammatory SASP factors were reported in the fat of GCV-treated p16-3MR.

7.5 Limitations of the current studies

One limitation of the study is the age of the mice used as part of the studies. The age used (24-months-old) as data from our group (Jackson, 2020, McArdle et al., 2019) and others (Brooks and Faulkner, 1988) show that mice begin to display characteristics in frailty, with a loss of muscle mass and function.

Another limitation is the marker for senescence, p16. Senescence in skeletal muscle has been identified using p21, and not p16.

Another limitation is the lack of diversity in the genders of the mice. The mice used in Chapters 4 and 6 were all male, however, due to the collaborative nature of this study, the P16-3MR mice used in Chapter 5 were of both sexes. Women and non-human female mammals are underrepresented in studies, whereby researchers assume results from males apply to females (Beery and Zucker, 2011). Researchers avoid the inclusion of females because of concerns that hormonal cycles decrease the homogeneity of study populations and confound effects of experimental manipulations (Beery and Zucker, 2011). Many drug studies using males often generate different results from those for women (Soldin and Mattison, 2009). In future studies, mice of each gender would be investigated in sufficient numbers to identify any gender related differences or trends in data.

Another limitation to the overall study was the multiplex cytokine analysis. The cytokine analysis performed in Chapters 3, 5, 6 made use of a 23-plex senescence cytokine array, the analysis on adult and old plasma and muscle in Chapter 4 were performed using a 33-plex array. This has caused issues whereby some cytokines were present on one array and not on another, preventing full comparison of cytokine between the different models used in this thesis (Table 7.1).

Key	
Not assayed	-
No difference	
Increased	
Decreased	

Cytokines	C2C12 myoblasts	Old mouse models		
		WT	P16-3MR	Fisetin
BCA-1/CXCL13	-		-	-
CTACK/CCL27	-		-	-
ENA-78/CXCL5	-		-	-
Eotaxin/CCL11				
Eotaxin-2/CCL24	-		-	-
Fractalkine/CX3CL1	-		-	-
G-CSF		-		p=0.0525
GM-CSF				
I-309/CCL1	-		-	-
IFN-γ				
IL-1α		-		
IL-1β				
IL-2				
IL-3		-		
IL-4				
IL-5		-		
IL-6				
IL-9		-		
IL-10				
IL-12(p40)		-		
IL-12(p70)		-		
IL-13		-		
IL-16	-		-	-
IL-17		-		
IP-10/CXCL10	-		-	-
I-TAC/CXCL11	-		-	-
KC/CXCL1				
MCP-1/CCL2				
MCP-2/CCL8	-	-	-	-
MCP-3/CCL7	-		-	-
MCP-5/CCL12	-		-	-
MDC/CCL22	-		-	-
MIP-1α/CCL3				
MIP-1β/CCL4				
MIP-2/CXCL2	-		-	-
MIP-3α/CCL20	-		-	-
MIP-3β/CCL19	-		-	-
RANTES/CCL5				
SCYB16/CXCL16	-		-	-
SDF-1α/CXCL-12	-		-	-
TARC/CCL17	-		-	-
TECK/CCL25	-		-	-
TNFα				

Table 7.1

Summary of cytokine analysis between different models of senescence. Old WT mice (24-months-old) compared with adult (8-12 months old) WT mice. GCV treated old (26-months-old) P16-3MR mice treated mice, compared with PBS treated old (26-months-old) P16-3MR mice. Fisetin treated old (24-months-old) WT mice compared with vehicle treated control old WT mice. Changes represent significant changes within the plasma of the mice compared with their controls.

7.6 Future directions.

7.6.1 Identification of the source of increased plasma cytokines in old mice and humans.

Inflammaging describes the chronic, low-grade systemic inflammation seen in ageing (Franceschi et al., 2000). The source of such inflammatory cytokines is unclear, but this inflammation appears to occur in the absence of infection and is primarily driven by endogenous signals. Data suggest that besides persistent infections; cell debris, misplaced self-molecules, and misfolded/oxidized proteins are major contributors to inflammaging (Franceschi and Campisi, 2014).

Data provided in this thesis and in other studies have supported a role for muscle, at least in part, in contributing to this systemic inflammation although data presented in this thesis do not support a role for senescence either in the systemic inflammation or in the muscle production of cytokines/chemokines.

Clearly, additional analysis is required to identify the source of the systemic inflammation in old mice (and humans) and to identify the components of this inflammation that may be potentially responsible for activation of NF-kB in muscle and the development of sarcopenia.

7.6.2 Examination of the local effects of muscle – derived cytokines on other cells and tissues.

The modified production of cytokines by skeletal muscle during ageing may not contribute in a significant way to the plasma concentration of cytokines/chemokines, but it may be that the release of cytokines/chemokines may play a role in the development of dysfunction in local tissues and cells. Of note is the local effect on

the peripheral nerve, interaction of which is crucial to maintenance of muscle mass and function. Additional studies on the effect of modified release of cytokines/chemokines is therefore warranted.

7.6.3 Lack of clear markers of senescence, particularly in terminally differentiated muscle cells.

None of the current markers for senescence are completely specific for senescence and are used in combination to characterise cellular senescence. The additional complication of the continued action of resident mononuclear stem cells in muscle (satellite cells) in proliferating and then differentiating to fuse and form terminally differentiated multinuclear cells provides an additional level of complexity. A number of classical indices of senescence are also involved in this cell cycle arrest and differentiation and a further understanding of the overlap of these processes in muscle tissue is required.

2001. Milestones in cell division. *Nat Cell Biol,* 3**,** E265.

ABDUL-AZIZ, A. M., SUN, Y., HELLMICH, C., MARLEIN, C. R., MISTRY, J., FORDE, E., PIDDOCK, R. E., SHAFAT, M. S., MORFAKIS, A., MEHTA, T., DI PALMA, F., MACAULAY, I., INGHAM, C. J., HAESTIER, A., COLLINS, A., CAMPISI, J., BOWLES, K. M. & RUSHWORTH, S. A. 2019. Acute myeloid leukemia induces protumoral p16INK4a-driven senescence in the bone marrow microenvironment. *Blood,* 133**,** 446-456.

ACKERT-BICKNELL, C. L., ANDERSON, L. C., SHEEHAN, S., HILL, W. G., CHANG, B., CHURCHILL, G. A., CHESLER, E. J., KORSTANJE, R. & PETERS, L. L. 2015. Aging Research Using Mouse Models. *Curr Protoc Mouse Biol,* 5**,** 95-133.

ACOSTA, J. C., BANITO, A., WUESTEFELD, T., GEORGILIS, A., JANICH, P., MORTON, J. P., ATHINEOS, D., KANG, T. W., LASITSCHKA, F., ANDRULIS, M., PASCUAL, G., MORRIS, K. J., KHAN, S., JIN, H., DHARMALINGAM, G., SNIJDERS, A. P., CARROLL, T., CAPPER, D., PRITCHARD, C., INMAN, G. J., LONGERICH, T., SANSOM, O. J., BENITAH, S. A., ZENDER, L. & GIL, J. 2013. A complex secretory program orchestrated by the inflammasome controls paracrine senescence. *Nat Cell Biol,* 15**,** 978-90.

ACOSTA, J. C., O'LOGHLEN, A., BANITO, A., GUIJARRO, M. V., AUGERT, A., RAGUZ, S., FUMAGALLI, M., DA COSTA, M., BROWN, C., POPOV, N., TAKATSU, Y., MELAMED, J., D'ADDA DI FAGAGNA, F., BERNARD, D., HERNANDO, E. & GIL, J. 2008. Chemokine signaling via the CXCR2 receptor reinforces senescence. *Cell,* 133**,** 1006-18.

ADHIKARI, A., XU, M. & CHEN, Z. J. 2007. Ubiquitin-mediated activation of TAK1 and IKK. *Oncogene,* 26**,** 3214-26.

AGUAYO-MAZZUCATO, C., ANDLE, J., LEE, T. B., JR., MIDHA, A., TALEMAL, L., CHIPASHVILI, V., HOLLISTER-LOCK, J., VAN DEURSEN, J., WEIR, G. & BONNER-WEIR, S. 2019. Acceleration of beta Cell Aging Determines Diabetes and Senolysis Improves Disease Outcomes. *Cell Metab,* 30**,** 129-142 e4.

AKBAR, A. N. & HENSON, S. M. 2011. Are senescence and exhaustion intertwined or unrelated processes that compromise immunity? *Nat Rev Immunol,* 11**,** 289-95.

AKBAR, A. N., HENSON, S. M. & LANNA, A. 2016. Senescence of T Lymphocytes: Implications for Enhancing Human Immunity. *Trends Immunol,* 37**,** 866-876.

AKIMA, H., KANO, Y., ENOMOTO, Y., ISHIZU, M., OKADA, M., OISHI, Y., KATSUTA, S. & KUNO, S. 2001. Muscle function in 164 men and women aged 20--84 yr. *Med Sci Sports Exerc,* 33**,** 220-6.

ALARCON-VARGAS, D. & RONAI, Z. 2002. p53-Mdm2--the affair that never ends. *Carcinogenesis,* 23**,** 541-7.

ALIMBETOV, D., DAVIS, T., BROOK, A. J., COX, L. S., FARAGHER, R. G., NURGOZHIN, T., ZHUMADILOV, Z. & KIPLING, D. 2016. Suppression of the senescence-associated secretory phenotype (SASP) in human fibroblasts using small molecule inhibitors of p38 MAP kinase and MK2. *Biogerontology,* 17**,** 305-15.

ALNAQEEB, M. A., ALZAID, N. S. & GOLDSPINK, G. 1984. Connective-Tissue Changes and Physical-Properties of Developing and Aging Skeletal-Muscle. *Journal of Anatomy,* 139**,** 677-689.

ALNAQEEB, M. A. & GOLDSPINK, G. 1987. Changes in fibre type, number and diameter in developing and ageing skeletal muscle. *J Anat,* 153**,** 31-45.

ALTUN, M., BESCHE, H. C., OVERKLEEFT, H. S., PICCIRILLO, R., EDELMANN, M. J., KESSLER, B. M., GOLDBERG, A. L. & ULFHAKE, B. 2010. Muscle wasting in aged, sarcopenic rats is associated with enhanced activity of the ubiquitin proteasome pathway. *J Biol Chem,* 285**,** 39597-608.

ARAI, Y., WATANABE, S., KIMIRA, M., SHIMOI, K., MOCHIZUKI, R. & KINAE, N. 2000. Dietary intakes of flavonols, flavones and isoflavones by Japanese women and the inverse correlation between quercetin intake and plasma LDL cholesterol concentration. *J Nutr,* 130**,** 2243-50.

ASHLEY, C. C. & RIDGWAY, E. B. 1968. Simultaneous recording of membrane potential, calcium transient and tension in single muscle fibers. *Nature,* 219**,** 1168-9.

AUNAN, J. R., WATSON, M. M., HAGLAND, H. R. & SOREIDE, K. 2016. Molecular and biological hallmarks of ageing. *Br J Surg,* 103**,** e29-46.

AVELAR, R. A., ORTEGA, J. G., TACUTU, R., TYLER, E. J., BENNETT, D., BINETTI, P., BUDOVSKY, A., CHATSIRISUPACHAI, K., JOHNSON, E., MURRAY, A., SHIELDS, S., TEJADA-MARTINEZ, D., THORNTON, D., FRAIFELD, V. E., BISHOP, C. L. & DE MAGALHAES, J. P. 2020. A multidimensional systems biology analysis of cellular senescence in aging and disease. *Genome Biol,* 21**,** 91.

BAEHR, L. M., WEST, D. W., MARCOTTE, G., MARSHALL, A. G., DE SOUSA, L. G., BAAR, K. & BODINE, S. C. 2016. Age-related deficits in skeletal muscle recovery following disuse are associated with neuromuscular junction instability and ER stress, not impaired protein synthesis. *Aging (Albany NY),* 8**,** 127-46.

BAGGIOLINI, M. 1998. Chemokines and leukocyte traffic. *Nature,* 392**,** 565-8.

BAKER, D. J., CHILDS, B. G., DURIK, M., WIJERS, M. E., SIEBEN, C. J., ZHONG, J., SALTNESS, R. A., JEGANATHAN, K. B., VERZOSA, G. C., PEZESHKI, A., KHAZAIE, K., MILLER, J. D. & VAN DEURSEN, J. M. 2016. Naturally occurring p16(Ink4a)-positive cells shorten healthy lifespan. *Nature,* 530**,** 184-9.

BAKER, D. J., JEGANATHAN, K. B., CAMERON, J. D., THOMPSON, M., JUNEJA, S., KOPECKA, A., KUMAR, R., JENKINS, R. B., DE GROEN, P. C., ROCHE, P. & VAN DEURSEN, J. M. 2004. BubR1 insufficiency causes early onset of aging-associated phenotypes and infertility in mice. *Nat Genet,* 36**,** 744-9.

BAKER, D. J., PEREZ-TERZIC, C., JIN, F., PITEL, K. S., NIEDERLANDER, N. J., JEGANATHAN, K., YAMADA, S., REYES, S., ROWE, L., HIDDINGA, H. J., EBERHARDT, N. L., TERZIC, A. & VAN DEURSEN, J. M. 2008. Opposing roles for p16Ink4a and p19Arf in senescence and ageing caused by BubR1 insufficiency. *Nat Cell Biol,* 10**,** 825-36.

BAKER, D. J., WEAVER, R. L. & VAN DEURSEN, J. M. 2013. p21 both attenuates and drives senescence and aging in BubR1 progeroid mice. *Cell Rep,* 3**,** 1164-74.

BAKER, D. J., WIJSHAKE, T., TCHKONIA, T., LEBRASSEUR, N. K., CHILDS, B. G., VAN DE SLUIS, B., KIRKLAND, J. L. & VAN DEURSEN, J. M. 2011. Clearance of p16Ink4a-positive senescent cells delays ageing-associated disorders. *Nature,* 479**,** 232-6.

BALAGOPAL, P., ROOYACKERS, O. E., ADEY, D. B., ADES, P. A. & NAIR, K. S. 1997. Effects of aging on in vivo synthesis of skeletal muscle myosin heavy-chain and sarcoplasmic protein in humans. *Am J Physiol,* 273**,** E790-800.

BANO, G., TREVISAN, C., CARRARO, S., SOLMI, M., LUCHINI, C., STUBBS, B., MANZATO, E., SERGI, G. & VERONESE, N. 2017. Inflammation and sarcopenia: A systematic review and meta-analysis. *Maturitas,* 96**,** 10-15.

BARANY, M. 1967. ATPase activity of myosin correlated with speed of muscle shortening. *J Gen Physiol,* 50**,** Suppl:197-218.

BARTEK, J. & LUKAS, J. 2001. Mammalian G1- and S-phase checkpoints in response to DNA damage. *Curr Opin Cell Biol,* 13**,** 738-47.

BAUR, J. A. 2010. Biochemical effects of SIRT1 activators. *Biochim Biophys Acta,* 1804**,** 1626-34.

BAZAN, J. F., BACON, K. B., HARDIMAN, G., WANG, W., SOO, K., ROSSI, D., GREAVES, D. R., ZLOTNIK, A. & SCHALL, T. J. 1997. A new class of membrane-bound chemokine with a CX3C motif. *Nature,* 385**,** 640-4.

BEERY, A. K. & ZUCKER, I. 2011. Sex bias in neuroscience and biomedical research. *Neurosci Biobehav Rev,* 35**,** 565-72.

BEINKE, S. & LEY, S. C. 2004. Functions of NF-kappaB1 and NF-kappaB2 in immune cell biology. *Biochem J,* 382**,** 393-409.

BENNETT, V. & BAINES, A. J. 2001. Spectrin and ankyrin-based pathways: Metazoan inventions for integrating cells into tissues. *Physiological Reviews,* 81**,** 1353-1392.

BERG, H. E., DUDLEY, G. A., HAGGMARK, T., OHLSEN, H. & TESCH, P. A. 1991. Effects of lower limb unloading on skeletal muscle mass and function in humans. *J Appl Physiol (1985),* 70**,** 1882-5.

BERNET, J. D., DOLES, J. D., HALL, J. K., KELLY TANAKA, K., CARTER, T. A. & OLWIN, B. B. 2014. p38 MAPK signaling underlies a cell-autonomous loss of stem cell self-renewal in skeletal muscle of aged mice. *Nat Med,* 20**,** 265-71.

BERRY, D. C., STENESEN, D., ZEVE, D. & GRAFF, J. M. 2013. The developmental origins of adipose tissue. *Development,* 140**,** 3939-49.

BILODEAU, P. A., COYNE, E. S. & WING, S. S. 2016. The ubiquitin proteasome system in atrophying skeletal muscle: roles and regulation. *Am J Physiol Cell Physiol,* 311**,** C392-403.

BJEDOV, I., TOIVONEN, J. M., KERR, F., SLACK, C., JACOBSON, J., FOLEY, A. & PARTRIDGE, L. 2010. Mechanisms of life span extension by rapamycin in the fruit fly Drosophila melanogaster. *Cell Metab,* 11**,** 35-46.

BODINE, S. C., LATRES, E., BAUMHUETER, S., LAI, V. K., NUNEZ, L., CLARKE, B. A., POUEYMIROU, W. T., PANARO, F. J., NA, E., DHARMARAJAN, K., PAN, Z. Q., VALENZUELA, D. M., DECHIARA, T. M., STITT, T. N., YANCOPOULOS, G. D. & GLASS, D.

J. 2001. Identification of ubiquitin ligases required for skeletal muscle atrophy. *Science,* 294**,** 1704-8.

BODNAR, A. G., OUELLETTE, M., FROLKIS, M., HOLT, S. E., CHIU, C. P., MORIN, G. B., HARLEY, C. B., SHAY, J. W., LICHTSTEINER, S. & WRIGHT, W. E. 1998. Extension of life-span by introduction of telomerase into normal human cells. *Science,* 279**,** 349-52.

BOSSOLA, M., PACELLI, F., COSTELLI, P., TORTORELLI, A., ROSA, F. & DOGLIETTO, G. B. 2008. Proteasome activities in the rectus abdominis muscle of young and older individuals. *Biogerontology,* 9**,** 261-8.

BOTTINELLI, R., CANEPARI, M., PELLEGRINO, M. A. & REGGIANI, C. 1996. Force-velocity properties of human skeletal muscle fibres: myosin heavy chain isoform and temperature dependence. *J Physiol,* 495 (Pt 2)**,** 573-86.

BRACK, A. S., CONBOY, M. J., ROY, S., LEE, M., KUO, C. J., KELLER, C. & RANDO, T. A. 2007. Increased Wnt signaling during aging alters muscle stem cell fate and increases fibrosis. *Science,* 317**,** 807-10.

BRAIG, M., LEE, S., LODDENKEMPER, C., RUDOLPH, C., PETERS, A. H., SCHLEGELBERGER, B., STEIN, H., DORKEN, B., JENUWEIN, T. & SCHMITT, C. A. 2005. Oncogene-induced senescence as an initial barrier in lymphoma development. *Nature,* 436**,** 660-5.

BROOKE, M. H. & KAISER, K. K. 1970. Three "myosin adenosine triphosphatase" systems: the nature of their pH lability and sulfhydryl dependence. *J Histochem Cytochem,* 18**,** 670-2.

BROOKS, S. V. & FAULKNER, J. A. 1988. Contractile properties of skeletal muscles from young, adult and aged mice. *J Physiol,* 404**,** 71-82.

BROOKS, S. V. & FAULKNER, J. A. 1990. Contraction-induced injury: recovery of skeletal muscles in young and old mice. *Am J Physiol,* 258**,** C436-42.

BROOKS, S. V. & FAULKNER, J. A. 1991. Maximum and sustained power of extensor digitorum longus muscles from young, adult, and old mice. *J Gerontol,* 46**,** B28-33.

BROOKS, S. V. & FAULKNER, J. A. 2001. Severity of contraction-induced injury is affected by velocity only during stretches of large strain. *Journal of Applied Physiology,* 91**,** 661-666.

BROOKS, S. V., ZERBA, E. & FAULKNER, J. A. 1995. Injury to muscle fibres after single stretches of passive and maximally stimulated muscles in mice. *J Physiol,* 488 (Pt 2)**,** 459-69.

BROWN, R. E., JARVIS, K. L. & HYLAND, K. J. 1989. Protein measurement using bicinchoninic acid: elimination of interfering substances. *Anal Biochem,* 180**,** 136-9.

BRUNK, U. T. & TERMAN, A. 2002. Lipofuscin: mechanisms of age-related accumulation and influence on cell function. *Free Radic Biol Med,* 33**,** 611-9.

BURKE, S. J., LU, D., SPARER, T. E., MASI, T., GOFF, M. R., KARLSTAD, M. D. & COLLIER, J. J. 2014. NF-kappaB and STAT1 control CXCL1 and CXCL2 gene transcription. *Am J Physiol Endocrinol Metab,* 306**,** E131-49.

BURSUKER, I., RHODES, J. M. & GOLDMAN, R. 1982. Beta-galactosidase--an indicator of the maturational stage of mouse and human mononuclear phagocytes. *J Cell Physiol,* 112**,** 385-90.

CAI, D., FRANTZ, J. D., TAWA, N. E., JR., MELENDEZ, P. A., OH, B. C., LIDOV, H. G., HASSELGREN, P. O., FRONTERA, W. R., LEE, J., GLASS, D. J. & SHOELSON, S. E. 2004. IKKbeta/NF-kappaB activation causes severe muscle wasting in mice. *Cell,* 119**,** 285-98.

CAMPBELL, M. J., MCCOMAS, A. J. & PETITO, F. 1973. Physiological changes in ageing muscles. *J Neurol Neurosurg Psychiatry,* 36**,** 174-82.

CAMPISI, J. 2013. Aging, cellular senescence, and cancer. *Annu Rev Physiol,* 75**,** 685-705.

CAMPISI, J. & D'ADDA DI FAGAGNA, F. 2007. Cellular senescence: when bad things happen to good cells. *Nat Rev Mol Cell Biol,* 8**,** 729-40.

CANTO, C., JIANG, L. Q., DESHMUKH, A. S., MATAKI, C., COSTE, A., LAGOUGE, M., ZIERATH, J. R. & AUWERX, J. 2010. Interdependence of AMPK and SIRT1 for metabolic adaptation to fasting and exercise in skeletal muscle. *Cell Metab,* 11**,** 213-9.

CARLSON, B. M. & FAULKNER, J. A. 1989. Muscle Transplantation between Young and Old Rats - Age of Host Determines Recovery. *American Journal of Physiology,* 256**,** C1262-C1266.

CASTILHO, R. M., SQUARIZE, C. H., CHODOSH, L. A., WILLIAMS, B. O. & GUTKIND, J. S. 2009. mTOR mediates Wnt-induced epidermal stem cell exhaustion and aging. *Cell Stem Cell,* 5**,** 279-89.

CHANG, B. D., XUAN, Y., BROUDE, E. V., ZHU, H., SCHOTT, B., FANG, J. & RONINSON, I. B. 1999. Role of p53 and p21waf1/cip1 in senescence-like terminal proliferation arrest induced in human tumor cells by chemotherapeutic drugs. *Oncogene,* 18**,** 4808-18.

CHATSIRISUPACHAI, K., PALMER, D., FERREIRA, S. & DE MAGALHAES, J. P. 2019. A human tissue-specific transcriptomic analysis reveals a complex relationship between aging, cancer, and cellular senescence. *Aging Cell,* 18**,** e13041.

CHELM, B. K. & GEIDUSCHEK, E. P. 1979. Gel electrophoretic separation of transcription complexes: an assay for RNA polymerase selectivity and a method for promoter mapping. *Nucleic Acids Res,* 7**,** 1851-67.

CHEN, C., LIU, Y., LIU, Y. & ZHENG, P. 2009. mTOR regulation and therapeutic rejuvenation of aging hematopoietic stem cells. *Sci Signal,* 2**,** ra75.

CHEN, C. C. & LAU, L. F. 2009. Functions and mechanisms of action of CCN matricellular proteins. *Int J Biochem Cell Biol,* 41**,** 771-83.

CHEN, L. K., LIU, L. K., WOO, J., ASSANTACHAI, P., AUYEUNG, T. W., BAHYAH, K. S., CHOU, M. Y., CHEN, L. Y., HSU, P. S., KRAIRIT, O., LEE, J. S., LEE, W. J., LEE, Y., LIANG, C. K., LIMPAWATTANA, P., LIN, C. S., PENG, L. N., SATAKE, S., SUZUKI, T., WON, C. W., WU, C. H., WU, S. N., ZHANG, T., ZENG, P., AKISHITA, M. & ARAI, H. 2014. Sarcopenia in Asia: consensus report of the Asian Working Group for Sarcopenia. *J Am Med Dir Assoc,* 15**,** 95-101.

CHEN, Q. N., FAN, Z., LYU, A. K., WU, J., GUO, A., YANG, Y. F., CHEN, J. L. & XIAO, Q. 2020. Effect of sarcolipin-mediated cell transdifferentiation in sarcopenia-associated skeletal muscle fibrosis. *Exp Cell Res,* 389**,** 111890.

CHEN, Z., TROTMAN, L. C., SHAFFER, D., LIN, H. K., DOTAN, Z. A., NIKI, M., KOUTCHER, J. A., SCHER, H. I., LUDWIG, T., GERALD, W., CORDON-CARDO, C. & PANDOLFI, P. P. 2005. Crucial role of p53-dependent cellular senescence in suppression of Pten-deficient tumorigenesis. *Nature,* 436**,** 725-30.

CHIEN, C. S., SHEN, K. H., HUANG, J. S., KO, S. C. & SHIH, Y. W. 2010. Antimetastatic potential of fisetin involves inactivation of the PI3K/Akt and JNK signaling pathways with downregulation of MMP-2/9 expressions in prostate cancer PC-3 cells. *Mol Cell Biochem,* 333**,** 169-80.

CHIEN, Y., SCUOPPO, C., WANG, X., FANG, X., BALGLEY, B., BOLDEN, J. E., PREMSRIRUT, P., LUO, W., CHICAS, A., LEE, C. S., KOGAN, S. C. & LOWE, S. W. 2011. Control of the senescence-associated secretory phenotype by NF-kappaB promotes senescence and enhances chemosensitivity. *Genes Dev,* 25**,** 2125-36.

CHRISTOPHER, L. J., CUI, D., WU, C., LUO, R., MANNING, J. A., BONACORSI, S. J., LAGO, M., ALLENTOFF, A., LEE, F. Y., MCCANN, B., GALBRAITH, S., REITBERG, D. P., HE, K., BARROS, A., JR., BLACKWOOD-CHIRCHIR, A., HUMPHREYS, W. G. & IYER, R. A. 2008. Metabolism and disposition of dasatinib after oral administration to humans. *Drug Metab Dispos,* 36**,** 1357-64.

CLAYTON, D. A., DODA, J. N. & FRIEDBERG, E. C. 1974. The absence of a pyrimidine dimer repair mechanism in mammalian mitochondria. *Proc Natl Acad Sci U S A,* 71**,** 2777-81.

COLLADO, M., BLASCO, M. A. & SERRANO, M. 2007. Cellular senescence in cancer and aging. *Cell,* 130**,** 223-33.

COLLADO, M. & SERRANO, M. 2010. Senescence in tumours: evidence from mice and humans. *Nat Rev Cancer,* 10**,** 51-7.

CONBOY, I. M., CONBOY, M. J., WAGERS, A. J., GIRMA, E. R., WEISSMAN, I. L. & RANDO, T. A. 2005. Rejuvenation of aged progenitor cells by exposure to a young systemic environment. *Nature,* 433**,** 760-4.

COPPE, J. P., DESPREZ, P. Y., KRTOLICA, A. & CAMPISI, J. 2010a. The senescence-associated secretory phenotype: the dark side of tumor suppression. *Annu Rev Pathol,* 5**,** 99-118.

COPPÉ, J. P., DESPREZ, P. Y., KRTOLICA, A. & CAMPISI, J. 2010. The senescence-associated secretory phenotype: The dark side of tumor suppression. *Annual Review of Pathology: Mechanisms of Disease.*

COPPE, J. P., PATIL, C. K., RODIER, F., KRTOLICA, A., BEAUSEJOUR, C. M., PARRINELLO, S., HODGSON, J. G., CHIN, K., DESPREZ, P. Y. & CAMPISI, J. 2010b. A human-like senescence-associated secretory phenotype is conserved in mouse cells dependent on physiological oxygen. *PLoS One,* 5**,** e9188.

COPPE, J. P., PATIL, C. K., RODIER, F., SUN, Y., MUNOZ, D. P., GOLDSTEIN, J., NELSON, P. S., DESPREZ, P. Y. & CAMPISI, J. 2008. Senescence-associated secretory phenotypes

reveal cell-nonautonomous functions of oncogenic RAS and the p53 tumor suppressor. *PLoS Biol,* 6**,** 2853-68.

COSGROVE, B. D., GILBERT, P. M., PORPIGLIA, E., MOURKIOTI, F., LEE, S. P., CORBEL, S. Y., LLEWELLYN, M. E., DELP, S. L. & BLAU, H. M. 2014. Rejuvenation of the muscle stem cell population restores strength to injured aged muscles. *Nat Med,* 20**,** 255-64.

CRISTOFALO, V. J. 2005. SA beta Gal staining: biomarker or delusion. *Exp Gerontol,* 40**,** 836-8.

CRUZ-JENTOFT, A. J., BAEYENS, J. P., BAUER, J. M., BOIRIE, Y., CEDERHOLM, T., LANDI, F., MARTIN, F. C., MICHEL, J. P., ROLLAND, Y., SCHNEIDER, S. M., TOPINKOVA, E., VANDEWOUDE, M., ZAMBONI, M. & EUROPEAN WORKING GROUP ON SARCOPENIA IN OLDER, P. 2010. Sarcopenia: European consensus on definition and diagnosis: Report of the European Working Group on Sarcopenia in Older People. *Age Ageing,* 39**,** 412-23.

CURRAIS, A., PRIOR, M., DARGUSCH, R., ARMANDO, A., EHREN, J., SCHUBERT, D., QUEHENBERGER, O. & MAHER, P. 2014. Modulation of p25 and inflammatory pathways by fisetin maintains cognitive function in Alzheimer's disease transgenic mice. *Aging Cell,* 13**,** 379-90.

CUTHBERTSON, D., SMITH, K., BABRAJ, J., LEESE, G., WADDELL, T., ATHERTON, P., WACKERHAGE, H., TAYLOR, P. M. & RENNIE, M. J. 2005. Anabolic signaling deficits underlie amino acid resistance of wasting, aging muscle. *FASEB J,* 19**,** 422-4.

D'ADDA DI FAGAGNA, F. 2008. Living on a break: cellular senescence as a DNA-damage response. *Nat Rev Cancer,* 8**,** 512-22.

D'ORAZI, G., SODDU, S. & SACCHI, A. 2000. Activation of p53/p21(waf1) pathway is associated with senescence during v-Ha-ras transformation of immortal C2C12 myoblasts. *Anticancer Research,* 20**,** 3497-3502.

DA SILVA, P. F. L., OGRODNIK, M., KUCHERYAVENKO, O., GLIBERT, J., MIWA, S., CAMERON, K., ISHAQ, A., SARETZKI, G., NAGARAJA-GRELLSCHEID, S., NELSON, G. & VON ZGLINICKI, T. 2019. The bystander effect contributes to the accumulation of senescent cells in vivo. *Aging Cell,* 18**,** e12848.

DAY, K., SHEFER, G., SHEARER, A. & YABLONKA-REUVENI, Z. 2010. The depletion of skeletal muscle satellite cells with age is concomitant with reduced capacity of single progenitors to produce reserve progeny. *Dev Biol,* 340**,** 330-43.

DE WAAL MALEFYT, R., ABRAMS, J., BENNETT, B., FIGDOR, C. G. & DE VRIES, J. E. 1991a. Interleukin 10(IL-10) inhibits cytokine synthesis by human monocytes: an autoregulatory role of IL-10 produced by monocytes. *J Exp Med,* 174**,** 1209-20.

DE WAAL MALEFYT, R., HAANEN, J., SPITS, H., RONCAROLO, M. G., TE VELDE, A., FIGDOR, C., JOHNSON, K., KASTELEIN, R., YSSEL, H. & DE VRIES, J. E. 1991b. Interleukin 10 (IL-10) and viral IL-10 strongly reduce antigen-specific human T cell proliferation by diminishing the antigen-presenting capacity of monocytes via downregulation of class II major histocompatibility complex expression. *J Exp Med,* 174**,** 915-24.

DEBACQ-CHAINIAUX, F., ERUSALIMSKY, J. D., CAMPISI, J. & TOUSSAINT, O. 2009. Protocols to detect senescence-associated beta-galactosidase (SA-betagal) activity, a biomarker of senescent cells in culture and in vivo. *Nat Protoc,* 4**,** 1798-806.

DEJONG, C. H., BUSQUETS, S., MOSES, A. G., SCHRAUWEN, P., ROSS, J. A., ARGILES, J. M. & FEARON, K. C. 2005. Systemic inflammation correlates with increased expression of skeletal muscle ubiquitin but not uncoupling proteins in cancer cachexia. *Oncol Rep,* 14**,** 257-63.

DELBONO, O. 2003. Neural control of aging skeletal muscle. *Aging Cell,* 2**,** 21-9.

DELDICQUE, L., THEISEN, D. & FRANCAUX, M. 2005. Regulation of mTOR by amino acids and resistance exercise in skeletal muscle. *Eur J Appl Physiol,* 94**,** 1-10.

DEMARIA, M., OHTANI, N., YOUSSEF, S. A., RODIER, F., TOUSSAINT, W., MITCHELL, J. R., LABERGE, R. M., VIJG, J., VAN STEEG, H., DOLLE, M. E., HOEIJMAKERS, J. H., DE BRUIN, A., HARA, E. & CAMPISI, J. 2014. An essential role for senescent cells in optimal wound healing through secretion of PDGF-AA. *Dev Cell,* 31**,** 722-33.

DEMONTIS, F., PICCIRILLO, R., GOLDBERG, A. L. & PERRIMON, N. 2013. Mechanisms of skeletal muscle aging: insights from Drosophila and mammalian models. *Dis Model Mech,* 6**,** 1339-52.

DENG, J., FU, R., LI, Q., WANG, Y., HU, W., SHEN, B., LI, H., HU, C., LIU, M., ZHANG, L., LIU, M., CAO, Q. & WANG, Y. 2019. Increased sFRP3 expression correlated to senescence of endothelial cells in the aging process of mice. *Am J Transl Res,* 11**,** 1810-1818.

DEOTARE, U., AL-DAWSARI, G., COUBAN, S. & LIPTON, J. H. 2015. G-CSF-primed bone marrow as a source of stem cells for allografting: revisiting the concept. *Bone Marrow Transplant,* 50**,** 1150-6.

DIMRI, G. P., LEE, X., BASILE, G., ACOSTA, M., SCOTT, G., ROSKELLEY, C., MEDRANO, E. E., LINSKENS, M., RUBELJ, I., PEREIRA-SMITH, O. & ET AL. 1995. A biomarker that identifies senescent human cells in culture and in aging skin in vivo. *Proc Natl Acad Sci U S A,* 92**,** 9363-7.

DOCK, J., RAMIREZ, C. M., HULTIN, L., HAUSNER, M. A., HULTIN, P., ELLIOTT, J., YANG, O. O., ANTON, P. A., JAMIESON, B. D. & EFFROS, R. B. 2017. Distinct aging profiles of CD8+ T cells in blood versus gastrointestinal mucosal compartments. *PLoS One,* 12**,** e0182498.

DUEY, W. J., BASSETT, D. R., JR., TOROK, D. J., HOWLEY, E. T., BOND, V., MANCUSO, P. & TRUDELL, R. 1997. Skeletal muscle fibre type and capillary density in college-aged blacks and whites. *Ann Hum Biol,* 24**,** 323-31.

DUMAZ, N. & MEEK, D. W. 1999. Serine15 phosphorylation stimulates p53 transactivation but does not directly influence interaction with HDM2. *EMBO J,* 18**,** 7002-10.

DUMBLE, M., MOORE, L., CHAMBERS, S. M., GEIGER, H., VAN ZANT, G., GOODELL, M. A. & DONEHOWER, L. A. 2007. The impact of altered p53 dosage on hematopoietic stem cell dynamics during aging. *Blood,* 109**,** 1736-42.

EDGERTON, V. R., SMITH, J. L. & SIMPSON, D. R. 1975. Muscle fibre type populations of human leg muscles. *Histochem J,* 7**,** 259-66.

EDWARDS, M. G., ANDERSON, R. M., YUAN, M., KENDZIORSKI, C. M., WEINDRUCH, R. & PROLLA, T. A. 2007. Gene expression profiling of aging reveals activation of a p53-mediated transcriptional program. *BMC Genomics,* 8**,** 80.

EISINGER, J. 1971. Visible gel electrophoresis and the determination of association constants. *Biochem Biophys Res Commun,* 44**,** 1135-42.

EVAN, G. I. & D'ADDA DI FAGAGNA, F. 2009. Cellular senescence: hot or what? *Curr Opin Genet Dev,* 19**,** 25-31.

EVANGELOU, K. & GORGOULIS, V. G. 2017. Sudan Black B, The Specific Histochemical Stain for Lipofuscin: A Novel Method to Detect Senescent Cells. *Methods Mol Biol,* 1534**,** 111-119.

EVANS, W. J. & CAMPBELL, W. W. 1993. Sarcopenia and age-related changes in body composition and functional capacity. *J Nutr,* 123**,** 465-8.

FAGGIOLI, F., WANG, T., VIJG, J. & MONTAGNA, C. 2012. Chromosome-specific accumulation of aneuploidy in the aging mouse brain. *Hum Mol Genet,* 21**,** 5246-53.

FALCON, L. J. & HARRIS-LOVE, M. O. 2017. Sarcopenia and the New ICD-10-CM Code: Screening, Staging, and Diagnosis Considerations. *Fed Pract,* 34**,** 24-32.

FARR, J. N., ROWSEY, J. L., ECKHARDT, B. A., THICKE, B. S., FRASER, D. G., TCHKONIA, T., KIRKLAND, J. L., MONROE, D. G. & KHOSLA, S. 2019. Independent Roles of Estrogen Deficiency and Cellular Senescence in the Pathogenesis of Osteoporosis: Evidence in Young Adult Mice and Older Humans. *J Bone Miner Res,* 34**,** 1407-1418.

FARR, J. N., XU, M., WEIVODA, M. M., MONROE, D. G., FRASER, D. G., ONKEN, J. L., NEGLEY, B. A., SFEIR, J. G., OGRODNIK, M. B., HACHFELD, C. M., LEBRASSEUR, N. K., DRAKE, M. T., PIGNOLO, R. J., PIRTSKHALAVA, T., TCHKONIA, T., OURSLER, M. J., KIRKLAND, J. L. & KHOSLA, S. 2017. Corrigendum: Targeting cellular senescence prevents age-related bone loss in mice. *Nat Med,* 23**,** 1384.

FAULKNER, J. A., BROOKS, S. V. & OPITECK, J. A. 1993. Injury to skeletal muscle fibers during contractions: conditions of occurrence and prevention. *Phys Ther,* 73**,** 911-21.

FAULKNER, J. A., BROOKS, S. V. & ZERBA, E. 1995. Muscle atrophy and weakness with aging: contraction-induced injury as an underlying mechanism. *J Gerontol A Biol Sci Med Sci,* 50 Spec No**,** 124-9.

FAULKNER, J. A., JONES, D. A. & ROUND, J. M. 1989. Injury to skeletal muscles of mice by forced lengthening during contractions. *Q J Exp Physiol,* 74**,** 661-70.

FAULKNER, J. A., RAMASWAMY, K., PALMER, M., VANDERMEULEN, J., RENOUX, A., KOSTROMINOVA, T. & MICHELE, D. 2011. Lateral transmission of force is impaired in skeletal muscles of dystrophic mice and very old rats. *Faseb Journal,* 25.

FENG, Z., HU, W., TERESKY, A. K., HERNANDO, E., CORDON-CARDO, C. & LEVINE, A. J. 2007. Declining p53 function in the aging process: a possible mechanism for the increased tumor incidence in older populations. *Proc Natl Acad Sci U S A,* 104**,** 16633-8.

FIELDING, R. A., VELLAS, B., EVANS, W. J., BHASIN, S., MORLEY, J. E., NEWMAN, A. B., ABELLAN VAN KAN, G., ANDRIEU, S., BAUER, J., BREUILLE, D., CEDERHOLM, T., CHANDLER, J., DE MEYNARD, C., DONINI, L., HARRIS, T., KANNT, A., KEIME GUIBERT, F., ONDER, G., PAPANICOLAOU, D., ROLLAND, Y., ROOKS, D., SIEBER, C., SOUHAMI, E., VERLAAN, S. & ZAMBONI, M. 2011. Sarcopenia: an undiagnosed condition in older adults. Current consensus definition: prevalence, etiology, and consequences. International working group on sarcopenia. *J Am Med Dir Assoc,* 12**,** 249-56.

FRANCESCHI, C. & BONAFE, M. 2003. Centenarians as a model for healthy aging. *Biochem Soc Trans,* 31**,** 457-61.

FRANCESCHI, C., BONAFE, M., VALENSIN, S., OLIVIERI, F., DE LUCA, M., OTTAVIANI, E. & DE BENEDICTIS, G. 2000. Inflamm-aging. An evolutionary perspective on immunosenescence. *Ann N Y Acad Sci,* 908**,** 244-54.

FRANCESCHI, C. & CAMPISI, J. 2014. Chronic inflammation (inflammaging) and its potential contribution to age-associated diseases. *J Gerontol A Biol Sci Med Sci,* 69 Suppl 1**,** S4-9.

FRANCISCO-CRUZ, A., AGUILAR-SANTELISES, M., RAMOS-ESPINOSA, O., MATA-ESPINOSA, D., MARQUINA-CASTILLO, B., BARRIOS-PAYAN, J. & HERNANDEZ-PANDO, R. 2014. Granulocyte-macrophage colony-stimulating factor: not just another haematopoietic growth factor. *Med Oncol,* 31**,** 774.

FRANCKHAUSER, S., ELIAS, I., ROTTER SOPASAKIS, V., FERRE, T., NAGAEV, I., ANDERSSON, C. X., AGUDO, J., RUBERTE, J., BOSCH, F. & SMITH, U. 2008. Overexpression of Il6 leads to hyperinsulinaemia, liver inflammation and reduced body weight in mice. *Diabetologia,* 51**,** 1306-16.

FRIED, M. & CROTHERS, D. M. 1981. Equilibria and kinetics of lac repressor-operator interactions by polyacrylamide gel electrophoresis. *Nucleic Acids Res,* 9**,** 6505-25.

FRONTERA, W. R. & OCHALA, J. 2015. Skeletal muscle: a brief review of structure and function. *Calcif Tissue Int,* 96**,** 183-95.

FRONTERA, W. R., SUH, D., KRIVICKAS, L. S., HUGHES, V. A., GOLDSTEIN, R. & ROUBENOFF, R. 2000. Skeletal muscle fiber quality in older men and women. *Am J Physiol Cell Physiol,* 279**,** C611-8.

FROST, R. A. & LANG, C. H. 2011. mTor signaling in skeletal muscle during sepsis and inflammation: where does it all go wrong? *Physiology (Bethesda),* 26**,** 83-96.

GARCIA-CAO, I., GARCIA-CAO, M., MARTIN-CABALLERO, J., CRIADO, L. M., KLATT, P., FLORES, J. M., WEILL, J. C., BLASCO, M. A. & SERRANO, M. 2002. "Super p53" mice exhibit enhanced DNA damage response, are tumor resistant and age normally. *EMBO J,* 21**,** 6225-35.

GARNER, M. M. & REVZIN, A. 1981. A gel electrophoresis method for quantifying the binding of proteins to specific DNA regions: application to components of the Escherichia coli lactose operon regulatory system. *Nucleic Acids Res,* 9**,** 3047-60.

GARTEL, A. L. & RADHAKRISHNAN, S. K. 2005. Lost in transcription: p21 repression, mechanisms, and consequences. *Cancer Res,* 65**,** 3980-5.

GATENBY, J. B. & MOUSSA, T. A. 1949. The sudan black B technique in cytology. *J R Microsc Soc,* 69**,** 72-5.

GE, Y., WALDEMER, R. J., NALLURI, R., NUZZI, P. D. & CHEN, J. 2013. RNAi screen reveals potentially novel roles of cytokines in myoblast differentiation. *PLoS One,* 8**,** e68068.

GERHARDT, C. C., ROMERO, I. A., CANCELLO, R., CAMOIN, L. & STROSBERG, A. D. 2001. Chemokines control fat accumulation and leptin secretion by cultured human adipocytes. *Mol Cell Endocrinol,* 175**,** 81-92.

GLEES, P. & HASAN, M. 1976. Lipofuscin in neuronal aging and diseases. *Norm Pathol Anat (Stuttg),* 32**,** 1-68.

GOLDSPINK, G., FERNANDES, K., WILLIAMS, P. E. & WELLS, D. J. 1994. Age-related changes in collagen gene expression in the muscles of mdx dystrophic and normal mice. *Neuromuscular Disorders,* 4**,** 183-191.

GOLLAPUDI, P., HASEGAWA, L. S. & EASTMOND, D. A. 2014. A comparative study of the aneugenic and polyploidy-inducing effects of fisetin and two model Aurora kinase inhibitors. *Mutat Res Genet Toxicol Environ Mutagen,* 767**,** 37-43.

GOMES, E. C., SILVA, A. N. & DE OLIVEIRA, M. R. 2012. Oxidants, antioxidants, and the beneficial roles of exercise-induced production of reactive species. *Oxid Med Cell Longev,* 2012**,** 756132.

GOMES, M. D., LECKER, S. H., JAGOE, R. T., NAVON, A. & GOLDBERG, A. L. 2001. Atrogin-1, a muscle-specific F-box protein highly expressed during muscle atrophy. *Proc Natl Acad Sci U S A,* 98**,** 14440-5.

GONG, H., SUN, L., CHEN, B., HAN, Y., PANG, J., WU, W., QI, R. & ZHANG, T. M. 2016. Evaluation of candidate reference genes for RT-qPCR studies in three metabolism related tissues of mice after caloric restriction. *Sci Rep,* 6**,** 38513.

GONZALEZ, E. & DELBONO, O. 2001. Age-dependent fatigue in single intact fast- and slow fibers from mouse EDL and soleus skeletal muscles. *Mech Ageing Dev,* 122**,** 1019-32.

GORBUNOVA, V. & SELUANOV, A. 2010. A Comparison of Senescence in Mouse and Human Cells. *In:* ADAMS, P. D. & SEDIVY, J. M. (eds.) *Cellular Senescence and Tumor Suppression.* New York, NY: Springer New York.

GORGOULIS, V. G. & HALAZONETIS, T. D. 2010. Oncogene-induced senescence: the bright and dark side of the response. *Curr Opin Cell Biol,* 22**,** 816-27.

GRAEFE, E. U., WITTIG, J., MUELLER, S., RIETHLING, A. K., UEHLEKE, B., DREWELOW, B., PFORTE, H., JACOBASCH, G., DERENDORF, H. & VEIT, M. 2001. Pharmacokinetics and bioavailability of quercetin glycosides in humans. *J Clin Pharmacol,* 41**,** 492-9.

GRIMBY, G. & SALTIN, B. 1983. The ageing muscle. *Clin Physiol,* 3**,** 209-18.

GROSSE, L., WAGNER, N., EMELYANOV, A., MOLINA, C., LACAS-GERVAIS, S., WAGNER, K. D. & BULAVIN, D. V. 2020. Defined p16(High) Senescent Cell Types Are Indispensable for Mouse Healthspan. *Cell Metab,* 32**,** 87-99 e6.

GUPTA, S. C., TYAGI, A. K., DESHMUKH-TASKAR, P., HINOJOSA, M., PRASAD, S. & AGGARWAL, B. B. 2014. Downregulation of tumor necrosis factor and other proinflammatory biomarkers by polyphenols. *Arch Biochem Biophys,* 559**,** 91-9.

HALL, B. M., BALAN, V., GLEIBERMAN, A. S., STROM, E., KRASNOV, P., VIRTUOSO, L. P., RYDKINA, E., VUJCIC, S., BALAN, K., GITLIN, I., LEONOVA, K., POLINSKY, A., CHERNOVA, O. B. & GUDKOV, A. V. 2016. Aging of mice is associated with p16(Ink4a)- and beta-galactosidase-positive macrophage accumulation that can be induced in young mice by senescent cells. *Aging (Albany NY),* 8**,** 1294-315.

HAMMOND, M. E., LAPOINTE, G. R., FEUCHT, P. H., HILT, S., GALLEGOS, C. A., GORDON, C. A., GIEDLIN, M. A., MULLENBACH, G. & TEKAMP-OLSON, P. 1995. IL-8 induces neutrophil chemotaxis predominantly via type I IL-8 receptors. *J Immunol,* 155**,** 1428-33.

HANDE, K. R. 1998. Etoposide: four decades of development of a topoisomerase II inhibitor. *Eur J Cancer,* 34**,** 1514-21.

HARA, E., SMITH, R., PARRY, D., TAHARA, H., STONE, S. & PETERS, G. 1996. Regulation of p16CDKN2 expression and its implications for cell immortalization and senescence. *Mol Cell Biol,* 16**,** 859-67.

HARLEY, C. B., FUTCHER, A. B. & GREIDER, C. W. 1990. Telomeres shorten during ageing of human fibroblasts. *Nature,* 345**,** 458-60.

HARRISON, D. E., STRONG, R., SHARP, Z. D., NELSON, J. F., ASTLE, C. M., FLURKEY, K., NADON, N. L., WILKINSON, J. E., FRENKEL, K., CARTER, C. S., PAHOR, M., JAVORS, M. A., FERNANDEZ, E. & MILLER, R. A. 2009. Rapamycin fed late in life extends lifespan in genetically heterogeneous mice. *Nature,* 460**,** 392-5.

HASLAM, E. & CAI, Y. 1994. Plant polyphenols (vegetable tannins): gallic acid metabolism. *Nat Prod Rep,* 11**,** 41-66.

HASTEN, D. L., PAK-LODUCA, J., OBERT, K. A. & YARASHESKI, K. E. 2000. Resistance exercise acutely increases MHC and mixed muscle protein synthesis rates in 78-84 and 23-32 yr olds. *Am J Physiol Endocrinol Metab,* 278**,** E620-6.

HAYASHIJI, N., YUASA, S., MIYAGOE-SUZUKI, Y., HARA, M., ITO, N., HASHIMOTO, H., KUSUMOTO, D., SEKI, T., TOHYAMA, S., KODAIRA, M., KUNITOMI, A., KASHIMURA, S., TAKEI, M., SAITO, Y., OKATA, S., EGASHIRA, T., ENDO, J., SASAOKA, T., TAKEDA, S. & FUKUDA, K. 2015. Erratum: G-CSF supports long-term muscle regeneration in mouse models of muscular dystrophy. *Nat Commun,* 6**,** 7295.

HAYFLICK, L. & MOORHEAD, P. S. 1961. The serial cultivation of human diploid cell strains. *Exp Cell Res,* 25**,** 585-621.

HE, G., SIDDIK, Z. H., HUANG, Z., WANG, R., KOOMEN, J., KOBAYASHI, R., KHOKHAR, A. R. & KUANG, J. 2005. Induction of p21 by p53 following DNA damage inhibits both Cdk4 and Cdk2 activities. *Oncogene,* 24**,** 2929-43.

HERBIG, U., FERREIRA, M., CONDEL, L., CAREY, D. & SEDIVY, J. M. 2006. Cellular senescence in aging primates. *Science,* 311**,** 1257.

HERBIG, U. & SEDIVY, J. M. 2006. Regulation of growth arrest in senescence: telomere damage is not the end of the story. *Mech Ageing Dev,* 127**,** 16-24.

HERNANDEZ-SEGURA, A., DE JONG, T. V., MELOV, S., GURYEV, V., CAMPISI, J. & DEMARIA, M. 2017. Unmasking Transcriptional Heterogeneity in Senescent Cells. *Curr Biol,* 27**,** 2652-2660 e4.

HERNANDEZ-SEGURA, A., NEHME, J. & DEMARIA, M. 2018. Hallmarks of Cellular Senescence. *Trends Cell Biol,* 28**,** 436-453.

HICKSON, L. J., LANGHI PRATA, L. G. P., BOBART, S. A., EVANS, T. K., GIORGADZE, N., HASHMI, S. K., HERRMANN, S. M., JENSEN, M. D., JIA, Q., JORDAN, K. L., KELLOGG, T. A., KHOSLA, S., KOERBER, D. M., LAGNADO, A. B., LAWSON, D. K., LEBRASSEUR, N. K., LERMAN, L. O., MCDONALD, K. M., MCKENZIE, T. J., PASSOS, J. F., PIGNOLO, R. J., PIRTSKHALAVA, T., SAADIQ, I. M., SCHAEFER, K. K., TEXTOR, S. C., VICTORELLI, S. G., VOLKMAN, T. L., XUE, A., WENTWORTH, M. A., WISSLER GERDES, E. O., ZHU, Y., TCHKONIA, T. & KIRKLAND, J. L. 2019. Senolytics decrease senescent cells in humans: Preliminary report from a clinical trial of Dasatinib plus Quercetin in individuals with diabetic kidney disease. *EBioMedicine,* 47**,** 446-456.

HU, Y., BAUD, V., DELHASE, M., ZHANG, P., DEERINCK, T., ELLISMAN, M., JOHNSON, R. & KARIN, M. 1999. Abnormal morphogenesis but intact IKK activation in mice lacking the IKKalpha subunit of IkappaB kinase. *Science,* 284**,** 316-20.

HUANG, T. T., WUERZBERGER-DAVIS, S. M., WU, Z. H. & MIYAMOTO, S. 2003. Sequential modification of NEMO/IKKgamma by SUMO-1 and ubiquitin mediates NF-kappaB activation by genotoxic stress. *Cell,* 115**,** 565-76.

HUSSAIN, T., TAN, B., YIN, Y., BLACHIER, F., TOSSOU, M. C. & RAHU, N. 2016. Oxidative Stress and Inflammation: What Polyphenols Can Do for Us? *Oxid Med Cell Longev,* 2016**,** 7432797.

HUXLEY, H. & HANSON, J. 1954. Changes in the cross-striations of muscle during contraction and stretch and their structural interpretation. *Nature,* 173**,** 973-6.

HUXLEY, H. E. 1957. The double array of filaments in cross-striated muscle. *J Biophys Biochem Cytol,* 3**,** 631-48.

HWANG, S. Y., KANG, Y. J., SUNG, B., JANG, J. Y., HWANG, N. L., OH, H. J., AHN, Y. R., KIM, H. J., SHIN, J. H., YOO, M. A., KIM, C. M., CHUNG, H. Y. & KIM, N. D. 2018. Folic acid is necessary for proliferation and differentiation of C2C12 myoblasts. *J Cell Physiol,* 233**,** 736-747.

IKEDA, H., TAUCHI, H. & SATO, T. 1985. Fine structural analysis of lipofuscin in various tissues of rats of different ages. *Mech Ageing Dev,* 33**,** 77-93.

IMAMURA, K., ASHIDA, H., ISHIKAWA, T. & FUJII, M. 1983. Human major psoas muscle and sacrospinalis muscle in relation to age: a study by computed tomography. *J Gerontol,* 38**,** 678-81.

INGJER, F. 1979. Capillary supply and mitochondrial content of different skeletal muscle fiber types in untrained and endurance-trained men. A histochemical and ultrastructural study. *Eur J Appl Physiol Occup Physiol,* 40**,** 197-209.

IWAI, K. 2012. Diverse ubiquitin signaling in NF-kappaB activation. *Trends Cell Biol,* 22**,** 355-64.

JACKSON, M. J. 2020. On the mechanisms underlying attenuated redox responses to exercise in older individuals: A hypothesis. *Free Radic Biol Med*.

JACKSON, M. J. & MCARDLE, A. 2011. Age-related changes in skeletal muscle reactive oxygen species generation and adaptive responses to reactive oxygen species. *J Physiol,* 589**,** 2139-45.

JACKSON, S. P. & BARTEK, J. 2009. The DNA-damage response in human biology and disease. *Nature,* 461**,** 1071-8.

JADHAV, K. S., DUNGAN, C. M. & WILLIAMSON, D. L. 2013. Metformin limits ceramide-induced senescence in C2C12 myoblasts. *Mech Ageing Dev,* 134**,** 548-59.

JANSSEN, I., HEYMSFIELD, S. B., WANG, Z. M. & ROSS, R. 2000. Skeletal muscle mass and distribution in 468 men and women aged 18-88 yr. *J Appl Physiol (1985),* 89**,** 81-8.

JANSSON, E. & SYLVEN, C. 1983. Myoglobin concentration in single type I and type II muscle fibres in man. *Histochemistry,* 78**,** 121-4.

JEON, O. H., KIM, C., LABERGE, R. M., DEMARIA, M., RATHOD, S., VASSEROT, A. P., CHUNG, J. W., KIM, D. H., POON, Y., DAVID, N., BAKER, D. J., VAN DEURSEN, J. M., CAMPISI, J. & ELISSEEFF, J. H. 2017. Local clearance of senescent cells attenuates the development of post-traumatic osteoarthritis and creates a pro-regenerative environment. *Nat Med,* 23**,** 775-781.

JEYAPALAN, J. C., FERREIRA, M., SEDIVY, J. M. & HERBIG, U. 2007. Accumulation of senescent cells in mitotic tissue of aging primates. *Mech Ageing Dev,* 128**,** 36-44.

JIANG, J., WANG, Y., SUSAC, L., CHAN, H., BASU, R., ZHOU, Z. H. & FEIGON, J. 2018. Structure of Telomerase with Telomeric DNA. *Cell,* 173**,** 1179-1190 e13.

JO, E., LEE, S. R., PARK, B. S. & KIM, J. S. 2012. Potential mechanisms underlying the role of chronic inflammation in age-related muscle wasting. *Aging Clin Exp Res,* 24**,** 412-22.

JUN, J. I. & LAU, L. F. 2010. The matricellular protein CCN1 induces fibroblast senescence and restricts fibrosis in cutaneous wound healing. *Nat Cell Biol,* 12**,** 676-85.

JUNG, C. H., KIM, H., AHN, J., JEON, T. I., LEE, D. H. & HA, T. Y. 2013. Fisetin regulates obesity by targeting mTORC1 signaling. *J Nutr Biochem,* 24**,** 1547-54.

JURK, D., WANG, C., MIWA, S., MADDICK, M., KOROLCHUK, V., TSOLOU, A., GONOS, E. S., THRASIVOULOU, C., SAFFREY, M. J., CAMERON, K. & VON ZGLINICKI, T. 2012. Postmitotic neurons develop a p21-dependent senescence-like phenotype driven by a DNA damage response. *Aging Cell,* 11**,** 996-1004.

JURK, D., WILSON, C., PASSOS, J. F., OAKLEY, F., CORREIA-MELO, C., GREAVES, L., SARETZKI, G., FOX, C., LAWLESS, C., ANDERSON, R., HEWITT, G., PENDER, S. L., FULLARD, N., NELSON, G., MANN, J., VAN DE SLUIS, B., MANN, D. A. & VON ZGLINICKI, T. 2014. Chronic inflammation induces telomere dysfunction and accelerates ageing in mice. *Nat Commun,* 2**,** 4172.

KAEBERLEIN, M., POWERS, R. W., 3RD, STEFFEN, K. K., WESTMAN, E. A., HU, D., DANG, N., KERR, E. O., KIRKLAND, K. T., FIELDS, S. & KENNEDY, B. K. 2005. Regulation of yeast replicative life span by TOR and Sch9 in response to nutrients. *Science,* 310**,** 1193-6.

KAKIMOTO, Y., OKADA, C., KAWABE, N., SASAKI, A., TSUKAMOTO, H., NAGAO, R. & OSAWA, M. 2019. Myocardial lipofuscin accumulation in ageing and sudden cardiac death. *Sci Rep,* 9**,** 3304.

KARIN, M. 1999. How NF-kappaB is activated: the role of the IkappaB kinase (IKK) complex. *Oncogene,* 18**,** 6867-74.

KAYO, T., ALLISON, D. B., WEINDRUCH, R. & PROLLA, T. A. 2001. Influences of aging and caloric restriction on the transcriptional profile of skeletal muscle from rhesus monkeys. *Proc Natl Acad Sci U S A,* 98**,** 5093-8.

KEFALOYIANNI, E., GAITANAKI, C. & BEIS, I. 2006. ERK1/2 and p38-MAPK signalling pathways, through MSK1, are involved in NF-kappaB transactivation during oxidative stress in skeletal myoblasts. *Cell Signal,* 18**,** 2238-51.

KENNEDY, A. L., MORTON, J. P., MANOHARAN, I., NELSON, D. M., JAMIESON, N. B., PAWLIKOWSKI, J. S., MCBRYAN, T., DOYLE, B., MCKAY, C., OIEN, K. A., ENDERS, G. H., ZHANG, R., SANSOM, O. J. & ADAMS, P. D. 2011. Activation of the PIK3CA/AKT pathway suppresses senescence induced by an activated RAS oncogene to promote tumorigenesis. *Mol Cell,* 42**,** 36-49.

KIHARA, S., HAYASHI, S., HASHIMOTO, S., KANZAKI, N., TAKAYAMA, K., MATSUMOTO, T., CHINZEI, N., IWASA, K., HANEDA, M., TAKEUCHI, K., NISHIDA, K. & KURODA, R. 2018. Cyclin-Dependent Kinase Inhibitor-1-Deficient Mice Are Susceptible to Osteoarthritis Associated With Enhanced Inflammation. *J Bone Miner Res,* 33**,** 2242.

KIM, H. N., CHANG, J., IYER, S., HAN, L., CAMPISI, J., MANOLAGAS, S. C., ZHOU, D. & ALMEIDA, M. 2019. Elimination of senescent osteoclast progenitors has no effect on the age-associated loss of bone mass in mice. *Aging Cell,* 18**,** e12923.

KIM, J. H., BACHMANN, R. A. & CHEN, J. 2009. Interleukin-6 and insulin resistance. *Vitam Horm,* 80**,** 613-33.

KIPLING, D. & COOKE, H. J. 1990. Hypervariable ultra-long telomeres in mice. *Nature,* 347**,** 400-2.

KIRKWOOD, T. B. & AUSTAD, S. N. 2000. Why do we age? *Nature,* 408**,** 233-8.

KLEIN, C. S., MARSH, G. D., PETRELLA, R. J. & RICE, C. L. 2003. Muscle fiber number in the biceps brachii muscle of young and old men. *Muscle Nerve,* 28**,** 62-8.

KOSAR, M., BARTKOVA, J., HUBACKOVA, S., HODNY, Z., LUKAS, J. & BARTEK, J. 2011. Senescence-associated heterochromatin foci are dispensable for cellular senescence, occur in a cell type- and insult-dependent manner and follow expression of p16(ink4a). *Cell Cycle,* 10**,** 457-68.

KRASIEVA, T. B., EHREN, J., O'SULLIVAN, T., TROMBERG, B. J. & MAHER, P. 2015. Cell and brain tissue imaging of the flavonoid fisetin using label-free two-photon microscopy. *Neurochem Int,* 89**,** 243-8.

KREILING, J. A., TAMAMORI-ADACHI, M., SEXTON, A. N., JEYAPALAN, J. C., MUNOZ-NAJAR, U., PETERSON, A. L., MANIVANNAN, J., ROGERS, E. S., PCHELINTSEV, N. A., ADAMS, P. D. & SEDIVY, J. M. 2011. Age-associated increase in heterochromatic marks in murine and primate tissues. *Aging Cell,* 10**,** 292-304.

KRISHNAMURTHY, J., TORRICE, C., RAMSEY, M. R., KOVALEV, G. I., AL-REGAIEY, K., SU, L. & SHARPLESS, N. E. 2004. Ink4a/Arf expression is a biomarker of aging. *J Clin Invest,* 114**,** 1299-307.

KRIZHANOVSKY, V., YON, M., DICKINS, R. A., HEARN, S., SIMON, J., MIETHING, C., YEE, H., ZENDER, L. & LOWE, S. W. 2008. Senescence of activated stellate cells limits liver fibrosis. *Cell,* 134**,** 657-67.

KROON, P. A., CLIFFORD, M. N., CROZIER, A., DAY, A. J., DONOVAN, J. L., MANACH, C. & WILLIAMSON, G. 2004. How should we assess the effects of exposure to dietary polyphenols in vitro? *Am J Clin Nutr,* 80**,** 15-21.

KRTOLICA, A., PARRINELLO, S., LOCKETT, S., DESPREZ, P. Y. & CAMPISI, J. 2001. Senescent fibroblasts promote epithelial cell growth and tumorigenesis: a link between cancer and aging. *Proc Natl Acad Sci U S A,* 98**,** 12072-7.

KUILMAN, T., MICHALOGLOU, C., MOOI, W. J. & PEEPER, D. S. 2010. The essence of senescence. *Genes Dev,* 24**,** 2463-79.

KUILMAN, T. & PEEPER, D. S. 2009. Senescence-messaging secretome: SMS-ing cellular stress. *Nat Rev Cancer,* 9**,** 81-94.

KYLE, U. G., GENTON, L., HANS, D., KARSEGARD, L., SLOSMAN, D. O. & PICHARD, C. 2001. Age-related differences in fat-free mass, skeletal muscle, body cell mass and fat mass between 18 and 94 years. *Eur J Clin Nutr,* 55**,** 663-72.

LABERGE, R. M., ADLER, D., DEMARIA, M., MECHTOUF, N., TEACHENOR, R., CARDIN, G. B., DESPREZ, P. Y., CAMPISI, J. & RODIER, F. 2013. Mitochondrial DNA damage induces apoptosis in senescent cells. *Cell Death Dis,* 4**,** e727.

LABERGE, R. M., SUN, Y., ORJALO, A. V., PATIL, C. K., FREUND, A., ZHOU, L., CURRAN, S. C., DAVALOS, A. R., WILSON-EDELL, K. A., LIU, S., LIMBAD, C., DEMARIA, M., LI, P., HUBBARD, G. B., IKENO, Y., JAVORS, M., DESPREZ, P. Y., BENZ, C. C., KAPAHI, P., NELSON, P. S. & CAMPISI, J. 2015. MTOR regulates the pro-tumorigenic senescence-associated secretory phenotype by promoting IL1A translation. *Nat Cell Biol,* 17**,** 1049-61.

LADNER, K. J., CALIGIURI, M. A. & GUTTRIDGE, D. C. 2003. Tumor necrosis factor-regulated biphasic activation of NF-kappa B is required for cytokine-induced loss of skeletal muscle gene products. *J Biol Chem,* 278**,** 2294-303.

LARSSON, L. & ANSVED, T. 1995. Effects of ageing on the motor unit. *Progress in Neurobiology,* 45**,** 397-458.

LARSSON, L., DEGENS, H., LI, M., SALVIATI, L., LEE, Y. I., THOMPSON, W., KIRKLAND, J. L. & SANDRI, M. 2019. Sarcopenia: Aging-Related Loss of Muscle Mass and Function. *Physiol Rev,* 99**,** 427-511.

LARSSON, L., SJODIN, B. & KARLSSON, J. 1978. Histochemical and biochemical changes in human skeletal muscle with age in sedentary males, age 22--65 years. *Acta Physiol Scand,* 103**,** 31-9.

LAURENTIUS, T., KOB, R., FELLNER, C., NOURBAKHSH, M., BERTSCH, T., SIEBER, C. C. & BOLLHEIMER, L. C. 2019. Long-Chain Fatty Acids and Inflammatory Markers Coaccumulate in the Skeletal Muscle of Sarcopenic Old Rats. *Dis Markers,* 2019**,** 9140789.

LEBRASSEUR, N. K., TCHKONIA, T. & KIRKLAND, J. L. 2015. Cellular Senescence and the Biology of Aging, Disease, and Frailty. *Nestle Nutr Inst Workshop Ser,* 83**,** 11-8.

LEE, B. Y., HAN, J. A., IM, J. S., MORRONE, A., JOHUNG, K., GOODWIN, E. C., KLEIJER, W. J., DIMAIO, D. & HWANG, E. S. 2006. Senescence-associated beta-galactosidase is lysosomal beta-galactosidase. *Aging Cell,* 5**,** 187-95.

LEHMAN, W., CRAIG, R. & VIBERT, P. 1994. Ca(2+)-induced tropomyosin movement in Limulus thin filaments revealed by three-dimensional reconstruction. *Nature,* 368**,** 65-7.

LENG, S. X., CAPPOLA, A. R., ANDERSEN, R. E., BLACKMAN, M. R., KOENIG, K., BLAIR, M. & WALSTON, J. D. 2004. Serum levels of insulin-like growth factor-I (IGF-I) and dehydroepiandrosterone sulfate (DHEA-S), and their relationships with serum interleukin-6, in the geriatric syndrome of frailty. *Aging Clin Exp Res,* 16**,** 153-7.

LEWIS-MCDOUGALL, F. C., RUCHAYA, P. J., DOMENJO-VILA, E., SHIN TEOH, T., PRATA, L., COTTLE, B. J., CLARK, J. E., PUNJABI, P. P., AWAD, W., TORELLA, D., TCHKONIA, T., KIRKLAND, J. L. & ELLISON-HUGHES, G. M. 2019. Aged-senescent cells contribute to impaired heart regeneration. *Aging Cell,* 18**,** e12931.

LEXELL, J., TAYLOR, C. C. & SJOSTROM, M. 1988. What is the cause of the ageing atrophy? Total number, size and proportion of different fiber types studied in whole vastus lateralis muscle from 15- to 83-year-old men. *J Neurol Sci,* 84**,** 275-94.

LI, M. & LARSSON, L. 2010. Force-generating capacity of human myosin isoforms extracted from single muscle fibre segments. *J Physiol,* 588**,** 5105-14.

LI, Y. P. & REID, M. B. 2000. NF-kappaB mediates the protein loss induced by TNF-alpha in differentiated skeletal muscle myotubes. *Am J Physiol Regul Integr Comp Physiol,* 279**,** R1165-70.

LIGHTFOOT, A. P., MCCORMICK, R., NYE, G. A. & MCARDLE, A. 2014. Mechanisms of skeletal muscle ageing; avenues for therapeutic intervention. *Curr Opin Pharmacol,* 16**,** 116-21.

LIO, D., SCOLA, L., CRIVELLO, A., COLONNA-ROMANO, G., CANDORE, G., BONAFE, M., CAVALLONE, L., FRANCESCHI, C. & CARUSO, C. 2002. Gender-specific association between-1082 IL-10 promoter polymorphism and longevity. *Genes and Immunity,* 3**,** 30-33.

LITWINIEC, A., GACKOWSKA, L., HELMIN-BASA, A., ZURYN, A. & GRZANKA, A. 2013. Low-dose etoposide-treatment induces endoreplication and cell death accompanied by cytoskeletal alterations in A549 cells: Does the response involve senescence? The possible role of vimentin. *Cancer Cell Int,* 13**,** 9.

LIU, F., WU, H. Y., WESSELSCHMIDT, R., KORNAGA, T. & LINK, D. C. 1996. Impaired production and increased apoptosis of neutrophils in granulocyte colony-stimulating factor receptor-deficient mice. *Immunity,* 5**,** 491-501.

LIU, Y., SANOFF, H. K., CHO, H., BURD, C. E., TORRICE, C., IBRAHIM, J. G., THOMAS, N. E. & SHARPLESS, N. E. 2009. Expression of p16(INK4a) in peripheral blood T-cells is a biomarker of human aging. *Aging Cell,* 8**,** 439-48.

LONG, X., LIN, Y., ORTIZ-VEGA, S., YONEZAWA, K. & AVRUCH, J. 2005. Rheb binds and regulates the mTOR kinase. *Curr Biol,* 15**,** 702-13.

LOPES-PACIENCIA, S., SAINT-GERMAIN, E., ROWELL, M. C., RUIZ, A. F., KALEGARI, P. & FERBEYRE, G. 2019. The senescence-associated secretory phenotype and its regulation. *Cytokine,* 117**,** 15-22.

LOPEZ-LAZARO, M., WILLMORE, E. & AUSTIN, C. A. 2010. The dietary flavonoids myricetin and fisetin act as dual inhibitors of DNA topoisomerases I and II in cells. *Mutat Res,* 696**,** 41-7.

LOZANO, G. 2010. Mouse models of p53 functions. *Cold Spring Harb Perspect Biol,* 2**,** a001115.

LUSHAJ, E. B., JOHNSON, J. K., MCKENZIE, D. & AIKEN, J. M. 2008. Sarcopenia accelerates at advanced ages in Fisher 344xBrown Norway rats. *J Gerontol A Biol Sci Med Sci,* 63**,** 921-7.

LUTZ, C. T. & QUINN, L. S. 2012. Sarcopenia, obesity, and natural killer cell immune senescence in aging: altered cytokine levels as a common mechanism. *Aging (Albany NY),* 4**,** 535-46.

MA, L., CHEN, Z., ERDJUMENT-BROMAGE, H., TEMPST, P. & PANDOLFI, P. P. 2005. Phosphorylation and functional inactivation of TSC2 by Erk implications for tuberous sclerosis and cancer pathogenesis. *Cell,* 121**,** 179-93.

MABB, A. M., WUERZBERGER-DAVIS, S. M. & MIYAMOTO, S. 2006. PIASy mediates NEMO sumoylation and NF-kappaB activation in response to genotoxic stress. *Nat Cell Biol,* 8**,** 986-93.

MABE, S., NAGAMUNE, T. & KAWAHARA, M. 2014. Detecting protein-protein interactions based on kinase-mediated growth induction of mammalian cells. *Sci Rep,* 4**,** 6127.

MACPHERSON, P. C., DENNIS, R. G. & FAULKNER, J. A. 1997. Sarcomere dynamics and contraction-induced injury to maximally activated single muscle fibres from soleus muscles of rats. *J Physiol,* 500 (Pt 2)**,** 523-33.

MAHER, P. 2015. How fisetin reduces the impact of age and disease on CNS function. *Front Biosci (Schol Ed),* 7**,** 58-82.

MAIER, B., GLUBA, W., BERNIER, B., TURNER, T., MOHAMMAD, K., GUISE, T., SUTHERLAND, A., THORNER, M. & SCRABLE, H. 2004. Modulation of mammalian life span by the short isoform of p53. *Genes Dev,* 18**,** 306-19.

MAKRIS, C., GODFREY, V. L., KRAHN-SENFTLEBEN, G., TAKAHASHI, T., ROBERTS, J. L., SCHWARZ, T., FENG, L., JOHNSON, R. S. & KARIN, M. 2000. Female mice heterozygous

for IKK gamma/NEMO deficiencies develop a dermatopathy similar to the human X-linked disorder incontinentia pigmenti. *Mol Cell,* 5**,** 969-79.

MALAQUIN, N., MARTINEZ, A. & RODIER, F. 2016. Keeping the senescence secretome under control: Molecular reins on the senescence-associated secretory phenotype. *Exp Gerontol,* 82**,** 39-49.

MARTIN, C., CHEN, S., HEILOS, D., SAUER, G., HUNT, J., SHAW, A. G., SIMS, P. F., JACKSON, D. A. & LOVRIC, J. 2010. Changed genome heterochromatinization upon prolonged activation of the Raf/ERK signaling pathway. *PLoS One,* 5**,** e13322.

MARTINS, L., GALLO, C. C., HONDA, T. S. B., ALVES, P. T., STILHANO, R. S., ROSA, D. S., KOH, T. J. & HAN, S. W. 2020. Skeletal muscle healing by M1-like macrophages produced by transient expression of exogenous GM-CSF. *Stem Cell Res Ther,* 11**,** 473.

MATHEU, A., MARAVER, A., KLATT, P., FLORES, I., GARCIA-CAO, I., BORRAS, C., FLORES, J. M., VINA, J., BLASCO, M. A. & SERRANO, M. 2007. Delayed ageing through damage protection by the Arf/p53 pathway. *Nature,* 448**,** 375-9.

MATSUOKA, S., ROTMAN, G., OGAWA, A., SHILOH, Y., TAMAI, K. & ELLEDGE, S. J. 2000. Ataxia telangiectasia-mutated phosphorylates Chk2 in vivo and in vitro. *Proc Natl Acad Sci U S A,* 97**,** 10389-94.

MAUGHAN, R. J., WATSON, J. S. & WEIR, J. 1984. Muscle strength and cross-sectional area in man: a comparison of strength-trained and untrained subjects. *Br J Sports Med,* 18**,** 149-57.

MAYA, R., BALASS, M., KIM, S. T., SHKEDY, D., LEAL, J. F., SHIFMAN, O., MOAS, M., BUSCHMANN, T., RONAI, Z., SHILOH, Y., KASTAN, M. B., KATZIR, E. & OREN, M. 2001. ATM-dependent phosphorylation of Mdm2 on serine 395: role in p53 activation by DNA damage. *Genes Dev,* 15**,** 1067-77.

MCARDLE, A., DILLMANN, W. H., MESTRIL, R., FAULKNER, J. A. & JACKSON, M. J. 2004. Overexpression of HSP70 in mouse skeletal muscle protects against muscle damage and age-related muscle dysfunction. *FASEB J,* 18**,** 355-7.

MCARDLE, A., POLLOCK, N., STAUNTON, C. A. & JACKSON, M. J. 2019. Aberrant redox signalling and stress response in age-related muscle decline: Role in inter- and intra-cellular signalling. *Free Radic Biol Med,* 132**,** 50-57.

MCKAY, B. R., OGBORN, D. I., BAKER, J. M., TOTH, K. G., TARNOPOLSKY, M. A. & PARISE, G. 2013. Elevated SOCS3 and altered IL-6 signaling is associated with age-related human muscle stem cell dysfunction. *Am J Physiol Cell Physiol,* 304**,** C717-28.

MCMAHON, D. K., ANDERSON, P. A., NASSAR, R., BUNTING, J. B., SABA, Z., OAKELEY, A. E. & MALOUF, N. N. 1994. C2C12 cells: biophysical, biochemical, and immunocytochemical properties. *Am J Physiol,* 266**,** C1795-802.

MELTON, L. J., 3RD, RIGGS, B. L., ACHENBACH, S. J., AMIN, S., CAMP, J. J., ROULEAU, P. A., ROBB, R. A., OBERG, A. L. & KHOSLA, S. 2006. Does reduced skeletal loading account for age-related bone loss? *J Bone Miner Res,* 21**,** 1847-55.

MENDRYSA, S. M., O'LEARY, K. A., MCELWEE, M. K., MICHALOWSKI, J., EISENMAN, R. N., POWELL, D. A. & PERRY, M. E. 2006. Tumor suppression and normal aging in mice with constitutively high p53 activity. *Genes Dev,* 20**,** 16-21.

MENG, S. J. & YU, L. J. 2010. Oxidative stress, molecular inflammation and sarcopenia. *Int J Mol Sci,* 11**,** 1509-26.

MICHALOGLOU, C., VREDEVELD, L. C., SOENGAS, M. S., DENOYELLE, C., KUILMAN, T., VAN DER HORST, C. M., MAJOOR, D. M., SHAY, J. W., MOOI, W. J. & PEEPER, D. S. 2005. BRAFE600-associated senescence-like cell cycle arrest of human naevi. *Nature,* 436**,** 720-4.

MINAMINO, T., ORIMO, M., SHIMIZU, I., KUNIEDA, T., YOKOYAMA, M., ITO, T., NOJIMA, A., NABETANI, A., OIKE, Y., MATSUBARA, H., ISHIKAWA, F. & KOMURO, I. 2009. A crucial role for adipose tissue p53 in the regulation of insulin resistance. *Nat Med,* 15**,** 1082-7.

MIQUEL, J., ECONOMOS, A. C., FLEMING, J. & JOHNSON, J. E., JR. 1980. Mitochondrial role in cell aging. *Exp Gerontol,* 15**,** 575-91.

MITCHELL, S., VARGAS, J. & HOFFMANN, A. 2016. Signaling via the NFkappaB system. *Wiley Interdiscip Rev Syst Biol Med,* 8**,** 227-41.

MIYAMOTO, S. 2011. Nuclear initiated NF-kappaB signaling: NEMO and ATM take center stage. *Cell Res,* 21**,** 116-30.

MONTANI, D., BERGOT, E., GUNTHER, S., SAVALE, L., BERGERON, A., BOURDIN, A., BOUVAIST, H., CANUET, M., PISON, C., MACRO, M., POUBEAU, P., GIRERD, B., NATALI, D., GUIGNABERT, C., PERROS, F., O'CALLAGHAN, D. S., JAIS, X., TUBERT-BITTER, P., ZALCMAN, G., SITBON, O., SIMONNEAU, G. & HUMBERT, M. 2012. Pulmonary arterial hypertension in patients treated by dasatinib. *Circulation,* 125**,** 2128-37.

MONTECUCCO, A., ZANETTA, F. & BIAMONTI, G. 2015. Molecular mechanisms of etoposide. *EXCLI J,* 14**,** 95-108.

MOORE, K. W., O'GARRA, A., DE WAAL MALEFYT, R., VIEIRA, P. & MOSMANN, T. R. 1993. Interleukin-10. *Annu Rev Immunol,* 11**,** 165-90.

MORLEY, J. E., ANKER, S. D. & VON HAEHLING, S. 2014. Prevalence, incidence, and clinical impact of sarcopenia: facts, numbers, and epidemiology-update 2014. *J Cachexia Sarcopenia Muscle,* 5**,** 253-9.

MORSE, C. I., THOM, J. M., REEVES, N. D., BIRCH, K. M. & NARICI, M. V. 2005. In vivo physiological cross-sectional area and specific force are reduced in the gastrocnemius of elderly men. *Journal of Applied Physiology,* 99**,** 1050-5.

MOSSER, D. D., THEODORAKIS, N. G. & MORIMOTO, R. I. 1988. Coordinate changes in heat shock element-binding activity and HSP70 gene transcription rates in human cells. *Mol Cell Biol,* 8**,** 4736-44.

MOURKIOTI, F., KRATSIOS, P., LUEDDE, T., SONG, Y. H., DELAFONTAINE, P., ADAMI, R., PARENTE, V., BOTTINELLI, R., PASPARAKIS, M. & ROSENTHAL, N. 2006. Targeted ablation of IKK2 improves skeletal muscle strength, maintains mass, and promotes regeneration. *J Clin Invest,* 116**,** 2945-54.

MUNOZ-ESPIN, D., CANAMERO, M., MARAVER, A., GOMEZ-LOPEZ, G., CONTRERAS, J., MURILLO-CUESTA, S., RODRIGUEZ-BAEZA, A., VARELA-NIETO, I., RUBERTE, J., COLLADO, M. & SERRANO, M. 2013. Programmed cell senescence during mammalian embryonic development. *Cell,* 155**,** 1104-18.

MUNOZ-ESPIN, D. & SERRANO, M. 2014. Cellular senescence: from physiology to pathology. *Nat Rev Mol Cell Biol,* 15**,** 482-96.

MUSCARITOLI, M., ANKER, S. D., ARGILES, J., AVERSA, Z., BAUER, J. M., BIOLO, G., BOIRIE, Y., BOSAEUS, I., CEDERHOLM, T., COSTELLI, P., FEARON, K. C., LAVIANO, A., MAGGIO, M., ROSSI FANELLI, F., SCHNEIDER, S. M., SCHOLS, A. & SIEBER, C. C. 2010. Consensus definition of sarcopenia, cachexia and pre-cachexia: joint document elaborated by Special Interest Groups (SIG) "cachexia-anorexia in chronic wasting diseases" and "nutrition in geriatrics". *Clin Nutr,* 29**,** 154-9.

NACHER, V., CARRETERO, A., NAVARRO, M., ARMENGOL, C., LLOMBART, C., RODRIGUEZ, A., HERRERO-FRESNEDA, I., AYUSO, E. & RUBERTE, J. 2006. The quail mesonephros: a new model for renal senescence? *J Vasc Res,* 43**,** 581-6.

NAGANO, T., NAKANO, M., NAKASHIMA, A., ONISHI, K., YAMAO, S., ENARI, M., KIKKAWA, U. & KAMADA, S. 2016. Identification of cellular senescence-specific genes by comparative transcriptomics. *Sci Rep,* 6**,** 31758.

NARITA, M., NUNEZ, S., HEARD, E., NARITA, M., LIN, A. W., HEARN, S. A., SPECTOR, D. L., HANNON, G. J. & LOWE, S. W. 2003. Rb-mediated heterochromatin formation and silencing of E2F target genes during cellular senescence. *Cell,* 113**,** 703-16.

NELSON, G., WORDSWORTH, J., WANG, C., JURK, D., LAWLESS, C., MARTIN-RUIZ, C. & VON ZGLINICKI, T. 2012. A senescent cell bystander effect: senescence-induced senescence. *Aging Cell,* 11**,** 345-9.

NEWMAN, A. B., HAGGERTY, C. L., GOODPASTER, B., HARRIS, T., KRITCHEVSKY, S., NEVITT, M., MILES, T. P., VISSER, M., HEALTH, A. & BODY COMPOSITION RESEARCH, G. 2003. Strength and muscle quality in a well-functioning cohort of older adults: the Health, Aging and Body Composition Study. *J Am Geriatr Soc,* 51**,** 323-30.

NIELSEN, S. & PEDERSEN, B. K. 2008. Skeletal muscle as an immunogenic organ. *Curr Opin Pharmacol,* 8**,** 346-51.

NOBORI, T., MIURA, K., WU, D. J., LOIS, A., TAKABAYASHI, K. & CARSON, D. A. 1994. Deletions of the cyclin-dependent kinase-4 inhibitor gene in multiple human cancers. *Nature,* 368**,** 753-6.

O'CALLAGHAN, C. & VASSILOPOULOS, A. 2017. Sirtuins at the crossroads of stemness, aging, and cancer. *Aging Cell,* 16**,** 1208-1218.

OECKINGHAUS, A. & GHOSH, S. 2009. The NF-kappaB family of transcription factors and its regulation. *Cold Spring Harb Perspect Biol,* 1**,** a000034.

OGRODNIK, M., MIWA, S., TCHKONIA, T., TINIAKOS, D., WILSON, C. L., LAHAT, A., DAY, C. P., BURT, A., PALMER, A., ANSTEE, Q. M., GRELLSCHEID, S. N., HOEIJMAKERS, J. H. J., BARNHOORN, S., MANN, D. A., BIRD, T. G., VERMEIJ, W. P., KIRKLAND, J. L., PASSOS, J. F., VON ZGLINICKI, T. & JURK, D. 2017. Cellular senescence drives age-dependent hepatic steatosis. *Nat Commun,* 8**,** 15691.

OGRODNIK, M., ZHU, Y., LANGHI, L. G. P., TCHKONIA, T., KRUGER, P., FIELDER, E., VICTORELLI, S., RUSWHANDI, R. A., GIORGADZE, N., PIRTSKHALAVA, T., PODGORNI, O., ENIKOLOPOV, G., JOHNSON, K. O., XU, M., INMAN, C., PALMER, A. K., SCHAFER, M., WEIGL, M., IKENO, Y., BURNS, T. C., PASSOS, J. F., VON ZGLINICKI, T., KIRKLAND,

J. L. & JURK, D. 2019. Obesity-Induced Cellular Senescence Drives Anxiety and Impairs Neurogenesis. *Cell Metab,* 29**,** 1233.

OHTANI, T., ISHIHARA, K., ATSUMI, T., NISHIDA, K., KANEKO, Y., MIYATA, T., ITOH, S., NARIMATSU, M., MAEDA, H., FUKADA, T., ITOH, M., OKANO, H., HIBI, M. & HIRANO, T. 2000. Dissection of signaling cascades through gp130 in vivo: reciprocal roles for STAT3- and SHP2-mediated signals in immune responses. *Immunity,* 12**,** 95-105.

OLAHARSKI, A. J., MONDRALA, S. T. & EASTMOND, D. A. 2005. Chromosomal malsegregation and micronucleus induction in vitro by the DNA topoisomerase II inhibitor fisetin. *Mutat Res,* 582**,** 79-86.

OLSON, B. J. & MARKWELL, J. 2007. Assays for determination of protein concentration. *Curr Protoc Protein Sci,* Chapter 3**,** Unit 3 4.

OSTROWSKI, K., SCHJERLING, P. & PEDERSEN, B. K. 2000. Physical activity and plasma interleukin-6 in humans--effect of intensity of exercise. *Eur J Appl Physiol,* 83**,** 512-5.

OU, H. L. & SCHUMACHER, B. 2018. DNA damage responses and p53 in the aging process. *Blood,* 131**,** 488-495.

PAGANO, M., PEPPERKOK, R., VERDE, F., ANSORGE, W. & DRAETTA, G. 1992. Cyclin A is required at two points in the human cell cycle. *EMBO J,* 11**,** 961-71.

PAJVANI, U. B., TRUJILLO, M. E., COMBS, T. P., IYENGAR, P., JELICKS, L., ROTH, K. A., KITSIS, R. N. & SCHERER, P. E. 2005. Fat apoptosis through targeted activation of caspase 8: a new mouse model of inducible and reversible lipoatrophy. *Nat Med,* 11**,** 797-803.

PAL, H. C., BAXTER, R. D., HUNT, K. M., AGARWAL, J., ELMETS, C. A., ATHAR, M. & AFAQ, F. 2015. Fisetin, a phytochemical, potentiates sorafenib-induced apoptosis and abrogates tumor growth in athymic nude mice implanted with BRAF-mutated melanoma cells. *Oncotarget,* 6**,** 28296-311.

PAL, H. C., DIAMOND, A. C., STRICKLAND, L. R., KAPPES, J. C., KATIYAR, S. K., ELMETS, C. A., ATHAR, M. & AFAQ, F. 2016a. Fisetin, a dietary flavonoid, augments the anti-invasive and anti-metastatic potential of sorafenib in melanoma. *Oncotarget,* 7**,** 1227-41.

PAL, H. C., PEARLMAN, R. L. & AFAQ, F. 2016b. Fisetin and Its Role in Chronic Diseases. *Adv Exp Med Biol,* 928**,** 213-244.

PAL, H. C., SHARMA, S., STRICKLAND, L. R., KATIYAR, S. K., BALLESTAS, M. E., ATHAR, M., ELMETS, C. A. & AFAQ, F. 2014. Fisetin inhibits human melanoma cell invasion through promotion of mesenchymal to epithelial transition and by targeting MAPK and NFkappaB signaling pathways. *PLoS One,* 9**,** e86338.

PALACIO, L., GOYER, M. L., MAGGIORANI, D., ESPINOSA, A., VILLENEUVE, N., BOURBONNAIS, S., MOQUIN-BEAUDRY, G., LE, O., DEMARIA, M., DAVALOS, A. R., DECALUWE, H. & BEAUSEJOUR, C. 2019. Restored immune cell functions upon clearance of senescence in the irradiated splenic environment. *Aging Cell,* 18**,** e12971.

PANGRAZZI, L. & WEINBERGER, B. 2020. T cells, aging and senescence. *Exp Gerontol,* 134**,** 110887.

PANTOJA, C. & SERRANO, M. 1999. Murine fibroblasts lacking p21 undergo senescence and are resistant to transformation by oncogenic Ras. *Oncogene,* 18**,** 4974-82.

PARRINELLO, S., SAMPER, E., KRTOLICA, A., GOLDSTEIN, J., MELOV, S. & CAMPISI, J. 2003. Oxygen sensitivity severely limits the replicative lifespan of murine fibroblasts. *Nat Cell Biol,* 5**,** 741-7.

PARRY, D. A. & SQUIRE, J. M. 1973. Structural role of tropomyosin in muscle regulation: analysis of the x-ray diffraction patterns from relaxed and contracting muscles. *J Mol Biol,* 75**,** 33-55.

PASPARAKIS, M., LUEDDE, T. & SCHMIDT-SUPPRIAN, M. 2006. Dissection of the NF-kappaB signalling cascade in transgenic and knockout mice. *Cell Death Differ,* 13**,** 861-72.

PATIL, P., DONG, Q., WANG, D., CHANG, J., WILEY, C., DEMARIA, M., LEE, J., KANG, J., NIEDERNHOFER, L. J., ROBBINS, P. D., SOWA, G., CAMPISI, J., ZHOU, D. & VO, N. 2019. Systemic clearance of p16(INK4a) -positive senescent cells mitigates age-associated intervertebral disc degeneration. *Aging Cell,* 18**,** e12927.

PAYETTE, H., ROUBENOFF, R., JACQUES, P. F., DINARELLO, C. A., WILSON, P. W., ABAD, L. W. & HARRIS, T. 2003. Insulin-like growth factor-1 and interleukin 6 predict sarcopenia in very old community-living men and women: the Framingham Heart Study. *J Am Geriatr Soc,* 51**,** 1237-43.

PETERSON, J. M. & PIZZA, F. X. 2009. Cytokines derived from cultured skeletal muscle cells after mechanical strain promote neutrophil chemotaxis in vitro. *J Appl Physiol (1985),* 106**,** 130-7.

PETROVA, N. V., VELICHKO, A. K., RAZIN, S. V. & KANTIDZE, O. L. 2016. Small molecule compounds that induce cellular senescence. *Aging Cell,* 15**,** 999-1017.

PIJET, B., PIJET, M., LITWINIUK, A., GAJEWSKA, M., PAJAK, B. & ORZECHOWSKI, A. 2013. TNF- alpha and IFN-s-dependent muscle decay is linked to NF-kappaB- and STAT-1alpha-stimulated Atrogin1 and MuRF1 genes in C2C12 myotubes. *Mediators Inflamm,* 2013**,** 171437.

POMMIER, Y., LEO, E., ZHANG, H. & MARCHAND, C. 2010. DNA topoisomerases and their poisoning by anticancer and antibacterial drugs. *Chem Biol,* 17**,** 421-33.

PORTER, M. M., VANDERVOORT, A. A. & LEXELL, J. 1995. Aging of human muscle: structure, function and adaptability. *Scand J Med Sci Sports,* 5**,** 129-42.

PRASATH, G. S. & SUBRAMANIAN, S. P. 2011. Modulatory effects of fisetin, a bioflavonoid, on hyperglycemia by attenuating the key enzymes of carbohydrate metabolism in hepatic and renal tissues in streptozotocin-induced diabetic rats. *Eur J Pharmacol,* 668**,** 492-6.

PRICE, F. D., VON MALTZAHN, J., BENTZINGER, C. F., DUMONT, N. A., YIN, H., CHANG, N. C., WILSON, D. H., FRENETTE, J. & RUDNICKI, M. A. 2014. Inhibition of JAK-STAT signaling stimulates adult satellite cell function. *Nat Med,* 20**,** 1174-81.

PROBIN, V., WANG, Y., BAI, A. & ZHOU, D. 2006. Busulfan selectively induces cellular senescence but not apoptosis in WI38 fibroblasts via a p53-independent but

extracellular signal-regulated kinase-p38 mitogen-activated protein kinase-dependent mechanism. *J Pharmacol Exp Ther,* 319**,** 551-60.

PROWSE, K. R. & GREIDER, C. W. 1995. Developmental and tissue-specific regulation of mouse telomerase and telomere length. *Proc Natl Acad Sci U S A,* 92**,** 4818-22.

RAY, P., DE, A., MIN, J. J., TSIEN, R. Y. & GAMBHIR, S. S. 2004. Imaging tri-fusion multimodality reporter gene expression in living subjects. *Cancer Res,* 64**,** 1323-30.

RAYMENT, I., RYPNIEWSKI, W. R., SCHMIDT-BASE, K., SMITH, R., TOMCHICK, D. R., BENNING, M. M., WINKELMANN, D. A., WESENBERG, G. & HOLDEN, H. M. 1993. Three-dimensional structure of myosin subfragment-1: a molecular motor. *Science,* 261**,** 50-8.

REBELO-MARQUES, A., DE SOUSA LAGES, A., ANDRADE, R., RIBEIRO, C. F., MOTA-PINTO, A., CARRILHO, F. & ESPREGUEIRA-MENDES, J. 2018. Aging Hallmarks: The Benefits of Physical Exercise. *Front Endocrinol (Lausanne),* 9**,** 258.

ROBERTS, A. W. 2005. G-CSF: a key regulator of neutrophil production, but that's not all! *Growth Factors,* 23**,** 33-41.

RODIER, F. & CAMPISI, J. 2011. Four faces of cellular senescence. *J Cell Biol,* 192**,** 547-56.

ROOS, C. M., ZHANG, B., PALMER, A. K., OGRODNIK, M. B., PIRTSKHALAVA, T., THALJI, N. M., HAGLER, M., JURK, D., SMITH, L. A., CASACLANG-VERZOSA, G., ZHU, Y., SCHAFER, M. J., TCHKONIA, T., KIRKLAND, J. L. & MILLER, J. D. 2016. Chronic senolytic treatment alleviates established vasomotor dysfunction in aged or atherosclerotic mice. *Aging Cell,* 15**,** 973-7.

ROTH, S. M., MARTEL, G. F., IVEY, F. M., LEMMER, J. T., METTER, E. J., HURLEY, B. F. & ROGERS, M. A. 2000. Skeletal muscle satellite cell populations in healthy young and older men and women. *Anat Rec,* 260**,** 351-8.

ROWAN, S. L., RYGIEL, K., PURVES-SMITH, F. M., SOLBAK, N. M., TURNBULL, D. M. & HEPPLE, R. T. 2012. Denervation causes fiber atrophy and myosin heavy chain co-expression in senescent skeletal muscle. *PLoS One,* 7**,** e29082.

RUSSO, G. L., RUSSO, M., SPAGNUOLO, C., TEDESCO, I., BILOTTO, S., IANNITTI, R. & PALUMBO, R. 2014. Quercetin: a pleiotropic kinase inhibitor against cancer. *Cancer Treat Res,* 159**,** 185-205.

SACHS, S., ZARINI, S., KAHN, D. E., HARRISON, K. A., PERREAULT, L., PHANG, T., NEWSOM, S. A., STRAUSS, A., KEREGE, A., SCHOEN, J. A., BESSESEN, D. H., SCHWARZMAYR, T., GRAF, E., LUTTER, D., KRUMSIEK, J., HOFMANN, S. M. & BERGMAN, B. C. 2019. Intermuscular adipose tissue directly modulates skeletal muscle insulin sensitivity in humans. *Am J Physiol Endocrinol Metab,* 316**,** E866-E879.

SACRAMENTO, C. B., CANTAGALLI, V. D., GRINGS, M., CARVALHO, L. P., BAPTISTA-SILVA, J. C., BEUTEL, A., BERGAMASCHI, C. T., DE CAMPOS JUNIOR, R. R., DE MORAES, J. Z., TAKIYA, C. M., SAMOTO, V. Y., BOROJEVIC, R., DA SILVA, F. H., NARDI, N. B., DOHMANN, H. F., JUNIOR, H. S., VALERO, V. B. & HAN, S. W. 2009. Granulocyte-macrophage colony-stimulating factor gene based therapy for acute limb ischemia in a mouse model. *J Gene Med,* 11**,** 345-53.

SAITO, S., GOODARZI, A. A., HIGASHIMOTO, Y., NODA, Y., LEES-MILLER, S. P., APPELLA, E. & ANDERSON, C. W. 2002. ATM mediates phosphorylation at multiple p53 sites, including Ser(46), in response to ionizing radiation. *J Biol Chem,* 277**,** 12491-4.

SAITO, Y., CHIKENJI, T. S., MATSUMURA, T., NAKANO, M. & FUJIMIYA, M. 2020. Exercise enhances skeletal muscle regeneration by promoting senescence in fibro-adipogenic progenitors. *Nat Commun,* 11**,** 889.

SALAMA, R., SADAIE, M., HOARE, M. & NARITA, M. 2014. Cellular senescence and its effector programs. *Genes Dev,* 28**,** 99-114.

SALMELA, A. L., POUWELS, J., VARIS, A., KUKKONEN, A. M., TOIVONEN, P., HALONEN, P. K., PERALA, M., KALLIONIEMI, O., GORBSKY, G. J. & KALLIO, M. J. 2009. Dietary flavonoid fisetin induces a forced exit from mitosis by targeting the mitotic spindle checkpoint. *Carcinogenesis,* 30**,** 1032-40.

SARTIPY, P. & LOSKUTOFF, D. J. 2003. Monocyte chemoattractant protein 1 in obesity and insulin resistance. *Proc Natl Acad Sci U S A,* 100**,** 7265-70.

SCALBERT, A., MORAND, C., MANACH, C. & REMESY, C. 2002. Absorption and metabolism of polyphenols in the gut and impact on health. *Biomed Pharmacother,* 56**,** 276-82.

SCHAAP, L. A., PLUIJM, S. M., DEEG, D. J. & VISSER, M. 2006. Inflammatory markers and loss of muscle mass (sarcopenia) and strength. *Am J Med,* 119**,** 526 e9-17.

SCHAFER, M. J., WHITE, T. A., EVANS, G., TONNE, J. M., VERZOSA, G. C., STOUT, M. B., MAZULA, D. L., PALMER, A. K., BAKER, D. J., JENSEN, M. D., TORBENSON, M. S., MILLER, J. D., IKEDA, Y., TCHKONIA, T., VAN DEURSEN, J. M., KIRKLAND, J. L. & LEBRASSEUR, N. K. 2016. Exercise Prevents Diet-Induced Cellular Senescence in Adipose Tissue. *Diabetes,* 65**,** 1606-15.

SCHAFER, M. J., WHITE, T. A., IIJIMA, K., HAAK, A. J., LIGRESTI, G., ATKINSON, E. J., OBERG, A. L., BIRCH, J., SALMONOWICZ, H., ZHU, Y., MAZULA, D. L., BROOKS, R. W., FUHRMANN-STROISSNIGG, H., PIRTSKHALAVA, T., PRAKASH, Y. S., TCHKONIA, T., ROBBINS, P. D., AUBRY, M. C., PASSOS, J. F., KIRKLAND, J. L., TSCHUMPERLIN, D. J., KITA, H. & LEBRASSEUR, N. K. 2017. Cellular senescence mediates fibrotic pulmonary disease. *Nat Commun,* 8**,** 14532.

SCHIAFFINO, S. & REGGIANI, C. 2011. Fiber types in mammalian skeletal muscles. *Physiol Rev,* 91**,** 1447-531.

SELL, H., DIETZE-SCHROEDER, D., KAISER, U. & ECKEL, J. 2006. Monocyte chemotactic protein-1 is a potential player in the negative cross-talk between adipose tissue and skeletal muscle. *Endocrinology,* 147**,** 2458-67.

SERINO, A. & SALAZAR, G. 2018. Protective Role of Polyphenols against Vascular Inflammation, Aging and Cardiovascular Disease. *Nutrients,* 11.

SERRANO, A. L. & MUNOZ-CANOVES, P. 2010. Regulation and dysregulation of fibrosis in skeletal muscle. *Exp Cell Res,* 316**,** 3050-8.

SERRANO, M., HANNON, G. J. & BEACH, D. 1993. A new regulatory motif in cell-cycle control causing specific inhibition of cyclin D/CDK4. *Nature,* 366**,** 704-7.

SERRANO, M., LIN, A. W., MCCURRACH, M. E., BEACH, D. & LOWE, S. W. 1997. Oncogenic ras provokes premature cell senescence associated with accumulation of p53 and p16INK4a. *Cell,* 88**,** 593-602.

SHAFIQ, S. A. & GORYCKI, M. A. 1965. Regeneration in skeletal muscle of mouse: some electron-microscope observations. *J Pathol Bacteriol,* 90**,** 123-7.

SHIEH, S. Y., AHN, J., TAMAI, K., TAYA, Y. & PRIVES, C. 2000. The human homologs of checkpoint kinases Chk1 and Cds1 (Chk2) phosphorylate p53 at multiple DNA damage-inducible sites (vol 14, pg 289, 2000). *Genes & Development,* 14**,** 750-750.

SIMONEAU, J. A., LORTIE, G., BOULAY, M. R., MARCOTTE, M., THIBAULT, M. C. & BOUCHARD, C. 1985. Human skeletal muscle fiber type alteration with high-intensity intermittent training. *Eur J Appl Physiol Occup Physiol,* 54**,** 250-3.

SMITH, P. K., KROHN, R. I., HERMANSON, G. T., MALLIA, A. K., GARTNER, F. H., PROVENZANO, M. D., FUJIMOTO, E. K., GOEKE, N. M., OLSON, B. J. & KLENK, D. C. 1985. Measurement of protein using bicinchoninic acid. *Anal Biochem,* 150**,** 76-85.

SOLDIN, O. P. & MATTISON, D. R. 2009. Sex differences in pharmacokinetics and pharmacodynamics. *Clin Pharmacokinet,* 48**,** 143-57.

SOSA, P., ALCALDE-ESTEVEZ, E., PLAZA, P., TROYANO, N., ALONSO, C., MARTINEZ-ARIAS, L., EVELEM DE MELO AROEIRA, A., RODRIGUEZ-PUYOL, D., OLMOS, G., LOPEZ-ONGIL, S. & RUIZ-TORRES, M. P. 2018. Hyperphosphatemia Promotes Senescence of Myoblasts by Impairing Autophagy Through Ilk Overexpression, A Possible Mechanism Involved in Sarcopenia. *Aging Dis,* 9**,** 769-784.

SOTO-GAMEZ, A., QUAX, W. J. & DEMARIA, M. 2019. Regulation of Survival Networks in Senescent Cells: From Mechanisms to Interventions. *J Mol Biol,* 431**,** 2629-2643.

SOUSA-VICTOR, P., GUTARRA, S., GARCIA-PRAT, L., RODRIGUEZ-UBREVA, J., ORTET, L., RUIZ-BONILLA, V., JARDI, M., BALLESTAR, E., GONZALEZ, S., SERRANO, A. L., PERDIGUERO, E. & MUNOZ-CANOVES, P. 2014. Geriatric muscle stem cells switch reversible quiescence into senescence. *Nature,* 506**,** 316-21.

SPELLMAN, P. T., SHERLOCK, G., ZHANG, M. Q., IYER, V. R., ANDERS, K., EISEN, M. B., BROWN, P. O., BOTSTEIN, D. & FUTCHER, B. 1998. Comprehensive identification of cell cycle-regulated genes of the yeast Saccharomyces cerevisiae by microarray hybridization. *Mol Biol Cell,* 9**,** 3273-97.

SPUDICH, J. A. 2001. The myosin swinging cross-bridge model. *Nat Rev Mol Cell Biol,* 2**,** 387-92.

STEENSBERG, A., VAN HALL, G., OSADA, T., SACCHETTI, M., SALTIN, B. & KLARLUND PEDERSEN, B. 2000. Production of interleukin-6 in contracting human skeletal muscles can account for the exercise-induced increase in plasma interleukin-6. *J Physiol,* 529 Pt 1**,** 237-42.

STORER, M., MAS, A., ROBERT-MORENO, A., PECORARO, M., ORTELLS, M. C., DI GIACOMO, V., YOSEF, R., PILPEL, N., KRIZHANOVSKY, V., SHARPE, J. & KEYES, W. M. 2013. Senescence is a developmental mechanism that contributes to embryonic growth and patterning. *Cell,* 155**,** 1119-30.

STROBER, W. 2015. Trypan Blue Exclusion Test of Cell Viability. *Curr Protoc Immunol,* 111**,** A3 B 1-A3 B 3.

STUDENSKI, S. A., PETERS, K. W., ALLEY, D. E., CAWTHON, P. M., MCLEAN, R. R., HARRIS, T. B., FERRUCCI, L., GURALNIK, J. M., FRAGALA, M. S., KENNY, A. M., KIEL, D. P., KRITCHEVSKY, S. B., SHARDELL, M. D., DAM, T. T. & VASSILEVA, M. T. 2014. The FNIH sarcopenia project: rationale, study description, conference recommendations, and final estimates. *J Gerontol A Biol Sci Med Sci,* 69**,** 547-58.

SUH, Y., AFAQ, F., KHAN, N., JOHNSON, J. J., KHUSRO, F. H. & MUKHTAR, H. 2010. Fisetin induces autophagic cell death through suppression of mTOR signaling pathway in prostate cancer cells. *Carcinogenesis,* 31**,** 1424-33.

SUN, S. C. 2011. Non-canonical NF-kappaB signaling pathway. *Cell Res,* 21**,** 71-85.

SUN, S. C., CHANG, J. H. & JIN, J. 2013. Regulation of nuclear factor-kappaB in autoimmunity. *Trends Immunol,* 34**,** 282-9.

SUNG, B., PANDEY, M. K. & AGGARWAL, B. B. 2007. Fisetin, an inhibitor of cyclin-dependent kinase 6, down-regulates nuclear factor-kappaB-regulated cell proliferation, antiapoptotic and metastatic gene products through the suppression of TAK-1 and receptor-interacting protein-regulated IkappaBalpha kinase activation. *Mol Pharmacol,* 71**,** 1703-14.

SYED, D. N., ADHAMI, V. M., KHAN, M. I. & MUKHTAR, H. 2013. Inhibition of Akt/mTOR signaling by the dietary flavonoid fisetin. *Anticancer Agents Med Chem,* 13**,** 995-1001.

TAHARA, H., SATO, E., NODA, A. & IDE, T. 1995. Increase in expression level of p21sdi1/cip1/waf1 with increasing division age in both normal and SV40-transformed human fibroblasts. *Oncogene,* 10**,** 835-40.

TAKEDA, T., HOSOKAWA, M. & HIGUCHI, K. 1991. Senescence-accelerated mouse (SAM): a novel murine model of accelerated senescence. *J Am Geriatr Soc,* 39**,** 911-9.

TAKEDA, T., HOSOKAWA, M., TAKESHITA, S., IRINO, M., HIGUCHI, K., MATSUSHITA, T., TOMITA, Y., YASUHIRA, K., HAMAMOTO, H., SHIMIZU, K., ISHII, M. & YAMAMURO, T. 1981. A new murine model of accelerated senescence. *Mech Ageing Dev,* 17**,** 183-94.

TALPAZ, M., SHAH, N. P., KANTARJIAN, H., DONATO, N., NICOLL, J., PAQUETTE, R., CORTES, J., O'BRIEN, S., NICAISE, C., BLEICKARDT, E., BLACKWOOD-CHIRCHIR, M. A., IYER, V., CHEN, T. T., HUANG, F., DECILLIS, A. P. & SAWYERS, C. L. 2006. Dasatinib in imatinib-resistant Philadelphia chromosome-positive leukemias. *N Engl J Med,* 354**,** 2531-41.

TE POELE, R. H., OKOROKOV, A. L., JARDINE, L., CUMMINGS, J. & JOEL, S. P. 2002. DNA damage is able to induce senescence in tumor cells in vitro and in vivo. *Cancer Res,* 62**,** 1876-83.

THOMA, A. & LIGHTFOOT, A. P. 2018. NF-kB and Inflammatory Cytokine Signalling: Role in Skeletal Muscle Atrophy. *Adv Exp Med Biol,* 1088**,** 267-279.

TIERNEY, M. T., AYDOGDU, T., SALA, D., MALECOVA, B., GATTO, S., PURI, P. L., LATELLA, L. & SACCO, A. 2014. STAT3 signaling controls satellite cell expansion and skeletal muscle repair. *Nat Med,* 20**,** 1182-6.

TODARO, G. J. & GREEN, H. 1963. Quantitative studies of the growth of mouse embryo cells in culture and their development into established lines. *J Cell Biol,* 17**,** 299-313.

TOHMA, H., HEPWORTH, A. R., SHAVLAKADZE, T., GROUNDS, M. D. & ARTHUR, P. G. 2011. Quantification of ceroid and lipofuscin in skeletal muscle. *J Histochem Cytochem,* 59**,** 769-79.

TOMLINSON, B. E. & IRVING, D. 1977. The numbers of limb motor neurons in the human lumbosacral cord throughout life. *J Neurol Sci,* 34**,** 213-9.

TOUSSAINT, O., DUMONT, P., DIERICK, J. F., PASCAL, T., FRIPPIAT, C., CHAINIAUX, F., SLUSE, F., ELIAERS, F. & REMACLE, J. 2000a. Stress-induced premature senescence. Essence of life, evolution, stress, and aging. *Ann N Y Acad Sci,* 908**,** 85-98.

TOUSSAINT, O., MEDRANO, E. E. & VON ZGLINICKI, T. 2000b. Cellular and molecular mechanisms of stress-induced premature senescence (SIPS) of human diploid fibroblasts and melanocytes. *Exp Gerontol,* 35**,** 927-45.

TOUSSAINT, O., REMACLE, J., DIERICK, J. F., PASCAL, T., FRIPPIAT, C., ZDANOV, S., MAGALHAES, J. P., ROYER, V. & CHAINIAUX, F. 2002. From the Hayflick mosaic to the mosaics of ageing. Role of stress-induced premature senescence in human ageing. *Int J Biochem Cell Biol,* 34**,** 1415-29.

TRESSERA-RIMBAU, A., ARRANZ, S., EDER, M. & VALLVERDU-QUERALT, A. 2017. Dietary Polyphenols in the Prevention of Stroke. *Oxid Med Cell Longev,* 2017**,** 7467962.

TU, Z., AIRD, K. M., BITLER, B. G., NICODEMUS, J. P., BEEHARRY, N., XIA, B., YEN, T. J. & ZHANG, R. 2011. Oncogenic RAS regulates BRIP1 expression to induce dissociation of BRCA1 from chromatin, inhibit DNA repair, and promote senescence. *Dev Cell,* 21**,** 1077-91.

TUTTLE, C. S. L., WAAIJER, M. E. C., SLEE-VALENTIJN, M. S., STIJNEN, T., WESTENDORP, R. & MAIER, A. B. 2020. Cellular senescence and chronological age in various human tissues: A systematic review and meta-analysis. *Aging Cell,* 19**,** e13083.

TYNER, S. D., VENKATACHALAM, S., CHOI, J., JONES, S., GHEBRANIOUS, N., IGELMANN, H., LU, X., SORON, G., COOPER, B., BRAYTON, C., PARK, S. H., THOMPSON, T., KARSENTY, G., BRADLEY, A. & DONEHOWER, L. A. 2002. p53 mutant mice that display early ageing-associated phenotypes. *Nature,* 415**,** 45-53.

VALENTIJN, F. A., FALKE, L. L., NGUYEN, T. Q. & GOLDSCHMEDING, R. 2018. Cellular senescence in the aging and diseased kidney. *J Cell Commun Signal,* 12**,** 69-82.

VAN DER MEULEN, J. H., MCARDLE, A., JACKSON, M. J. & FAULKNER, J. A. 1997. Contraction-induced injury to the extensor digitorum longus muscles of rats: the role of vitamin E. *J Appl Physiol (1985),* 83**,** 817-23.

VAN DEURSEN, J. M. 2014. The role of senescent cells in ageing. *Nature,* 509**,** 439-46.

VANDEN BERGHE, W., PLAISANCE, S., BOONE, E., DE BOSSCHER, K., SCHMITZ, M. L., FIERS, W. & HAEGEMAN, G. 1998. p38 and extracellular signal-regulated kinase mitogen-activated protein kinase pathways are required for nuclear factor-kappaB p65 transactivation mediated by tumor necrosis factor. *J Biol Chem,* 273**,** 3285-90.

VANHOOREN, V. & LIBERT, C. 2013. The mouse as a model organism in aging research: usefulness, pitfalls and possibilities. *Ageing Res Rev,* 12**,** 8-21.

VARSHAVSKY, A. J., BAKAYEV, V. V. & GEORGIEV, G. P. 1976. Heterogeneity of chromatin subunits in vitro and location of histone H1. *Nucleic Acids Res,* 3**,** 477-92.

VASILAKI, A., IWANEJKO, L. M., MCARDLE, F., BROOME, C. S., JACKSON, M. J. & MCARDLE, A. 2003. Skeletal muscles of aged male mice fail to adapt following contractile activity. *Biochem Soc Trans,* 31**,** 455-6.

VASILAKI, A., MCARDLE, F., IWANEJKO, L. M. & MCARDLE, A. 2006. Adaptive responses of mouse skeletal muscle to contractile activity: The effect of age. *Mech Ageing Dev,* 127**,** 830-9.

VELLAI, T., TAKACS-VELLAI, K., ZHANG, Y., KOVACS, A. L., OROSZ, L. & MULLER, F. 2003. Genetics: influence of TOR kinase on lifespan in C. elegans. *Nature,* 426**,** 620.

VERDIJK, L. B., SNIJDERS, T., DROST, M., DELHAAS, T., KADI, F. & VAN LOON, L. J. 2014. Satellite cells in human skeletal muscle; from birth to old age. *Age (Dordr),* 36**,** 545-7.

VISSER, M., PAHOR, M., TAAFFE, D. R., GOODPASTER, B. H., SIMONSICK, E. M., NEWMAN, A. B., NEVITT, M. & HARRIS, T. B. 2002. Relationship of interleukin-6 and tumor necrosis factor-alpha with muscle mass and muscle strength in elderly men and women: the Health ABC Study. *J Gerontol A Biol Sci Med Sci,* 57**,** M326-32.

VOLPI, E., SHEFFIELD-MOORE, M., RASMUSSEN, B. B. & WOLFE, R. R. 2001. Basal muscle amino acid kinetics and protein synthesis in healthy young and older men. *JAMA,* 286**,** 1206-12.

VON ZGLINICKI, T. 2002. Oxidative stress shortens telomeres. *Trends Biochem Sci,* 27**,** 339-44.

VON ZGLINICKI, T., NILSSON, E., DOCKE, W. D. & BRUNK, U. T. 1995. Lipofuscin accumulation and ageing of fibroblasts. *Gerontology,* 41 Suppl 2**,** 95-108.

VON ZGLINICKI, T., WAN, T. & MIWA, S. 2020. Senescence in Post-Mitotic Cells: A Driver of Aging? *Antioxid Redox Signal*.

WAAIJER, M. E., PARISH, W. E., STRONGITHARM, B. H., VAN HEEMST, D., SLAGBOOM, P. E., DE CRAEN, A. J., SEDIVY, J. M., WESTENDORP, R. G., GUNN, D. A. & MAIER, A. B. 2012. The number of p16INK4a positive cells in human skin reflects biological age. *Aging Cell,* 11**,** 722-5.

WALL, B. T., GORISSEN, S. H., PENNINGS, B., KOOPMAN, R., GROEN, B. B., VERDIJK, L. B. & VAN LOON, L. J. 2015. Aging Is Accompanied by a Blunted Muscle Protein Synthetic Response to Protein Ingestion. *PLoS One,* 10**,** e0140903.

WALSH, K. 1997. Coordinate regulation of cell cycle and apoptosis during myogenesis. *Prog Cell Cycle Res,* 3**,** 53-8.

WANG, J. & WALSH, K. 1996. Resistance to apoptosis conferred by Cdk inhibitors during myocyte differentiation. *Science,* 273**,** 359-61.

WELLE, S., BROOKS, A. I., DELEHANTY, J. M., NEEDLER, N., BHATT, K., SHAH, B. & THORNTON, C. A. 2004. Skeletal muscle gene expression profiles in 20-29 year old and 65-71 year old women. *Exp Gerontol,* 39**,** 369-77.

WERNER, C., FURSTER, T., WIDMANN, T., POSS, J., ROGGIA, C., HANHOUN, M., SCHARHAG, J., BUCHNER, N., MEYER, T., KINDERMANN, W., HAENDELER, J., BOHM, M. & LAUFS, U. 2009. Physical exercise prevents cellular senescence in circulating leukocytes and in the vessel wall. *Circulation,* 120**,** 2438-47.

WIEMANN, S. U., SATYANARAYANA, A., TSAHURIDU, M., TILLMANN, H. L., ZENDER, L., KLEMPNAUER, J., FLEMMING, P., FRANCO, S., BLASCO, M. A., MANNS, M. P. & RUDOLPH, K. L. 2002. Hepatocyte telomere shortening and senescence are general markers of human liver cirrhosis. *FASEB J,* 16**,** 935-42.

WILEY, C. D., FLYNN, J. M., MORRISSEY, C., LEBOFSKY, R., SHUGA, J., DONG, X., UNGER, M. A., VIJG, J., MELOV, S. & CAMPISI, J. 2017. Analysis of individual cells identifies cell-to-cell variability following induction of cellular senescence. *Aging Cell,* 16**,** 1043-1050.

WILLIAMS, R. J., SPENCER, J. P. & RICE-EVANS, C. 2004. Flavonoids: antioxidants or signalling molecules? *Free Radic Biol Med,* 36**,** 838-49.

WILSON, D., JACKSON, T., SAPEY, E. & LORD, J. M. 2017. Frailty and sarcopenia: The potential role of an aged immune system. *Ageing Res Rev,* 36**,** 1-10.

WOLFE, R. R. 2006. The underappreciated role of muscle in health and disease. *Am J Clin Nutr,* 84**,** 475-82.

WU, Z. H., SHI, Y., TIBBETTS, R. S. & MIYAMOTO, S. 2006. Molecular linkage between the kinase ATM and NF-kappaB signaling in response to genotoxic stimuli. *Science,* 311**,** 1141-6.

XIONG, Y., HANNON, G. J., ZHANG, H., CASSO, D., KOBAYASHI, R. & BEACH, D. 1993. p21 is a universal inhibitor of cyclin kinases. *Nature,* 366**,** 701-4.

XU, M., BRADLEY, E. W., WEIVODA, M. M., HWANG, S. M., PIRTSKHALAVA, T., DECKLEVER, T., CURRAN, G. L., OGRODNIK, M., JURK, D., JOHNSON, K. O., LOWE, V., TCHKONIA, T., WESTENDORF, J. J. & KIRKLAND, J. L. 2017. Transplanted Senescent Cells Induce an Osteoarthritis-Like Condition in Mice. *J Gerontol A Biol Sci Med Sci,* 72**,** 780-785.

XU, M., PALMER, A. K., DING, H., WEIVODA, M. M., PIRTSKHALAVA, T., WHITE, T. A., SEPE, A., JOHNSON, K. O., STOUT, M. B., GIORGADZE, N., JENSEN, M. D., LEBRASSEUR, N. K., TCHKONIA, T. & KIRKLAND, J. L. 2015a. Targeting senescent cells enhances adipogenesis and metabolic function in old age. *Elife,* 4**,** e12997.

XU, M., PIRTSKHALAVA, T., FARR, J. N., WEIGAND, B. M., PALMER, A. K., WEIVODA, M. M., INMAN, C. L., OGRODNIK, M. B., HACHFELD, C. M., FRASER, D. G., ONKEN, J. L., JOHNSON, K. O., VERZOSA, G. C., LANGHI, L. G. P., WEIGL, M., GIORGADZE, N., LEBRASSEUR, N. K., MILLER, J. D., JURK, D., SINGH, R. J., ALLISON, D. B., EJIMA, K., HUBBARD, G. B., IKENO, Y., CUBRO, H., GAROVIC, V. D., HOU, X., WEROHA, S. J.,

ROBBINS, P. D., NIEDERNHOFER, L. J., KHOSLA, S., TCHKONIA, T. & KIRKLAND, J. L. 2018. Senolytics improve physical function and increase lifespan in old age. *Nat Med,* 24**,** 1246-1256.

XU, M., TCHKONIA, T., DING, H., OGRODNIK, M., LUBBERS, E. R., PIRTSKHALAVA, T., WHITE, T. A., JOHNSON, K. O., STOUT, M. B., MEZERA, V., GIORGADZE, N., JENSEN, M. D., LEBRASSEUR, N. K. & KIRKLAND, J. L. 2015b. JAK inhibition alleviates the cellular senescence-associated secretory phenotype and frailty in old age. *Proc Natl Acad Sci U S A,* 112**,** E6301-10.

YABLUCHANSKIY, A., TARANTINI, S., BALASUBRAMANIAN, P., KISS, T., CSIPO, T., FULOP, G. A., LIPECZ, A., AHIRE, C., DELFAVERO, J., NYUL-TOTH, A., SONNTAG, W. E., SCHWARTZMAN, M. L., CAMPISI, J., CSISZAR, A. & UNGVARI, Z. 2020. Pharmacological or genetic depletion of senescent astrocytes prevents whole brain irradiation-induced impairment of neurovascular coupling responses protecting cognitive function in mice. *Geroscience*.

YAFFE, D. & SAXEL, O. 1977. Serial passaging and differentiation of myogenic cells isolated from dystrophic mouse muscle. *Nature,* 270**,** 725-7.

YANG, H. S. & HINDS, P. W. 2003. Increased ezrin expression and activation by CDK5 coincident with acquisition of the senescent phenotype. *Mol Cell,* 11**,** 1163-76.

YANG, X., SCHADT, E. E., WANG, S., WANG, H., ARNOLD, A. P., INGRAM-DRAKE, L., DRAKE, T. A. & LUSIS, A. J. 2006. Tissue-specific expression and regulation of sexually dimorphic genes in mice. *Genome Res,* 16**,** 995-1004.

YOUSEFZADEH, M. J., ZHU, Y., MCGOWAN, S. J., ANGELINI, L., FUHRMANN-STROISSNIGG, H., XU, M., LING, Y. Y., MELOS, K. I., PIRTSKHALAVA, T., INMAN, C. L., MCGUCKIAN, C., WADE, E. A., KATO, J. I., GRASSI, D., WENTWORTH, M., BURD, C. E., ARRIAGA, E. A., LADIGES, W. L., TCHKONIA, T., KIRKLAND, J. L., ROBBINS, P. D. & NIEDERNHOFER, L. J. 2018. Fisetin is a senotherapeutic that extends health and lifespan. *EBioMedicine,* 36**,** 18-28.

ZHANG, R., CHEN, W. & ADAMS, P. D. 2007. Molecular dissection of formation of senescence-associated heterochromatin foci. *Mol Cell Biol,* 27**,** 2343-58.

ZHU, S., TIAN, Z., TORIGOE, D., ZHAO, J., XIE, P., SUGIZAKI, T., SATO, M., HORIGUCHI, H., TERADA, K., KADOMATSU, T., MIYATA, K. & OIKE, Y. 2019. Aging- and obesity-related peri-muscular adipose tissue accelerates muscle atrophy. *PLoS One,* 14**,** e0221366.

ZHU, Y., TCHKONIA, T., FUHRMANN-STROISSNIGG, H., DAI, H. M., LING, Y. Y., STOUT, M. B., PIRTSKHALAVA, T., GIORGADZE, N., JOHNSON, K. O., GILES, C. B., WREN, J. D., NIEDERNHOFER, L. J., ROBBINS, P. D. & KIRKLAND, J. L. 2016. Identification of a novel senolytic agent, navitoclax, targeting the Bcl-2 family of anti-apoptotic factors. *Aging Cell,* 15**,** 428-35.

ZHUO, W., ZHANG, L., ZHU, Y., ZHU, B. & CHEN, Z. 2015. Fisetin, a dietary bioflavonoid, reverses acquired Cisplatin-resistance of lung adenocarcinoma cells through MAPK/Survivin/Caspase pathway. *Am J Transl Res,* 7**,** 2045-52.

ZOU, L. 2007. Single- and double-stranded DNA: building a trigger of ATR-mediated DNA damage response. *Genes Dev,* 21**,** 879-85.

Appendix

9.1 Abstracts

9.1.1 BSRA - 2017

Shigdar S.[1] shigdars@liv.ac.uk, Staunton C.[1], Vasilaki A.[1], McArdle A.[1]

[1]Department of Musculoskeletal Biology, William Henry Duncan Building, Institute of Ageing and Chronic Disease, University of Liverpool, UK. MRC-Arthritis Research UK Centre for Integrated research into Musculoskeletal Ageing (CIMA).

Do resident senescent cells drive the ageing phenotype of skeletal muscle?

Loss of skeletal muscle mass and function are critical factors in the development of frailty. The number of senescent cells increases with age in rodents (Krishnamurthy *et al*., 2004) and primates (Kreiling *et al*., 2011). We hypothesise that these cells trigger a local and/or systemic chronic inflammatory response leading to the rapid loss of muscle mass and function and that eliminating senescent cells will correct the accelerated loss of muscle mass and function in rodent models of sarcopenia.

Initial studies have investigated whether a C2C12 mouse muscle cell line could be induced into senescence and if so, whether key senescence-associated molecules are upregulated and/or released as the senescence–associated secretory phenotype (SASP).

Myoblasts were treated with Etoposide (50μM) to induce senescence and monitored for up to 5 days for SA-β-Gal staining and for p16 and p21 by immunocytochemistry. Myoblasts exhibited a significantly altered morphology, increased β-Galactosidase activity, and p16 and p21 levels compared with untreated healthy controls.

These data suggest that C2C12 myoblasts can undergo senescence. Further work will characterise the SASP of muscle cells and parallel work will elucidate the accumulation of senescent cells with age in a range of tissues of mouse ageing models and determine the effects of this accumulation on muscle.

Work generously funded by the BSRA.

9.1.2 Rosetrees Trust Symposium – 2017

Rosetrees Trust 30th Anniversary Symposium -Thursday 14th September 2017
Hosted by Rosetrees at the UCL Institute of Child Health.
Name: Shahjahan Miah Shigdar Institute: Institute of Ageing and Chronic Disease, Department of Musculoskeletal Biology
Rosetrees Project Title: Determining the mechanism responsible for frailty in older people: opportunities for novel interventions Rosetrees Grant Number: A1259

Do resident senescent cells drive ageing of skeletal muscle?

Shigdar S (shigdars@liv.ac.uk)[1], Staunton C[1], Richardson A[2], Vasilaki A[1], McArdle A[1]
[1]Department of Musculoskeletal Biology, William Henry Duncan Building, Institute of Ageing and Chronic Disease, University of Liverpool, UK. MRC-Arthritis Research UK Centre for Integrated research into Musculoskeletal Ageing (CIMA).
[2]University of Oklahoma Health Science Center and Oklahoma City VA Medical Center.

Loss of muscle mass and function are critical factors in the development of frailty, leading to immobility, falls and need for residential care, making sarcopenia one of the major factors in poor quality of life in old age. Despite this, only modest progress has been made in determining the mechanism(s) by which age-associated muscle loss occurs and this represents a critical barrier to developing optimal therapies for frailty in older people.

As we age, some individual cells within the body lose their ability to divide and grow (become senescent), these cells produce molecules, including inflammatory cytokines, which are known to be detrimental to tissues. We hypothesise that the production of these molecules by senescent cells either in close proximity to (resident stem cells) or distant to (fat cells) the muscle plays a major role in muscle loss with old age.

Preliminary data has characterised senescence in muscle stem cells (myoblasts) in culture and will now examine muscles of old mice for evidence of senescent myoblasts. Future studies will use a transgenic mouse in which senescent cells can be abolished. We hypothesise that this will prevent age-related loss of muscle mass and strength and lead to the development of novel therapies.

9.1.3 Institute of Ageing and Chronic Disease Science Day - 2018

Shigdar S.[1], Staunton C.[1], Vasilaki A.[1], McArdle A.[1]

[1]Department of Musculoskeletal Biology, William Henry Duncan Building, Institute of Ageing and Chronic Disease, University of Liverpool, UK, L7 8TX. MRC-Arthritis Research UK Centre for Integrated research into Musculoskeletal Ageing (CIMA).

shigdars@liv.ac.uk

Do Resident Senescent Cells Drive the Ageing Phenotype Of Skeletal Muscle?

Loss of skeletal muscle mass and function are critical factors in the development of frailty. The number of senescent cells increases with age in rodents (Krishnamurthy *et al*., 2004) and primates (Kreiling *et al*., 2011). We hypothesise that these cells trigger a local and/or systemic chronic inflammatory response leading to the rapid loss of muscle mass and function and that eliminating senescent cells will correct the accelerated loss of muscle mass and function in rodent models of sarcopenia.

Initial studies have investigated whether a C2C12 mouse muscle cell line could be induced into senescence and if so, whether key senescence-associated molecules are upregulated and/or released as the senescence associated secretory phenotype (SASP).

Myoblasts were treated with Etoposide to induce senescence and monitored for up to 5 days for SA-β-Gal staining, immunocytochemistry and western blot analysis. Myoblasts exhibited a significantly altered morphology, increased β-Galactosidase activity, and cyclin-dependent kinase inhibitor levels compared with untreated healthy controls.

These data suggest that C2C12 myoblasts can undergo senescence. Further work will characterise the SASP of muscle cells and parallel work will elucidate the accumulation of senescent cells with age in a range of tissues of mouse ageing models and determine the effects of this accumulation on muscle.

Work generously funded by the BSRA.

Shigdar S. [1] (shigdars@liv.ac.uk), Staunton C.[1], Vasilaki A.[1], McArdle A.[1]

[1]MRC-Arthritis Research UK Centre for Integrated research into Musculoskeletal Ageing (CIMA), Department of Musculoskeletal Biology, Institute of Ageing and Chronic Disease, William Henry Duncan Building, University of Liverpool, UK.

Do Resident Senescent Cells Drive The Ageing Phenotype Of Skeletal Muscle?

Loss of skeletal muscle mass and function are critical factors in the development of frailty. The number of senescent cells increases with age in rodents (Krishnamurthy *et al*., 2004) and primates (Kreiling *et al*., 2011). We hypothesise that these cells trigger a local and/or systemic chronic inflammatory response with the production of Senescence Associated Secretory Phenotype molecules (SASPs), including inflammatory cytokines leading to muscle dysfunction and loss. We further hypothesise that eliminating senescent cells will correct the accelerated loss of muscle mass and function in mouse models of sarcopenia.

Initial studies have investigated whether a C2C12 mouse muscle myoblast cell line could be induced into senescence and if so, whether key senescence associated molecules (such as p16, p21, and p53) are upregulated and/or released as part of the SASP.

Myoblasts were treated with the topoisomerase II inhibitor, Etoposide, to cause DNA damage and induce senescence. Treated C2C12 myoblasts were monitored for up to 5 days for Senescence Associated β-Galactosidase (SAβ-Gal) staining, immunocytochemistry for p16 and p21, and western blot analysis for p16, p21, and p53 on cell lysates. Treated myoblasts exhibited a significantly altered morphology, increased SAβ-Gal activity, and cyclin-dependent kinase inhibitor levels compared with untreated healthy controls.

These data suggest that C2C12 myoblasts can be induced into a senescent phenotype. Further work will characterise the SASP of C2C12 cell enriched media, adult and old murine skeletal muscle cell lysates, as well as plasma from these mice. Parallel work will determine the accumulation of senescent cells with age in a range of mouse tissues from a range of models ($CuZnSOD^{-/-}$, p16-3MR, and WT) and determine the effects of this accumulation on skeletal muscle function.

References

Kreiling, J.A., M. Tamamori-Adachi, *et al*. (2011). Age-associated increase in heterochromatic marks in murine and primate tissues. Aging Cell 10, 292-304.

Krishnamurthy, J., C. Torrice, *et al*., (2004). Ink4a/Arf expression is a biomarker of aging. J Clin Invest 114, 1299-1307.

Work generously funded by the British Society for Research into Ageing and the Rosetrees Trust.

9.1.5 Experimental Biology – 2018

Shigdar S. [1] (shigdars@liv.ac.uk), Staunton C.[1], Vasilaki A.[1], McArdle A.[1]

[1]MRC-Arthritis Research UK Centre for Integrated research into Musculoskeletal Ageing (CIMA), Department of Musculoskeletal Biology, Institute of Ageing and Chronic Disease, William Henry Duncan Building, University of Liverpool, UK.

Do Resident Senescent Cells Drive The Ageing Phenotype Of Skeletal Muscle?

Loss of skeletal muscle mass and function are critical factors in the development of frailty. The number of senescent cells increases with age in rodents (Krishnamurthy *et al*., 2004) and primates (Kreiling *et al*., 2011). We hypothesise that these cells trigger a local and/or systemic chronic inflammatory response with the production of senescence associated secretory phenotype molecules (SASPs), including inflammatory cytokines leading to muscle dysfunction and loss. We further hypothesise that eliminating senescent cells will correct the accelerated loss of muscle mass and function in mouse models of sarcopenia.

Initial studies have investigated whether key senescence associated molecules (such as p16, p21, and p53) are upregulated in aged (24 months old) compared to young (3 months old) C57BL6 WT mice skeletal muscles, and to characterise any potential SASPs produced.

Quadriceps from young and old mice were subjected to western blot analysis for senescence associated cyclin-dependent kinase inhibitors; p16, p21 and p53. Quadriceps were also snap frozen and cryosectioned transversely (12µm thickness) before being subjected to immunohistochemistry for p21 and p53, and a range of other senescent markers. Western blot analysis results outlined that muscle from aged mice showed a significantly increased expression of p16, p21, and p53 compared to that of young skeletal muscles ($p<0.05$).

In light of this data, we found that aged murine skeletal muscle expresses a range of senescence associated markers and current studies are characterising the senescent content (SASP) of plasma from these mice using a multiplex ELISA to try and determine its impact on aged skeletal muscle function.

Future work will examine the skeletal muscle as well as other tissues as such as the neuronal tissue and adipose tissue from young and old mice in a range of mouse aging models ($CuZnSOD^{-/-}$, p16-3MR, and WT) to determine the effects of this accumulation and its role in skeletal muscle structure and function.

References

Kreiling, J.A., M. Tamamori-Adachi, *et al*. (2011). Age-associated increase in heterochromatic marks in murine and primate tissues. Aging Cell 10, 292-304.

Krishnamurthy, J., C. Torrice, *et al*., (2004). Ink4a/Arf expression is a biomarker of aging. J Clin Invest 114, 1299-1307.

Work generously funded by the British Society for Research into Ageing and the Rosetrees Trust.

Shigdar S. [1] (shigdars@liv.ac.uk), Staunton C.[1], Brooks S., Vasilaki A.[1], Richardson A., McArdle A.[1]

[1]MRC-Arthritis Research UK Centre for Integrated research into Musculoskeletal Ageing (CIMA), Department of Musculoskeletal Biology, Institute of Ageing and Chronic Disease, William Henry Duncan Building, University of Liverpool, UK.

Senescence in myoblasts; role in age-related muscle dysfunction

Loss of muscle mass and function are critical factors in the development of frailty although the mechanisms involved are poorly understood. The number of senescent cells increases with age[1-2]. It is proposed that the presence of these cells plays a role in age-related muscle dysfunction via chronic activation of the nuclear factor k-B (NF-κB) mediated inflammatory pathway[3]. We hypothesise that resident satellite, or potentially other cells local to muscle, become senescent and exert detrimental effects on mature muscle fibres; including the chronic activation of NF-κB via the senescence associated secretory phenotype molecules (SASP) by the bystander effect[4].

In vitro studies have also investigated whether C2C12 myoblasts could become senescent, whether senescence associated cyclin-dependent kinase inhibitors (CDKI) are upregulated, and to determine the nature of the SASP. Myoblasts were treated with Etoposide to induce senescence. Treated myoblasts exhibited significantly altered morphology consistent with a senescent phenotype, increased SA-β-Gal activity, CDKI levels, and SASP factors (IL-6, IL-12(p40), and RANTES), compared with untreated cells.

Additional studies examined muscles from old (24months) and young (3months) C57BL6 Wild-Type (WT) mice for evidence of increased senescence markers. Muscles from old mice had a significantly increased (4-fold) content of senescence CDKIs compared with muscles of young mice ($p<0.05$).

Data suggest that myoblasts can develop a senescent phenotype. Further work will investigate the effect on mature myotubes co-cultured with senescent myoblasts on NF-κB activity. Furthermore, we will determine the role of senescence *in vivo* on skeletal muscle and NF-κB activity in muscle using p16-3MR mice and senolytic agents.

Work generously funded by the British Society for Research into Ageing and the Rosetrees Trust.

1. Krishnamurthy, J., C. Torrice, *et al*., (2004). Ink4a/Arf expression is a biomarker of aging. J Clin Invest 114, 1299-1307.

2. Kreiling, J.A., M. Tamamori-Adachi, *et al*. (2011). Age-associated increase in heterochromatic marks in murine and primate tissues. Aging Cell 10, 292-304.

3. Vasilaki A, McArdle F, Iwanejko LM, McArdle A. (2006). Adaptive responses of mouse skeletal muscle to contractile activity: The effect of age. Mech Ageing Dev. 127(11):830-9.

9.2 Posters

9.2.1 BSRA – 2017

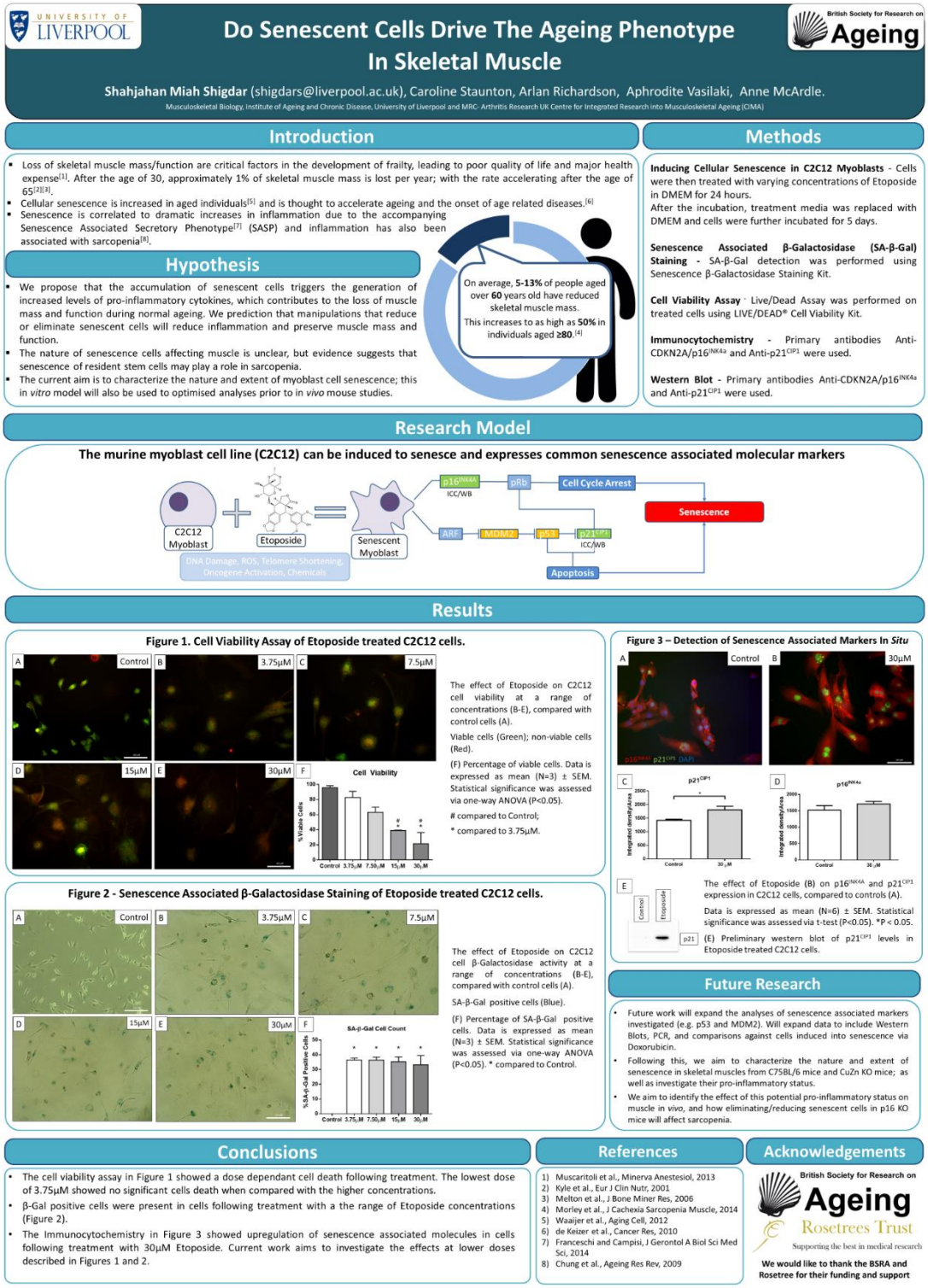

9.2.2 Institute of Ageing and Chronic Disease Science Day - 2018

Do Senescent Cells Drive The Ageing Phenotype In Skeletal Muscle

Shahjahan M Shigdar (shigdars@liverpool.ac.uk), Caroline Staunton, Arlan Richardson, Aphrodite Vasilaki, Anne McArdle.

Musculoskeletal Biology, Institute of Ageing and Chronic Disease, University of Liverpool and MRC- Arthritis Research UK Centre for Integrated Research into Musculoskeletal Ageing (CIMA)

Introduction

- Loss of skeletal muscle mass and function are critical factors in the development of frailty, leading to poor quality of life and major health expense[1].
- Cellular senescence is increased in aged individuals[5] and is thought to accelerate ageing and the onset of age related diseases[6].
- Senescence is correlated to increases in inflammation due to the accompanying Senescence Associated Secretory Phenotype[7] (SASP) and increases in inflammatory cytokines has also been associated with sarcopenia[8].

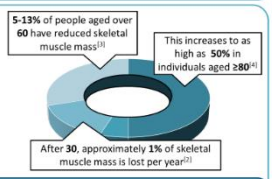

Hypothesis

- We propose that the accumulation of senescent cells results in increased levels of pro-inflammatory cytokines, which contributes to the loss of muscle mass/function during normal ageing.
- Manipulations that reduce/eliminate senescent cells may reduce inflammation and preserve muscle mass/function.
- The nature of senescence cells affecting muscle is unclear, but evidence suggests that senescence of resident or distant stem cells may play a role in sarcopenia.

Methods

Inducing Cellular Senescence in C2C12 Myoblasts - Cells were treated with varying concentrations of Etoposide in DMEM for 24 hours. After the incubation, treatment media was replaced with supplemented DMEM and cells were further incubated for 5 days.

Senescence Associated β-Galactosidase (SA-β-Gal) Staining - SA-β-Gal detection was performed using a Senescence β-Galactosidase Staining Kit.

Cell Viability Assay - Live/Dead Assay was performed on treated cells using LIVE/DEAD® Cell Viability Kit.

Immunocytochemistry - Primary antibodies Anti-CDKN2A/p16^{INK4a} and Anti-p21^{CIP1} were used.

Western Blot - Primary antibodies Anti-p53, Anti-MDM2, Anti-CDKN2A/p16^{INK4a} and Anti-p21^{CIP1} were used.

Research Models

The murine myoblast cell line (C2C12) can be induced to senesce and express senescence associated molecular markers

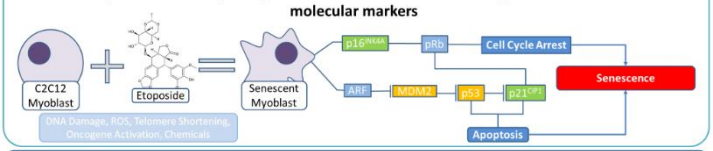

Characterising senescence in young, aged, WT C57BL/6, and p16-3MR mice

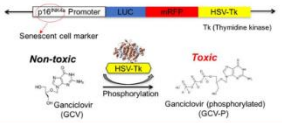

In Vitro Results

Figure 1. Cell Viability Assay of Etoposide treated C2C12 cells.

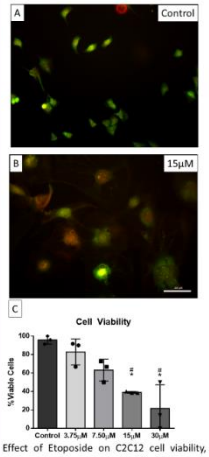

Effect of Etoposide on C2C12 cell viability, compared with control cells (A). Viable cells (Green); non-viable cells (Red).

(C) Percentage of viable cells. Data is expressed as mean (N=3) ± SEM. Statistical significance was assessed via one-way ANOVA (P<0.05) with Tukey's test.

compared to Control

* compared to 3.75μM

Figure 2 – SA-β-Gal Stain of Etoposide treated C2C12 cells.

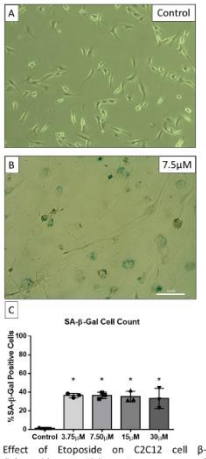

Effect of Etoposide on C2C12 cell β-Galactosidase activity at a range of concentrations, compared with control cells (A). SA-β-Gal positive cells (Blue).

(C) Percentage of SA-β-Gal positive cells. Data is expressed as mean (N=3) ± SEM. Statistical significance was assessed via one-way ANOVA (P<0.05) with Tukey's test.

* compared to Control

Figure 3 – Detection of Senescence Associated Markers in *Situ*

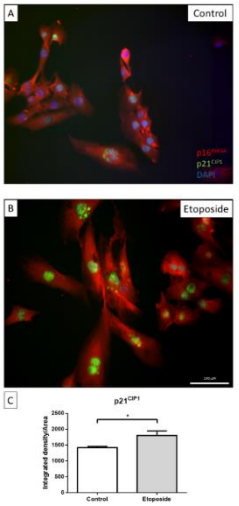

The effect of Etoposide (B) on p16^{INK4A} and p21^{CIP1} expression in C2C12 cells, compared with controls (A).

(C) Data is expressed as mean (N=6) ± SEM. Statistical significance was assessed via t-test (P<0.05). *P < 0.05.

In Vivo Results

Figure 4 – Detection of Senescence Associated Markers in quadriceps of young and old mice

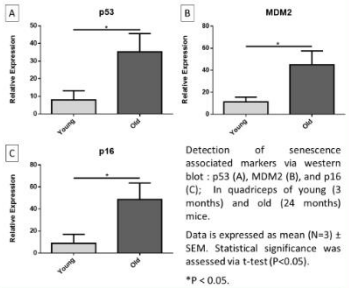

Detection of senescence associated markers via western blot : p53 (A), MDM2 (B), and p16 (C); In quadriceps of young (3 months) and old (24 months) mice.

Data is expressed as mean (N=3) ± SEM. Statistical significance was assessed via t-test (P<0.05).

*P < 0.05.

Ongoing Research

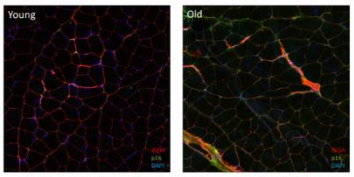

p16^{INK4A} expression in quadriceps of young (left) and old (right) mice. Current works aims to investigate the presence of senescence associated markers in *vivo* using immunohistochemistry.

Future works aims to use p16-3MR mice to characterise and manipulate senescence in *vivo*.

Conclusions

- The cell viability assay showed a concentration dependant C2C12 cell death following treatment with Etoposide. The lowest concentration (3.75μM) showed no significant loss of cell viability when compared with the higher concentrations.
- β-Gal positive cells were present in cells following treatment in a range of Etoposide treatments.
- Immunocytochemistry showed upregulation of senescence associated molecules in cells following treatment with Etoposide.
- Western blot analysis of quadriceps of young and old mouse showed an upregulation senescence associated molecules. Current work aims to investigate the location of these markers using immunofluorescence.

References

1) Muscaritoli et al., Minerva Anestesiol, 2013
2) Kyle et al., Eur J Clin Nutr, 2001
3) Melton et al., J Bone Miner Res, 2006
4) Morley et al., J Cachexia Sarcopenia Muscle, 2014
5) Waaijer et al., Aging Cell, 2012
6) de Keizer et al., Cancer Res, 2010
7) Franceschi and Campisi, J Gerontol A Biol Sci Med Sci, 2014
8) Chung et al., Ageing Res Rev, 2009

Acknowledgements

British Society for Research on Ageing
Rosetrees Trust
Supporting the best in medical research
We would like to thank the BSRA and Rosetree Trust for their funding and support

9.2.3 Experimental Biology – 2018

Senescence in myoblasts; role in age-related muscle dysfunction

Shahjahan M Shigdar (shigdars@liverpool.ac.uk), Caroline Staunton, Aphrodite Vasilaki, Anne McArdle.

1MRC-Arthritis Research UK Centre for Integrated research into Musculoskeletal Ageing (CIMA), Department of Musculoskeletal Biology, Institute of Ageing and Chronic Disease, University of Liverpool

Introduction

- Loss of skeletal muscle mass and function are critical factors in the development of frailty, leading to poor quality of life and major health expense[1].
- Cellular senescence is increased in old individuals[5] and is thought to accelerate ageing and the onset of age-related diseases[6].
- Senescence is correlated to increases in inflammation due to the accompanying Senescence Associated Secretory Phenotype[7] (SASP) and increases in inflammatory cytokines have also been associated with sarcopenia[8].
- We propose that the accumulation of senescent cells results in increased levels of pro-inflammatory cytokines, which contributes to the loss of muscle mass/function during normal ageing.
- Manipulations that reduce/eliminate senescent cells may reduce inflammation and preserve muscle mass/function.
- The nature of senescence cells affecting muscle is unclear, but evidence suggests that senescence of resident or distant stem cells may play a role in sarcopenia.

Materials and Methods

Inducing Cellular Senescence in C2C12 Myoblasts - Cells were treated Etoposide in DMEM for 24 hours. Media was replaced with DMEM and cells were incubated for a further 5 days.

Senescence Associated β-Galactosidase (SA-β-Gal) Staining - SA-β-Gal detection was performed using a Senescence β-Galactosidase Staining Kit (Cell Signalling Technology).

Cell Viability Assay – Viability was assessed in cells using LIVE/DEAD® Cell Viability Kit.

Immunocytochemistry - Primary antibody Anti-$p21^{CIP1}$ was used. Cunter stained with phalloidin and DAPI.

Western Blot - Primary antibody Anti-$p21^{CIP1}$ was used.

Multiplex Cytokine Analysis – Bioplex Luminex Kit was used.

Aims: to investigate whether the C2C12 mouse muscle myoblast cell line could be induced into senescence, whether key senescence associated molecules are expressed; and the nature of the SASP produced.

Results

Figure 1. Viability Of C2C12 Myoblasts Treated With Etoposide

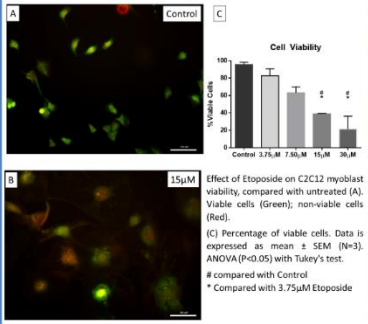

Effect of Etoposide on C2C12 myoblast viability, compared with untreated (A). Viable cells (Green); non-viable cells (Red).

(C) Percentage of viable cells. Data is expressed as mean ± SEM (N=3). ANOVA (P<0.05) with Tukey's test.

compared with Control

* Compared with 3.75μM Etoposide

Figure 2. Etoposide treated C2C12 myoblasts display Senescence Associated β-Galactosidase staining.

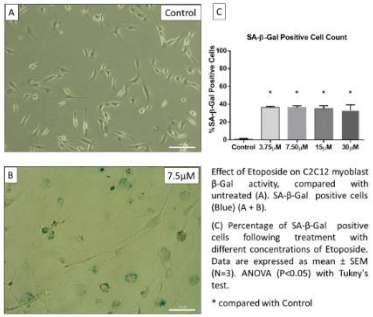

Effect of Etoposide on C2C12 myoblast β-Gal activity, compared with untreated (A). SA-β-Gal positive cells (Blue) (A + B).

(C) Percentage of SA-β-Gal positive cells following treatment with different concentrations of Etoposide. Data are expressed as mean ± SEM (N=3). ANOVA (P<0.05) with Tukey's test.

* compared with Control

Figure 3. Etoposide treated C2C12 myoblasts have increased levels of $p21^{CIP1}$

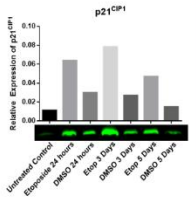

Effect of 3.75μM Etoposide on p21 protein levels in C2C12 myoblasts, compared with untreated and DMSO controls.

Figure 4. Detection of $p21^{CIP1}$ in *Situ*

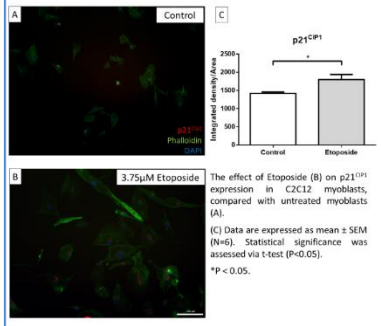

The effect of Etoposide (B) on $p21^{CIP1}$ expression in C2C12 myoblasts, compared with untreated myoblasts (A).

(C) Data are expressed as mean ± SEM (N=6). Statistical significance was assessed via t-test (P<0.05).

*P < 0.05.

Figure 5 – Analysis of the SASP from Etoposide treated C2C12 myoblasts.

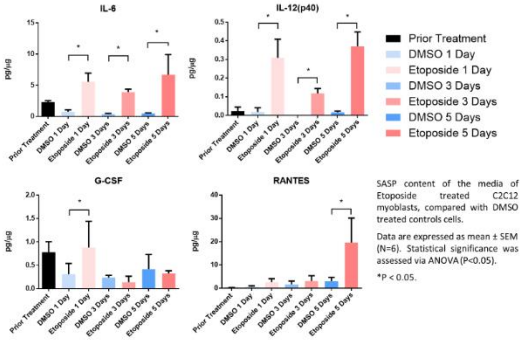

SASP content of the media of Etoposide treated C2C12 myoblasts, compared with DMSO treated controls cells.

Data are expressed as mean ± SEM (N=6). Statistical significance was assessed via ANOVA (P<0.05).

*P < 0.05.

Conclusions

- A concentration dependant C2C12 myoblast death following treatment with Etoposide was evidenced.
- Senescence Associated β-Galactosidase positive myoblasts were present following treatment by a range of Etoposide concentrations.
- Western blot and immunocytochemistry analysis showed upregulation of senescence associated molecule, $p21^{CIP1}$, in myoblasts following treatment with Etoposide.
- SASP analysis of media from C2C12 myoblasts treated with Etoposide showed significantly increased SASP at various time points post-senescence induction.
- C2C12 myoblasts treated with Etoposide demonstrate senescence.

References

1) Muscaritoli et al., Minerva Anestesiol, 2013
2) Kyle et al., Eur J Clin Nutr, 2001
3) Melton et al., J Bone Miner Res, 2006
4) Morley et al., J Cachexia Sarcopenia Muscle, 2014
5) Waaijer et al., Aging Cell, 2012
6) de Keizer et al., Cancer Res, 2010
7) Franceschi and Campisi, J Gerontol A Biol Sci Med Sci, 2014
8) Chung et al., Ageing Res Rev, 2009

Contacts Details

Mr Shahjahan Shigdar BSc (Hons)
E: shigdars@Liverpool.ac.uk
Institute of Ageing and Chronic Disease,
William Henry Duncan Building,
6 West Derby Street,
Liverpool,
L7 8TX

Acknowledgements

We would like to thank the BSRA, Rosetrees Trust, and Physiological Society for their generous support.

Do Senescent Cells Drive The Ageing Phenotype In Skeletal Muscle

Shahjahan M Shigdar (shigdars@liverpool.ac.uk), Caroline Staunton, Arlan Richardson, Aphrodite Vasilaki, Anne McArdle.
Musculoskeletal Biology, Institute of Ageing and Chronic Disease, University of Liverpool and MRC- Arthritis Research UK Centre for Integrated Research into Musculoskeletal Ageing (CIMA)

Introduction

- Loss of skeletal muscle mass and function are critical factors in the development of frailty, leading to poor quality of life and major health expense[1].
- Cellular senescence is increased in aged individuals[5] and is thought to accelerate ageing and the onset of age related diseases[6].
- Senescence is correlated to increases in inflammation due to the accompanying Senescence Associated Secretory Phenotype[7] (SASP) and increases in inflammatory cytokines has also been associated with sarcopenia[8].
- We propose that the accumulation of senescent cells results in increased levels of pro-inflammatory cytokines, which contributes to the loss of muscle mass/function during normal ageing.
- Manipulations that reduce/eliminate senescent cells may reduce inflammation and preserve muscle mass/function.
- The nature of senescence cells affecting muscle is unclear, but evidence suggests that senescence of resident or distant stem cells may play a role in sarcopenia.

Materials and Methods

Mice – C57BL6 wild type mice were used, at ages 8-12 months for young, and 24 months+ for old.

Senescence Associated β-Galactosidase (SA-β-Gal) Staining - SA-β-Gal detection was performed using a Senescence β-Galactosidase Staining Kit.

Western Blot - Primary antibody Anti-p53, Anti-MDM2, and Anti-$p21^{CIP1}$ was used.

Immunocytochemistry - Primary antibody Anti-$p21^{CIP1}$ was used. Counter stained with rhodamine labelled Wheat Germ Agglutinin and DAPI.

Aims: to investigate the presence of senescent cells within the muscle of young and old mice

Results

Figure 1 –Haematoxylin and Eosin Staining of Muscle From Young And Old Mice

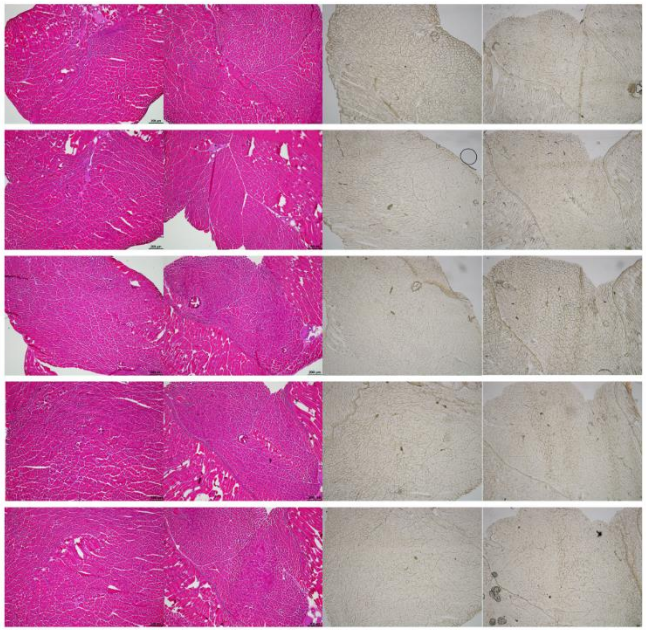

Serial Haematoxylin and Eosin staining of the gastrocnemius muscle of young (right) and old (left) mice.

Figure 2 –Senescence Associated β-Galactosidase Staining of Muscle From Young And Old Mice

Serial Senescence Associated β-Galactosidase staining of the *gastrocnemius* muscle of young (right) and old (left) mice.

Figure 3 – Detection of Senescence Associated Markers in muscles of young and old mice

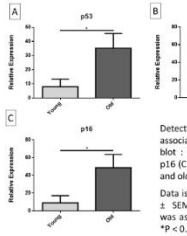

Detection of senescence associated markers via western blot : p53 (A), MDM2 (B), and p16 (C); In quadriceps of young) and old mice.

Data is expressed as mean (N=3) ± SEM. Statistical significance was assessed via t-test (P<0.05). *P < 0.05.

Figure 4 – Detection of Senescence Associated Markers in muscles of young and old mice *in Situ*

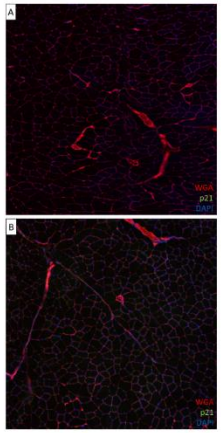

Immunofluorescent detection of senescence associated marker $p21^{CIP1}$; In quadriceps of young (B) and old (A) mice.

Conclusions

- The serial sectioning and staining for Senescence Associated β-Galactosidase showed negative results in the *gastrocnemius* muscles; in both young and old of mice.
- Western Blot analysis for protein levels for Senescence Associated Markers in quadriceps muscles of young and old mice showed upregulation of several senescence markers.
- Immunofluorescence of to visualise the aforementioned senescence marker $p21^{CIP1}$ showed negative results; in both young and old mice.
- From these data, we can conclude that muscles themselves are not senescent; and are not contributing to the chronic NFκB we see during ageing.

References

1) Muscaritoli et al., Minerva Anestesiol, 2013
2) Kyle et al., Eur J Clin Nutr, 2001
3) Melton et al., J Bone Miner Res, 2006
4) Morley et al., J Cachexia Sarcopenia Muscle, 2014
5) Waaijer et al., Aging Cell, 2012
6) de Keizer et al., Cancer Res, 2010
7) Franceschi and Campisi, J Gerontol A Biol Sci Med Sci, 2014
8) Chung et al., Ageing Res Rev, 2009

Contacts Details

Mr Shahjahan Shigdar BSc (Hons)
E: shigdars@Liverpool.ac.uk
Institute of Ageing and Chronic Disease,
William Henry Duncan Building,
6 West Derby Street,
Liverpool,
L7 8TX

Acknowledgements

We would like to thank the BSRA, Rosetree Trust, and Physiological Society for their funding and support

9.2.5 BSRA – 2018

Senescence in myoblasts; role in age-related muscle dysfunction

Shahjahan Shigdar[1] (shigdars@liv.ac.uk), Caroline Staunton[1], Susan Brooks[2], Aphrodite Vasilaki[1], Arlan Richardson[3], Anne McArdle[1]

[1]MRC-Arthritis Research UK Centre for Integrated research into Musculoskeletal Ageing (CIMA), Department of Musculoskeletal Biology, Institute of Ageing and Chronic Disease, University of Liverpool
[2]University of Michigan, Department of Molecular and Integrative Physiology
[3]University of Oklahoma Health Science Center, Oklahoma City VA Medical Center

Introduction

- Loss of skeletal muscle mass and function are critical factors in the development of frailty, leading to poor quality of life and major health expense[1].
- Cellular senescence is increased in old individuals[2] and is thought to accelerate ageing and the onset of age-related diseases[3].
- Senescence is correlated to increases in inflammation due to the accompanying Senescence Associated Secretory Phenotype[4] (SASP) and increases in inflammatory cytokines have also been associated with sarcopenia[5].
- We propose that the accumulation of senescent cells results in increased levels of pro-inflammatory cytokines, which contributes to the loss of muscle mass/function during normal ageing.
- Manipulations that reduce/eliminate senescent cells may reduce inflammation and preserve muscle mass/function. The nature of senescence cells affecting muscle is unclear, but evidence suggests that senescence of resident or distant stem cells may play a role in sarcopenia.

Aims

To investigate whether the C2C12 mouse muscle myoblast cell line could be induced into senescence, whether key senescence associated molecules are expressed; and the nature of the SASP produced.
We also aim to investigate whether senescent cells drive the ageing phenotype in skeletal muscle.

Materials and Methods

Inducing Cellular Senescence in C2C12 Myoblasts - Cells were treated with Etoposide in DMEM for 24 hours. Media was replaced with DMEM and cells were incubated for a further 5 days.

Senescence Associated β-Galactosidase (SA-β-Gal) Staining - SA-β-Gal detection was performed using Senescence β-Galactosidase Staining Kit (Cell Signalling Technology).

Cell Viability Assay – Viability was assessed in cells using LIVE/DEAD® Cell Viability Kit.

Western Blotting - Primary antibodies Anti-p53, Anti-MDM2, and Anti-p21CIP1 were used.

Immunohistochemistry Primary antibody Anti-$p21^{CIP1}$ was used. C2C12 cells counter stained with phalloidin and DAPI. Muscle sections counter stained with wheat germ agglutinin and DAPI.

Multiplex Cytokine Analysis – Bioplex Luminex Kit was used.

Mice – C57BL6 wild type mice were used; age 8-12 months for young/adult, and 24 months+ for old.

Results

Figure 1. Viability of C2C12 myoblasts treated with Etoposide

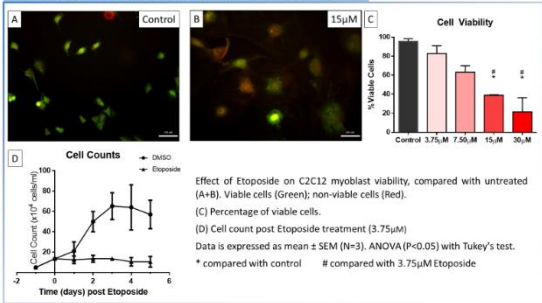

Effect of Etoposide on C2C12 myoblast viability, compared with untreated (A+B). Viable cells (Green); non-viable cells (Red).
(C) Percentage of viable cells.
(D) Cell count post Etoposide treatment (3.75μM)
Data is expressed as mean ± SEM (N=3). ANOVA (P<0.05) with Tukey's test.
* compared with control # compared with 3.75μM Etoposide

Figure 2. Etoposide treated C2C12 myoblasts stained for Senescence Associated β-Galactosidase

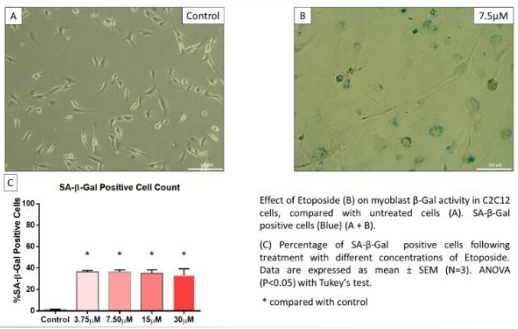

Effect of Etoposide (B) on myoblast β-Gal activity in C2C12 cells, compared with untreated cells (A). SA-β-Gal positive cells (Blue) (A + B).

(C) Percentage of SA-β-Gal positive cells following treatment with different concentrations of Etoposide. Data are expressed as mean ± SEM (N=3). ANOVA (P<0.05) with Tukey's test.

* compared with control

Figure 3. Etoposide treated C2C12 myoblasts have increased levels of $p21^{CIP1}$

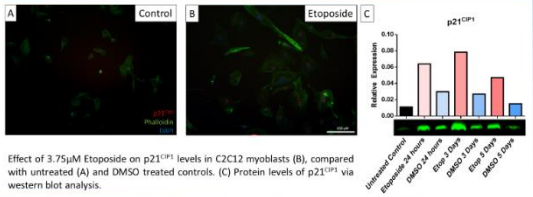

Effect of 3.75μM Etoposide on $p21^{CIP1}$ levels in C2C12 myoblasts (B), compared with untreated (A) and DMSO treated controls. (C) Protein levels of $p21^{CIP1}$ via western blot analysis.

Figure 4 – Analysis of the SASP from Etoposide treated C2C12 myoblasts.

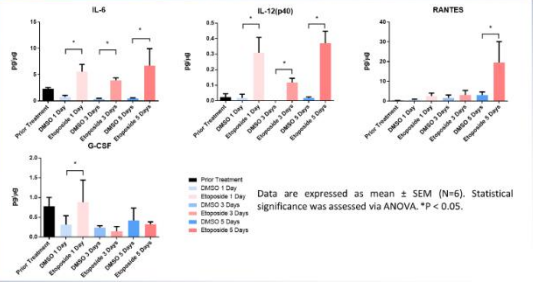

Data are expressed as mean ± SEM (N=6). Statistical significance was assessed via ANOVA. *P < 0.05.

Figure 5 – Detection of senescence associated markers in muscles of mice

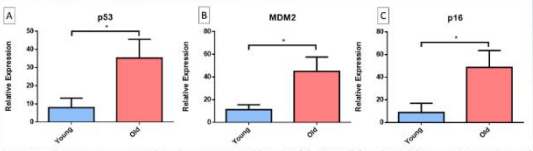

Detection of senescence associated markers via western blot : p53 (A), MDM2 (B), and p16 (C); In quadriceps of young) and old mice.

Data is expressed as mean (N=3) ± SEM. Statistical significance was assessed via t-test. *P < 0.05.

Figure 6 – *in Situ* detection of senescence associated markers in muscles of mice

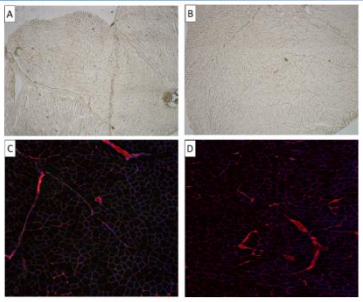

Senescence Associated β-Galactosidase staining of the gastrocnemius muscle of young (A) and old (B) mice.

Immunofluorescent detection of senescence associated marker $p21^{CIP1}$; In quadriceps of young (C) and old (D) mice.

Conclusions

- A concentration dependant C2C12 myoblast death following treatment with Etoposide was evidenced. Cells did not continue to divide following treatment with Etoposide.
- SA-β-Gal positive myoblasts were present following treatment with Etoposide as was increased content of $p21^{CIP1}$
- Analysis of media from Etoposide treated C2C12 myoblasts showed significantly increased SASP at various time points post treatment.
- These data demonstrate that C2C12 myoblasts demonstrate senescence following treatment with Etoposide .
- Western blot analysis for senescence markers showed upregulation of several senescence markers in aged mice, compared with young. SA-β-Gal activity and Immunofluorescence for the senescence markers p53, p21 and p16 showed negative results; in both young and old mice.

References

1) Muscaritoli et al., Minerva Anestesiol, 2013
2) Waaijer et al., Aging Cell, 2012
3) de Keizer et al., Cancer Res, 2010
4) Franceschi and Campisi, J Gerontol A Biol Sci Med Sci, 2014
5) Chung et al., Ageing Res Rev, 2009

Acknowledgements

British Society for Research on Ageing
Rosetrees Trust
Supporting the best in medical research

We would like to thank the BSRA and Rosetree Trust for their generous support.